Investigating the Relationship Between Markers of Ageing & Cardiometabolic Disease

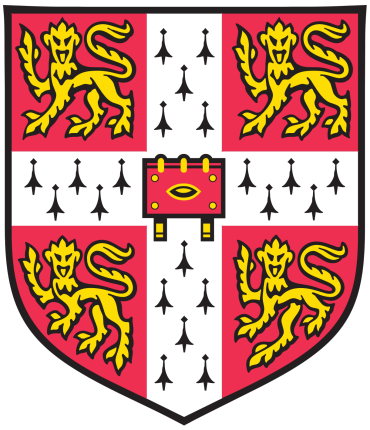

Daniel John Wright

Darwin College

University of Cambridge

January (Lent) 2018

This thesis is submitted in fulfilment of the requirements
for the degree of Doctor of Philosophy (Ph.D.)

Felix qui potuit rerum cognoscere causas

The work contained herein was conducted at the Medical Research Council Epidemiology Unit between October 2014 and September 2017, under the supervision of Professor Nicholas Wareham, Dr John Perry, and (until September 2016) Dr Robert Scott.

This dissertation is the result of my own work, and includes nothing which is the outcome of work done in collaboration with others except as specified in the *Contributions* section of each chapter, or otherwise noted in the text. No part of this work - or any work substantially similar to it - has previously been submitted, nor will in future be submitted, for a degree at the University of Cambridge or any other University.

As required by the Degree Committee for the Faculties of Clinical Medicine and Clinical Veterinary Medicine, this dissertation does not exceed 60,000 words (exclusive of tables, figures, supplementary materials and references).

The approximate word count of this document is 41,700.

DANIEL J. WRIGHT

Darwin College, University of Cambridge
January 2018, Lent Term

This thesis is the product of a great deal of discussion, collaboration, and thought-wrangling. It simply would not have been possible without the immeasurable help and support I have been lucky to receive from my friends and colleagues both inside and outside the MRC Epidemiology Unit; whether helping me grapple code, concepts, or just supplying coffee (or, more importantly, beer)...

My particular thanks go to my supervisors - Nick, Robert and John - who have guided me through the PhD process with patience and careful thought. Although, Felix, I feel you have most certainly borne the brunt of my day-to-day crises. A huge thank you for *your* patience and considered advice. You are a veritable fount of knowledge, and what's more, it's mostly useful.

To my fellow PhDs. Tom, you have withstood my babbling and nonsense for many a year but I've got a feeling you'll miss my incessant presence - don't tell me I'm wrong. Emma, you have been a wonderful friend, weathering even the most absurd of my Edina Monsoon outbursts with poise. Eirini, it's been a pleasure. And Sherly, your advice gave me the strength to just keep pushing. I am also very grateful to Clara for pragmatic advice and emotional support.

My thanks also to Nicola Kerrison, Isobel Stewart, Amy Ahern, Andrew Cooper and Jian'an Luan for all contributing in their own way to my PhD experience, and for helping me retain my sanity.

Finally, to Matt. Thank you for your unwavering love and support, and for always believing in me. You give me perspective on what *really* matters, and for that - and for you - I am truly thankful.

Summary

Human ageing is accompanied by characteristic metabolic and endocrine changes, including altered hormone profiles, insulin resistance and deterioration of skeletal muscle. Obesity and diabetes may themselves drive an accelerated ageing phenotype. Untangling the causal web between ageing, obesity and diabetes is a priority in order to understand their aetiology and improve prevention and management.

The role of biological ageing in determining the risk of obesity and associated conditions has often been examined using mean leukocyte telomere length (LTL), a marker of replicative fatigue and senescence. However, considering phenotypes which represent different domains of biological and functional ageing as exposures for obesity and related traits could allow the elucidation of new understudied phenotypes relevant to cardio-metabolic risk in the wider population.

This PhD considers the causal role of (1) hand grip strength (HGS), a marker of overall strength and physical functioning, and (2) resting energy expenditure, an indicator of overall energy metabolism and the major component of daily energy expenditure, in cardio-metabolic risk. I also characterise a new and readily-quantifiable marker of age-related genomic instability, mosaic loss of the Y chromosome (mLOY). Observational evidence implicates each of these phenotypes in cardio-metabolic conditions and intermediate phenotypes. However, it is not possible to infer causality from these observational associations due to confounding and reverse-causality. Mendelian randomisation offers a solution to these limitations and can allow the causal nature of these relationships to be investigated. Using population-based data including UK Biobank, this thesis presents the first large-scale genetic discovery effort for each trait and provides new biological insight into their shared and separate aetiology. I used identified variants to investigate the bidirectional causal associations of each trait with cardio-metabolic outcomes, intermediate phenotypes and other related traits such as frailty and mortality. In total I identified 16 loci for hand grip strength, 19 for mLOY, and one signal for REE. I have shown that HGS is likely to be causally linked to fracture risk, and I have identified the important shared genetic architecture between mLOY, glycaemic traits and cancer. I have also demonstrated that at least one known genetic variant contributing to obesity risk acts partially via reduced REE.

Overall the findings of my PhD contribute to our wider understanding of the aetiological role of ageing processes in metabolic dysfunction, and have implications for both basic science and translational applications.

Publications

⋆ denotes joint first authorship.

Published

Willems S.M.⋆, **Wright D.J.**⋆, Day F.R., Trajanoska K. . . .(72 authors). . . Wareham N.J. & Scott R.A. (2017) Large-scale GWAS identifies multiple loci for hand grip strength providing biological insights into muscular fitness. *Nature Communications*. **8**, DOI:10.1038/ncomms16015.

Wright D.J.⋆, Day F.R.⋆, Kerrison N.D.⋆, Zink F.⋆ . . .(13 authors). . . Stefansson K. & Perry J.R.B. (2017). Genetic variants associated with mosaic Y chromosome loss highlight cell cycle genes and overlap with cancer susceptibility. *Nature Genetics*. **49**, 674-679.

In Preparation or Review

Trajanoska K.⋆, Morris J.A.⋆, Oei L.⋆, Zheng H.F.⋆ . . .(11 authors). . . **Wright D.J.**. . .(157 authors). . . Scott R.A., Evans D.M., Kiel D.P., Ohlsson C., Richards J.B. & Rivadeneira F. (2018) Leveraging genetic associations to evaluate clinical risk factors for osteoporotic fractures. *British Medical Journal* (in review).

Wright D.J., Noordam R.R., Couture C., Piaggi P., Tanaka T., Tayo B., Li-Gao R., Schrack J., Cooper R., Luke A., Bouchard C., Pérusse L., Bogardus C., Baier L., Mook-Kanamori D., Brage S., Wareham N.J. & Scott R.A. Common European and Transethnic signals for objectively assessed resting energy expenditure provide biological insight (Working Title) (2018) *In Preparation.*

Abbreviations

Common abbreviations and acronyms used throughout this thesis are specified with a brief description below. Other abbreviations are defined on an *ad-hoc* basis throughout the main text.

REE	Resting energy expenditure, the minimum 24-hour energy requirement of a wakeful, fasted adult at complete physical and mental rest
PAEE	Physical activity energy expenditure, 24-hour energy expenditure due to skeletal muscle contraction (volitional and non-volitional)
TEF	Thermic effect of food, the 24-hour uplift in energy expenditure corresponding to post-absorptive digestion of food and assimilation of nutrients
TEE	Total energy expenditure, the sum of REE, TEF and PAEE
HGS	Maximal isometric hand grip strength across both hands, unless otherwise specified
mLOY	Mosaic loss of the Y chromosome
T1D/T2D	Type 1/Type 2 Diabetes Mellitus
GWAS	Genome-wide association study (from array genotyping)
EDTA	Ethylenediaminetetraacetic acid, a preservative used in blood sampling
1000G	1000 Genomes reference panel
HRC	Haplotype Reference Consortium
LD	Linkage Disequilibrium
HLA	Human Leukocyte Antigen complex (Major Histocompatibility Complex) at chromosome 6p21. As specified throughout this document, this region is often discounted from genetic discovery and downstream analyses due to structural complexities
HWE	Hardy-Weinberg Equilibrium
DXA	Dual X-ray Absorptiometry, the gold standard for assessment of compartmentalised and tissue-specific body masses
UKB	UK Biobank cohort
GEFOS	GEnetic Factors for OSteoporosis Consortium
CHARGE	Cohorts for Health and Ageing Research in Genetic Epidemiology Consortium
CARDIoGRAMplusC4D	Coronary ARtery DIsease Genome wide Replication and Meta-analysis plus Coronary Artery Disease Consortia
GIANT	GEnetic Investigation of ANthropometric Traits Consortium
SNP	Single nucleotide polymorphism (usually biallelic)
CI	Confidence interval
MR	Mendelian randomisation
EPIC	European Prospective Study of Nutrition and Cancer
FDR	False discovery rate, at $\alpha \geq 0.05$ unless otherwise specified.

Contents

List of Tables

List of Figures

Chapter 1

Background and Areas of Opportunity

Obesity, type 2 diabetes (T2D) and associated cardio-metabolic disorders are amongst the most pressing of threats to global public health. In 2012, more than a third of adults and 17% of children were clinically obese in the United States[1] on the basis of body mass index (BMI) $\geq$30kg/m^2. This level is rapidly being approached by the United Kingdom and other European countries[2], and represents only the uppermost subset of the considerably larger overweight population. Excess weight (BMI$\geq$25kg/m^2) affects more than half of adults in the US, for example, with the burden concentrated in those of middle and older age[1]. Moreover, obesity and its related conditions are now a truly globalised epidemic as the epidemiological transition sees their prevalence rising rapidly throughout the developing world[3–5]. The burden which these conditions place on quality of life is immense, and their economic and social consequences unsustainable in even the most developed nations[6,7]. There is, therefore, a clear imperative to advance our understanding of their aetiology, with a view to improving translational prevention and management.

1.1 Introduction

Age is an established risk factor for non-communicable disease, but, biologically, individuals age at different rates. Indeed, ageing is a composite of multiple processes which should be considered as separate concepts to chronological age. These domains reflect aspects of biological, physiological and functional ageing which are not adequately summarised by lifespan alone[8–11]. The theorised link between metabolism and ageing extends back many years to the 'Rate of Living' hypothesis - the first to speculate on possible associations between elevated metabolic rate and decreased lifespan[12]. Whilst the major principles of this hypothesis are now considered largely inaccurate[13], later hypotheses - namely that age-

ing is driven by oxidative damage resulting from metabolic production of reactive oxygen species (ROS)[14] - remain central to our concept of ageing[8]. The close relationship between ageing and metabolism is now well established. Data from *in vitro* and *in vivo* models and human populations suggests that ageing is characterised by a range of metabolic alterations, including (i) changes in circulating growth and steroid hormones such as insulin-like growth factor I, (ii) altered body composition as a result of increased adiposity and sarcopenia (age-related degeneration of skeletal muscle), (iii) increased insulin resistance, and (iv) mitochondrial dysfunction[15]. It has been argued that the established cellular hallmarks of ageing universally have important metabolic repercussions, and are major aetiological drivers of age-related metabolic dysfunction[15,16].

In recent years there has been substantial interest in characterising the aetiological role of biological and functional ageing in the development of obesity, T2D, and associated conditions at population level. Biological ageing has most commonly been modelled using leukocyte telomere length (LTL). Telomeres are highly repetitive sequences which cap the ends of chromosomes and play a crucial role in maintaining the stability of genomic DNA[17]. To overcome the 'end-replication problem' - the fact that the end-most sections of genomic DNA cannot be copied in full by the cell's replicative machinery[18] - telomeres are progressively degraded with successive cell divisions until, at a threshold level of shortening, the cell enters senescence[18,19]. Shortening can be observed in humans at population level[20] and, as a combined indicator of both senescence and oxidative stress[21], is conventionally considered a good marker of biological age[11].

Population-based studies have observed a moderate association between lower LTL and obesity[22,23], glycaemic traits and diabetes[24–26] and coronary heart disease[27]; the cross-sectional design of much of this work, however, makes the establishment of causal directionality in the exposure-outcome association particularly challenging. Altered physiological milieu associated with cardio-metabolic outcomes (such as chronic low-grade inflammation or hyperglycaemia), for example, may in fact act as a driver of telomere attrition, rather than the reverse, highlighting the issues raised by confounding and reverse causality when considering LTL as an observational exposure. Studies of alternative ageing metrics such as hand grip strength - a widely used proxy for functional ageing prospectively associated with mortality risk, diabetes and CHD - are inherently prone to the same set of limitations.

Modern genetic methods offer a robust solution to the limitations of observational epidemiology in establishing causality. The principle of Mendelian randomisation (MR) leverages the fact that alleles contributing to variation in a phenotypic trait are randomly and independently allocated at conception, to model genetically-predicted variation in that trait at population level. Given that an individual's allele allocation is fixed throughout the lifespan, and not susceptible to external confounders according to the classical definition of confounding, the association between this genetically-modelled trait and an observed outcome of interest can be interpreted causally. MR and its many extensions have gained traction as an

epidemiological tool in recent years, and are now a widely-accepted method for causal inference.

Mendelian randomisation approaches considering LTL as a causal exposure for cardiometabolic conditions do exist[28,29], and have provided some initial insights into these conditions as downstream effects of biological ageing processes. Sixteen common variants (10 independent loci) for LTL have been identified to date[28], primarily in a large cohort of 48,000 Europeans[30], but further progress in modelling telomere length as a causal exposure will require this instrument to be substantially expanded in order to increase the variance explained, as power in MR is partially a function of the phenotypic variance accounted for by the instrument. A sufficiently expanded discovery effort is precluded by the availability of additional samples with intersecting LTL quantification and genome-wide genotyping. In addition, it could be argued that LTL is a relatively abstract concept in terms of modelling age and, importantly, is non-modifiable. Considering the specific role of other physiological and metabolic correlates of human ageing may allow us to focus more closely on the underlying biology predisposing to metabolic dysfunction.

In this thesis, I present an alternative approach to investigating the role of ageing in cardiometabolic dysfunction, focussing on selected markers of physiological ageing and physical functioning: hand grip strength, resting energy expenditure, and mosaic loss of the Y chromosome, an emerging marker of stem cell dynamics and genomic instability with age. Observational evidence suggests an association between each of these phenotypes and metabolic conditions, but the underlying genetic variants in each case are poorly characterised, and robust establishment of causal direction has so far not been possible. Each trait may also be of relevance as a continuous risk factor in the extended population, not restricted to those of older age.

Using large population-based studies such as UK Biobank, this PhD focusses on new genetic discovery for each REE, HGS and mLOY and applies a range of downstream analyses based on tissue enrichment, expression profiles, and pathway analysis to gain detailed biological insight into each trait. These discovery efforts represent the largest and most informative genome-wide association studies (GWAS) to date for these phenotypes, and allow me to investigate the shared genetic architecture of ageing phenotypes with cardiometabolic traits. As an adjunct to this, I conduct detailed observational mediation analyses to establish whether known genetic variants for BMI exert their effect on adiposity through population-level variation in REE.

Where possible, variants identified are utilised as instrumental variables to allow them to be modelled as causal exposures for cardiometabolic traits, intermediate phenotypes (e.g. continuous glycaemic traits) and other potential outcomes of interest such as mortality, within a Mendelian randomisation framework. To fully detangle the causal direction of the ageing-metabolism association, the role of selected metabolic traits as causal drivers of these ageing traits is also considered.

1.2 Hand Grip Strength

Muscle strength is a key determinant of quality of life amongst the elderly[31,32], an established frailty marker[33,34], and a prospective predictor of physical decline[35,36], functional limitation[37,38] and loss of independence in activities of daily living[38,39] in middle- and older age. Most commonly, limb strength is assessed at population scale and in the clinic using isometric hand grip strength (HGS) - an accessible and readily-applied measure which correlates with other indices of skeletal muscle strength[40,41] including knee extensor force (Pearson's ρ ~0.7). Decreased HGS forms part of the consensus definition of sarcopenia[42] - pathological age-related reduction in muscle mass and function - and, as a commonplace, easily-assessed quantitative indicator of strength, has been suggested as an ideal phenotype to facilitate genetic characterisation of late-life physical functioning phenotypes[43]. Efforts to identify underlying genetic variants have so far been few and far between, despite the commonplace measurement of HGS as a functional phenotype. Various candidate approaches have highlighted the possible role of a handful of genes based on hypothesised biological priors, but GWAS approaches have yet to be applied in sufficiently-powered samples to rigorously implicate variants in a hypothesis-free manner[44].

Lower HGS robustly predicts all-cause mortality[35,45–48] independently of changes in muscle mass, and has recently been characterised as a prognostic indicator of CHD with potential clinical utility in low-resource settings[49]. Strong observational links with age-related morbidity and mortality have strengthened the perception of HGS as a marker of ageing. However, the capacity of HGS to reflect underlying undiagnosed and early pathological processes through reverse causation - for example in the case of diabetes[50–52] and obesity[53,54] - highlights the need to unpick directionality in the association of HGS with health outcomes. Based on data from Scandinavian conscripts, it has also been suggested that - outside the more commonly-studied timeframe of middle and older age - adolescent grip strength may be an important predictor of mortality over the lifecourse[55].

1.3 Resting Energy Expenditure

1.3.1 Definition and Measurement

Resting energy expenditure (REE) is defined as the energy required by a fasted adult to maintain physiological homeostasis and vital functions whilst wakeful, and physically and mentally at rest, in a thermoneutral environment[56–59]. REE corresponds to the baseline minimum energy requirement to sustain life without the additional energy costs attributable to movement or digestion and assimilation of nutrients. It should be differentiated from the basal metabolic rate, which refers to the baseline energy requirement of an individual whilst asleep. Dependent on how sedentary a lifestyle an individual leads, REE contributes around 60% of total daily energy expenditure (TEE)[56], which otherwise comprises energy expenditure resulting from contraction of skeletal muscle (physical activity energy expenditure, PAEE) and the energetic cost of digestion (thermic effect of food, TEF; Figure 1.1). For purposes of thermoregulation, energy may additionally be expended as non-shivering or shivering thermogenesis, which are regarded as subsets of REE and PAEE for most intents and purposes. Taken in the context of total energy intake, REE forms one side of overall energy balance. Intuitive interest in REE as an aetiological factor for weight gain and cardiometabolic dysfunction has been driven by the fact that obesity is a condition of chronic energy balance, and REE constitutes the majority of daily energy expenditure. Its complex association with both body composition and ageing (discussed in detail below) highlights the gains which might be made by genetic characterisation and causal inference of this trait.

The definitive measure of REE is direct calorimetry, which assesses energy use by direct measurement of radiated heat, based on the thermodynamic principle that all energy utilised by endotherms is ultimately lost as heat[60,61]. The accepted gold-standard for assessment of REE in a clinical and research setting, however, is indirect calorimetry: measurement of the relative fractions of inspired and expired O_2 and CO_2 to derive metabolic O_2 consumption (VO_2) and CO_2 production (VCO_2). In turn, these parameters are used to calculate REE according to standard formulae which account for substrate use by calculation of the respiratory exchange ratio ($\frac{VCO_2}{VO_2}$) and correspondingly assign a caloric equivalent to VO_2 based on findings from bomb calorimetry of macronutrients[62].

1.3.2 Non-Genetic Determinants

Age, Sex and Body Composition Nearly a century of research begun by the 1918 work of Harris and Benedict[63] supports the central and highly intuitive role that body size - and composition - plays in the determination of REE. REE is predominantly determined by fat-free mass (FFM)[64,65], is lower in women relative to men[63,66,67], and inversely related to age, independent of sex-related differences in body composition or overall changes in relative fat and fat-free compartments[68–70]. Age-related decreases in REE

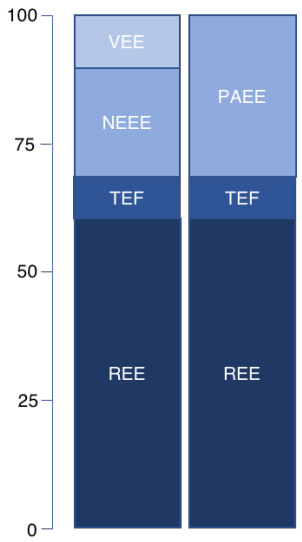

Figure 1.1: Contribution of REE to total daily energy expenditure. REE contributes around 60% of total daily energy needs, dependent on activity levels. The remainder of total energy expenditure comprises the thermic effect of food (TEF) and physical activity energy expenditure (PAEE). PAEE can be split into incidental movement attributable to daily living (Non-exercise energy expenditure, NEEE), and volitional exercise-induced energy expenditure (VEE) resulting from deliberate exertion.

might be explained by changes in the metabolic rate of specific organs over the lifecourse[68], whilst absolute fat mass may also play an important independent role[71], though literature is inconsistent[72]. Effects on REE observed per unit fat mass are considerably less than for FFM, reflecting the known disparity in the metabolic activity of these tissues. For example, in a healthy cohort of 150 adults, Johnstone and colleagues[73] have reported that dual x-ray absorptiometry (DXA)-derived fat-mass explains 6.7% variance in REE ($p<0.01$), in contrast to 63% explained by FFM.

Ancestry REE is lower in black, relative to Caucasian, individuals, independent of body composition[74–76]. A particular body of evidence supports this observation amongst African-American women[77–83], who represent a demographic of special interest due to their disproportionate predisposition to obesity, and increased risk of weight gain[84], for which REE has been hypothesised as an aetiological driver[85]. Lower REE amongst blacks is suggested to be mediated by decreased functional organ mass by comparison to whites[86]. Differences in REE continue to be observed when ethnicity is modelled as a continuous trait. Amongst African-Americans, REE is lower with higher African admixture[87], whilst increased European admixture correlates with increased REE[88], suggesting an underlying genetic component to the ethnic observation.

Stimulants and Alcohol Nicotine is acutely thermogenic[89–91], yet the influence of long-term smoking status is relatively under-studied. Adjusted for body composition parameters, existing work suggests that REE is greater in current relative to never smokers amongst obese African-American[83] and Caucasian[92] populations, albeit in small samples. Most recently, Blauw et al.[93] have replicated this finding in 6,673 Dutch nationals, reporting that elevated REE is restricted to smoking in the current vs. never subcohort, with no continuous effects per pack-year smoked. Similarly, alcohol[91,94] and caffeine[89,95,96] intake are associated with short-term increases in REE, but the effect of habitual intake as a lifestyle exposure

remains to be elucidated. Nonetheless, these correlates highlight the need to ensure that participants in whom REE is measured are free of stimulants and alcohol[57].

1.3.3 Genetic Determinants

Family and twin studies ranging from the mid-1980s to the present[72,97–99] consistently estimate the heritable component of REE at around 30%, yet underlying variants remain uncharacterised. Existing literature for the most part comprises candidate gene studies utilising biologically plausible genes identified by prior work in animal models or high-profile obesity-related genes in humans[100–106]. Though significant gene-REE associations are reported in a number of cases, this work is afflicted by the standard limitations of early candidate gene studies, being underpowered, lacking replication of findings in appropriate independent samples, and accounting for neither key confounders such as body size, age and sex, nor multiple testing.

Whilst hypothesis-free approaches are not altogether absent, they have been of limited value and mostly pre-date the modern GWAS era. Genome-wide linkage studies utilising microsatellite panels have previously been conducted in French Canadians[107], Nigerians[108] and (for baseline metabolic rate as opposed to REE) Pima Indians[109]. The Pima Indian population has also recently provided a modern GWAS for objectively-measured REE[110] (n=507), implicating a variant intronic in *GPR158*. Even this latest effort is notably underpowered for genome-wide discovery, and an absence of replication in comparable populations limits interpretation and highlights the need for further discovery work pooling many thousands of samples with objective assessments of REE.

1.3.4 REE as an Aetiological Factor

The intuitive role of REE in cardiometabolic disease (particularly obesity) is clear, and has generated interest for many decades. A popular historic approach has been to quantify REE in so-called 'post-obese' subjects relative to never-obese controls; such studies report lower REE amongst previously obese participants who have returned to normal weight[111]. These retrospective observational approaches are particularly prone to confounding by 'adaptive thermogenesis'; change in REE corresponding to altered energy intake, which exceeds the change attributable to changes in body composition alone[112–115]. Indeed, negative energy balance at the level required for safe weight loss induces adaptive responses which persist over subsequent periods of weight maintenance[116–118]. Studies reporting lower REE amongst obese relative to normal weight participants[119,120] are liable to reverse causation, even after adjustment for body composition. REE prospectively predicts weight gain during follow-up of American Indians independent of age, sex and body composition[121], and Italians[122] normalised for fat-free body mass, but not amongst a multi-ethnic cohort of American men[123], the largest such study to date. The complex relationship of REE

with body mass, and its vulnerability to confounding and reverse causation, highlight the advances which might be made through the application of techniques for robust causal inference.

1.4 Mosaic Loss of Y Chromosome

Of the three main phenotypes considered within this thesis, mosaic loss of Y (mLOY) has the least developed body of literature concerning a possible aetiological role in cardiometabolic dysfunction; but, as an outcome of genomic instability, has a strong theoretical basis as an ageing phenotype[8].

mLOY is a post-zygotic aneuploidy acquired during the lifecourse, and involving complete loss of the Y chromosome in a proportion of somatic cells, resulting in genomic mosaicism for the Y chromosome. mLOY constitutes one of a wider set of post-zygotic variations with relatively high prevalence at population level, which are increasingly recognised as of relevance to disease processes[124]. Described for many decades[125,126], Y mosaicism in peripheral blood is the most common chromosomal aneuploid event in humans by an order of magnitude and is strongly associated with age. More than one fifth of men aged >80 years had detectable Y mosaicism in peripheral blood in a recent study, though mLOY of some extent is commonly observed from middle age onwards[127]. Y loss represents a binary event at the cellular level (lost/retained), but can be expressed as a proportion of affected blood cells at the individual level[128], using fluorescence estimates of Y chromosome abundance from standard genome-wide genotyping arrays. The high prevalence of mLOY clearly demonstrates that peripheral blood cells are able to survive in the absence of the Y chromosome, and offers a unique scenario in which a severe chromosomal defect is able to be observed and quantified at population scale in apparently healthy men.

Whilst conventionally considered an innocuous age-related phenomenon rather than an aetiologically-significant factor for health[129,130], the recent recognition that greater mLOY is associated with prospective risk of Alzheimer's disease[127], non-haematological cancers[131–133] and mortality[131] has ignited interest in mLOY as both an important biological correlate of ageing, and an independent exposure for disease risk[124,128]. Large-scale autosomal mosaicism has also been associated with cardiovascular outcomes amongst people with diabetes[134], highlighting the potential aetiological importance of mLOY in cardiometabolioc dysfunction. However, the fact that mLOY is a post-zygotic mutation and consequently subject to confounding in the same way as any other observational exposure - for example by behavioural factors such as smoking[135] - prevents robust examination of mLOY as a causal exposure for these traits in current work.

The ease with which mLOY can be assessed, and the fact that it can be derived from existing large scale genome-wide genotype data, makes it a particularly attractive phenotype for future work, and particularly for very large scale genetic discovery. Identification of *autosomal* variants underlying mLOY in men may provide fundamental insights into the common biology of genomic instability in both sexes, and its intersection with disease risk, whilst allowing the significance of chromosomal mosaicism as an age-related causal disease exposure to be formally assessed.

1.5 Summary of Rationale and Objectives

The rationale and areas of opportunity for this thesis can be summarised as follows:

1. Ageing is a complex and multi-factorial exposure which is inherently of interest in disease risk, and is closely associated with obesity and related cardiometabolic dysfunction.
2. Understanding the directionality of ageing as an exposure or outcome of disease will have translational benefit.
3. Hand grip strength, resting energy expenditure, and Y chromosome mosaicism each represent different functional and biological aspects of ageing, and are observationally implicated in the aetiology of cardiometabolic disease either directly or (in the case of mLOY) through related phenomena.
4. Considering these wider functional and biological phenotypes of ageing will allow relevant biology and physiology to be more closely interrogated, and will facilitate the study of these phenotypes as exposures for disease in the wider population, and outside the immediate context of ageing.
5. Standard observational approaches preclude causal inference given their liability to reverse causation and confounding.
6. Mendelian randomisation offers a solution robust to these limitations.
7. Highly-powered and informative genetic discovery efforts for HGS, REE and mLOY are absent in the literature, and will provide new and valuable insights into the biology of these traits.

Through application of genome-wide discovery efforts in very large-scale population-based data including UK Biobank and very deeply phenotyped cohorts such as the Fenland Study, this thesis will characterise common genetic variants underpinning variation in these phenotypes. Detailed downstream analyses will be used to prioritise genes at identified loci and to maximise biological insight. Variants implicated will be applied as instrumental variables to facilitate causal inference of each phenotype on key cardiometabolic outcomes and intermediate traits, and allow the directionality of known observational associations to be examined under a bidirectional Mendelian randomisation framework.

Chapter 2

Major Data Sources and Common Methods

2.1 Cohort Studies

The work presented in this thesis utilises large observational cohorts as the principal data source for genetic discovery and associated analyses. Whereas cohorts used for replication and functional insight or follow-up vary between chapters, and dependent on the availability of necessary phenotype data, a core of studies are common throughout. Brief procedural details of these cohorts - particularly the genotyping, quality control and imputation protocols for extracted DNA - are provided here. Elements of the study which are particularly salient to certain chapters (such as the assessment of chapter-specific phenotypes) are discussed more fully in the relevant chapter.

2.1.1 UK Biobank

First conceptualised in the early 2000s as a joint venture of the UK Medical Research Council and the Wellcome Trust[136,137], UK Biobank (ukbiobank.ac.uk) is a large population-based observational cohort designed to facilitate highly-powered research of the aetiology and mechanisms of chronic disease, with a particular focus on genetics[138,139]. The study contains more than 500,000 British participants who have provided a broad range of health data at high resolution, including biological samples (blood, saliva, urine), detailed physiological and anthropometric measures, and information on lifestyle factors. Most recently, in collaboration with a UK-wide working group, UKB has delivered objective assessments of cardiorespiratory fitness and physical activity from triaxial wrist-mounted accelerometry in nearly a fifth of its participants. Additionally, the study is integrated into the reporting frameworks of the UK National Health Service (NHS), for automated and ongoing linkage and ascertainment of healthcare events, outcomes and mortality. UKB has the particular distinction of being fully open access for research undertaken in the public interest.

Recruitment and Initial Assessment

Between 2006-2010, a total of 503,325 middle- and older-aged (40-69 years) British residents were recruited from centralised NHS primary care registrations. Upon enrollment, participants attended an initial assessment visit at one of 22 centres located throughout England, Scotland and Wales, during which a comprehensive catalogue of anthropometric, physical, lifestyle and behavioural exposures were assessed, and biological samples (blood, urine and saliva) were drawn. UK Biobank provides a centralised catalogue of data collected, and detailed protocols for each variable, on its Data Showcase (ctsu.ox.ac.uk/crystal). Overarching protocols for the study have been described previously[139]. Briefly, UKB used a touch screen-delivered questionnaire to initially assess lifestyle factors including diet (food frequency questionnaire, FFQ) and habitual physical activity (modified short-form Recent Physical Activity

Questionnaire, RPAQ[140]), self-reported medical history, psychosocial factors and sociodemographics, as well as cognitive function. Aspects of this touch screen questionnaire were clarified and expanded upon during a personal interview with trained personnel. Basic physical measures - for example heart rate, blood pressure, bone mineral density, hand grip strength and anthropometric phenotypes (e.g. height, weight) were assessed by a research nurse using standard equipment, and blood samples were drawn. Participants provided their own urine and saliva samples whilst at the assessment location. Standardisation of assessment by reference to centrally-issued standard operating protocols was mandated by UKB to minimise random and systematic error, and optimise comparability of measures across the network of research staff and assessment centres within which the study operated. All participants provided informed consent at the start of their assessment visit. UKB attained ethical approval from the UK National Research Ethics Committee North West and was conducted in full compliance with the principles of the World Medical Association Declaration of Helsinki. A relatively low response rate of 5.5% during recruitment[141] (likely due to the untargeted, systematic canvassing of eligible individuals within certain geographic locale, and high participant burden of enrolment by contrast to some other cohorts) means that UKB demonstrates a degree of healthy-volunteer effect, and should not be interpreted as a representative sample of the UK population (see Chapter 7). Such limitations, however, do not preclude valid and generalisable assessment of epidemiological associations if there is sufficient variability in phenotypes within the cohort.

Anthropometric measures Weight was measured as part of bioimpedance assessment using a BC418MA Body Composition Analyser (Tanita Europe BV, Amsterdam, the Netherlands), with the participant dressed in light clothing. Standing height was measured on a rigid stadiometer (Seca, Birmingham, UK).

Genetic Data

The analyses presented in this thesis primarily use imputed data from UKB's interim genotyping release (May 2015), restricted to biallelic SNPs with MAF $\geq$0.1%. This release covers approximately the first 30% of the cohort; the remaining participants were released in July 2017, however, this largely fell outside the timeframe available for analysis within the scope of this PhD. Genotyping and imputation were conducted using a central pipeline in collaboration with industrial and academic partners, and overseen by UKB.

DNA Extraction and Genotyping To ensure the preservation and long-term stability of biosamples, UKB devised and applied a standardised sample-handling protocol for blood encompassing prescribed procedures for the sampling process itself and initial handling at the assessment location, followed by temperature-controlled shipping to central -80°C and -196°C archives across primary and back-up sites[142].

DNA was extracted from EDTA buffy coat using standard approaches with a particular focus on between-batch consistency before shipping to Affymetrix Research Services (Santa Clara, CA) for centralised genotyping. Samples were genotyped at >800,000 loci on one of two custom-configured arrays (UK Biobank Axiom array or UK BiLEVE Axiom array) with 95% common content designed to optimise the quality and quantity of variants for imputation, whilst directly genotyping selected exome content and rare coding variants.

Imputation After restriction to biallelic SNPs with MAF $\geq$0.1 and additional genotyping quality control, including the removal of SNPs with missing data, multiallelic variants, and 1,037 sample outliers, a subset of 641,081 autosomal SNPs from 152,256 samples were available for imputation, which was conducted centrally on behalf of UK Biobank at the Wellcome Trust Centre for Human Genetics, University of Oxford. SNPs were pre-phased using SHAPEIT3 software[143], and imputed (using a modified version of IMPUTE2) to a merged reference panel containing combined haplotypes from the UK10K consortium[144] and 1000 Genomes consortium, Phase III[145]. This approach has previously been shown to provide a high quality imputation reference in populations of mixed ancestry[143]. Full details of the genotyping and QC protocol applied (biobank.ctsu.ox.ac.uk/crystal/docs/genotyping_qc.pdf), and the phasing and imputation approach (biobank.ctsu.ox.ac.uk/crystal/docs/impute_ukb_v1.pdf) are available centrally from UKB.

Subsetting Unrelated Europeans To account for relatedness and population structure within the genotyped sample, UKB centrally defined a subset of unrelated European participants which complied to a strict white European genetic ancestry based on principal components analysis, and were free of overt relatedness. This subsample was used in sensitivity analyses and methods within which population structure could not otherwise be accounted for, as indicated throughout.

Box 2.1 | Fenland Study: *A priori* exclusion criteria

- Clinical diagnosis of diabetes mellitus
- Terminally ill with prognosis of less than one year
- Suffering from a psychotic illness
- Pregnant or breastfeeding
- Unable to walk unassisted

2.1.2 The Fenland Study

Coordinated from the MRC Epidemiology Unit, Cambridge, phase one of the Fenland study (Fenland) is a population-based cross-sectional cohort designed to enable enhanced investigation of the joint and separate effects of genetic and lifestyle factors on intermediate traits relevant to T2D, obesity, and related metabolic disorders. To achieve this, the study combines large sample size with very complete and detailed phenotyping, with a particular focus on metabolic profiling and the assessment of continuous intermediate traits which offer power advantages for analysis and interpretation, by comparison to binary disease classifications. Fenland was the first cohort to implement truly population-scale assessment of objective resting energy expenditure by indirect calorimetry as a standard element of the baseline visit, and remains unique in the volume of calorimetry data it holds.

Recruitment and Initial Assessment

Over the course of ten years from 2005, 12,342 British adults aged 30-55 years were recruited from NHS primary care practice lists in Cambridge and rural Cambridgeshire, and attended an initial assessment visit at one of three MRC Epidemiology Unit field centres located in Wisbech, Ely or Cambridge. To facilitate robust study of the early pathogenesis of chronic conditions before clinical intervention or confounding by comorbidities, recruitment was focussed on younger and middle-aged participants free of pre-existing conditions. Potential participants were identified by their general practitioner and approached for inclusion (n=46,020; 27% response rate). Individuals were excluded from further consideration if they fulfilled any one of the criteria outlined in Box 2.1.

Anthropometric Measures Extensive compartmentalised body composition was obtained by dual x-ray absorptiometry (DXA), the *de facto* gold standard. Compartment-specific (fat, lean, bone) masses were measured on a Lunar Prodigy device (GE Healthcare, Buckinghamshire, UK), processed using proprietary software, and manually partitioned into trunk and peripheral compartments. Total body weight was measured using callibrated scales, and standing height using a rigid stadiometer.

Indirect Calorimetry Participants were requested to fast and refrain from intake of thermogenic stimulants (caffeine, nicotine) from 22.00 on the evening preceding their assessment. Indirect calorimetry was assessed approximately one hour into the visit; in the intervening time, participants had generally been sedentary and physically at rest. With the participant fully reclined, open-circuit indirect calorimetry (Jaeger Oxycon Pro, CareFusion) was assessed for six consecutive minutes using continuous flow (breath by breath) sampling. The participant breathed normally through a fitted facemask, and remained wakeful, still and quiet throughout. Live output was monitored by trained research personnel throughout to ensure data quality. Observed oxygen consumption (VO_2) and carbon dioxide elimination (VCO_2) were cleaned and applied to derive resting energy expenditure (kcal/day) by a standardised protocol using established formulae based on the calorimetric equivalents of the cardiorespiratory parameters. Full details of this process are provided in Chapter 4).

Genetic Data

DNA was extracted from EDTA whole blood by standard technique at Whatman Biosciences (Cambridge, UK), and array-genotyped at the MRC Epidemiology Unit on one of three commercial platforms; the majority on the UK Biobank Axiom array (Affymetrix) utilised for UK Biobank's centralised genotyping effort (n=9,368), or, alternatively, on Human Genome-wide SNP 5.0 (Affymetrix, n=1,402) and Infinium CoreExome-24 (Illumina, n=1,664) arrays. Standard proprietary calling algorithms were used. After sample quality control (sample call rate $\geq$95%, heterozygosity thresholds), and omission of variants demonstrating deviation from Hardy-Weinberg equilibrium ($p_{HWE}=5\times10^{-6}$), variants were imputed (IMPUTE2) against 1000G Europeans. The exact 1000G version applied for imputation purposes varied by array and date of imputation.

2.1.3 EPIC-Norfolk Subcohort

EPIC-Norfolk is one of the two UK-based subcohorts contributing to the European Prospective Study on Nutrition and Cancer (EPIC), a multi-centre prospective cohort totalling 500,000 participants throughout ten Western Europe and Scandinavian countries[146]. EPIC was established in 1989 with the objective of investigating the role of diet, lifestyle and environment in the development of chronic conditions, with a particular focus on cancer. With detailed phenotyping spanning multiple prospective timepoints, EPIC and each of its sub-cohorts have become valuable resources for chronic disease epidemiology and the exploration of genetic risk.

Recruitment and Initial Assessment

EPIC-Norfolk[147] comprises 25,639 British adults aged 40-79 years, recruited from general practice lists (n=35) in Norwich and surrounding Norfolk between 1993 and 1997. All registered individuals in the prescribed age range were canvassed for participation unless flagged as unsuitable by the practitioner: of the 77,630 approached, 30,445 consented to participate, and 25,639 were ultimately enrolled[148], a response rate of 33%. Participants attended a initial first health-check (1HC) upon recruitment, during which a standard range of anthropometric and physical measures were taken, lifestyle exposures were assessed and blood was sampled. Since the first health check, participants have routinely been invited to re-attend for assessment on two occasions; three, thirteen, and twenty years after their initial baseline assessment. Given its relatively static population and the oversight of care provision by one NHS Trust, Norfolk was selected as the recruitment setting with the intention of minimising participant attrition and maximising outcome ascertainment over decades of follow-up; full details of participant response rates and characteristics between health checks have been published previously[148]. The assessment process in subsequent health checks retains the standard elements of the baseline visit but has been expanded and developed to include new measures with time. For example, assessment of hand grip strength as an important indicator of overall strength with aging was introduced in the third health check (3HC, n=8,623, response rate of 46.9% amongst the 18,380 surviving individuals consented before 1HC, who had not previously withdrawn consent or been lost to follow-up[148]). The third health check is the primary source of data for this thesis. There was approximately equal attrition of men and women from the study between 1HC and 3HC, but those attending both 3HC and 1HC were significantly younger, leaner, more educated, of higher socioeconomic status, more physically active, and less likely to smoke that those who attended 1HC alone[148], highlighting a healthy cohort effect which becomes more pronounced throughout the course of follow-up.

Anthropometric Measures With the participant dressed in light clothing and barefoot, weight was measured to the nearest 0.2kg using a digital scale (Salter, UK), and standing height (nearest mm) with a rigid stadiometer[147].

Genetic Data

DNA was extracted from EDTA buffy coat using standard methods. Samples were genotyped at >800,000 SNPs on the UK Biobank Axiom Array (Affymetrix) at the MRC Epidemiology Unit. After removal of SNPs failing Hardy-Weinberg equilibrium ($p \leq 5 \times 10^{-6}$), variants were pre-phased (ShapeIT v2.r790) and imputed (IMPUTE v2.3.13) to 1000G Phase III individuals (October 2014).

2.2 Methods

Each of the chapters of this thesis follow a broadly similar analytical trajectory comprising genetic discovery, followed by independent replication of variants where appropriate data are available, and downstream analyses to (i) provide biological insight (ii) infer causality, and (iii) investigate shared genetic architecture. In the interests of brevity and to reduce duplication of content, the methods applied commonly within this analytical pipeline, including detailed discussion of their rationale and context, are provided as a single point of reference here. Details of methods which do not fall into this overarching pipeline of genetic discovery and application (for example derivation and measurement of chapter-specific phenotypes) are outlined in each chapter, as are specific analytic details which vary between cohorts and analyses.

2.2.1 Genetic Discovery and Meta-Analysis

Linear Mixed Models

Linear mixed models (LMMs) offer a robust solution to handle confounding arising from sub-ethnic population stratification and cryptic relatedness in genome-wide association studies, and confer power advantages in large population-based cohorts[149]. Discovery analyses presented in this thesis were preferentially run using LMM implemented in BOLT-LMM (v2.2). Primary analyses assumed additive (per-allele) effect and were restricted post-analysis to biallelic variants with MAF$\geq$0.1% and imputation quality (IMPUTE 'info' parameter) $\geq$0.4. Independent loci were defined on the basis of physical proximity, using a 1mb window centred on the index SNP (i.e., 500kb flanking each side). For replication cohorts and meta-analytical discovery approaches (e.g., REE discovery, Chapter 4) used in this thesis, SNP associations were most commonly calculated externally, and therefore used a range of approaches and softwares aligned with the collaborators' usual analysis pipeline. External study-specific methods are detailed on a chapter-by-chapter basis.

Heritability Estimation

Unless otherwise specified, narrow-sense heritability (h^2) was estimated using a Restricted Estimate Maximum Likelihood variance components analysis implemented in an extension of the algorithm used for main association analyses, BOLT-REML (v2.2). This approach is based on the same principles as conventional methods of heritability estimation such as genomic-relatedness-based restricted maximum-likelihood approaches[150], but incorporates speed enhancements when working with large datasets[151]. As an alternative for meta-analytical discovery samples combining data from multiple cohorts, heritability was estimated using LD Score Regression[152–154].

Distinguishing Inflation from Polygenicity

Genomic inflation provides an indication of residual population stratification present in GWAS, and is conventionally expressed as a genomic control factor (λ_{GC}); the observed divided by the expected median of the χ^2 distribution[155,156]. This value can be used to assess the degree of residual confounding from population structure, and to correspondingly correct the genome-wide test statistics. Given that apparent inflation of λ_{GC} can, however, be attributable to complex polygenicity of the trait[157], the intercept from LD Score Regression (LDSC) has recently been suggested as a measure of inflation robust to this effect[154]. We calculated both the standard λ_{GC} and LD score regression intercept using recently-described LDSC software (v1.1.0), based on pre-calculated European LD scores[154] derived using the 1000G European subset. To avoid confounding by imputation quality, calculations were restricted to variants available in Hapmap Phase III, as recommended by the program developers. Statistically significant inflation was defined on the basis of a significant LD score regression intercept at $\alpha \leq 0.05$, and summary statistics were adjusted manually for the intercept point estimate in such cases. Details are provided on a case-by-case basis throughout.

Meta-Analysis

When (i) generating a combined discovery sample or (ii) calculating combined p-values for stage one variants replicated in external (European) cohorts, variants were meta-analysed using a fixed-effects, inverse variance-weighted approach implemented in METAL[158]. Genomic control factors (defined as the intercept from LD-Score Regression) were applied during the meta-analysis process, if required. Given that a standard fixed-effect is underpowered for meta-anlysis of estimates across ethnically-discordant groups[159], specific methods developed to maximise power in transethnic analyses were applied where necessary, as discussed in Chapter 4.

Linkage Structure and Secondary Signals

To examine local LD structure, regional plots were generated in LocusZoom[160] using LD reference values from 1000G Phase I Europeans. To investigate the presence of multiple independent signals at a locus as appropriate, conditional analyses were run on each discovery locus prior to replication. Using approximate conditional analyses in Genome-wide Complex Trait Analysis[161,162] (GCTA, v1.25.3), variant p-values at each locus were conditioned on the genotype of the index variant and their conditional p-values re-examined using the genome-wide threshold to define the presence of a secondary signal.

2.2.2 LD Score Regression

Using genome-wide summary statistics from discovery (either in UKB alone or meta-analysed discovery in the case of REE), the LD Score Regression method recently described by Bulik-Sullivan and colleagues[154] was applied, as appropriate, to (i) estimate genetic correlation between the trait of interest and other phenotypes and (ii) derive tissue-specific partitioned heritability of traits based on pre-calculated European LD scores. To avoid confounding by imputation quality, all LDSC analyses were restricted to variants available in HapMap Phase III.

Tissue-specific Partitioned Heritability

Partitioned heritability can provide an indication of whether certain cell types are enriched for functional gene categories which disproportionately contribute to the heritability of a phenotype[163]. In this way, over-represented effector tissues important within the aetiology of the phenotype can be identified. LDSC is distributed with eight curated tissue classes, each of which contain functional categories of variants which act in a manner specific to that tissue. Partitioned heritability analyses were run separately for each tissue class, adjusting in each case for heritability explained by each functional category of variants across the genome (that is, in a non-tissue-specific manner). A Bonferroni-corrected p-value accounting for eight tests was used to define statistical significance.

Genetic Correlations

To gauge the shared contribution of variants across the genome to the trait of interest (e.g. hand grip strength) and other phenotypes, we calculated genetic correlations (r_G) from LD score regression[153]. Analyses were run using either the standalone LDSC executable or the LD Hub facility[164], a web application which aggregates published genome-wide summary statistics from large consortia, for rapid calculation of r_G). Correlations were run in a hypothesis-free manner restricting to potentially correlated traits of biological relevance, and using a Bonferroni-corrected p-value adjusted for the number of independent tests to define significance. Exact details are provided in each chapter.

2.2.3 Imputed Transcriptome Analyses

To explore the potential functional significance of variants in gene expression, and to prioritise functional genes falling within identified loci, a number of variant- and gene-centric expression analyses were undertaken. Initially, lead variants (or their best proxy, $r^2 \geq 0.8$) were looked up in cell types relevant to the trait (see Chapter methods) in the GTEx resource[165] to identify *cis*-eQTL associations. Variants passing

GTEx criteria for tissue-specific eQTL association, and additionally high LD ($r^2 \geq 0.8$) with the best eQTL for the transcript in question in the tissue of interest were considered eQTLs.

To supplement this variant-centric approach, three new methods for integrating genome wide summary statistics with expression associations from independent samples were applied: TWAS, SMR and MetaXcan. By utilising established eQTL data sets as reference, these approaches are able to effectively model expected variation in the transcriptome of the GWAS sample based on variation in autosomal variants across the genome (genetically-predicted gene expression, GPGE), and subsequently test for independent associations between imputed transcript levels and the phenotype of interest.

SMR Summary Mendelian Randomisation (SMR) uses summary-level gene expression data to map potentially functional genes to trait-associated SNPs[166], and investigate whether trait associations at a locus are driven by differential expression, under the assumption of a single causal variant/eQTL. Using publicly-available whole blood eQTL data from Westra and colleagues[167], we tested for associations between transcript abundance in whole blood and our GWAS traits. A conservative significance threshold was set at $p=4.9\times10^{-6}$, reflecting the number of transcripts tested.

TWAS The recently-described Transcriptome-wide Association Study (TWAS) approach[168] was used to infer gene expression associations in whole blood data sets (Young Finns Study and the Netherlands Twin Registry cohorts). The threshold for significance was set to correct for the number of studies and genes ($p=1\times10^{-5}$).

MetaXcan MetaXcan, a meta-analysis extension of the PrediXcan method[169] modified to take summary statistics as input in place of individual-level data[170], was used to infer associations between tissue-specific genetically-predicted gene expression (GPGE) derived from GTEx[165], and GWAS traits considered in this thesis. PrediXcan is a gene-based data aggregation and integration method which incorporates data from observed gene expression and GWAS to translate evidence of association between a phenotype and a variant to the gene level. Briefly, PrediXcan first imputes gene expression at an individual level using prediction models trained on directly-measured transcriptomic data sets with intersecting genome-wide genotyping, before regressing the phenotype of interest on imputed GPGE. MetaXcan extends the application of PrediXcan to allow inference of the direction and magnitude of GPGE-phenotype associations using only GWAS summary statistics, which is advantageous when SNP-phenotype associations are obtained from meta-analysis, and when individual-level data are not available. Pre-calculated tissue-specific expression prediction weights generated from GTEx were downloaded from the PredictDB resource (http://predictdb.org/) as transcriptome reference. Tissue-specific analyses were run, restricting to tissues selected on the basis of biological relevance to the trait under consideration. The threshold for

statistical significance was conservatively set using a Bonferroni correction considering each gene-based association in each tissue as a separate and statistically independent test. Further details on the selection of tissues, and corresponding Bonferroni thresholds, are supplied in each chapter.

2.2.4 Pathway Analyses

Trait associations across the genome were tested for enrichment of genes falling within known biological pathways, or sharing common functional annotation using the Meta-Analysis Gene set ENrichment of varianT Associations (MAGENTA). By using pre-specified gene set definitions as reference, MAGENTA applies a gene set enrichment analysis (GSEA)-based approach which has been previously described[171].

Briefly, each autosomal gene is mapped to a single index SNP, defined as the SNP with the lowest association p-value within a 100kb upstream and 40kb downstream window. After adjustment for possible confounders including gene size, SNP density and LD, this p-value (which represents a gene score) is ranked relative to all scored genes in the genome. At a given significance threshold (95^{th} or 75^{th} percentile), the observed number of gene scores ranked above the threshold in a given pathway is calculated and compared to the expected number of gene scores above this threshold under a null hypothesis, based on the distribution of one million randomly-permuted pathways of identical size. This process generates an empirical permutation-based GSEA p-value for each pathway.

Enrichment was assessed in a hypothesis-free manner across gene sets drawn from six public databases of gene ontology (GO), functional annotation and canonical or curated pathways: GO Terms, the Protein Analysis through Evolutionary Relationships (PANTHER) database, Ingenuity, the Kyoto Encyclopaedia of Genes and Genomes (KEGG), Biocarta, and Reactome pathways (downloaded *via* the Molecular Signatures Database, mSigDB, July 2011). Analyses were restricted to 3,216 gene sets with an effective size $\geq$10 genes after filtering of proximal genes and genes not containing variants for analysis. Genes in the HLA region were excluded due to difficulties in accounting for gene density and linkage structure. For some phenotypes, custom gene sets of particular biological or mechanistic relevance were additionally defined and tested. Details are provided on a chapter-by-chapter basis. Pathway significance for hypothesis-free tests was defined using a FDR$\leq$0.05 at either threshold, considering each pathway as a statistically independent test. In hypothesis-driven gene set testing, a pathway GSEA p-value accounting for the number of candidate pathways tested was applied.

2.2.5 Gene-based Association

By aggregating the contribution of multiple variants within a gene to variation in a phenotype, gene-based testing is can be used to prioritise genes from genome-wide summary statistics. Against the

Box 2.2 | Assumptions of Mendelian randomisation

1. The instrument is robustly associated with the exposure
2. The instrument is associated with the outcome only *via* the modeled exposure
3. The instrument is independent of factors confounding the observational association between the exposure and the outcome

backdrop of a lower burden of correction for multiple-testing, genes containing multiple associated variants which do not exceed the genome-wide threshold for significance can be highlighted. Such approaches have previously been shown to be effective when considering protein-coding variation in exome-based analyses[172], and are widely used to assess candidates of particular biological interest in GWAS summary statistics. Recently, and with the release of packages to streamline the analytic process[173], application of systematic gene-based testing across the genome (genome-wide gene association study, GWGAS) using summary statistics has increased substantially, particularly in very large-scale studies such as UKB[174–177]

In these analyses, a combination of these two approaches were applied. For hypothesis-driven investigation of gene associations, the VErsatile Gene-based Association Study (VEGAS) algorithm[178] was used, calculating LD from HapMap Europeans and restricting to directly typed and well-imputed (info$\geq$0.8) variants. For GWGAS, we applied the newly-described MAGMA permutation-based approach[173], using 1000G Phase 3 as the LD reference. In all cases, conservative Bonferroni correction accounting for the number of tests run, and assuming all tests were independent, was used to account for an $\alpha \leq 0.05$.

2.2.6 Mendelian Randomisation

Mendelian randomisation (MR) provides a solution to circumvent many of the issues of confounding and reverse causation which can affect the robust inference of directionality and causality in classical observational epidemiology. Conceptualised as a 'natural randomised trial'[179] (Fig 2.3), MR applies Mendel's first and second laws (that alleles independently segregate during meiosis and are randomly assigned at conception) to model genetically-predicted variation in an exposure using variants as a genetic instrument. As alleles are fixed for the lifespan, and therefore cannot in theory be confounded by known or unknown factors, associations between the instrument and an observed outcome can be interpreted causally, given that assumptions hold[180,181] (see Box 2.2, Fig 2.3).

Constructing Scores

Additive genetic risk scores were calculated as the sum of aligned (e.g. effect-increasing) alleles at SNPs associated with the exposure, and expressed as either (i) a per-allele score or (ii) a weighted score. For the latter, each allele dosage was weighted by its effect on the exposure, allowing the effect of the

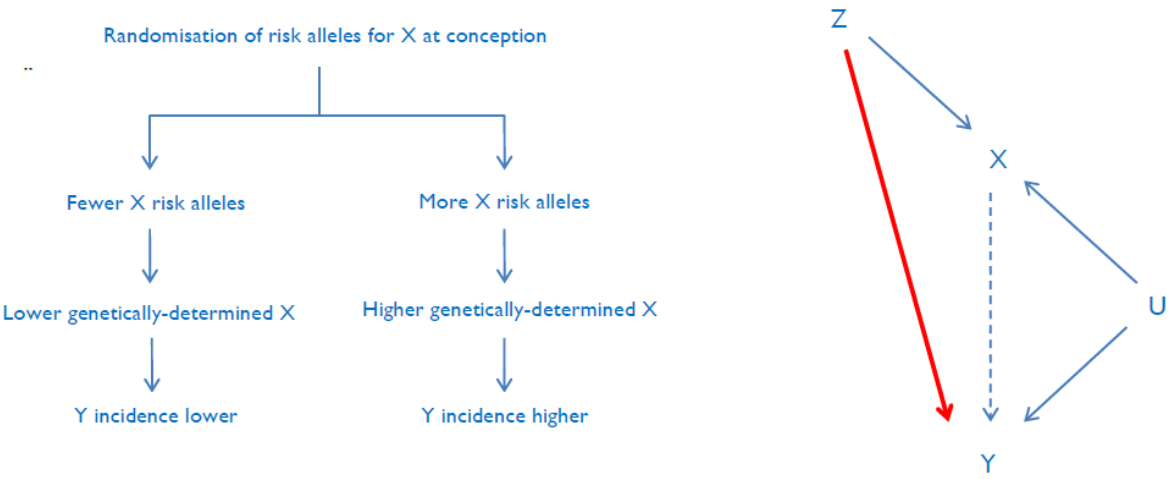

Figure 2.3: Concept and theory of Mendelian randomisation. *Left:* MR is conceptualised as analogous to an intervention-based RCT. Random assignment at conception of risk alleles for the exposure, X, leads to variation in genetically-determined levels of X within the population, for which altered phenotypes in the outcome Y can be observed. *Right:* Under observational epidemiology, the association between an exposure X and an outcome Y is subject to known, unknown, and residual confounding (U). When genetic variants associated with X can be used as an instrumental variable Z, the direct relationship between Z and Y (red arrow) is theoretically unconfounded and, subject to the assumptions of MR, can be used to infer causality in the X-Y association. After Hingorani & Humphries[179], Lawlor *et al.*[180]

instrument to be interpreted per genetically-predicted change in the exposure. Effect weights were most commonly drawn from combined stage one + two analyses. Further details follow in the Methods sections of each chapter. Scores were restricted to variants passing the genome-wide threshold for significance to minimise the risk of pleiotropy and weak instrument issues.

Main Analyses

We applied two-sample MR, in which causal associations are investigated in a second sample independent of the population used to derive the genetic risk score[182,183]. Where outcome and genotype were available in an intersecting sample, MR was implemented using individual participant data (IPD) in an appropriate study cohort with the required phenotypes available, regressing the outcome on individually-derived genetic scores. For the most part, however, we applied the recently-described summary statistic approach, which extends the two-sample approach to leverage summary data of the score-exposure and score-outcome association[184,185]. The score-outcome effect is regressed on the score-exposure association for each variant, and the resulting β provides an indication of the overall causal estimate. Given that summary statistics can be sourced from publicly-available consortium meta-analyses representing the largest possible sample size for many traits, the range of outcomes and exposures for causal inference is substantially expanded. Assuming that the outcome and exposure associations are drawn from ethnically- and demographically-similar populations, summary statistic MR increases power whilst minimising the risk of a false positive due to weak instrument bias[183]. Bias from weak instruments shifts the estimate toward the null in this context (i.e. it is conservative), in contrast to one-sample approaches, in which weak instruments artificially inflate the causal estimate.

Summary-statistic MR was implemented using either in-house scripts, or the MR-Base two-sample MR package for R[186], which streamlines the process of extracting exposure or outcome data from published summary statistics, aligning alleles between the exposure and outcome, and identifying suitable proxies for instrumental variants. Where effect estimates were drawn from consortia meta-analyses, full details are provided in each chapter. Inverse variance-weighted (IVW) regression was applied as the standard model. This approach weights the regression at each variant by the precision of its effect on the outcome, and thus ensures that the contribution of each variant to the overall causal estimate is decreased where there is increased error in its causal estimate. Where a variant was not available in outcome summary statistics, we used its nearest proxy ($r^2 \geq 0.8$) defined from 1000G using either LDLink[187] (https://analysistools.nci.nih.gov/LDlink/) or the in-built functionality of MR-Base.

Sensitivity Analyses

Amongst the assumptions required for an MR to be valid and informative, only the first (robust association between the instrument and the modelled exposure) can be tested directly. Approaches to indicate whether an assumption may have been violated, and to mitigate for it in sensitivity analyses, are available, as detailed below. These stages were pursued only when MRs indicated a statistically significant result (accounting for multiple testing), based on IVW estimation.

Directional Pleiotropy Horizontal pleiotropy - when a variant is associated with an outcome via multiple biologically heterogeneous pathways - can lead to violation of assumptions in MR, specifically if the combined pleiotropic effect of a score is directional[183]. Directional pleiotropy occurs when there is residual association between the gene score and the outcome, which persists after the effect of the score on the exposure has been accounted for, implying that the residual effect acts through pathways external to the modelled exposure[188]. Under this situation, the causal estimate from MR is biased away from the null. To circumvent possible issues of directional pleiotropy in our instruments, we applied MR-Egger[189], a modification of Egger's regression[190] which relaxes the strict set of assumptions normally required for IVW MR, and does not restrain the intercept to the origin. By allowing variants to violate the second assumption of MR (Box 2.2), the intercept generated by MR-Egger provides a formal assessment of directional pleiotropy, and the corresponding β indicates a causal estimate robust even if all variants in the score influence the outcome through directionally pleiotropic pathways.

Multiple Invalid Instruments To allow for a situation in which some variants violated more than one assumption of MR, a weighted median approach was applied[191]. By weighting the causal estimates toward their median, this approach provides consistent causal estimates when as many as 50% of the variants in a score violate the second or third assumption of MR.

Chapter 3

Using Genetics to Investigate the Causal Relationship between Ageing and Hand Grip Strength

Chapter Published as

Willems S.⋆, **Wright D.J.**⋆, Day F.R⋆, Trajanoska K.⋆, Joshi P.K. *et al*. (2017)
Large-scale GWAS identifies multiple loci for hand grip strength providing biological insights into muscular fitness. Nat Commun. *8*, DOI: 10.1038/ncomms16015

And contributes to:
Trajanoska K.⋆, Morris J.A.⋆, Oei L.⋆, Zheng H.⋆ . . . **Wright D.J.** . . . *et al.* (2017)
Leveraging genetic associations to evaluate clinical risk factors for osteoporotic fractures. New Eng J Med (submitted, in review)

Hand grip strength is a widely-used proxy of muscular fitness, a marker of frailty and predictor of a range of morbidities and all-cause mortality. To investigate the genetic determinants of variation in grip strength, we performed a large-scale genetic discovery analysis in a combined sample of 195,180 individuals and identify 16 loci associated with grip strength ($p \leq 5 \times 10^{-8}$) in combined analyses. A number of these loci contain genes implicated in structure and function of skeletal muscle fibres (*ACTG1*), neuronal maintenance and signal transduction (*PEX14, TGFA, SYT1*), or monogenic syndromes with involvement of psychomotor impairment (*PEX14, LRPPRC* and *KANSL1*). Mendelian randomisation analyses are consistent with a causal effect of lower genetically-predicted grip strength on higher fracture risk. In conclusion, our findings provide new biological insight into the mechanistic underpinnings of grip strength and the causal role of muscular strength in age-related morbidities and mortality. This chapter contains work completed in collaboration with a number of internal and external colleagues. Contributions are detailed in Section 3.5.

3.1 Introduction

Muscle strength, measured by isometric hand grip strength, is an accessible and widely-used proxy of muscular fitness. Lower grip strength is associated with impaired quality of life in older adults, and is an established marker of frailty, predicting physical decline and functional limitation in daily living[35,38,39]. The value of grip strength as a clinical predictor of fracture risk has been demonstrated in different populations[192,193], and higher grip strength has been found to be prognostic of walking recovery after hip fracture surgery in later life[194]. Grip strength has also been shown to predict cardiovascular disease (CVD) and all-cause mortality over many years of follow-up[45,49,55]. Whilst it remains unclear whether these prospective associations with fracture risk, CVD and mortality are causal - or reflect early manifestation of underlying disease processes - the role of muscular strength as a predictor of functional capacity highlights the importance of understanding its aetiology.

Grip strength is highly heritable (h^2=30-65%)[195–197]. Whilst candidate gene approaches have implicated multiple loci in this phenotype, including thermogenic and myogenic factors[198,199], there remain few robustly replicated associations. Two genome-wide association studies in up to 27,000 individuals have been reported to date[44,200], yielding one intergenic genome-wide significant association[200] at rs752045.

Here, in a combined sample size of 195,180 individuals, including 142,035 individuals from the UK Biobank (UKB) cohort[138], we identified 16 genome-wide significant loci associated with grip strength. We also performed Mendelian randomisation (MR) analyses, which showed no evidence for causality in the associations of grip strength with cardiovascular disease or all-cause mortality, but were suggestive of a causal effect of muscular strength on fracture risk.

3.2 Methods

Assessment of Grip Strength and Covariates Isometric hand grip strength was measured at UKB baseline using a calibrated *Jamar J00105* hydraulic hand dynamometer with peak force indicator (Lafayette Instrument Company, IN, USA), adjusted to the individual's hand size. With the participant seated, elbow bent, and forearm horizontal and supported, one measurement was taken per hand, and maximal hand grip (kg) was taken as the higher of the two readings. The protocol for height and body mass measurement has previously been described in Chapter 2. Phenotyping details for each of the stage two cohorts are detailed in Supplementary Table 1.

Genotyping and Imputation Imputed variants from UKB's interim genotyping release (May 2015) were used for stage one association analyses: full details of the underlying genotyping and imputation protocols applied centrally by UKB have been detailed in Chapter 2. Stage II cohorts applied imputation in line with their usual practices - full details are provided in Supplementary Table 1.

17q21.31 Haplotype Imputation and Analyses In collaboration with colleagues at the University of Leicester (L. Wain, M. Tobin, N. Shrine, see Section 3.5), nine structural haplotypes previously reported at the 17q21.31 cytoband were imputed according to existing protocols[201–203]. Imputation was based on a haplotype reference panel from Boettger and colleagues[202], which uniquely coded each structural haplotype using a combination of twelve surrogate, virtual binary markers. In addition, the file contained 6,302 flanking variant haplotypes. IMPUTE v2.3.2 was used to impute the genotypes of the surrogate markers against the reference panel. The panel contained 284 genotyped variants within the reference region, pre-phased with SHAPEIT v2.837. Variants within the copy-number variable region, with MAF <0.01, or evidence of deviation from Hardy-Weinberg equilibrium $p_{HWE}=1\times10^{-6}$ were excluded. Surrogate markers were subsequently decoded into the corresponding nine structural haplotypes for analysis. Association of haplotypes (inverted versus non-inverted, continuous structural variant [$\alpha/\beta/\gamma$] copy number, and nine common haplotypes as a categorical exposure) with grip strength was modelled using linear regression adjusted for age, sex, height (m), BMI (kg/m^2) and genotyping chip in up to 111,860 unrelated genetic white Europeans defined centrally by UKB.

Genome-wide association analyses of grip strength 142,035 UKB participants had imputed genetic data, grip strength and full covariate availability for genome-wide association analyses; all were of self-identified white ancestry, with the majority (94.6%) reporting as white British. Discovery analyses for maximal grip strength (n=142,035) were run using a Bayesian linear mixed model (LMM) adjusted for age (years), sex, height (m) and BMI (kg/m^2), implemented in BOLT-LMM software (v2.2), as described in Chapter 2. Primary analyses assumed additive (per-allele) effect. Analyses were restricted to biallelic

variants with MAF$\geq$0.1% which had been directly typed, or imputed with imputation quality (IMPUTE2 info)$\geq$0.4.

Independent loci were defined based on proximity using a 1mB window around the index variant reaching genome-wide significance. Independent lead variants (n=21) were followed-up in up to 53,145 individuals from international collaborating cohorts (stage two). In cases where an index variant was not typed or imputed at sufficient quality, appropriate proxies were defined as the variant with the next-lowest p-value within 500kb of the index (Supplementary Table 4). Each stage two cohort accounted for population structure according to its usual practice. Full details of the analytical approach and model specification of each replication cohort are summarized in Supplementary Table 1. Stage I and II results for each of the 21 variants were combined by inverse variance-weighted fixed-effect meta-analysis using METAL. Sixteen loci reached genome-wide significance in combined meta-analysis and were considered to be associated with grip strength.

To examine local linkage disequilibrium structure of replicated loci, regional plots for each of the 16 replicated loci were generated in LocusZoom using LD reference values from the CEU panel of 1000G Phase 1. To investigate possible independent signals at each of the 16 replicated loci, approximate conditional analyses were undertaken using Genome-Wide Complex Trait Analysis software (GCTA, Version 1.25.2).

LD-Score Regression Using genome-wide summary statistics from our UKB phase one analyses, the recently-described LD Score Regression method described by Bulik-Sullivan and colleagues (implemented in LDSC software, v1.0.0) was used to (i) estimate genetic correlation between grip strength and other phenotypes, and (ii) derive tissue-specific partitioned heritability of grip strength. The main principles and practical considerations of this approach have been described in Chapter 2 - details specific to the grip strength analyses are provided here.

Genetic Correlations

Genetic correlations of grip strength were calculated with CHD risk, lean mass index (LMI), fat mass index (FMI) and bone mineral density (BMD) measured at the forearm, femoral neck or lumbar spine. For CHD and BMD, publicly available GWAS summary statistics from the CARDIoGRAMplusC4D[204] and GEFOS[205] consortia, respectively, were used. Summary statistics for LMI and FMI were generated *de novo* by conducting GWAS in a combined sample of 12,851 individuals from the Fenland Study and EPIC-Norfolk. Details of these cohorts are provided in Chapter 2, and descriptive details of anthropometric parameters are provided in Supplementary Table 2. LMI and FMI (kg/m^2) were defined as DXA-derived lean mass or fat mass, respectively, divided by the square of DXA-derived height (GE Lunar Prodigy processed using Lunar EnCORE v14.1, GE Healthcare). GWAS were conducted

separately in each cohort using BOLT-LMM as for the main hand grip analyses. FMI analyses were adjusted for age and sex. Because of the sex specific distribution of the phenotype, LMI analyses were run sex stratified and adjusted for age. Results from both cohorts were combined by fixed-effect inverse variance-weighted meta-analysis using METAL.

Tissue-specific Partitioned Heritability

Partitioned heritability was run individually for each of the eight curated tissue classes distributed with LDSC, adjusting in each case for heritability explained by each functional category of variants across the genome (that is, in a non-tissue-specific manner).

Integration of Expression Data To investigate the direct associations of gene transcript levels with hand grip, and prioritise genes falling within the 16 identified loci, we combined variant-centric and wider genome-wide approaches. Initially, a look-up of all 16 replicated grip strength variants or their best proxy (r2>0.8) was conducted in skeletal muscle, transformed fibroblasts, nervous system and brain regions in the GTEx resource to identify eQTL associations. Variants passing GTEx criteria for tissue-specific eQTL association, and in high LD (r2$\geq$0.8) with the best eQTL for the transcript in question in the tissue of interest were considered significant eQTLs. To consider the combined effect of genetically-predicted gene expression on hand grip across the genome, we additionally took advantage of SMR and MetaXcan approaches, using transcriptome reference from Westra and colleagues (whole blood), and multiple tissues from GTEx, respectively. This process is detailed fully in Chapter 2. We conservatively considered predicted expression of a gene to be associated with grip strength at a MetaXcan p-value$\leq 2.52\times10^{-7}$, taking each gene association in each tissue as an independent test for the purposes of Bonferroni correction

Gene Set Enrichment Analyses Genome-wide discovery results from the UKB cohort were tested for enrichment of pre-specified gene sets based on common functional annotation or known biological pathways in MAGENTA (v2.4)[171]. Enrichment was assessed in a hypothesis-free manner across gene sets drawn from six public databases of gene ontology, functional annotation and canonical/curated pathways, as described in Chapter 2. In collaboration with colleagues at the Broad Institute (D.G. MacArthur, M. Lek, see Section 3.5), custom sets were defined from literature review, incorporating genes with known function in pathways or processes relevant to muscle development and maintenance (Supplementary Table 11. Given their established pro-atrophic role and candidacy as a potential drug target to maintain muscle mass and function, genes involved in the transduction of myostatin/activin signalling *via* activin A type II receptors (*ACVR2A* and *ACVR2B*) were defined from Han et al.[206]. Monogenic genes implicated in muscular dystrophies and myopathies were based on Kaplan & Hamroun (2014)[207], with additional manual curation (M. Lek) to include collagen IV-opathies, congenital myopathies and glycogen storage diseases which may present which present with a similar pattern of limb-girdle muscle weakness.

Gene-based Tests Genes involved in myostatin/activin signalling via activin type II receptors (*FST, MSTN, ACVR2A, ACVR2B*) and known atrophy effectors (*TRIM63, FBXO32*) were identified from literature[206,208] and defined as candidate genes for grip strength based on their biological prior for an involvement in skeletal muscle trophism. Gene-based association tests were performed for each candidate using the Versatile Gene-based Association Study (VEGAS) algorithm[178], calculating LD from HapMap Europeans. VEGAS was applied to the grip strength discovery-phase association results across the whole genome, restricting to directly typed and well-imputed variants (IMPUTE info>0.8).

Role of Variants in Muscle Structure & Histology To identify whether grip strength variants were associated with elements of muscle histology, the association of the 16 replicated HGS variants with muscle histology parameters was examined in 656 men from three independent cohorts of Swedish ancestry (see Supplementary Note). In collaboration with colleagues, the additive association of each of the 16 lead SNPs with percentage of (i) type I fibres, (ii) type IIA fibres and (iii) type IIB fibres from muscle biopsy, as well as capillary density (calculated as the number of capillaries divided by the total number of fibres) was calculated. Phenotypes were inverse-normalized prior to analysis. To better quantify power in this sample, formal power calculations were performed using Quanto (biostats.ucsc.edu/Quanto.html).

Mendelian Randomisation Summary statistic MR (see Chapter 2) was used to examine sex and growth hormone-related phenotypes as causal exposures for grip strength. Primary analyses comprised of the standard inverse variance-weighted approach; as sensitivity analyses for robust causal inference, heterogeneity was assessed using Cochran's *Q*-statistic, and MR-Egger, weighted median, and penalised weighted median estimators of causal effect were applied. The advantages of this approach are detailed elsewhere in this thesis. Additive genetic instruments weighted for the effect of each variant on the intermediate phenotype were constructed for circulating sex hormone-binding globulin (SHBG)[209], dehydroepiandrosterone sulphate (DHEA-S)[210], insulin-like growth factor I (IGF-1)[211], fasting insulin[212], and insulin secretion[213] on the basis of published findings. Full details of each instrument are contained in Supplementary Table 17. Grip strength effect estimates were obtained from the stage one discovery GWAS in UKB.

To infer causality in the association of grip strength with CHD, myocardial infarction (MI), fracture risk, BMD (forearm, lumbar spine, femoral neck), LMI and FMI, summary statistic MR was implemented as above, using the 16 identified loci as instrumental variable for genetically-determined grip strength. Summary statistics for BMD, CHD, LMI and FMI were the same as those used in genetic correlations. Summary statistics for MI were obtained from CARDIoGRAMplusC4D[204]. Fracture risk utilised summary statistics from an ongoing analysis by GEFOS (Supplementary Note), as well as individual participant-level data in EPIC-Norfolk. Where HGS variants were not available in outcome phenotype summary statistics, proxies

were defined as the variant with the next-lowest association p-value for HGS within 500kb of the index in stage one analyses.

Re-weighting MRs incorporating EPIC-Norfolk outcomes

Because EPIC-Norfolk was included in genomewide association meta-analyses for FMI and LMI outcomes, and provided data for the individual participant-level analyses of fracture risk, the HGS instrument was re-weighted using effect estimates exclusive of EPIC-Norfolk samples for the summary statistic analyses of FMI/LMI, and the individual participant level analyses (Supplementary Table 5. For the latter, unconditional logistic regression adjusted for age and sex was used to model the association of an individually-calculated genetic risk score for HGS with fracture risk. This analysis was then meta-analysed (fixed effects) together with results from the summary statistic HGS-fracture risk MR in GEFOS to provide a single result.

All-cause mortality

To test the causal relationship of HGS with all-cause mortality, genetically-determined HGS was modelled on a per-individual basis in EPIC-Norfolk (n_{Total}=21,043, $n_{Deceased}$=5,699), using effect estimates from combined stage one plus two analyses, and excluding estimates derived from EPIC-Norfolk, as above. The association of the genetic risk score to mortality was tested under a Cox proportional hazards model, adjusted for age and sex. Proportional hazards were confirmed using standard technique (Schoenfeld residuals, Kaplan-Meier curve).

Parental Lifespan

To enhance power, and in line with previous work[214], an individual participant level MR of HGS-parental lifespan, as a proxy for survival, was conducted in UKB. The concept of exploring genetic associations by proxy for conditions or traits which are rare, lethal or for which the accrual of cases within a standard observational cohort setting carries an unacceptable time overhead (for example, mortality) is gaining traction in the literature, and has been shown not only to recapitulate signals obtained from standard approaches, but also to confer significant power advantages in discovery approaches[215]. In collaboration with P. Joshi, parental lifespan and vital status (paternal n_{Total}=133,123, $n_{Deceased}$=102,072; maternal n_{Total}=133,123, $n_{Deceased}$=102,072) were regressed on the genetically-predicted handgrip of offspring (modelled as previously, inclusive of EPIC-Norfolk estimates) using Cox proportional hazards, in effect imputing parental genotype at each HGS variant from that of the offspring. The effects generated reflect the influence of offspring genotype on parental longevity, and the expected allele dosages in the parental generation are half the observed dosages in offspring. Effect

estimates per parental allele are correspondingly twice that observed per offspring allele. For clarity, the inferred effect on parental lifespan per parental allele is presented in this work.

Association of Loci with Elite Athletic Status Using data from four multi-ethnic cohorts of elite athletes (Japanese $n_{Athletes}$=54, $n_{Controls}$=406; African American $n_{Athletes}$=79, $n_{Controls}$=391; Jamaican $n_{Athletes}$=88, $n_{Controls}$=87; European $n_{Athletes}$=395, $n_{Controls}$=726; see Supplementary Note), the association of the 16 replicated HGS loci with odds of attaining elite athletic status was assessed by conditional logistic regression relative to age-, sex-, and ethnicity-matched controls. Analyses were performed separately in each cohort before meta-analysing to provide a single point of reference.

Tests of Model Fit To test for departure from additivity in the main grip strength stage one analyses, we applied a dominance deviation approach including two terms for 'best guess' genotypes (i.e. allele codings restricted to integers, rather than allowing continuous terms reflecting the uncertainty in genotype introduced by imputation). One term encoded the major allele homozygotes, heterozygotes, and minor allele homozygotes as 0,1,2, respectively, and the other as 0,1,0, to test the hypothesis that heterozygotes have mean grip strength values intermediate between the two heterozygote terms. The second model allows departure from additivity to be detected.

Checks for Allele Selection by Age Given that observational grip strength is strongly predictive of longitudinal mortality[45], two complementary analyses were run in UKB to ensure that strength increasing alleles from combined stage one plus two analyses were not under selection by age. Modelling each variant as strength-increasing allele dosage, the linear association of age with allele dosage was quantified, considering age as the dependent variable. To gauge whether allele dosage was predicted by age, the inverse of this regression was subsequently run, considering age as the independent variable. This approach has recently been applied to test for selection of variants by age in the Genetic Epidemiology Research on Ageing (GERA) cohort[216]. Analyses were restricted to centrally-defined unrelated white Europeans (n=112,337) to minimise confounding by population structure, and adjusted for sex and UKB genotyping array.

3.3 Results

3.3.1 Multiple novel loci are associated with grip strength

In stage one analyses, we tested the association of >17 million variants (minor allele frequency (MAF) $\geq$0.1%, imputation quality >0.4), in 142,035 white European individuals from UK Biobank with maximal grip strength. Genome-wide SNP-based heritability was estimated at 23.9% (SE 2.7%). Twenty-one loci showed genome-wide significant associations ($p \leq 5 \times 10^{-8}$) in stage one (Supplementary Figure 1), and were subsequently followed up in stage two analyses of up to 53,145 individuals from 8 additional studies (Supplementary Table 1, Supplementary Note) including the Cohorts for Heart and Aging Research in Genomic Epidemiology (CHARGE) consortium[200]. Twelve loci were independently replicated (directional consistency with stage one, p <0.05) in stage two cohorts (Supplementary Table 5) and 16 loci contained genome-wide significant associations ($p \leq 5 \times 10^{-8}$) in combined analyses. Effect sizes on grip strength ranged from 0.14-0.42 kg per allele under an additive model (Table 3.1, Supplementary Table 5). Given the discordance in sample size between stage one and two analyses, and in the interests of maximising power, we considered there to be evidence of association at any locus reaching genome-wide significance in combined analyses, and pursued all 16 in downstream analyses. Lead SNPs at the 16 grip strength-associated loci included common variants (MAF$\geq$5%) in or near *POLD3, TGFA, ERP27, HOXB3, GLIS1, PEX14, MGMT, LRPPRC, SYT1, GBF1, KANSL1, SLC8A1, IGSF9B, ACTG1*, a low-frequency variant (MAF 3%) in *DEC1*, and a further common variant falling within the human leukocyte antigen (HLA) region (Table 3.1, Supplementary Figure 2). Approximate conditional analyses identified no additional signals at genome-wide significance at these 16 loci after conditioning on their respective lead SNPs.

At two loci, we saw evidence for a departure from additivity ($p=3.13 \times 10^{-3}$) under a dominance deviation model (Supplementary Figure 3); at the *GBF1* locus, there was evidence of a dominant effect of the grip strength-raising A allele ($p_{domdev}=2.3 \times 10^{-3}$), and at the *SYT1* locus, evidence for a recessive effect of the grip strength-raising A allele $p_{domdev}=3.0 \times 10^{-3}$. No individual variants showed significant effect modification by age or sex. The association of the 16-variant genetic score (modelled as the sum of the grip strength-increasing allele dosage at each variant per individual) showed no interaction with age ($p_{interaction}=0.30$), but was stronger in men than in women (men: β = 0.20 kg per grip strength-increasing allele, $p=2.38 \times 10^{-48}$; women: β = 0.13 kg per grip strength-increasing allele, $p=3.61 \times 10^{-43}$; $p_{interaction}=1.56 \times 10^{-5}$ (Figure 3.1). Age at recruitment was independent of strength-increasing allele dosage at each of the sixteen SNPs from combined analyses. Equally, allele frequency at each SNP was not predicted by age, suggesting that there is no selection of alleles by age at these loci[216]. We did not replicate the previously-reported association at rs752045 with grip strength[200] (β per minor allele = 0.01 (95% CI -0.06, 0.08), p=0.75).

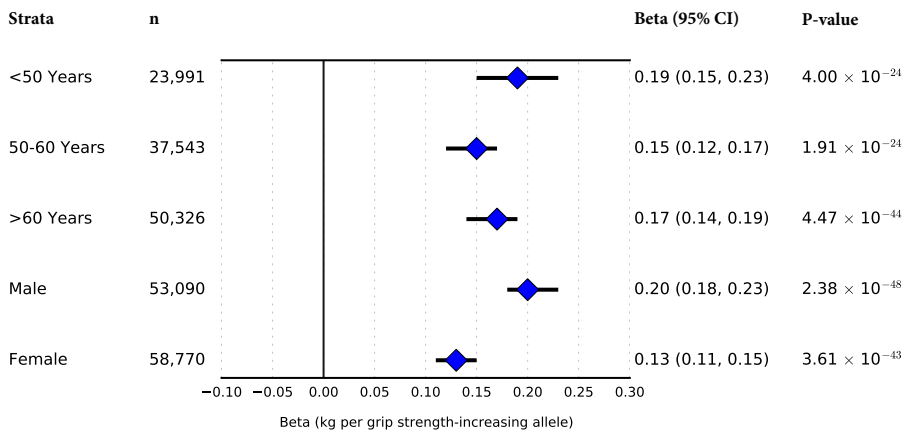

Figure 3.1: Association of the HGS 16-SNP score with grip strength by age and sex strata
Association of the grip strength-increasing genetic score showed no interaction with observed grip strength by age ($p_{interaction}$=0.30), but was stronger in men than women ($p_{interaction}$=1.56×10^{-5}) in a subset of 111,860 unrelated UKB participants from stage one analyses. Associations shown are from linear regression

A number of associated loci contained genes with biologically plausible roles in strength and neuromuscular fitness, through effects on the structure and function of skeletal muscle (*ACTG1*), excitation-contraction coupling (*SLC8A1*), evidence for neurotrophic roles (*TGFA*), or involvement in the regulation of neurotransmission (SYT1). *ACTG1* (Actin, γ1A) encodes a key component of the costamere, a protein complex localised to the Z-disc of skeletal muscle which physically tethers myofibrils to the cell membrane and transmits contractile force generated at the sarcomere to the extracellular matrix via the dystrophin glycoprotein complex (DGC)[217,218]. Monogenic loss of elements of the DGC results in muscular dystrophies[219], whilst *Actg1* knock-out mice display overt muscle weakness, progressive myopathy and decreased isometric twitch force[220]. *SLC8A1* encodes a transmembrane $Na^+/Ca2^+$ exchanger which is vital to restoring $Ca2^+$ concentration to pre-excitation levels in excitable cells. Muscle-specific overexpression of *SLC8A1* has been shown to induce dystrophy-like skeletal muscle pathology[221]. Synaptotagmin-1, encoded by *SYT1*, is an integral synaptic membrane protein which regulates $Ca2^+$-dependent neurotransmitter release at the presynaptic terminal[222], and is implicated in development of neuromuscular junction pathology in rodent models of spinal muscular atrophy[223]. *TGFA* encodes transforming growth factor α, a well-characterised growth factor which plays a key neurotrophic role in the central and peripheral nervous systems[224], and is upregulated during the acute injury response of motor neurons, promoting neuronal survival[225,226].

Three lead variants for grip strength map to or near to genes implicated in monogenic syndromes characterised by neurological and/or psychomotor impairment (Table 3.1, Supplementary Figure 2). rs10186876 ($p_{Combined}$=9.75×10^{-11}) lies 15kb upstream of *LRPPRC* (leucine-rich pentacotripeptide-containing), which has been implicated in the French-Canadian variant of Leigh Syndrome (Mendelian Inheritance in Man (MIM) ID: 220111), a cytochrome C oxidase deficiency with features including developmental delay, hypotonia and weakness[227]. Mutations in *PEX14* (Peroxisomal Biogenesis Factor 14) (intronic lead variant rs6687430) underlie certain forms of Zellweger Spectrum Peroxisomal Biogenesis Disorder (MIM:

Table 3.1 | Sixteen HGS loci reaching genome-wide significance in combined analyses

				Stage One (UKB)			Stage Two Cohorts			Combined			
rsID	Gene⋆	All.	EAF	Effect	SE	*p*	Effect	SE	*p*	Effect	SE	*p*	N
rs958685	*TGFA*	A/C	0.52	0.154	0.026	2.8×10^{-9}	0.164	0.04	3.8×10^{-5}	0.157	0.022	4.8×10^{-13}	191,754
rs72979233	*POLD3*	A/G	0.76	0.210	0.03	3.7×10^{-12}	0.112	0.041	5.8×10^{-3}	0.175	0.024	5.0×10^{-13}	192,490
rs11614333	*ERP27*	C/T	0.62	0.181	0.027	5.0×10^{-11}	0.117	0.04	3.5×10^{-3}	0.16	0.023	1.6×10^{-12}	195,154
rs2288278	*HOXB3*	A/G	0.66	0.162	0.027	3.0×10^{-9}	0.147	0.04	2.8×10^{-4}	0.157	0.023	3.8×10^{-12}	195,133
rs4926611	*GLIS1*	C/T	0.64	0.173	0.027	1.3×10^{-10}	0.115	0.041	5.1×10^{-3}	0.156	0.023	4.8×10^{-12}	192,964
rs6687430	*PEX14*	G/A	0.46	0.15	0.026	7.6×10^{-9}	0.124	0.04	1.7×10^{-3}	0.142	0.022	5.6×10^{-11}	195,176
rs10186876	*LRPPRC*	A/G	0.36	0.162	0.027	2.7×10^{-9}	0.113	0.041	6.2×10^{-3}	0.147	0.023	9.8×10^{-11}	192,490
rs374532236	*MGMT*	T/C	0.38	0.157	0.027	5.5×10^{-9}	0.121	0.042	4.2×10^{-3}	0.147	0.023	1.1×10^{-10}	189,701
rs10861798	*SYT1*	A/G	0.43	0.145	0.026	4.3×10^{-8}	0.159	0.047	7.4×10^{-4}	0.148	0.023	1.3×10^{-10}	189,160
rs78325334	HLA Region	T/C	0.84	0.228	0.038	2.4×10^{-9}	0.113	0.05	0.024	0.186	0.03	9.6×10^{-10}	193,127
rs2273555	*GBF1*	A/G	0.61	0.153	0.027	9.1×10^{-9}	0.096	0.041	0.019	0.136	0.022	1.1×10^{-9}	191,754
rs80103986	*KANSL1*	A/T	0.81	0.201	0.033	1.8×10^{-9}	0.098	0.052	0.059	0.171	0.028	1.2×10^{-9}	193,090
rs2110927	*SLC8A1*	C/T	0.27	0.161	0.029	4.4×10^{-8}	0.098	0.045	0.029	0.142	0.025	7.7×10^{-9}	192,490
rs6565586	*ACTG1*	A/T	0.25	0.169	0.03	2.2×10^{-8}	0.096	0.064	0.14	0.156	0.027	1.2×10^{-8}	187,072
rs72762373	*DEC1*	A/G	0.03	0.424	0.078	4.9×10^{-8}	0.359	0.255	0.16	0.418	0.074	1.8×10^{-8}	152,162
rs34845616	*IGSF9B*	A/G	0.25	0.168	0.03	1.7×10^{-8}	0.07	0.049	0.15	0.141	0.025	2.7×10^{-8}	189,666

All, alleles (effect/other); EAF, effect allele frequency; *N*, sample size; HLA, Human Leukocyte Antigen
Results are sorted by combined stage one + stage two p-value
⋆ Nearest gene to the index variant
Stage one analyses include 142,035 participants
Effect estimates are in kg, per additional effect allele

614887), a syndrome characterised by absence of functional peroxisomes and systemic neurological impairment[228]. Finally, rs80103986 is intronic in *KANSL1*, which has been implicated in the complex impaired-psychomotor phenotype of Koolen-de Vries syndrome (MIM: 610443)[229]. Further, the signal at *KANSL1* is in a large linkage disequilibrium (LD) block also containing *MAPT* (rs754512, $p_{discovery} = 3.7 \times 10^{-8}$), which encodes the microtubule-associated τ protein. *MAPT* has been implicated in a suite of so-called tauopathies characterised by progressive neurological deficit, and is also a well-characterised risk locus for Parkinson's disease[230]. 17q21.31 has a complex haplotype structure comprising an inversion and three structural copy number variants arising from duplication events, which has previously been shown to be of relevance to health[201]. After imputing the nine common structural haplotypes at this locus[201–203], the inverted haplotype was associated with lower strength by reference to the non-inverted (β = -0.17kg, $p=3.85 \times 10^{-6}$), independent of age, sex, height and BMI (Supplementary Table 6). This association appeared to be driven by the inverted $\alpha 2.\gamma 2$ structural variant (β = -0.18 kg, $p=1.24 \times 10^{-5}$).

In sensitivity analyses, we re-tested associations of the 16 grip strength variants in UKB after exclusion of up to 8,676 individuals with T1D, cancer, or other prevalent disease with potential to influence muscle strength. No loci showed significant attenuation of effect relative to overall analyses (Supplementary Tables 7, 8).

3.3.2 Signals are enriched for biologically relevant tissues

To identify enrichment of association signals across different tissues and identify likely effector tissues, we performed cell type-specific partitioned heritability analyses on genome-wide association results from the

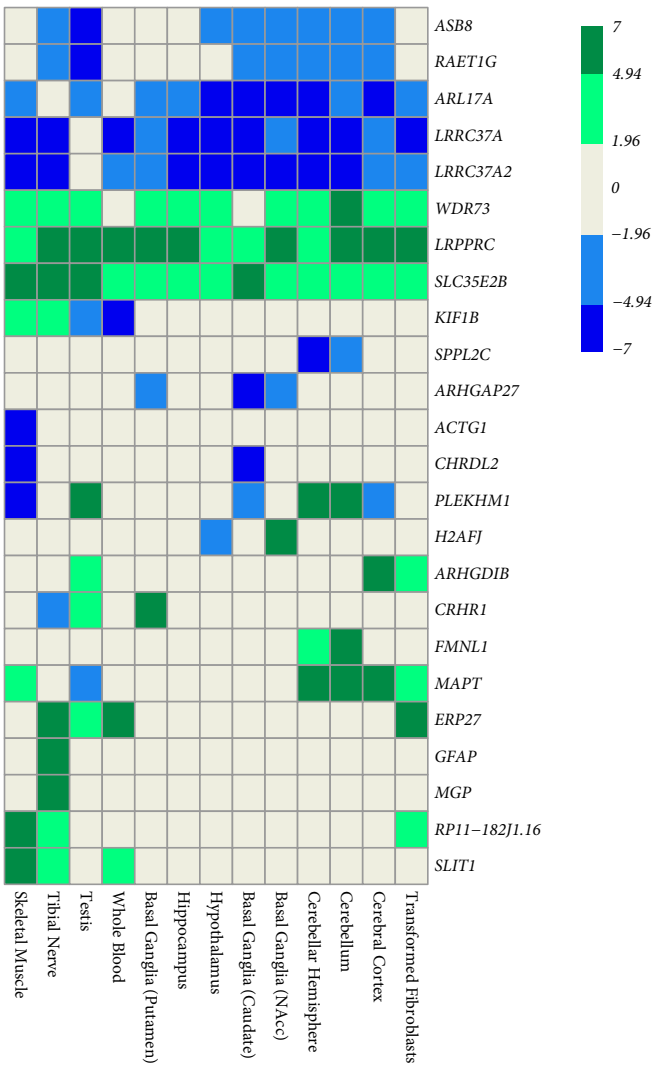

Figure 3.2: MetaXcan-predicted association of imputed gene transcript levels with grip strength across biologically-relevant tissues in GTEx
Data are shown for all genes at which altered transcription was significantly associated with grip strength in at least one biologically-relevant tissue, after accounting for multiple testing. Data are z-scores of transcript level association with higher handgrip strength, clustered by tissue. Direction of z-score indicates whether higher or lower gene expression is associated with higher grip strength. Absolute z-score > 1.96 indicates nominal significance at $p \leq 0.05$, and ≥ 4.94 indicates significance after adjustment for multiple testing ($p \leq 7.91 \times 10^{-7}$). NAcc, Nucleus accumbens.

discovery phase. After adjustment for multiple testing across nine distinct tissue types ($p < 0.0056$), we observed significant enrichments of associations with grip strength in tissue-specific regulatory regions for a number of tissues, including bone/connective tissue ($p = 2.03 \times 10^{-10}$), skeletal muscle ($p = 1.88 \times 10^{-9}$) and the CNS ($p = 7.37 \times 10^{-8}$). Enrichments at weaker levels of statistical significance were also observed in cardiovascular and gastrointestinal tissue, as well as the adrenal/pancreas axis, and 'other' tissues (Supplementary Figure 4).

3.3.3 Integration of gene expression data

Guided by tissue-specific enrichments, we sought to identify putative effector transcripts underlying these associations by investigating associations of lead SNPs or their proxies ($r^2>0.8$) with transcript levels in brain, tibial nerve and skeletal muscle in GTEx. The grip strength-increasing allele at *ACTG1* (rs6565586) was associated with lower expression of *ACTG1* in skeletal muscle ($p_{EXP\text{-}Lead}=3.81 \times 10^{-13}$, $p_{EXP\text{-}Best\ eQTL}=2.64 \times 10^{-13}$, $r^2=0.85$). At *LRPPRC* (rs10186876), the strength-increasing allele was associated with higher *LRPPRC* expression levels in cerebellum ($p_{EXP\text{-}Lead}=6.35 \times 10^{-7}$, $p_{EXP\text{-}Best\ eQTL}=9.35 \times 10^{-8}$,

r^2=0.93) and cerebellar hemisphere ($p_{EXP\text{-}Lead}$=1.29$\times$10^{-6}, $p_{EXP\text{-}Best\ eQTL}$=3.62$\times$10^{-8}, r^2=1.00), which appears directionally concordant with previously-characterised loss of function and otherwise damaging mutations associated with the disease phenotype of French-Canadian Leigh Syndrome[231]. At rs1161433 (*ERP27* locus), the grip strength-increasing allele was associated with higher levels of *MGP* expression in tibial nerve ($p_{EXP\text{-}Lead}$=5.90$\times$10^{-10}, $p_{EXP\text{-}Best\ eQTL}$=2.19$\times$10^{-12}, r^2=0.84). *MGP* (Matrix Gla Protein) is a well-characterised inhibitor of vascular tissue and cartilage calcification, and consequently acts as a key regulator of bone formation[232].

We also performed integrated transcriptome- and genome-wide analyses using MetaXcan and SMR approaches. Accounting for 5,973 independent expression probes (Bonferroni-corrected p=8.37$\times$10^{-6}), and potential coincidental overlap of eQTL signals with GWAS loci, SMR analyses using whole blood transcriptome data[167] suggested correlation between higher grip strength and lower expression levels of ERP27(p_{SMR}=2.50$\times$10^{-9}) and *KANSL1* (p_{SMR}=3.05$\times$10^{-7}), both of which are implicated genes from our GWAS analysis.

MetaXcan analysis identified 25 protein-coding transcripts implicated in grip strength at Bonferroni-corrected significance in at least one of twelve biologically-relevant tissues from the GTEx resource (neuronal, muscle, connective, androgenic tissues and whole blood; transcripts showed concordantly altered expression across a number of these candidate tissue types (Figure 3.2, Supplementary Table 9). For *LRPPRC*, for example, we observed association of higher expression levels across a number of brain tissue types, tibial nerve, whole blood and testis, with higher grip strength. Higher *MAPT* expression in multiple brain regions known to be implicated in motor coordination (cortex, cerebellum and cerebellar hemisphere) was also associated with higher grip strength.

3.3.4 Pathways underlying variation in grip strength

Hypothesis-free gene set enrichment analysis (GSEA) based on gene-sets of common functional annotation, or belonging to pre-defined canonical pathways (Supplementary Table 10, indicated five-fold enrichment of association in/near genes implicated in 'positive regulation of protein catabolic process' (gene ontology (GO): 1903364, false discovery rate (FDR)=0.026), and nominal enrichment of associations near genes implicated in 'dual excision repair in global genomic nucleotide excision repair' (Reactome: R-HSA-5696400, FDR=0.047). Given the identification of established psychomotor disease loci amongst index variants for grip strength, we additionally interrogated our association results for enrichment of genes known to be implicated in monogenic myopathies and dystrophies (Supplementary Tables 10 and 11). Grip strength associations were nominally enriched in the myopathy-linked gene set (p=0.017), but not at loci implicated in dystrophic conditions (p=0.47).

3.3.5 Insights into overlap with pro-atrophic signalling

Myokine signalling via activin type II receptors (ActRII) has been recognised as a key pathway by which muscle mass might be preserved in many clinical contexts[206,208]: yet, we saw no evidence for enrichment of associations around genes in a custom-defined pathway of myostatin/activin signalling through ActRII[206] (Supplementary Table 10 and 11). We also performed gene-based association analyses using VEGAS for genes encoding receptors and ligands in the ActRII signalling pathway, as well as known atrophy effectors (Supplementary Table 12). Two genes (*ACVR2B* and *FBXO32*) showed a significant association with grip strength ($p<0.0071$, accounting for seven gene-based tests) (Supplementary Table 12). *ACVR2B*, for which we found the strongest evidence for gene-based association ($p=0.0002$), encodes the principal transmembrane receptor of myostatin: the target of BYM338, a monoclonal antibody-based inhibitor of ActRIIB, which has shown early promise in reversing muscle atrophy and promoting hypertrophy in phase I trials[233,234]. *FBXO32* encodes the E3 ubiquitin ligase Atrogin-1/MAFbx, which is recognised as fundamental effector of atrophy[206]. These associations are an indication of notable biology at ACVRB2 and FBXO32, though the fact that the VEGAS algorithm calculates gene-level association as the mean of variant associations within the gene means that gene associations may be influenced by single variants, and results must therefore be interpreted with care.

3.3.6 Implication of loci in elite athletic performance

Whilst low grip strength is normally considered a marker of frailty, we also investigated the role of grip strength-associated SNPs in the opposite extreme of physiology: elite athlete status. We examined the association of grip strength-associated SNPs with odds of being an elite sprint/power athlete in a meta-analysis of four studies of sprint and power athletes ($n_{Athletes}=616$, $n_{Controls}=1610$) (see Methods and Supplementary Note for further details of methods and participants). Among the 14 available SNPs, we saw no evidence of association with elite athlete status (Supplementary Table 13). Previously, a nonsense mutation (R577X) in *ACTN3*, which encodes the actin-binding protein α-actinin 3 in skeletal muscle, has been associated with elite athlete status[235]. We found a nominally significant association of the stop-gain variant (T allele) with lower grip strength (additive: β = -0.062 kg, p = 0.018) (Supplementary Table 14) although we found no evidence for any departure from an additive genetic model at this locus (dominance deviation model p = 0.72; Supplementary Figure 5).

3.3.7 Variant association with muscle histology

We also examined whether the lead SNPs at grip strength-associated loci were associated with muscle fibre type and capillary density in a small sample in which muscle fibre type histology and genome-wide

data were available (13 of 16 SNPs were available; Supplementary Table 15). Allowing for 13 tests ($p=3.8\times10^{-3}$), the grip strength-raising allele at *TGFA* was associated with a lower proportion of type I (slow-twitch oxidative) muscle fibres (β=-0.16, $p=3.3\times10^{-3}$), and a tendency towards higher proportion of type IIB (fast-twitch glycolytic) muscle fibres (β=0.16, $p=5.5\times10^{-3}$) (Supplementary Table 15). We acknowledge limited power in this small sample to identify modest effect sizes. Given a minor allele frequency of 0.1 and a sample size of 656 individuals, we estimated 80% power to detect an effect size of ~0.35 SDs.

3.3.8 MR of intermediate phenotypes on muscle strength

Given the roles of sex- and growth hormones and related phenotypes in muscle growth and development[236–238], we performed summary statistic MR to test whether genetically-determined sex hormone binding globulin (SHBG), dehydroepiandrosterone sulphate (DHEA-S), insulin and insulin-like growth factor-I (IGF-I) levels were associated with grip strength. Using genome-wide significantly associated SNPs for SHBG[209], DHEA-S[210] and IGF-1 levels[211], we saw no evidence for a causal association with grip strength (Supplementary Table 16). We saw some indication of causality of insulin resistance and fasting insulin levels in grip strength (Supplementary Table 16) in inverse-variance and median-weighted analyses, although the considerable heterogeneity in inverse-variance weighted results warrants a cautious interpretation (Supplementary Table 16, Supplementary Figure 6).

3.3.9 Muscle strength as a possible causal exposure

Using a MR approach, we investigated the potentially causal role of muscular strength in both mortality and disease outcomes, utilising the 16 replicated loci as an instrumental variable to model genetically-determined grip strength as a proxy of wider muscular strength.

Mortality We found no evidence for a causal relationship between muscular strength and all-cause mortality in 21,043 participants (5,699 deaths) drawn from the EPIC-Norfolk cohort (hazard ratio (HR) per kg higher grip strength 0.96 (95%CI 0.91, 1.03), p = 0.265; Figure 3.3A). However, given wide CIs we also sought to improve power using a recently published approach applying data on parental lifespan[214] as a proxy for longevity. Using this approach in UKB (102,072 paternal deaths, 83,315 maternal deaths), we again found no evidence for causality, with greater precision (HR [95% CI]: 1.00 [0.98, 1.03], p = 0.739) (Figure 3.3A).

Coronary Heart Disease We next investigated a causal role for grip strength in cardiovascular disease using genome-wide association results for CHD (60,801 cases, 123,504 controls) and myocardial infarc-

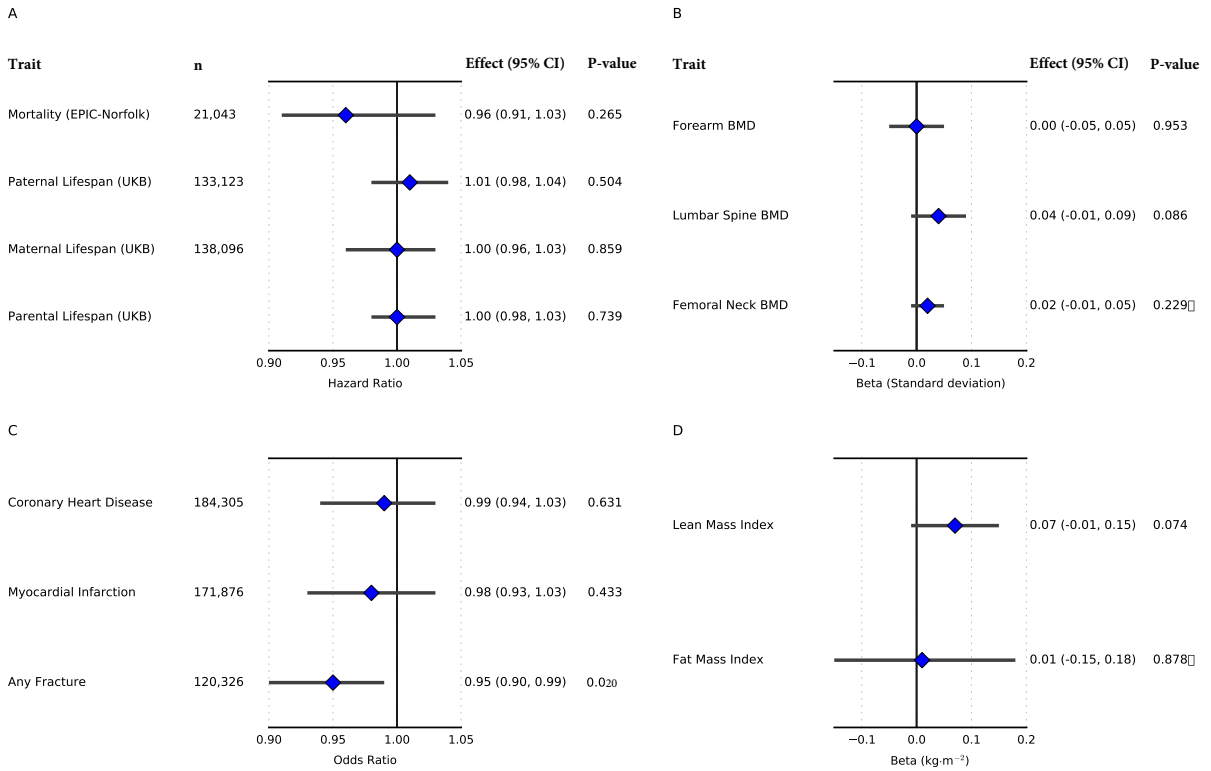

Figure 3.3: Mendelian randomisation of grip strength to mortality, morbidity and anthropometric phenotypes
(**a**) Mortality and parental lifespan in UKB & EPIC-Norfolk; (**b**) Forearm, lumbar spine and femoral neck bone mineral density in GEFOS; (**c**) Coronary heart disease and myocardial infarction in CARDIoGRAMplusC4D and all-fracture risk in GEFOS + EPIC-Norfolk; (**d**) lean mass and fat mass indexes in the Fenland Study + EPIC-Norfolk (n=12,851). Error bars reflect 95% CI

tion (MI; 43,677 cases, 128,199 controls) from the CARDIoGRAMplusC4D Consortium[204] (Figure 3.3C). We found no evidence for a causal relationship between grip strength and CHD (odds ratio (OR) per genetically predicted kg higher grip strength 0.99 (95% CI 0.94, 1.03), p = 0.631) or MI (OR 0.98 (95% CI 0.93, 1.03), p = 0.433; Supplementary Table 18). This result was further supported by cross-trait LD Score regression results showing no significant genetic correlation between grip strength and CHD (r_G= -0.045, p = 0.362; Supplementary Table 19).

Fracture risk and bone mineral density We performed MR analyses of fracture risk using a meta-analysis of (1) summary statistics MR results for fracture risk from the GEFOS consortium (20,439 cases, 78,843 controls; Supplementary Note, Supplementary Table 18) and (2) logistic regression results from association of the weighted grip strength genetic score with fracture risk in the EPIC-Norfolk study (1,002 cases, 20,042 controls). Meta-analysis results suggested a causal association of genetically-predicted higher grip strength with lower risk of fracture (OR per genetically predicted kg higher grip strength 0.95 (95% CI 0.90, 0.99), p = 0.02) (Figure 3.3B). Summary statistic MR of genetically-determined grip strength on publicly available bone mineral density (BMD) GWAS results[205] did not show significant associations between grip strength and BMD (Figure 3.3C, Supplementary Table 18). However, we did find positive genome-wide genetic correlations of bone mineral density with grip strength (femoral neck BMD: r_G = 0.123, p=9.5×10^{-3}; lumbar spine BMD: r_G = 0.156, p=6×10^{-4}; Supplementary Table 19), supportive of a

role for genetically predicted higher grip strength in fracture risk.

Similar to the BMD results, MR analyses of genetically-determined grip strength on meta-analysed GWAS results comprising 12,851 participants from the Fenland and EPIC-Norfolk cohorts did not show significant associations between grip strength and lean mass index (LMI) or fat mass index (FMI) (LMI β = .072 kg/m^2, p = .074; FMI β = .013 kg/m^2, p = .878) (Figure 3.3D, Supplementary Table 18). We did observe, however, a significant genetic correlation between grip strength and LMI (r_G = 0.258, p=2.8$\times$10^{-5}), but not FMI (Supplementary Table 19).

3.4 Discussion

We have identified 16 loci associated with maximal hand grip strength at genome-wide significance. A number of the lead variants were located within or close to genes implicated in structure and function of skeletal muscle fibres, neuronal maintenance, and signal transduction in the central and peripheral nervous systems. Partitioned heritability analyses indicated significant tissue-specific enrichment of skeletal muscle, central nervous system, connective tissue and bone in the genome-wide grip strength results. We observed evidence of shared genetic aetiology of lean mass and grip strength levels, while pathway analyses indicated a role for genes involved in regulation of protein catabolism in the aetiology of grip strength.

Due to the well-established observational associations of higher grip strength with reduced risk of mortality and incident CHD it has been hypothesised that improvement of muscle strength might increase longevity and reduce risk of adverse cardiovascular events[49]. Our MR analyses do not find evidence supportive of a causal role of muscular strength in mortality risk, nor in risk of cardiovascular events (CHD and MI), leaving open the possibility that these observational associations may be attributable to confounding and/or reverse causality. In the absence of causality, it is likely that apparent prospective associations between hand grip strength and cardiovascular disease are driven by a subset of undiagnosed participants amongst whom early, sub-clinical disease processes in the pathogenesis of CHD and related conditions have begun to adversely influence grip strength, whether through direct atrophic pathways or indirect loss of muscle condition, perhaps due to reduced physical activity. Regardless, this does not negate the importance of maintaining strength and muscle mass during ageing as a strategy to maintain physical function[205], and we acknowledge the potential limitations of our MR, especially to conclude on the absence of a causal association given a null result. For example, the limited variance in intermediate traits explained by genetic variants leaves uncertainty over the presence of a small causal effect. Thus, expanded genetic discovery efforts and greater availability of large-scale studies of disease outcomes will improve the precision of MR analyses in future. We saw evidence for shared genetic aetiology of bone mineral density and lean mass with grip strength, and MR results suggested a causal role for higher

muscular strength in lower risk of fracture. Collectively, these results suggest that the determinants of muscular strength are shared with the determinants of fracture risk and are consistent with those from intervention studies to increase muscle strength, which have been shown to improve functional capacity and reduce the rate of falls[239], as well as attenuating the rate of functional decline and increased frailty which often follows major fracture among the elderly[240]. Despite the established decline in grip strength with increasing age, we did not observe heterogeneity in the effect of grip strength-associated variants with grip strength by age. The cumulative effect of the genetic score was greater in men than women, however, perhaps suggesting differences in the underlying genetic component of muscle strength by sex.

We saw evidence of enrichment of associations with grip strength around genes implicated in myopathies. We also noted three loci with genome-wide significant associations containing genes (*KANSL1, PEX14* and *LRPPRC*) implicated in rare, severe clinical syndromes characterised by phenotypes of progressive psychomotor impairment, muscle hypotonia and neuropathy[227,229]. Within the UKB discovery cohort, the association of all three loci with grip strength persisted at genome-wide significance even after sensitivity analyses restricted to participants without any form of self-reported condition which might affect muscle mass or function. Whilst these clinical conditions represent the extreme phenotype of highly deleterious rare mutations in these genes, we demonstrate that proximal common variants are likely to underpin more subtle population-level variation in strength in healthy populations.

Finally, we found that common variation at *ACVR2B*, the principal receptor of myostatin and activin in skeletal muscle, is associated with population-level variation in grip strength. Ongoing clinical trials and development of pharmaceutical agents targeting this pathway have demonstrated potential to reverse atrophy, and improve muscle function in numerous clinical contexts, both within and separate from the context of frailty and ageing[233,234]. Most notably, Bimagrumab (a monoclonal antibody antagonist of ActRII) has progressed to Phase III for the treatment of spontaneous inclusion body myositis[234] (a rare and severe myopathy), and trials are progressing for related indications including cachexia, hip fracture and chronic obstructive pulmonary disease[233]. Our association of common variation in *ACVR2B* with muscle strength provides some level of genetic support for pharmaceutical targeting of ActRII in this context.

In conclusion, we identified 16 loci robustly implicated in grip strength and provide insight into the underlying biology of this important, widely studied, yet poorly characterised trait. MR analyses suggest no causal role for muscular strength in mortality, but do provide evidence for a causal role in fracture risk, highlighting the importance of interventions to improve muscle strength as a means to reduce fracture risk and resultant morbidities. Further genetic and functional work to characterise these loci will elucidate new pathways involved in the regulation of muscle strength and inform the development of drugs to tackle muscle wasting and weakness.

3.5 Contributions

The full list of contributors to the work presented in this chapter is as follows:

Sara M. Willems, Daniel J. Wright, Felix R. Day, Katerina Trajanoska, Peter K. Joshi, John A. Morris, Amy M. Matteini, Fleur C. Garton, Niels Grarup, Nikolay Oskolkov, Anbupalam Thalamuthu, Massimo Mangino, Jun Liu, Ayse Demirkan, Monkol Lek, Liwen Xu, Guan Wang, Christopher Oldmeadow, Kyle J. Gaulton, Luca A. Lotta, Eri Miyamoto-Mikami, Manuel A. Rivas, Tom White, Po-Ru Loh, Mette Aadahl, Najaf Amin, John R. Attia, Krista Austin, Beben Benyamin, Søren Brage, Yu-Ching Cheng, Paweł Cięszczyk, Wim Derave, Karl-Fredrik Eriksson, Nir Eynon, Allan Linneberg, Alejandro Lucia, Myosotis Massidda, Braxton D. Mitchell, Motohiko Miyachi, Haruka Murakami, Sandosh Padmanabhan, Ashutosh Pandey, Ioannis Papadimitriou, Deepak K. Rajpal, Craig Sale, Theresia M. Schnurr, Francesco Sessa, Nick Shrine, Martin D. Tobin, Ian Varley, Louise V. Wain, Naomi R. Wray, Cecilia M. Lindgren, Daniel G. MacArthur, Dawn M. Waterworth, Mark I. McCarthy, Oluf Pedersen, Kay-Tee Khaw, Douglas P. Kiel, GEFOS Anytype of Fracture Consortium, Yannis Pitsiladis, Noriyuki Fuku, Paul W. Franks, Kathryn N. North, Cornelia M. van Duijn, Karen A. Mather, Torben Hansen, Ola Hansson, Tim Spector, Joanne M. Murabito, J. Brent Richards, Fernando Rivadeneira, Claudia Langenberg, John R.B. Perry, Nick J. Wareham, Robert A. Scott

D.J.W. conceived and performed all main analyses in particular collaboration with S.M.W. and R.A.S. Oversaw and co-ordinated replication efforts and additional analyses in external data sources. Combined and presented findings, prepared narrative and manuscript, and enacted modifications throughout review process between September 2016 and final publication in July 2017.

R.A.S., C.L., J.R.B.P., S.B. and N.J.W. had oversight of the project and analyses. K.K., A.M.M., J.M.M., D.P.K, A.T., K.A.M., C.O., J.R.A., M. Mangino, T.S., J.L., A.D., C.M.van D. M.A., A. Linneberg., T.H., T.M.S. provided stage two data and/or analysis. F.R.D., L.A.L., T.W., F.C.G., K.N.N., N.R.W., P.C., A. Lucia, M. Massidda, I.P., F.S., W.D., B.B., G.W., Y.P., K.A., Y-C.C., B.D.M., S.P., C.S., I.V., E.M-M., M. Miyachi, H.M., N.F., B.R., F.R., K.T., J.M., N.G., N.O., O.P, O.H., P.W.F., K-F.E., C.M.L., D.G.M., M.L., L.X., K.J.G., M.A.R., T.W., L.A.L., P-R.L., D.M.W., A.P., D.K.R., N.S., L.V.W., M.D.T., N.E., M.McC. and the GEFOS consortium contributed additional data and/or analysis.

Chapter 4

REE-Gen: A Global Effort to Identify and Apply Genetic Associations for Resting Energy Expenditure

Resting energy expenditure (REE) constitutes the majority of daily total energy requirements, is a cornerstone of basic metabolism and energy balance, and may be of aetiological importance to weight gain and obesity. A number of genes have been pursued as candidates influencing REE, but genetic variants influencing REE are poorly characterised. To identify these variants, we performed a large genetic discovery analysis in up to 11,164 European individuals, and identified one common locus to the 3' of *GOT2* associated with REE, independently of body size. *GOT2* is an indispensable component of the malate-aspartate shuttle, which translocates high energy electrons from glycolysis in the cytoplasm, to the mitochondrial matrix, where they enter the electron transport chain. By inclusion of a further 700 transethnic samples, we additionally identify two further signals for REE, which offer high biological plausibility for an involvement in energy metabolism. REE associations across the genome were nominally enriched for major biochemical respiratory processes independent of age and sex, and showed intuitive positive genetic correlation with body size parameters. We present the first large-scale discovery of REE in Europeans, and provide insight into the biology underlying variation in basic energy metabolism.

4.1 Introduction

Resting energy expenditure (REE) is the minimum level of energy required by an adult to maintain vital function whilst at rest, it forms the main component of total daily energy expenditure in all but the most physically active individuals[56]. REE varies primarily as a function of age, sex and basic anthropometric factors, driven by body size, and has typically been considered a fixed energy cost for an individual of given body size and composition[64–70]. Family and twin studies[97–99] have consistently estimated the heritable component of REE at 30%, yet no underlying variants have been characterised. Whilst certain candidate genes (e.g. *UCP1, UCP3, MC4R*) have been reported as associated with REE in specific populations[100–106], the current literature is based on nominal significance thresholds ($p<0.05$), and is underpowered for genetic effect.

As a major component of energy balance, REE has clear theoretical implications in obesity. However, observational approaches to assess whether REE plays a role in weight gain have been inconclusive, and are limited by their high potential for confounding, especially when using retrospective methods. Amongst known loci for BMI and adiposity, the mechanisms by which variants aetiologically underpin higher body size and fat mass are unknown. Whether variants are linked to positive energy balance through increased energy intake, or decreased expenditure - and whether their effects act through behavioural or physiological routes - is unclear. Recent work in mice and human cell lines provides an initial suggestion that *FTO* may mediate higher BMI through decreasing net thermogenesis[241], yet further work is required.

To characterise genetic variants associated with REE independently of body size, we conducted a genome-wide association study (GWAS) of REE measured by indirect calorimetry in up to 11,164 Europeans, and an additional transethnic sample of 697.

4.2 Methods

For each contributing cohort (Supplementary Table 20), cardiorespiratory exchange was measured in rested and overnight-fasted individuals by open circuit indirect calorimetry under thermoneutral climate-controlled conditions, according to best practice[57]. After quality control to ensure steady-state respiration (a prerequisite for the accurate inference of REE[57]), REE was derived from observed respiratory exchange parameters using established equations[62,242]. For the Fenland Study, respiratory exchange data collected over the course of recruitment was processed, cleaned and used to derive REE *de novo* for the purposes of this work, as detailed below. For other cohorts, REE phenotypes were based on the existing measurement, quality control, and derivation procedures applied by each study; exact details of these protocols are outlined in Supplementary Table 20.

Fenland: Measurement of cardiorespiratory exchange at rest

In the Fenland study, participants provided measurements approximately an hour into the assessment visit, having primarily been seated and at rest for that time. After a short period of acclimation, respiratory exchange was quantified (Jaeger Oxycon Pro, Carefusion, CA) using breath-by-breath (BxB) sampling with a facemask interface, for six consecutive minutes. Heart rate was measured contemporaneously using two independent devices: (i) a telemetric sensor (Polar, Warwick, UK) providing real-time read-out of pulse, and (ii) the ActiHeart combined heart rate/activity monitor (CamNTech, Cambridge, UK) set to sample RR interval at 15s epochs The participant was supine, still and wakeful throughout.

Running quality assurance of data Real-time output was monitored by trained personnel throughout the test to identify instability in the measured phenotypes, and HR was tracked to ensure steady-state at resting levels (per a baseline reference measure). Participants with erratic or inconsistent breathing profile, respiratory exchange, or elevated HR were reminded to relax, and breathe normally. Testing duration may have been extended at the operator's discretion should the six-minute protocol be judged insufficient to gauge stable exchange phenotypes from normal breathing. In case of anomalies indicative of equipment error, malfunction or sampling line leaks, the test was paused and errors rectified, before resuming for a further six minutes.

Pre-test calibration The *Oxycon Pro* was calibrated for (i) ambient condition sensing (air temperature, atmospheric pressure and humidity), (ii) volume measurement, and (iii) gas analysis, on a standard schedule according to manufacturer instructions. All calibrations were run twice daily, with additional calibration for volume and ambient conditions between participants. Analyser calibration used gas of standard composition (15% O_2, 5% CO_2, 80% N_2; BOC Industrial Gases, Guildford, UK). Volume calibration was via a

Table 4.1 | Inclusion criteria for individual breaths	
Parameter	Acceptable Range
VO_2/kg	1-6ml/kg/min
RER	0.6-1.2
V_E	$\pm$3 SDs of participant's mean V_E in last 120s
T_{IN}	0.5-10s
T_{EX}	0.5-10s
$pEtCO_2$	3.3-6kPa (25-45mmHg)

fixed-volume pump.

Fenland: Derivation of resting energy expenditure

Cardiorespiratory exchange data collected within Fenland is uniquely large, and gathered in a research context distinct to the clinical environment from which calorimetry usually originates. By contrast to the clinical setting[57], Fenland applied a shorter, standard measurement protocol centred on maximising data quality whilst minimising inconvenience to the participant. Output was monitored to ensure quality, yet testing duration was standardised and interpretation of data was not contemporary with the test. Efficient processing of this data necessitated the development of a novel quality control and interpretation pipeline. The procedure was split into two parts (Supplementary Figure 7): within-participant cleaning and smoothing of the BxB time-series, followed by cohort-level masking of participants with inadequate or poor-quality data.

Within-participant filtering Under BxB sampling, exchange data are continuously assessed and reported by breath, in contrast to mixing-chamber protocols, which collect and sample expired air at fixed intervals, introducing a degree of averaging. To manage the noisier nature of BxB output (Figure 4.1), an initial within-participant cleaning stage was constructed to retain stable, physiologically plausible breaths representative of underlying respiratory exchange at rest. Absolute and distribution-based filters were applied (Table 4.1) to remove physiologically spurious breaths, anomalies (e.g. coughs, sneezes, hiccups), hardware error, and exchange parameters suggestive of non-resting states. BxB filtering focused first on removal of non-valid breaths, and secondly on ensuring steady-state exchange within the remaining time-series (Supplementary Figure 7).

Restriction to valid breaths To remove physiologically implausible breaths within each individual's timeseries of breaths (Supplementary Figure 7), VO_2 was normalised to body weight and restricted to the range 1 - 6mL/kg/min. Thresholds were selected to maintain true variation and avoid artificial truncation of the distribution within the range of plausible VO_2 values at rest, whilst ensuring that extreme and erroneous values were removed. Missing values of VO_2/kg and VCO_2/kg were dropped by default.

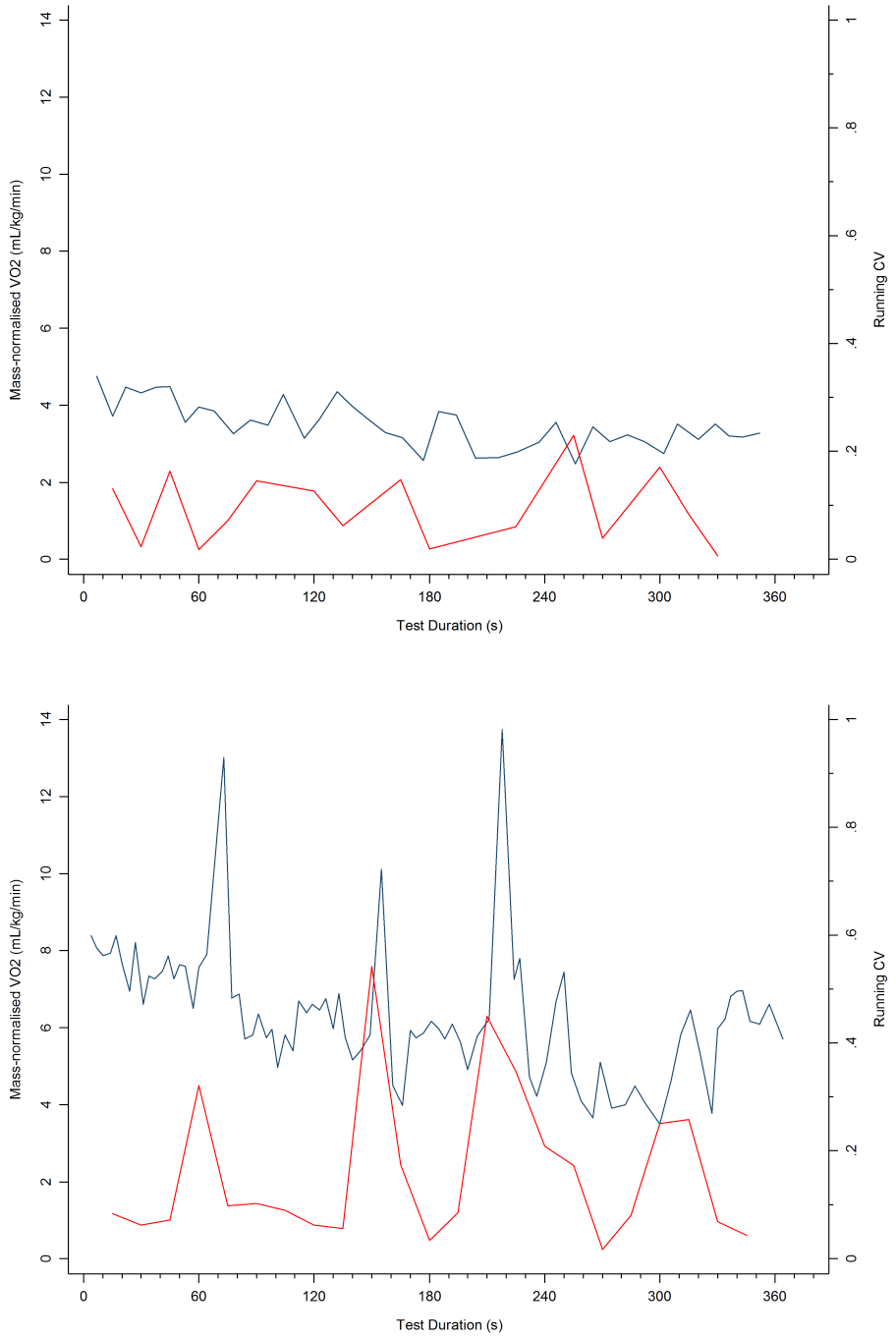

Figure 4.1: Breath by breath VO_2 timeseries in two participants with differing degrees of data noise prior to filtering. Data are observed body mass-adjusted VO_2 reported by breath. Red trace (right axis), rolling coefficient of variation (CV) of VO_2 for consecutive 15s epochs. Upper plot, six-minute timeseries from a participant with mean VO_2 correspondonding to the standard MET (3.5mL/kg/min). Lower plot, equivalent timeseries for a participant with a high mean observed VO_2. Combined, these plots demonstrate the variability in the stability of observed respiratory exchange parameters which must be consistently processed to retain breaths representative of underlying respiration.

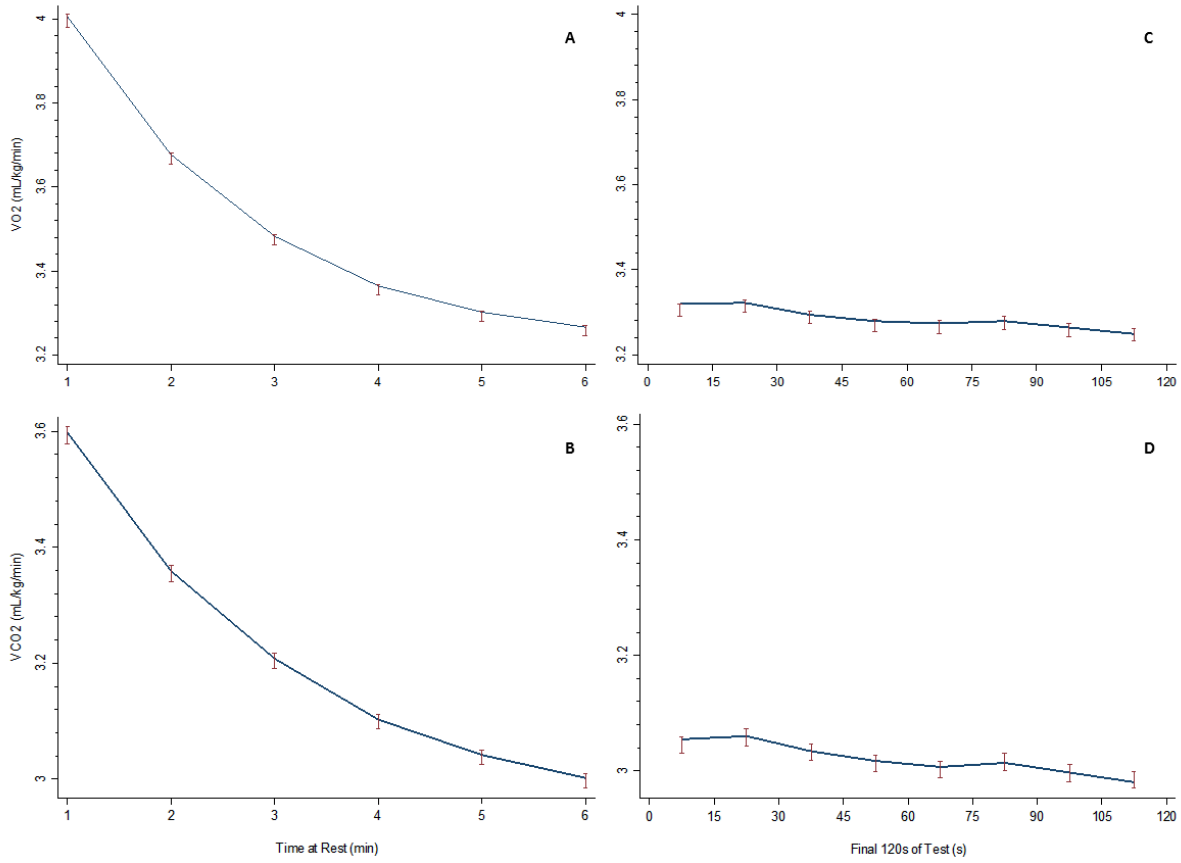

Figure 4.2: Population trend in VO_2 & VCO_2 over duration of indirect calorimetry. Data shown are population-level means of individual-level means calculated using unsmoothed valid breaths, with 95% CI. Time is calculated relative to the full test duration of each participant. A and B, Trend over six-minute test duration; C and D, Detail of trend over last 120s of protocol by 15s epoch.

Breath-wise respiratory exchange ratio (RER) was limited to the range 0.6-1.2. RER usually equates to the true respiratory quotient (RQ) of 0.7-1.0 at cellular level - however there is a need to allow for physiological processes such as bicarbonate buffering which increase the gradient between the RQ and RER. Anomalous breaths and those registered in error were further flagged by removing breaths corresponding to an outlying respiratory minute volume (V_E), more than 3 SDs from the participant's mean, and those with extreme inspiratory and expiratory durations (T_{IN} and T_{EX}, respectively; Table 4.1).

Metabolic representativeness of remaining breaths was assessed on the basis of their end-tidal partial pressure of CO_2 ($pEtCO_2$, the concentration carbon dioxide in the breath at the end of exhalation); values reflecting hypo- or hyperventilation (i.e. respiratory exchange in excess or deficit of underlying metabolic requirements) were removed. $pEtCO_2$ is applied as a proxy indicator of arterial oxygen tension ($paCO_2$), and has a clinically-acceptable range of 30-45mmHg corresponding to a normal paCO2 range of 35-45mmHg, accounting for the established arterial-end tidal oxygen gradient. In the interest of conserving observations whilst ensuring that true hyperventilation was removed, the minimum limit applied was lowered to 25mmHg. The upper limit remained unchanged, as CO_2 retention exceeding this threshold would correspond to clinical ventilatory failure.

Phenotype stability Steady-state respiration is a prerequisite to accurate interpretation of indirect calorimetry[57]. As an initial step in identifying population-level stabilisation of respiration, minute-by-minute mean VO_2 and VCO_2 were calculated for each participant based on valid breaths from the previous stage, and averaged across the whole test population (Figure 2.2, panels A-B). Each minute was defined relative to the end-time of the participant's test to account for differing test durations. At population level, VO_2 and VCO_2 continued to decrease substantially over the first three to four minutes of rest, and begin to plateau from minute five (Figure 2.2, panels C-D). Individual time-series were therefore truncated to the last 120s.

A five-breath rolling median was applied to all physiologically-valid breaths in this timeframe to generate a smoothed time-series and reduce the influence of remaining phenotype fluctuations. To systematically address instability in the time-series, smoothed VO_2 and VCO_2 were regressed separately on underlying time within each individual, and mean VO_2 and VCO_2 values of valid breaths across the 120s calculated by participant. Breaths with a residual VO_2 or VCO_2 exceeding 10% of the participant mean VO_2 or VCO_2, respectively, were identified as contributing to substantial fluctuation in the phenotype, and removed, leaving a final cleaned time-series of smoothed breaths judged to be physiologically plausible and metabolically representative (Supplementary Figure 7).

Between-participant filtering Based on the requirement for steady-state respiratory exchange, participants with a substantial directional trend in cleaned VO_2 or VCO_2 were removed from the analytical dataset (Supplementary Figure 7). To achieve this, cleaned VO_2 and VCO_2 for each participant was regressed on underlying time, and participants with an outlying β-coefficient (>3 SDs from the mean population β, and with a significant Bonferroni-corrected p-value at α=0.05) omitted. Participants with <6 or >50 breaths were dropped. To ensure representativeness, participants were additionally dropped if this cleaned time-series represented <50% of all valid breaths taken in the last 120s of the test (i.e. those remaining after restricting to valid breaths).

Calculation of REE from standard equations For participants passing all stages of QC, total daily resting energy expenditure (kcal/24hr) was derived according to the Abbreviated Weir formula, an adaptation of Weir's classic formula which omits the physiologically negligible contribution of protein metabolism to energy expenditure[62,243]. After calculation, REE was converted to kJ/day (1 kcal = 4.184 kJ).

$$REE = 1.44(3.9VO_2 + 1.1VCO_2)$$

NEO and the Pima Indian study used slight, but very closely aligned, variations of the above formula derived by Elia and Livesey[244], and Lusk[242], respectively.

Cross-sectional analyses in Fenland

To check associations of REE with known correlates, we ran initial cross-sectional analyses with age, sex, bodyweight, height and compartmentalised lean, fat and bone masses using linear regression (Stata 14; StataCorp, TX, USA) in a subset of Fenland samples only (n=7,689; corresponding to the analytic set used in Chapter 5). All models were adjusted for ambient temperature, calorimeter device and whether or not the participant has ingested as standard dose (75g) of glucose as part of an oral glucose tolerance test prior to measurement of respiratory parameters. Tissue-specific masses were measured by dual x-ray absorptiometry (DXA; Lunar Prodigy, GE Healthcare), processed using manufacturer's proprietary software, and manually partitioned into trunk and peripheral (limbs) compartments.

European association analyses & signal selection

Two variant discovery models were run: the first adjusting for age and sex, and the second for age, sex and bodyweight (kg). To account for between study-heterogeneity, we obtained the residual of REE for each model from linear regression adjusted for the model terms and study-specific covariates as detailed in Supplementary Table 20. Residuals were transformed to obtain a distribution of mean 0 and standard deviation 1.

Genome-wide associations of autosomal SNPs with transformed residuals were calculated separately in each contributing European study - Fenland, the Baltimore Longitudinal Study of Ageing (BLSA), the Netherlands Epidemiology of Obesity study (NEO), and the Quebec Family Study (QFS) - and additionally for each genotyping array within cohorts where multiple arrays were used. Details of each study are provided in Supplementary Table 20; a standardised analysis plan was followed by each collaborating cohort (Appendix 1). Linear mixed models (LMM) implemented in BOLT-LMM were applied preferentially; otherwise, study-specific measures to account for population structure were applied (Supplementary Table 20). SNPs with MAF <0.5% or imputation quality < 0.4 were excluded post-analysis. Fixed effects (inverse variance-weighted) meta-analysis of European cohorts was conducted in METAL without genomic correction. Variants with an association $p \leq 5 \times 10^{-8}$were considered genome-wide significant. Independent loci were defined on physical distance using a 500kb window either side of the index SNP. To confirm the absence of inflation in the association results, LD Score Regression intercept was calculated using LDSC *via* LD-Hub. Regional plots were produced for significant loci using LocusZoom with 1000G as LD reference.

Addition of trans-ethnic samples

Inclusion of diverse ancestral samples in GWAS may increase power to detect variant effects, yet can be adversely affected by between-study heterogeneity[159]. We performed a trans-ethnic meta-analysis by including REE data from two multi-ethnic cohorts: Pima Indians in Arizona (Pima, n=509) and the Nigerian individuals enrolled in the International Collaborative Study on Hypertension in Blacks (ICSHIB; n=188). See Supplementary Table 20 for descriptive details of these cohorts, and their protocol for REE derivation.

Genome-wide associations were calculated separately in ICSHIB and Pima data, adjusting for age, sex, study-specific covariates and population structure. After restricting to variants available in the European meta-analysis, results were meta-analysed together with the European discovery summary statistics in METASOFT[245] using (i) standard fixed-effects, (ii) Han and Eskin's modified random effects model (robust to heterogeneous direction of effect between studies)[245], and (iii) a binary effects model which increases power where a variant has an effect in some cohorts but not others[246]. After removing variants not available in either Pima or ICSHIB, trans-ethnic association results were available for 3,916,937 variants.

Metabolome Look-ups

Associations of rs61520068 with circulating metabolite levels were extracted from the GWAS summary statistics of two UK cohorts with metabolomic profiling. Metabolite measures were measured in up to 9,363 Fenland participants using the targeted Biocrates AbsoluteIDQ p180 Kit (Life Sciences AG, Austria), and up to 5,841 individuals from EPIC-Norfolk using the untargeted Metabolon Discovery-HD4 platform (Metabolon, NC, USA). In each study, separate GWAS analyses were run for each metabolite level (log-transformed and standardised) using BOLT-LMM (or SNPTEST where BOLT-LMM failed due to invalid heritability estimates). Models were adjusted for age and sex (and batch within EPIC-Norfolk). In Fenland, analyses were performed separately within two separate genotyping arrays, and meta-analysed. These analyses form part of an ongoing large-scale systematic genetic discovery effort for metabolites overseen by L. Lotta and I. Stewart, and were used by kind permission. Conservative Bonferroni correction, considering each tested metabolite as an independent statistical test, was applied within each array to define statistical significance.

Signal annotation & expression-based analyses

HaploReg[247] was used to functionally annotate REE variants from European and trans-ethnic discovery (and their proxies; $r^2 \geq 0.8$), including details on *cis*-eQTLs. Expression-based analyses were expanded to leverage associations with REE across the genome using imputed transcriptome-based models (TWAS,

MetaXcan, and SMR) based on expression in whole blood, and across multiple tissues from GTEx, as described in Chapter 2

Gene Set Enrichment Analyses

To test for biological and functional enrichment of associations with REE across the whole genome, we conducted hypothesis-free pathway-based analysis using MAGENTA, as previously described. Statistical enrichment of a pathway was defined as a permutation-based false discovery rate (FDR) $\leq$0.05 across all pathways. Taking a hypothesis-driven approach, associations with REE across the genome were additionally tested for enrichment of candidate pathways involved in cellular processes of glycolysis and aerobic respiration. Pathways were identified by querying mSigDB for key respiratory processes (Supplementary Table 24). Twenty-one pathways with >10 genes were identified; significant enrichment was defined using a conservative p-value threshold $\leq$(0.05/21), though nominal associations at p<0.05 were also reported given that adjustment for each pathway as an independent test is likely to be over-conservative when the contents of the gene sets are overlapping between pathways and between versions of the same pathway drawn from different databases.

4.3 Results

Of the 10,079 participants for whom indirect calorimetry measures were available in Fenland, REE was derived for 9,372 participants (92.9%; 91.1% of original men , and 93.6% of original women), who retained valid, steady-state respiratory time-series after restriction to valid breaths and removal of individuals with unstable phenotypes. Univariate anthropometric and respiratory phenotypes amongst this analytic subcohort are summarised in Supplementary Table 21. On average, participants passing quality control were somewhat overweight (mean BMI 26.8$\pm$4.7kg/m^2), with mean age 48.9 years. The 707 excluded participants weighed less on average (mean body mass 74.4kg vs. 78.1kg in the analytic set, p<0.001), and had a correspondingly decreased BMI. Age did not differ between quality control successes and failures. Over the last 120s of measurement, our observed VO_2 was concordant with expected ranges from literature[248]. In men and women combined, mean REE was 1748.17$\pm$432.55kcal/24hr; REE was normally distributed overall, and within the sexes (Supplementary Figure 8).

Of the 9,372 with derived REE, array genotyping and full covariate data was available in 8,491 participants; once combined with data from contributing discovery-stage cohorts (NEO, QFS, BLSA), objective REE was available in up to 11,164 individuals of European descent from Fenland, plus three additional cohorts in the Netherlands, Canada and United States. Based on a subset of data from the Fenland study we confirmed known observational associations of REE, which was negatively correlated with age, higher in men relative to women, and cross-sectionally predicted by body size, including separate independent effects of lean mass and fat mass (Supplementary Table 22).

4.3.1 A common variant near *GOT2* is associated with REE

To identify novel genetic associations with objectively-assessed REE from indirect calorimetry, I performed a genome-wide association study of REE in up to 11,164 individuals of European descent, with and without adjustment for body mass (Supplementary Figure 9). Whole genome heritability of REE adjusted for age and sex was estimated at 14.3% (2.3% after adjustment for bodyweight) using LD score regression. After accounting for multiple testing, heritability was not enriched for any particular tissue based on partitioned heritability analyses.

We identified one common (MAF = 0.50) intergenic signal for REE, independent of age and sex (rs61520068, p=4.11$\times10^{-8}$), to the 3' of *GOT2* (Mitochondrial Glutamic-Oxaloacetic Transaminase II), associated with a 0.08 SD increase in REE per effect allele (Figure 4.3). No signals reached genome-wide significance upon additional adjustment for bodyweight. Association p-values were not significantly inflated in either model on the basis of LD-score regression intercept, and apparent inflation of GC was attributable to high polygenicity of REE (Supplementary Figure 9). Approximate conditional analyses confirmed the ab-

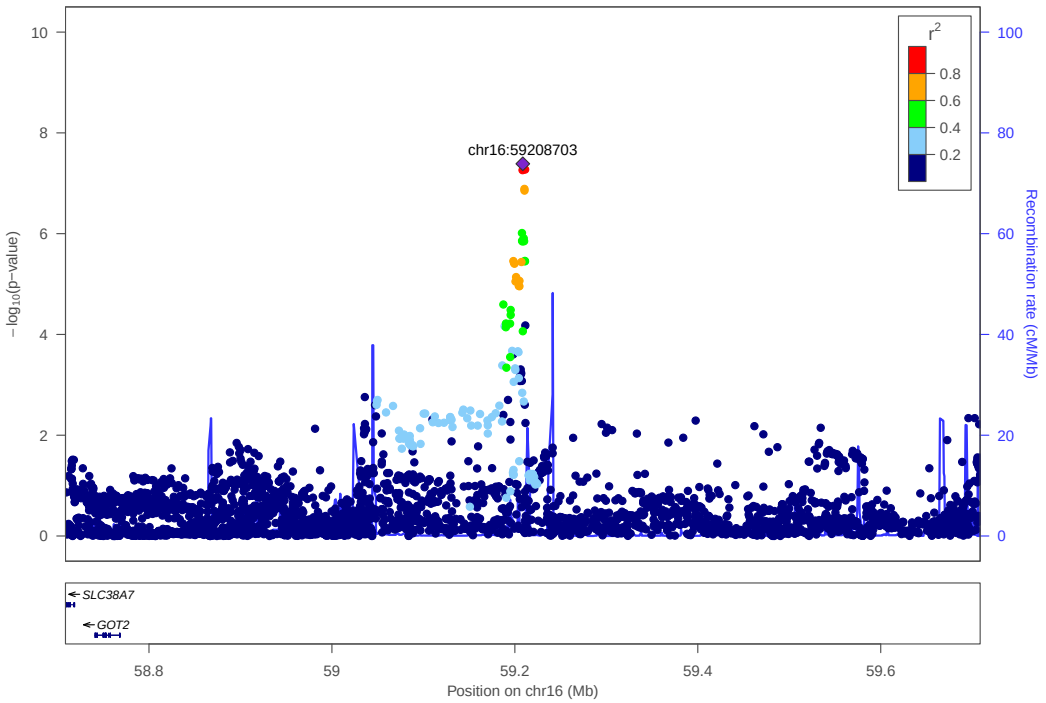

Figure 4.3: Regional association of rs61520068 with REE in European discovery analyses adjusted for age and sex

sence of any secondary signal at rs61520068. rs61520068 was not a significant *cis*-quantitative trait locus for either tissue-specific gene expression or methylation based on look-ups in GTEx (via the HaploReg browser) and the BiOS QTL Browser (http://www.genenetwork.nl/biosqtlbrowser/), and we additionally found no evidence of association with circulating metabolite levels in either the Fenland or EPIC-Norfolk cohorts. Summary statistics from the initial (age- and sex-adjusted) model were used as the main source of associations for subsequent analyses.

4.3.2 Genetic signals are independent of major confounders

To check that the signal at rs61520068 was not influencing REE through an underlying association with body size, we looked up the variant in the most recent consortium-based GWAS for BMI[249], height[250], hip and waist circumferences[251], and body fat percentage[252], and confirmed an absence of signal within a 2mb window around the variant (Supplementary Figure 10). Additionally, *GOT2* encodes aspartate aminotransferase (AST), which is routinely used as a clinical indicator of liver function. As compromised liver function may confound observed genetic associations with metabolic function, we further confirmed that rs61520068 was not associated with plasma AST in the EPIC-Interact cohort[253,254] in standard association analyses assuming additive effect and accounting for age, sex and population structure (p=0.59, n=15,332).

4.3.3 Transethnic analyses implicate additional intronic signals

The addition of ethnically-diverse samples to GWAS may offer power benefits for variant discovery by exploiting differences in allele frequency, but requires tailored approaches to appropriately handle heterogeneity and population structure. We performed a trans-ethnic GWAS by meta-analysing Native American (n=509) and black African (n=188) individuals from two additional studies together with our main European population. A combination of meta-analysis techniques optimised to detect consistent and inconsistent directions of effect between ethnicities, as well as lack of effect in some ancestries, were applied to maximise power. These included fixed effects, Han and Eskin's modification of random effects and binary effects approaches, respectively[245,246].

Combined analyses revealed two additional intronic signals at genome-wide significance ($p \leq 5 \times 10^{-8}$) in *HCRTR2* (rs12527963), and *VTCN1* (rs12034996), with frequencies varying from 0.01-0.50 between ancestries (Supplementary Table 23). The lead variant at *VTCN1* remained significant after adjustment of REE for bodyweight ($p_{Binary}=3.43 \times 10^{-9}$). The European signal near *GOT2* fell just short of genome-wide significance in transethnic analyses adjusted for age and sex ($p_{Han\text{-}Eskin}=3.86 \times 10^{-7}$, $p_{Binary}=1.15 \times 10^{-7}$), but the magnitude and direction of its effect remained concordant with the European discovery model. This attenuation of statistical significance likely reflects the increased heterogeneity of transethnic analyses.

4.3.4 Enrichment for respiratory processes

Hypothesis-free gene set enrichment analyses (GSEA) using MAGENTA did not indicate statistically-significant enrichment of European REE associations across the genome for underlying canonical biological pathways or gene ontology groupings. To more closely investigate enrichment of association for specified biological processes and phenotypes relevant to energy balance and REE, we undertook hypothesis-driven GSEA using curated gene sets from mSigDB implicated in cellular respiration or its sub-processes (Supplementary Table 24). Suggestive enrichment of associations for genes involved in the citrate cycle (KEGG TCA Cycle p=0.022; GO TCA Cycle Enzyme Complex p=0.034), and implicated in the mitochondrial electron transport chain (Biocarta, p=0.0499) was observed, though should be interpreted with caution as these associations do not survive strict correction for multiple testing across 21 pathways (p=0.002). Nonetheless, there would appear to be biologically interesting enrichment at these pathways, especially considering the high level of correlation between their constituent genes, such that adjustment for 21 independent tests is likely over-conservative. Enrichment for the GO TCA Cycle Enzyme Complex term was statistically strengthened after adjustment for bodyweight (p=0.008).

4.3.5 Gene-based variant and expression analyses

Genome-wide gene-based association analyses are increasingly being applied to supplement variant-centric approaches in genetic discovery, and are particularly attractive due to their lower burden of multiple testing. Using MAGMA to test the mean association of all SNPs in each gene with REE across the genome, *PRKCSH* (glucosidase II β-subunit) showed gene-level association with REE, independent of body weight ($p_{MAGMA}=1.50\times10^{-6}$). We further applied a range of integrated transcriptome analyses (MetaXcan,SMR,TWAS) to gauge whether altered expression of genes in whole blood and a range of tissues was associated with REE. These approaches did not, however, implicate transcript levels in any tissue with REE.

4.3.6 Shared genetic basis with cardiometabolic phenotypes

In light of the fact that European discovery efforts identified only one variant at genome-wide significance in age and sex-adjusted models, formal assessment of REE as a causal exposure using MR techniques was not possible. Whilst the construction of polygenic instruments containing only variants associated with the modelled phenotype at sub-genomewide significance has been advocated[255], the risks of violating major assumptions of MR analyses by such an approach are very high. Selecting variants falling below the genome-wide threshold may weaken the assumption of robust association between the instrument and modelled intermediate, and also markedly increases the likelihood for pleiotropy and heterogeneity which cannot appropriately be mitigated through the use of sensitivity analyses. For this reason, we considered the shared genetic architecture of REE with selected anthropometric, cardiometabolic and ageing phenotypes, using associations across the whole genome (Supplementary Table 25). After accounting for multiple testing, REE (age and sex-adjusted) showed positive genetic correlation only with body size phenotypes, including standing height ($p=3.10\times10^{-8}$) and BMI ($p=1.18\times10^{-7}$). These findings are concordant with the observation that body size is the primary driver of whole-body energy requirements, and highlight the close relationship between these phenotypes. No further associations were observed, however. Genetic correlations using genome-wide associations for REE further adjusted for body mass were not possible, as the narrow-sense heritability observed in this model fell below the threshold required for correlation analyses by LD Score Regression.

4.4 Discussion

We have identified one common signal for REE in Europeans at genome-wide significance, and a further two signals after inclusion of 700 individuals of Native American or African ancestry. Associations appear to be independent of confounding by body size. Signals fall in or near to genes implicated in cellular respiration (*GOT2, SLC38A7*), T cell-mediated immunity (*VTCN1*) and orexigenic factors (*HCRTR2*). Across the genome, associations with REE are nominally enriched for the two major processes of aerobic respiration: the citrate cycle and the mitochondrial electron transport chain.

GOT2 encodes the mitochondrial form of glutamic-oxaloacetic transaminase, a core component of the malate-aspartate shuttle (MAS). This process vitally facilitates translocation of the high-energy reducing equivalents generated in glycolysis to the mitochondrial matrix, where they enter the electron transport chain (Figure 4.4). The intrinsic role of *GOT2* in electron transfer gives a high biological prior for association with REE. *GOT2* knockdown in lung cancer cells lines has previously been demonstrated to reduce ATP production by nearly a half[256], and decrease mitochondrial aspartate availability[257], whilst *GOT2* acetylation regulates the rate of the MAS in non-cancer cells[258]. Of note, the *GOT2* locus also partially contains *SLC38A7*, which encodes the major mitochondrial transporter of glutamine. Glutamine is the precursor amino-acid of glutamate, the substrate of *GOT2* in the MAS, where it is converted to α-ketoglutarate and feeds into the citrate cycle. Neither *GOT2* - nor any other gene - is functionally implicated by rs61520086, but, in the absence of alternative means to prioritise genes, the fact that *GOT2* is the only gene wholly contained within the 1mB locus centred on the index (Figure 4.3 strengthens its position as a gene of interest at this locus.

Transethnic analyses shed further light on potential genetic signals underlying REE: in particular, the implication of the neuropeptide orexin (*HCRTR2*) was of interest. Orexin (also known as hypocretin) is most well-characterised as a regulator of food intake, appetite and wakefulness[260–263], though a direct role in thermogenesis and adipocyte browning has been described more recently. Orexin is necessary for brown fat differentiation[264], reverses brown adipose dysfunction in ageing mice[265], and has been shown to be a key modulator of non-shivering thermogenesis in brown adipose tissue[264,266,267]. Whilst transethnic analyses in this case do add further biological insight, the low additional sample size contributed by transethnic samples to this analysis and the relatively low frequency of the identified variants means that these associations should be interpreted with caution pending further replication in diverse ancestral samples

This work represents the largest genetic discovery of objectively-assessed REE to date - and the first in Europeans - with a combined sample size exceeding other recent GWAS efforts by more than twenty-fold[110]. Through concerted international collaboration, the pooled sample used in these analyses incorporates the majority of REE data available from indirect calorimetry (with array-based genotyping also

available) on a global scale. Nonetheless, the absolute sample size used here is relatively small and it must be acknowledged that - despite best efforts - these analyses are likely to be underpowered. Limited discovery of associated variants has precluded the intended formal assessment of REE as a causal exposure, and the subsequent use of genetic correlations to assess shared genetic architecture of REE with cardiometabolioc traits across the genome only confirms known observational drivers of REE, rather than providing new insight.

Given that all available data have been utilised to maximise discovery sample size, our capacity to replicate associations in independent samples has been restricted. Follow-up of our identified locus at *GOT2* should be pursued in further work, though enhanced discovery efforts with improved sample size should be prioritised in order to maximise identification of independent variants for REE and generate a robust instrument for REE. This, however, represents a medium to long-term objective, as it will require substantial new phenotyping efforts in many thousands of individuals, or *de novo* genotyping of existing large population-based samples with REE already assessed. A particular frustration amongst existing population-based cohorts with indirect calorimetry measures (e.g. POUNDS-LOST[268], Health-ABC) is that the availability of biosamples suitable for genotyping is limited, having been stored only for a small proportion of the population (POUNDS-LOST), or otherwise not made collaboratively available to us (Health-ABC). In the short term, functional validation of the major genes implicated here by knock-down or knock-out in cell lines or animal models likely represents the next immediate avenue to investigate the role of these genes in energy expenditure. Dedicated systems (e.g. Seahorse Analysers, Agilent Technologies, Santa Clara, CA) allowing the direct effect of cellular perturbations on the respiratory profile of cell lines to be quantified through direct measurement of oxygen consumption and respiratory intermediates, are in wide research use, and could be applied to such knock-down cell lines in collaboration with partners.

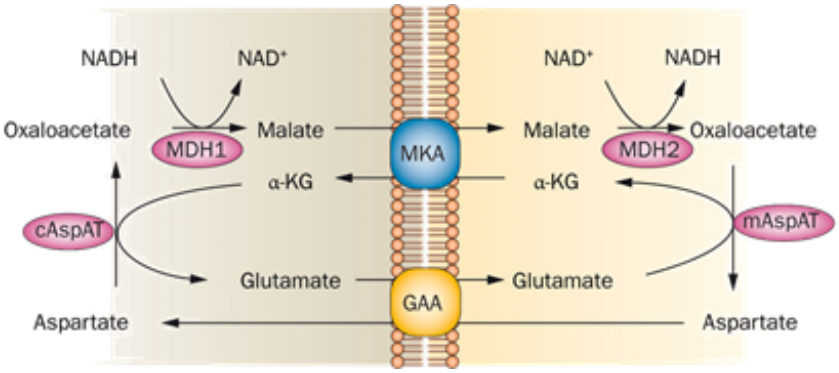

Figure 4.4: The malate-aspartate shuttle (MAS). As the inner mitochondrial membrane is impermeable to reduced cofactors, the MAS represents the main mechanism by which reducing equivalents for respiration are translocated between the cytosol (shaded blue) and the mitochondrial matrix (shaded orange). NADH oxidation in the intermembrane space is coupled to NAD reduction in the matrix, regenerating NADH for oxidative phosphorylation, and maintaining the cytoplasmic supply of NAD required for glycolysis. Glutamic-oxaloacetic transaminase is denoted here as cytosolic/mitochondrial aspartate aminotransferase, mAspAT. α-KG, α-ketoglutarate; MDH2, malate dehydrogenase; GAA, glutamate-aspartate antiporter; MKA, malate-α-ketoglutarate antiporter; cAspAT, cytosolic/mitochondrial aspartate aminotransferase. Reproduced from Menzies *et al.*[259]

4.5 Contributions

The full list of contributors to the work presented in this chapter is as follows:

Raymond R. Noordam, Christian Couture, Paolo Piaggi, Toshiko Tanaka, Bamidele Tayo, Ruifang Li-Gao, Jennifer Schrack, Richard Cooper, Amy Luke, Claude Bouchard, Louis Pérusse, Clifton Bogardus, Leslie Baier, Dennis O. Mook-Kanamori, Luca A. Lotta, Isobel Stewart, Kate Westgate, Robert A. Scott, Søren Brage, Nicholas J. Wareham.

D.J.W.: Conceived project, prepared overall consortium analysis plan, and performed main analyses. Constructed and applied systematic processing and quality control pipeline for raw respiratory exchange parameters to obtain analytic REE phenotype, according to best practice. Co-ordinated *de novo* formation of the REE-Gen consortium from international collaborators in 2015 and maintained engagement and compliance of collaborators to the analysis plan and its deliverables over the course of the PhD. Prepared the manuscript.

Provision of discovery GWAS summary statistics from additional discovery cohorts: R.R.N, D.O,M-K. (NEO Cohort); C.C., C.B., L.P. (QFS Cohort); T.T., J.S. (BLSA Cohort); P.P., C.B., L.B. (Pima Cohort); B.T., A.L., R.C. (ICSHIB Cohort). Metabolite GWAS data and look-up in EPIC-Norfolk data: L.A.L., I.S. Indirect calorimetry measurements and technical assistance with REE derivation: S.B., K.W. Guidance, support and oversight throughout: R.A.S., N.J.W.

Chapter 5

Do BMI Variants Influence Adiposity *via* Resting Energy Expenditure?

Ninety-seven genetic loci have been identified for body mass index (BMI), yet the mechanisms underpinning genetic risk for obesity are poorly characterised. Whilst some variants are thought to play a role in behavioural determinants of energy intake, consideration of the mediating role of energy expenditure has been incomplete. This is particularly true in the case of resting energy expenditure (REE), which represents the majority of daily energy expenditure and is typically considered non-modifiable for an individual of given body size and composition. Common BMI variants in *FTO* and *MC4R* have been reported to exert some of their effect on body weight via REE both in model organisms and small human studies, yet these findings lack replication. To inform the mechanistic basis of genetic obesity risk, this chapter details the first systematic assessment of the association of all BMI-increasing variants with REE in a large population-based cohort, and assesses the potential of REE as a mediating factor of 95 known biallelic risk loci for obesity, both in combination, and on a variant-by-variant basis. Obesity is interpreted with a particular focus on adiposity, using DXA-derived body fat percentage (BFP). One variant near *MTCH2* associated with higher adiposity as gauged by BMI and BFP was associated with lower daily REE after accounting for body size (β = -73.72 kJ/24hr per BMI-increasing allele, p=4.65×10^{-4}). We did not replicate previously-published associations of common BMI-associated variation near *FTO* and *MC4R* with REE.

BMI-increasing genetic variation near *MTCH2* (mitochondrial homolog carrier 2) appears to influence BFP partially *via* lower genetically-determined REE. Our results do not support previous work suggesting that common variation near *FTO* and *MC4R* acts via REE to affect BMI.

5.1 Introduction

Large-scale genetic discovery has identified many common single nucleotide polymorphisms (SNPs) associated with BMI, with 97 independent loci reaching genome-wide significance in the most recent European meta-analysis totalling more than 500,000 individuals[249]. This literature has provided valuable insight into the underlying genetic aetiology of body composition and obesity, and allowed shared genetic architecture with other relevant traits to be interrogated. Yet, the biological mechanisms by which BMI-associated variants predispose to obesity - and specifically whether they act through modulation of energy intake or energy expenditure - remain poorly understood.

Current population-based work has largely assessed the role of BMI-associated genes in energy intake, on the hypothesis that - in the context of a ubiquitous obesogenic environment - genetic risk for obesity operates through central regulation of eating behaviour[269]. In support of this, when modelled as a combined genetic risk score, the additive effect of BMI-increasing variants is associated with higher emotional and uncontrolled eating in US adults[270]. *FTO* has been associated with diminished satiety responsiveness in children[271], binge-eating in adolescence[272], and poorer cognitive restraint[270] and disinhibition[273] in adults. *MC4R* is associated with uncontrolled eating[274] and shows sex-specific effects on emotional eating in adults[275]. Examination of the mediating role of energy expenditure (both REE and physical activity energy expenditure, PAEE) in genetic BMI risk has similarly been restricted mainly to *FTO* variants[276]. As the predominant component of total daily energy expenditure[56] (and largely considered fixed for an individual of given body size and composition) REE has long been recognised as a possible risk factor for weight gain, though observational studies have often been confounded or subject to reverse causation[95,277,278]. Recently, in detailed work using rodent models and human cell lines, Claussnitzer and colleagues have reinvigorated discussion that REE may be a mechanistic factor in *FTO*-associated BMI risk by suggesting that *FTO* influences adipocyte differentiation and browning, and upregulates cellular thermogenesis[241]. This finding is, however, at odds with previous - albeit small - population-based samples which report no association between *FTO* and REE after accounting for the confounding effect of body size[276]. Reduction of REE (normalised to body weight) has also been implicated as a potential route by which variation near *MC4R* (melanocortin 4 receptor) may predispose to higher BMI in the Pima People of Arizona[103].

Whilst these candidate genes have received considerable attention, their reported effect on REE is inconsistent between evidence from animal models, cells lines and human cohorts, remains to be replicated in large population-based samples, and must be interpreted in the context of the wider genetic component of obesity risk. The extent to which known BMI-associated variants aside from *FTO* and *MC4R* influence energy balance through REE in human populations is unknown. To characterise whether genetic predisposition to obesity operates through REE, we systematically examined, for the first time, whether the effect of all known BMI-increasing variants on adiposity was mediated by objectively-measured REE in up

to 7,689 middle- to older-aged British adults from the Fenland Study.

5.2 Methods

Obtaining a measure of REE independent of body size REE was derived from respiratory parameters at rest as described in the previous chapter. REE is confounded by body size, and appropriate adjustment is necessary to gain physiologically valid and comparable findings of genetic associations with REE, but discussion of how best to normalise REE for body size has been ongoing in the literature for many years[276]. Taking BMI as an aggregate measure of overall body size, we generated residuals (REE_{RES}) by linear regression of whole-body REE (kJ/24hr) on BMI (kg/m^2), adjusting for age, sex and technical artefacts of the calorimetry measurement (calorimeter device ID, ambient test temperature). As participants were administered a standard 75g oral glucose tolerance test (OGTT) at the outset of the assessment visit, we additionally adjusted this regression for OGTT test status (received/not received). Of those participants with genotyping, up to 7,689 had derived REE and complete data for all residualised covariates, and were used in analyses.

Association of adiposity with known BMI variants Ninety-five biallelic variants associated with BMI in the latest GIANT consortium discovery effort[249] were extracted from imputed genotypes for each of the participants with REE and complete covariate data, and expressed as the BMI-increasing allele dosage, using the BMI-increasing allele reported by GIANT. The association of allele dosage at each variant with (i) REE residualised only for age, sex, OGTT and technical parameters (REE_{AS}), (ii) REE_{RES}, (iii) BMI residualised for age and sex and (iv) DXA-derived body fat percentage residualised for age and sex, was assessed by linear models additionally adjusted in each case for genotyping array and four topmost genomic principal components as a indicator of underlying population structure. To consider the combined additive effect of all 95 variants in aggregate, we additionally tested for association between each of these phenotypes and a genetic risk score (GRS_{95}) comprised of the BMI-increasing allele dosage summed across all 95 variants within each participant.

Identifying variants potentially affecting adiposity through REE According to the logic of Baron and Kenny[279], for REE_{RES} to potentially act as a mediator of genetic association with body fat percentage, it must be associated with both allele dosage at the variant, and independently with BFP. Amongst those variants associated at nominal significance ($p \leq 0.05$) with BFP, we defined a subset of variants at which the observed effect on adiposity was potentially mediated by REE as variants which were additionally associated with REE_{RES} after accounting for 95 independent tests ($p=5.26 \times 10^{-4}$).

Mediation analyses of adiposity To assess the possible mediating effect of variant-BFP association by REE_{RES}, three individual linear regressions were run within a Sobel-Goodman testing framework. The direct effect of allele dosage on BFP_{AS} was drawn from the set of regressions previously performed,

and the indirect effect *via* REE_{RES} was gauged by regressing REE_{RES} on allele dosage, and repeating the regression of BFP_{AS} on dosage with additional adjustment for REE_{RES}. All models were additionally adjusted for genotyping array and the four genomic PCs, as previously. Mediation was formally quantified using a parametric Sobel-Goodman test, comparing the direct and indirect effect (*via* REE_{RES}) of the variant on BFP_{AS}.

Sensitivity analyses To increase the statistical power and robustness of mediation analyses, standard errors and the indirect effect of rs3817334 on BFP *via* REE_{RES} were bootstrapped (1000 iterations, case resampling) to produce normal distribution-based, percentile-based and bias-corrected 95% confidence intervals, in line with best practice for assessing mediation.

5.3 Results

Accounting for age and sex, whole-body REE (kJ/24hr) was associated with higher BMI (β = 2.93 kg/m^2 per SD increase in REE, p<5$\times10^{-300}$). After removing the variance in REE attributable to BMI by residualisation (REE_{RES}), no statistical association existed between REE_{RES} and BMI (p=1.00), and REE_{RES} was normally distributed, suggesting that the linear model applied provides a measure of REE adequately adjusted for the important effect of body size on REE, and offers a good indication of whether an individual has a particularly high or low REE given their size. Importantly, higher REE_{RES} was associated with lower BFP (β=-0.58% per SD increase in REE_{RES}, p=2.53$\times10^{-11}$, consistent with the hypothesis that low REE normalised for body size is an aetiological factor for higher body fat accumulation.

Of the 95 variants considered, only one associated with REE independently of age and sex after accounting for multiple testing (rs7138803, β=102.6 kJ/24hr per BMI-increasing allele, p=3.93$\times10^{-5}$, Supplementary Table 26. This locus (*FAIM2*) was also one of the most significantly-associated with higher BMI (p=8.08$\times10^{-5}$). On adjustment of REE for BMI, four variants were associated with REE_{RES} at nominal significance (p$\leq$0.05), including rs7138803 (β=49.93, p=0.02), and variants in or near *CALCR*, *ERBB4* and *FPGT-TNNI3K*. One variant (rs3817334, *MTCH2*) survived Bonferroni correction and was associated with a decrease of 73.72 kJ/24hr in REE_{RES} per BMI-increasing allele (p=4.65$\times10^{-4}$). All five variants associated with REE_{RES} had consistent directions of effect between the age and sex-adjusted model, and after additional adjustment for BMI. Of the five, only the *MTCH2* and *FAIM2* loci were associated with BMI or BFP after accounting for age and sex. Aggregated dosage across all 95 variants expressed as an additive genetic risk score was strongly associated with higher REE_{AS}, BMI and BFP, but showed no statistical association with REE_{RES}, highlighting the extent to which the association with higher REE_{AS} is likely driven by larger body size (Supplementary Table 26).

For REE to be considered a possible mediator of genetic adiposity risk (higher BFP), BMI-increasing variants must be associated with both BFP and REE. To ensure adequate power, we restricted downstream mediation analyses to variants associated with REE_{RES} after accounting for multiple testing, and nominally associated with BFP. Only rs3817334 fulfilled this criterion (β_{BFP}=0.24% per BMI-increasing allele, p=0.023), and was taken forward for statistical examination as a mediator.

5.3.1 A variant near *MTCH2* predisposes to adiposity *via* lower REE

Using Sobel's test, we observed evidence for partial mediation of the genetic effect of rs3817334 on BFP by REE_{RES} ($p_{Mediation}$=1.39$\times10^{-3}$). This association was independent of the underlying correlation between body size and REE. Specifically, higher genetically-determined BFP at rs3817334 was mediated by lower REE ($\beta_{Indirect}$ of rs3817334 on BFP via REE_{RES} = 0.033% per additional BMI-increasing allele,

Table 5.1 | Mediation analyses of genetic risk on body fat percentage

	REE_{RES} (kJ/24hr)			BFP (%)			BFP *adj.* REE_{RES} (%)			Mediation		
	Beta	SE	p-value	Beta	SE	p-value	Beta	SE	p-value	p_{Sobel}	Beta	SE
rs3817334												
	-73.72	21.05	4.65E-04	0.24	0.11	0.023	0.207	0.105	0.049	1.39E-03	0.033	0.010

REE_{RES} is REE residualised for age, sex, BMI (kg/m^2), ambient temperature during calorimetry, calorimeter device ID, and OGTT test status (Y/N). Betas are effect per BMI-increasing allele as defined from GIANT Consortium meta-analyses, in the units indicated. In mediation analyses, Beta and SE refer to the indirect additive effect per BMI-increasing allele on BFP *via* REE_{RES}.

95% CI 0.013, 0.053%), corresponding to approximately 13.7% of the genetic predisposition to higher BFP at rs3817334 being transmitted through REE_{RES}.

5.3.2 Sensitivity Analyses

In sensitivity analyses, we sought to improve power in our mediation analyses by bootstrapping to generate non-parametric standard errors and 95% CIs of the indirect effect of rs3817334 on BFP *via* REE_{RES}. Bias-corrected and percentile-based 95% CIs were not materially different from normal-based CIs, and did not alter interpretation.

5.3.3 Functional profiling of the *MTCH2* locus

To examine the effect of rs3817334 on gene expression, we performed a look-up of the variant in the GTEx resource, which has systematically identified expression quantitative trait loci (eQTLs) for genes in a range of human tissues. The BMI-increasing allele (T) at rs3817334 was associated with higher MTCH2 transcript levels in skeletal muscle. Using data from the Exome Aggregation Consortium (ExAC)[280], we additionally identified a common missense variant in *MTCH2* (rs1064608)) which is in strong LD with rs3817334. (r^2=0.80 in 1000G Phase 3 CEU reference panel).

5.4 Discussion

Our study is the first to systematically assess the role of REE as an aetiological factor across all established genetic risk loci for obesity. We report that genetic risk for increased adiposity at rs3817334 - an intronic variant in *MTCH2* - is mediated in part by lower residual REE after accounting for the known correlations between REE and body size.

MTCH2 encodes mitochondrial carrier homolog 2, a transport protein localised to the outer mitochondrial membrane with an established role in apoptotic signalling[281], and a repressor of oxidative phosphorylation in haematopoietic stem cells[282]. *MTCH2* knockout in mouse skeletal muscle protects against diet-induced obesity through increased energy expenditure mediated by upregulation of oxidative phosphorylation and increased mitochondrial mass, and also promotes resistance to hyperinsulinemia[283]. Correspondingly, overexpression in rodents is correlated with diet-induced hyperglycaemia and lipid accumulation[284]. In humans, the BMI-increasing allele (T) of rs3817334 is correlated with higher expression of MTCH2 in skeletal muscle ($p_{GTEx}=1.05\times10^{-5}$)[165], providing directional consistency of *MTCH2* transcript levels and observed effect on adiposity and REE between functional models and our large population-based human sample. Further, rs3817334 is in strong linkage disequibilibrium (r2 = 0.81 in Europeans) with a known missense variant (rs1064608) in *MTCH2*, which is again an established eQTL for *MTCH2*

The common BMI signal in *FTO* (rs1558902 from Locke *et al*[249]) has recently been reported to influence adipocyte differentiation and regulate adipocyte browning and thermogenesis in animal models and human cell lines[241]. The lack of association between this locus and REE in our data (REE_{RES} β=-2.14 kJ/24hr per BMI-increasing allele, p=0.92) provides a clear indication that these observations are not translated to a meaningful correlation with REE at population level once REE has been normalised to body size. In agreement with previous population-based work in smaller cohorts[276], our findings do not support the hypothesis that *FTO* influences adiposity via REE, after appropriate adjustment for body size. Rather, given the body of evidence which supports a role for *FTO* variation in regulation of appetitive traits, it would seem that the locus near *FTO* primarily confers risk for obesity through an increased behavioural propensity for higher energy intake.

Equally, our observations for the BMI locus including *MC4R* (lead SNP rs6567160, REE_{RES} p=0.71) are not consistent with the energy balance phenotype of *MC4R* characterised by loss-of-function variants in Pima Indians in whom loss of *MC4R* predisposes to obesity through lower REE[103]. Discussion continues over whether *MC4R* functional variants influence BMI through energy expenditure or hypothalamic control of energy intake[285]: our findings for the common non-coding BMI-associated locus near MC4R contribute to this debate.

Only a subset of the known BMI variants associate at statistical significance with BMI in our sample; we are, therefore, likely underpowered to detect underlying associations with REE for some variants.

For variants of large effect (including *FTO* and *MC4R*), which are associated with BMI in this sample, it is reasonable to assume that we retain adequate power, and our results are informative, however. Nonetheless, this sample represents the largest cohort with objectively assessed REE currently presented in literature. To facilitate replication of our findings and increase power to investigate the aetiological role of REE in genetic risk for obesity, additional work in other cohorts with REE measurements and pooled analyses incorporating all available data will be required.

It should be noted that the association between REE and body size is complex and bidirectional: whilst it is hypothesised that lower REE drives increased fat deposition through the creation of an energy surfeit, larger body size may conversely increase REE, possibly even masking an underlying aetiological mechanism linking lower REE to adipose accumulation. The optimal approach to modelling REE independent of body size remains a topic of debate in the literature[276], but the lack of association between REE_{RES} and BMI in our analyses provides some confidence that our approach provides a measure of REE independent of body size, which indicates whether an individual has a high or low REE for their size. The bidirectional relationship between REE and body size also makes mediation analyses particularly challenging, as formal assessment of mediation requires there to be an association between the hypothesised mediating phenotype and the outcome phenotype of interest. In a model in which REE is adjusted for BMI, therefore, it is impossible to consider REE as a mediator for genetic risk for higher BMI directly. Instead, in this chapter, I have applied DXA-derived body fat percentage to allow the mediating effect of REE normalised to body size in genetic predisposition to increased adiposity to be examined. BMI variants drive body size substantially through adiposity[286], and the two phenotypes are correlated. Given that a reduction in REE resulting in energy surfeit is hypothesised to induce weight gain through increased fat deposition, considering BFP as an outcome is arguably superior to an aggregated measure such as BMI. Our results should, however, be interpreted with care and in the context of further work due to the risk of collinearity and other statistical artefacts. In addition, the extent of mediated effect described here (13% of genetic risk for adiposity at one SNP) is small, and, whilst informative, must be judged cautiously pending independent replication and expanded analyses. This work demonstrates for the first time in a large human population-based sample that known genetic risk for adiposity (modelled as BFP) may operate partly through decreased REE, and informs current debate on the mechanistic role of BMI risk loci in energy balance. We additionally demonstrate in the largest sample of objectively-measured REE to date that the previously-suggested mechanistic basis by which *MC4R* and *FTO* influence obesity through REE (observed in rodent models and cell lines) does not appear to be upheld in large-scale human populations.

5.5 Contributions

The full list of individuals who have contributed to the work presented in this chapter is as follows:

Tom White, Søren Brage, Kate Westgate, Robert A. Scott & Nick J. Wareham

D.J.W. Conceived the project, derived REE analytical phenotype, ran primary analyses, interpreted and presented findings.

Indirect calorimetry measurements and technical assistance with REE derivation as presented in the previous chapter: T.W., S.B., K.W. Conceived the project, provided guidance and oversight throughout: R.A.S., N.J.W.

Chapter 6

Identifying and Applying Genetic Determinants of Y-Chromosome Mosaicism as a Novel Marker of Ageing

Chapter Published as

Wright D.J.⋆, Day F.R.⋆, Kerrison N.D.⋆, Zink F.⋆ *et al.* (2017). Genetic variants associated with mosaic Y chromosome loss highlight cell cycle genes and overlap with cancer susceptibility. Nature Genetics. 49, 674-679.

The Y chromosome is frequently lost in haematopoietic cells, representing the single most common somatic aneuploidy amongst men, and is increasingly recognised as a biological marker of ageing. Recent reports suggest that mosaic loss of chromosome Y (mLOY) is a risk factor for malignancies and cardiometabolic dysfunction, yet the mechanisms that regulate mLOY, and its clinical relevance, are unknown. In this chapter, Y chromosome intensity data, as well as sequence reads from 85,542 men were applied to identify 19 genomic regions ($p \leq 5 \times 10^{-8}$) associated with mLOY. Cumulatively, these loci predicted X chromosome loss in women (n = 96,123; $p = 4.0 \times 10^{-6}$). Additional epigenome-wide methylation analyses using whole blood highlighted 36 differentially-methylated sites associated with mLOY. The genes identified converge on aspects of cell proliferation and cell cycle regulation, including DNA synthesis (*NPAT*), DNA damage response (*ATM*), mitosis (*PMF1, CENPN* and *MAD1L1*) and apoptosis (*TP53*). We highlight the shared genetic architecture between mLOY and cancer susceptibility, in addition to inferring a causal effect of smoking on mLOY. Collectively, our results demonstrate that intensity data from commercial genotyping arrays in extensive use enables a measure of cell cycle efficiency at population scale, offers a novel indicator of biological ageing, and identifies genes implicated in aneuploidy, genome instability and cancer susceptibility. This chapter contains work completed in collaboration with a number of internal and external colleagues. Contributions are detailed at the end of this chapter.

6.1 Introduction

Post-zygotic errors in cell division that result in too few or too many chromosomes in somatic daughter cells have been described for over a century: a cytogenetic feature known as aneuploidy. Although a well-established feature of human cancer cells[287,288], it remains unclear whether aneuploidy is a cause or consequence of tumorigenesis[287–291]. Research into the molecular mechanisms of aneuploidy has focused largely on the role of mitosis and mitotic checkpoint signaling, primarily in cellular and animal models[287,292]. Recent human genomic studies have shown that aneuploidy can be estimated using chromosome intensity data derived from standard genotyping arrays; an approach that has been validated by DNA sequencing[131,132,293]. These population-based studies have demonstrated that mLOY is more frequent than other mosaic chromosomal and structural alterations, exceeding the frequency of X chromosome mosaicism, the next most-common aneuploid event, by an order of magnitude. Detectable Y mosaicism in blood correlates with chronological age comparably to mean leukocyte telomere length (LTL)[294], with prevalence reaching 20% amongst men aged >80 years[131]. Such prevalence clearly reflects the capacity of some somatic cells to survive without the Y chromosome, and highlights mLOY as a potential model system of severe yet well-tolerated aneuploidy in blood, and a novel biological marker for ageing.

Although mLOY is a common feature in the general population, whether it is relevant to disease susceptibility, or whether cells in tissues other than peripheral blood undergo similar rates of chromosomal loss, remains unclear. Population studies have identified correlations between mLOY and smoking status, an association that seems to be transient and reversible after smoking cessation[135]. Such epidemiological studies have also identified associations with non-haematological cancers[131,293], Alzheimer's disease[127] and type 2 diabetes[134]; however, these observations are inconsistent[132] and possibly subject to confounding or reverse-causality.

The ability to assay a common measure of aneuploidy in large array-genotyped populations could facilitate the systematic identification of variants and genes involved in cell division errors. This would, in turn, enable a better understanding of the mechanisms involved and of the potential causal consequences of aneuploidy on cancer risk and other morbidities, which may subsequently be inferred using Mendelian randomisation approaches. To date, a single genetic association with mLOY near *TCL1A* has been reported (n = 12,369), suggesting that germline variation influencing mosaic chromosome loss can be detected[132]. Here, we used data from up to 85,542 men in UK Biobank and two further European cohorts to highlight widespread genomic, transcriptomic and epigenetic signatures of mosaic Y chromosome loss, and demonstrate that this approach concordantly identifies genes implicated in cell cycle regulation, genome instability and cancer susceptibility.

6.2 Methods

Estimation of Y chromosome mosaicism mLOY was estimated in the May 2015 genotyping release of UKB by calculating the normalised average signal intensity of all SNPs on the male-specific region of the Y chromosome (MSY)[295]. Signal intensity, genotype call and confidence files from genotyping (Affymetrix Power Tools) were analysed using the PennCNV-Affy pipeline[296] to generate a log-R ratio (LRR) for each SNP. SNPs without LRR calculable on both arrays, or those flagged by UKB as QC failures, were excluded. Fluorescence signal of the whole Y chromosome was summarised as the mean LRR across all Y chromosome SNPs (mLRR-Y). After omission of monomorphic variants and of genotyping and QC failures, 253 SNPs were available across all participants for the calculation of mLRR-Y.

Genetic discovery and signal selection Autosomal SNPs were analysed for linear association with the derived mLRR-Y phenotype by linear mixed models implemented in BOLT-LMM, adjusting for age and an indicator of genotyping array as covariates. This method has particular advantages regarding robustness to cryptic relatedness and population structure, as previously discussed. Analyses were restricted to white Europeans as defined using a K-means clustering approach applied to the first four genomic principal components, and ratified by self-reported ancestry. A maximum of 67,034 men with intersecting genotyping and mLRR-Y were available for analysis. SNPs with imputation quality <0.4 or MAF <0.1% were excluded after analysis. Independent loci were defined on the basis of proximity using a 1Mb window centred on the index. Fifteen independent loci were omitted from further consideration in downstream analyses due to concerns of technical artefact. Each of these 15 loci fulfilled at least two of the following criteria: (i) singletons in regional association plots, (ii) statistically significant association with genotype array status, and/or (iii) association with mLRR-Y in female samples, suggesting that the association observed in men was primarily with technical background intensity, as opposed to true physiological variation.

Signal follow-up & replication Replication was performed in two large independent populations using techniques complimentary to the discovery effort. The first comprised 9,793 men drawn from the EPIC-Norfolk subcohort, in whom mLRR-Y was derived from array intensity data as detailed above for UKB. Secondly, genome sequences from 8,715 Icelandic men in the deCODE study[297] (age range 41-105 years, mean 63 years) who had provided whole blood for sequencing (Illumina) to a mean depth of 37$\times$ were analysed. In the deCODE sample, the average read depth over chromosome Y (restricted to X-degenerate regions[295]) was interpreted as an estimate of Y copy number. Read depth was calculated by our Icelandic colleagues in SAMtools[298] using PLINK .bam-files aligned to hg38 and normalised relative to genome-wide sequencing coverage within each participant. Twelve individuals with copy number estimates >1.25 for chromosome Y were excluded. Y chromosome copy number was strongly negatively

correlated with age at blood draw (Spearman's ρ=0.50). For individuals older than 60 years at the time of sample collection, the distribution of chromosome Y copy-number had a heavy negative skew, with copy numbers as low as 0.08.

Genome-wide association adjusted for chronological age at blood draw was run in BOLT-LMM for both replication samples. deCODE copy number estimates were inverse normalised prior to analysis, and effect sizes for $\log_2$(Y copy number) were estimated *via* robust linear regression (rlm funtion from MASS R package[299]) to enable comparison with effect estimates obtained from array intensity-derived mLRR-Y in UKB and EPIC-Norfolk. The fraction of variation explained by a given variant was calculated as $2fa^2(1-f)$ where f denotes the minor allele frequency of the variant,and a is the additive effect expressed in standard deviations. An upper limit of heritability for Y mosaicism was estimated in deCODE as the Spearman rank correlation of derived Y copy number (as opposed to mLRR-Y) between sibling pairs (n=1,488), an approach commonly applied in this cohort[300–302].

Determinants of X chromosome loss Female X chromosome mosaicism was estimated by an equivalent protocol to mLOY, using array intensity data in UKB (n=75,595) and EPIC-Norfolk (n=11,248), in addition to sequence reads in 9,302 deCODE women with a mean sequencing depth of 36$\times$. As for Y, X chromosome copy number was estimated from average read depth over the X chromosome, excluding the pseudoautosomal regions *PAR1* and *PAR2*, the X-transposed region[295], and the centromere. This estimate was normalised against the participant's sequencing coverage across the genome and adjusted for sequencing protocol. Twenty-two outliers with non-physiological copy numbers (X copy number >2.5, or <1.5) were excluded. X Copy number was negatively correlated with age at blood sampling (Spearman's ρ = -0.28).

Methylation analyses DNA methylation in whole blood was measured in EPIC-Norfolk (n=1,378) using the Human Methylation 450k BeadChip (Illumina), a widely-applied array covering 96% of human genes with multiple probes, and 99% of characterised CpG islands across the genome, to facilitate high-throughput hypothesis-free analysis of the human methylome[303]. After setting methylation markers with detection p-value $\geq$ 0.01 to missing, methylation beta values were calculated for each marker. Quantile normalisation of methylation betas was applied separately to different marker groups based on colour channel, probe type and M/U subtypes[304]. Samples with a sample call rate $\leq$0.99 were removed (n=77). Methylation beta value distributions of the X, Y and autosomal chromosome markers were analysed separately and a further 11 sample outliers were excluded. Within each sample, markers with a marker call rate $\leq$0.95 were excluded (n=4,423).

All downstream analyses were restricted to autosomal methylation markers. Signal detection of methylation intensities can be affected by several factors, including SNPs on the probe, repetitive DNA, and

cross-reactive probes. We thus calculated the proportion of missing data at each CpG site (marker call rate); 8,775 CpGs with a call rate $\leq$0.95 were excluded. 3,295 CpGs with multimodal distributions of methylation intensities, identified by the R package ENmix[305], which typically arise from technical artefacts were also excluded. A further 18,874 CpG sites which were previously identified as mapping to more than 1 genomic location[306] were also excluded. The final cleaned dataset comprised 442,920 autosomal CpG sites. To account for cell composition variability, we estimated counts of T lymphocyte subtypes, natural killer cells, monocytes, granulocytes and B lymphocytes using the minfi R package[307,308]. These were included as covariates in subsequent epigenome-wide regression models.

To examine the association between methylation markers and mLOY, we performed an epigenome-wide association analysis in all male EPIC-Norfolk methylation samples (n=569). mLRR-Y was regressed separately on each methylation marker, adjusted for type 2 diabetes status, age, current smoking status, estimated cell counts, and sample plate. Bonferroni correction was applied, accounting for the number of markers tested ($p=1\times10^{-7}$). Furthermore, we checked that no significant CpG sites had sequences which also mapped to the Y chromosome.

Association statistics for genetic variants within the probe vicinity and corresponding methylation levels (i.e cis-meQTLs) were available from the BIOS QTL browser (http://www.genenetwork.nl/biosqtlbrowser/)

Genetic susceptibility to all-cause cancer To understand the shared genetic architecture of mLOY and cancer, an 'any prevalent cancer' variable was defined in UKB using linked NHS cancer registrations. The UK's system of mandatory cancer registration provides not only complete and systematic ascertainment of cases, but also a rigorous case definition, minimising potential for ascertainment biases. Cases were defined as individuals with a recorded date of diagnosis and corresponding diagnostic codes; controls as individuals with neither a cancer registration nor self-reported cancerous condition. Participants with inconsistent diagnostic details (e.g. a recorded diagnostic code, but no corresponding age at diagnosis) were set to missing to avoid heterogeneity of definition. GWAS analysis was performed in BOLT-LMM, including age, sex, and genotyping array as covariates.

Bidirectional associations with ageing, cancer and cardiometabolic risk Genetic correlations (r_g) between mLRR-Y and summary statistics for (i) cancer risk defined from UKB, (ii) hand grip strength, parental longevity and multi-site BMD as indicators of functional and biological ageing, and (iii) type II diabetes status, CHD risk, basic anthropometric traits and continuous intermediate glycaemic phenotypes as markers of cardiometabolic dysfunction, were calculated by LD-score regression. Hand grip strength analyses leveraged the summary statistics generated in Chapter 3. Summary statistics for other traits were obtained from the latest publicly-available European consortium meta-analyses, prioritising sample size over latest date of publication where multiple efforts existed. References for each phenotype are

detailed in the main text, Table 6.2

To assess the possible causal links between mLOY and cancer, and establish directionality in the potentially confounded associations with cardiometabolic conditions, two-sample summary statistic MR was applied using the 15 biallelic replicated mLOY signals as an additive (per-allele) instrument to model mLRR-Y as a causal exposure. Due to the complexities of applying insertion-deletion variants in MR either directly or *via* an assigned proxy, these variants were omitted. In bidirectional analyses, fasting insulin (17 variants)[309], fasting glucose (29 variants)[309], HbA_{1c} (11 variants)[310], BMI (96 variants)[249] and type 2 diabetes case-control status (49 variants)[311] were modelled as causal exposures for mLOY using previously reported biallelic risk loci at $p \leq 5 \times 10^{-8}$. Due to the considerable heterogeneity of cancer pathologies and the relative lack of genome-wide summary statistics for site and tissue-specific cancers, bidirectional cancer analyses were restricted to considering prostate cancer as a causal exposure, based on 90 published susceptibility loci[312,313]. Main IVW models, as well as sensitivity estimators robust to heterogeneity, partial invalidation of instrumental variable assumptions, and directional pleiotropy, were run as previously detailed (Chapter 2.

Further analyses for biological insight Replicated loci were looked up in HaploReg for eQTL associations and other functional annotations, and imputed expression analyses leveraging genetically-predicted gene expression were run in whole blood and multiple GTEx tissues using the three methods - SMR, MetaXcan and TWAS - previously described. Hypothesis-free GSEA was implemented in MAGENTA using the canonical pathways and GO Terms downloaded from mSigDB. Study-wise significance was determined when an individual pathway reached a false discovery rate (FDR) <0.05 in either MAGENTA's 95% or 75% significance threshold (see Chapter 2. In total, 3216 pathways from Gene Ontology, PANTHER, KEGG and Ingenuity were tested for enrichment of multiple modest associations with mLRR-Y.

Table 6.1 | Nineteen mLOY loci reaching genome-wide significance in combined analyses

					UK Biobank n=67,034		EPIC-Norfolk n=9,793		deCODE n=8,715			
rsID	Chr.	EA	AA	EAF	Effect [A]	p	Effect [A]	p	Effect [B]	p	$p_{Combined}$	Gene
rs17758695	18	C	T	0.97	-0.010	6.4E-21	-0.014	3.7E-04	-0.020	9.1E-13	1.3E-33	*BCL2*
rs1122138	14	C	A	0.84	-0.005	3.6E-23	-0.006	4.3E-04	-0.007	1.5E-04	6.3E-31	*TCL1A*
rs78378222	17	G	T	0.01	-0.013	1.3E-15	-0.032	1.8E-06	-0.026	3.8E-10	3.4E-28	*TP53*
rs59633341	3	D	I	0.16	-0.004	2.6E-18	-0.009	7.5E-07	-0.007	1.1E-05	4.1E-28	*TSC22D2*
rs2736609	1	T	C	0.36	-0.003	1.9E-12	-0.003	4.9E-02	-0.006	2.5E-07	2.0E-19	*PMF1* *SEMA4A*
rs13191948	6	C	T	0.54	-0.002	1.2E-11	-0.006	5.4E-06	-0.005	3.8E-05	2.2E-19	*SMPD2* *CCDC162P*
rs60084722	20	I	D	0.79	-0.003	6.6E-13	-0.002	2.5E-01	-0.006	9.4E-05	1.6E-17	*TPX2* *BCL2L1* *HM13*
rs381500	6	C	A	0.55	-0.002	5.7E-11	-0.002	1.9E-01	-0.005	1.1E-07	5.0E-16	*QKI*
rs56084922	5	G	A	0.08	-0.005	2.9E-13	-0.004	1.2E-01	-0.005	1.6E-03	3.0E-15	*NREP*
rs137952017	14	D	I	0.85	-0.003	1.2E-09	-0.010	1.3E-07	-0.004	4.0E-04	4.0E-15	*DLK1*
rs4721217	7	T	C	0.4	-0.002	6.5E-10	-0.005	2.8E-04	-0.003	1.1E-05	3.5E-14	*MAD1L1*
rs35091702	8	D	I	0.74	-0.002	4.2E-10	-0.004	6.0E-03	-0.002	3.9E-02	9.5E-12	*RBPMS*
rs4754301	11	A	G	0.55	-0.002	1.3E-09	-0.001	5.4E-01	-0.002	2.8E-02	6.5E-11	*NPAT* *ATM* *ACAT1*
rs12448368	16	C	T	0.13	-0.003	9.8E-10	-0.002	2.5E-01	-0.003	2.4E-02	7.1E-11	*CENPN* *ATMIN*
rs11082396	18	C	T	0.13	-0.003	3.3E-09	-0.004	6.7E-02	-0.003	1.2E-01	1.2E-10	*SETBP1*
rs13088318	3	G	A	0.34	-0.002	4.1E-09	0.000	7.7E-01	-0.003	1.7E-02	2.7E-10	*SENP7*
rs77522818	17	A	T	0.96	-0.005	1.3E-09	-0.004	3.0E-01	-0.002	2.4E-01	8.8E-10	*FAM117A*
rs10687116	13	I	D	0.8	-0.002	2.6E-08	-0.001	5.8E-01	-0.003	5.8E-02	8.8E-10	*WBP4*
rs115854006	3	C	T	0.96	-0.006	3.7E-08	-0.007	5.4E-02	0.002	9.3E-01	4.5E-08	*TREX1* *PLXNB1*

[A] Change in mLRR-Y per additional effect allele; [B] Change in copy number-transformed $\log_2$(Y copy number) per additional effect allele. Results are ordered by combined p-value, which reflects meta-analysis of associations across all studies. Insertion-deletion variant alleles are denoted I/D. Unless otherwise specified, gene shown is nearest gene to the index variant, or a candidate gene falling within the locus. Red highlight, index or one of its proxies ($r^2 \leq 0.8$) is a non-synonymous coding variant in the gene. Blue highlight, expression of gene is mediated by mLRR-Y associated SNPs. EA, effect allele; AA, alternative allele, EAF, effect allele frequency

6.3 Results

As a proxy for mLOY, mean intensity log-R ratio of all array-genotyped Y-chromosome SNPs (mLRR-Y) was estimated in a sample of 67,034 male participants from the interim genotyping release of UKB[138]. Further details of this derivation can be found in Methods. A normal distribution centred around zero was observed (standard deviation = 0.067), with negative values indicating reduced Y chromosome abundance in the clonal blood cell population (Supplementary Figure 11).

Consistent with previous reports[132,135,294], a strong negative correlation was observed between mLRR-Y and age (r=-0.21). 'Ever smoking' status (defined as self-reported current or former tobacco smoking) was also observationally associated with lower mLRR-Y (i.e. higher mLOY; $p=3.05\times10^{-82}$), and in combination with age explained 4.74% of the trait variance (age alone = 4.45%). To demonstrate the causal relationship between smoking and mLOY, we applied the principles of Mendelian randomisation, using an established and widely-utilised genetic instrument for smoking frequency[314]. By modelling genetic variants robustly associated with smoking volume (cigarettes per day) at the *CHRNA5-CHRNA3-CHRNB4* locus, which encodes various subunits of the major cholinergic nicotine receptor, we inferred a causal effect of smoking on decreased mLRR-Y in UKB (rs1051730 p=0.03; $p_{never\text{-}smokers}=0.41$; $p_{ever\text{-}smokers}=0.04$). This genetic association was confirmed in independent replication samples (EPIC Norfolk plus deCODE; combined n=18,508, replication p=0.009, discovery plus replication overall p=0.004).

6.3.1 Many autosomal variants are associated with mLOY

To identify novel genetic variants associated with mLOY, we performed a genome-wide association study of mLRR-Y as a quantitative trait in UKB. After stringent quality control (see Methods), the most significantly-associated SNPs were located at the previously reported[132] mLOY locus, *TCL1A* ($p=3.6\times10^{-23}$). We additionally identified a further 18 novel signals at genome-wide significance ($p\leq5\times10^{-8}$), with no evidence for significant inflation of test statistics genome-wide ($\lambda_{GC}=1.05$, Supplementary Figures 12 and 13). Replication was subsequently performed in an independent set of 9,793 men with array intensity data, in addition to 8,715 men from deCODE with Y loss estimated using sequence read abundance (see Methods). Both replication datasets provided strong statistical support for the identified loci, with all 19 loci retaining genome-wide significance in a combined model (Table 6.1). As evaluated in the deCODE data, these loci cumulatively explained 2.7% of total variance in Y chromosome copy number. Overall heritability was estimated at 34% (95% CI 25.2%, 42.4%), suggesting many additional associated variants of modest or small effect remain to be discovered.

HaploReg[247] and sequence data from the deCODE cohort were next applied to functionally annotate identified variants and genes. Four genes containing missense variants in strong linkage with the index signal

were highlighted, implicating *MAD1L1* (rs1801368, r^2>0.98), *PMF1* (rs1052053, r^2=1), *NREP* (rs11559, r^2=0.74) and *NPAT* (rs2070661, r^2=0.97) as potential functional candidates.

Genome-wide pathway analyses conducted on association results for continuous mLRR-Y highlighted five pre-defined biological pathways enriched for association (FDR<0.05), the most significant of which was 'Apoptosis', defined per the Kyoto Encyclopaedia of Genes and Genomes (KEGG). Other significant pathways (all defined from KEGG) included susceptibility to colorectal, prostate and thyroid cancers, and progesterone-mediated oocyte maturation.

6.3.2 Identified variants determine Y loss rather than gain

To ascertain whether mLRR-Y signals more likely reflect gain or loss of Y chromosome material, two analyses were run, comparing the bottom and top 5% of mLRR-Y ranked individuals to the median 25% (i.e. those falling between the 37.5th and 62.5th percentiles), as a dichotomous indicator of extreme Y-chromosome loss or gain, respectively. All nineteen loci exhibited consistently stronger associations with the odds of falling within the bottom 5% of mLRR-Y (i.e. greatest degree of mLOY) than the top 5% (Supplementary Table 27), suggesting that their effect is predominantly on mosaic Y chromosome loss. Analysis of mLRR-Y as a continuous trait across all individuals, however, remained the most powerful approach for variant discovery, as only two of the signals reached genome-wide significance in the dichotomised analysis (Supplementary Table 27).

6.3.3 mLOY variants influence X chromosome loss in women

To establish whether mlRR-Y signals acted only on the Y chromosome in a male-specific manner, or more generally promoted aneuploidy across chromosomes and the sexes, we considered the combined effect of the mLOY variants on mosaic loss of X chromosome (the next most common aneuploidy at population-level) in women. Using a combined sample of 96,123 women from the three study cohorts, and an equivalent approach to that used to ascertain mLOY, we quantified X chromosome loss both *via* array intensity data modelled as mean log-R ratio of X (mLRR-X; n=86,843 from UKB and EPIC-Norfolk), and sequence reads in deCODE (n=9,280, Figure 6.1). Heritability of X chromosome copy number was estimated at 26% (95% CI 17.4%, 36.2%) in deCODE; comparable to that of mLOY. Cumulatively, the 19 mLOY variants (aligned to mLRR-Y increasing allele dosage) significantly predicted mLRR-X in women alone, with the anticipated direction of effect, $p=4\times10^{-6}$, Figure 6.2).

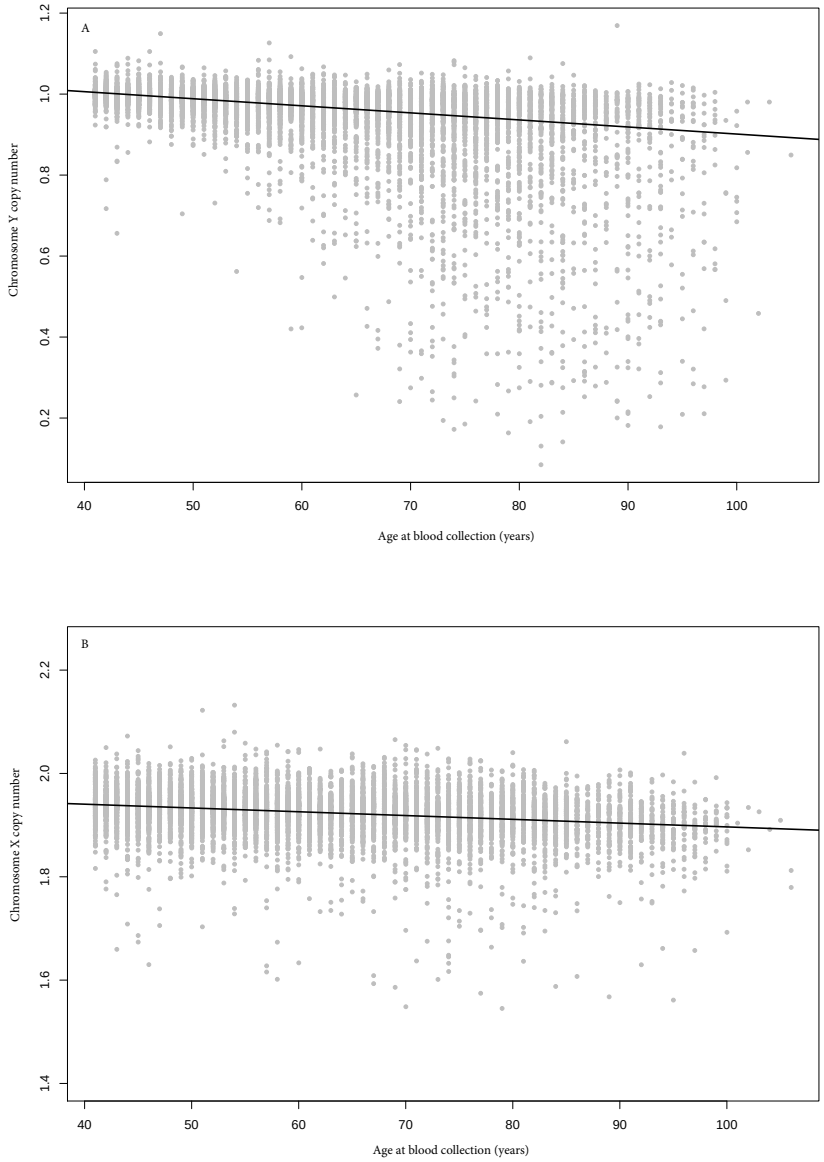

Figure 6.1: Estimated X and Y chromosome abundance with age in the Icelandic deCODE cohort. (A) Average Y chromosome copy number in 8,703 males. (B) Average X chromosome copy number in 9,280 females. In each case, copy number is estimated from whole genome sequencing in whole blood. Black line indicates line of best fit with age at blood collection as a linear predictor.

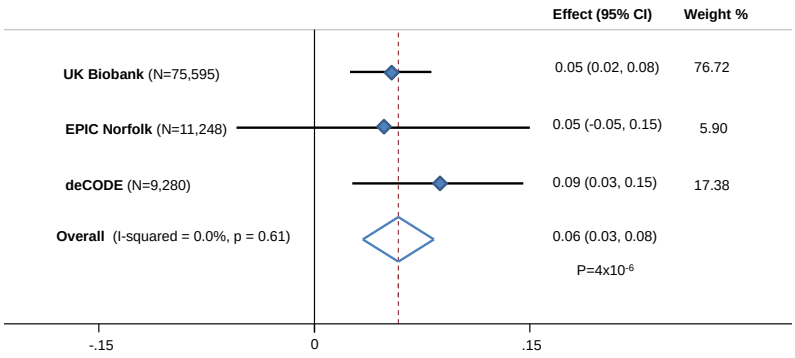

Figure 6.2: Cumulative effect of the 19 mLOY variants on X chromosome loss (higher mLRR-X) in women. 19 variants are modelled as an additive genetic score, aligned to mLRR-Y increasing (mLOY-decreasing) allele dosage

6.3.4 Transcriptomic and epigenetic signatures of mLOY

To identify potential functional transcripts mediating Y chromosome loss, summary statistic approaches to infer gene expression associations were applied, using three analytical imputation approaches[168,169,315], each based on independent whole-blood expression datasets (see Methods). Across these datasets, transcript abundance of eight genes (*HM13, SMPD2, TCL1A, SENP7, NPAT, ATM, ACAT1, CENPN*) was significantly associated with mLRR-Y after conservative Bonferroni correction. All expression signals identified in this way mapped near to one of the 19 associated genetic signals from GWAS (Table 6.1).

Using directly-assessed methylation data in 569 whole blood samples from EPIC-Norfolk, 36 differentially-methylated CpG positions (DMPs) correlated with mLRR-Y were additionally identified (Supplementary Table 28). Of note, all significant DMPs were in genomic regions distinct (>500kb distant) from the 19 original genetic loci, with the single exception of four correlated methylation probes within the *TP53* gene region. To investigate whether the observed DMPs represented causal drivers of mLOY, *cis*-methylation quantitative trait loci (meQTLs) were identified for all associated probes in publicly-available data[316]. In total, 20 probes had one or more genetic variants in *cis* which were associated with methylation levels of the corresponding site (Supplementary Table 29). None of these genetic variants were correlated with the 19 genomic loci; however, one *cis*-meQTL survived multiple test correction for association with mLRR-Y (rs7208523; CpG position cg20116579; meQTL $p=5.6\times10^{-31}$, mLRR-Y $p=9\times10^{-4}$). rs7208523 is 280kB from the GWAS index variant identified at the *TP53* locus (rs78378222), but is in total linkage equilibrium with this variant in 1000G Europeans ($r^2=0.0021$). This finding suggests that genetic variation at the *TNK1* locus, a gene with known involvement in tumor growth and survival[317], may be associated with increased mLOY via an epigenetic mechanism.

6.3.5 Genetic overlap with cancer susceptibility

Three mLOY signals are correlated with signals previously reported for basal cell carcinoma[318], glioma[319], neuroblastoma[320] (*TP53*), or testicular cancer[321,322] (*SEMA4A/PMF1* and *MAD1L1*). In each case, the

Table 6.2 | Genetic correlations of mLRR-Y with selected ageing, cardiometabolic and anthropometric traits

Trait	Author	Ref	r_g	SE	*Z*-score	p-value
Fasting Insulin	Manning, 2012	[309]	0.3396	0.0949	3.5791	0.0003
BMD (Femoral Neck)	Zheng, 2015	[205]	-0.1649	0.0739	-2.2302	0.0257
Paternal Lifespan	Pilling, 2016	[324]	0.2555	0.1219	2.0963	0.0361
BMI	Locke, 2015	[249]	0.045	0.0397	1.142	0.2534
Body Fat	Lu, 2016	[252]	0.0776	0.0695	1.1157	0.2646
Fasting Pro-insulin	Dupuis, 2010	[325]	0.151	0.1482	1.0187	0.3083
Waist Circumference	Shungin, 2015	[251]	0.052	0.0519	1.0011	0.3168
Fasting Glucose	Manning, 2012	[309]	0.0685	0.0762	0.8989	0.3687
BMD (Lumbar Spine)	Zheng, 2015	[205]	-0.0641	0.0757	-0.8465	0.3973
Type 2 Diabetes	Morris, 2012	[311]	0.0526	0.0788	0.6678	0.5043
Maternal Lifespan	Pilling, 2016	[324]	-0.07	0.1157	-0.6054	0.5449
Parental Lifespan	Pilling, 2016	[324]	0.0816	0.1429	0.5708	0.5681
Hand Grip Strength	Willems, 2017	[326]	0.0286	0.0627	0.456	0.6484
BMD (Forearm)	Zheng, 2015	[205]	-0.0672	0.1694	-0.3967	0.6916
HbA1c	Soranzo, 2010	[310]	0.0384	0.1073	0.3578	0.7205
Coronary Heart Disease	Nikpay, 2015	[204]	-0.0152	0.0585	-0.2606	0.7944
Waist-Hip Ratio	Shungin, 2015	[251]	-0.0026	0.0506	-0.0514	0.959

r_g, genetic correlation; SE, standard error of correlation; BMD, bone mineral density; HbA1c, circulating glycated haemoglobin. Note data reflects correlation of the trait with mLRR-Y, for which higher values indicates lower mLOY.

mLRR-Y decreasing allele (i.e increased mLOY) was associated with increased cancer susceptibility. We performed a reciprocal lookup of 90 loci previously reported for prostate cancer susceptibility[312,313] (Supplementary Table 30), the most common male non-skin cancer in western populations. There was no obvious enrichment of signal across these loci and no apparent dose-response relationship between the allelic effects on prostate cancer and mLOY ($p_{MR\text{-}Egger}$ = 0.26, Supplementary Figure 14). Under the hypothesis that susceptibility to many types of cancer may have a common basis in mitotic error, GWAS was run in UKB, defining men with any diagnosed cancer on the basis of linked UK cancer registrations as a case (n= 7,745 cases, 58,562 controls). This approach was recently used for multiple reproductive cancers, yielding several novel loci[323]. Applying the 19 mLRR-Y signals as an additive genetic instrument, there was no evidence of a dose-response relationship between genetically-modelled mLOY and cancer risk in men ($p_{MR\text{-}Egger}$ = 0.94, Supplementary Figure 15). To test the relationship between cancer risk and mLOY more comprehensively, the extent of shared genetic architecture across the whole genome was estimated using LD score regression. This revealed an overall significant inverse relationship between mLRR-Y and cancer risk (r_g=-0.42, p=0.02), which was not significant when considering only female cancer cases (r_g=-0.06, p=0.64).

6.3.6 Genetic overlap with ageing and cardiometabolic indicators

Given that Y chromosome mosaicism is a recognised correlate of age, implicated in cancer, and has been associated with type 2 diabetes, further genetic correlations were run to inform the potential for bidirectional causal inference between mLOY and existing markers of biological/functional ageing and

cardiometabolic dysfunction (Table 6.2). After accounting for multiple testing, we observed some evidence of shared genetic architecture between mLRR-Y and fasting insulin, based on MAGIC Cosortium data (r_g=0.3396, p=3$\times10^{-4}$), suggesting that a greater degree of mLOY shares a common genetic basis with lower fasting insulin.

To investigate directionality of association in the previously-reported association between large clonal mosaicism and diabetes risk[134], two-sample bidirectional MR was applied between mLRR-Y and diabetes status, as well as BMI, and a selected number of intermediate glycaemic markers (fasting insulin, fasting glucose, HbA_{1c}; Supplementary Table 32). No evidence was observed in support of a causal association in either direction between mLOY and diabetes risk or continuous glycaemic status. Lower genetically-predicted mLRR-Y (higher Y loss) was associated with lower BMI (β_{IVW} = -1.15kg/m^2 per unit decrease in mLRR-Y, p_{IVW}=0.016, MR-Egger Intercept p=0.610). A penalised weighted median estimator of the causal effect offered confidence that this association was robust to potential heterogeneity in the mLOY instrument (p_{HET}=0.005, β_{PWM}=-1.29kg/m^2 per unit decrease in mLRR-Y, p_{PWM}=0.034, Supplementary Figure 16), though it should be noted that this association only reached nominal statistical significance ($p \leq 0.05$) and did not survive adjustment for multiple testing (p=0.05/10). BMI was not a reciprocal causal exposure for mLOY in these data (p_{IVW}=0.923)

6.4 Discussion

Our findings, together with previous reports, demonstrate that loss of the Y chromosome in peripheral blood represents a promising new proxy trait for cell cycle fidelity and cellular ageing in large-scale population-based studies, which is highly prevalent and can readily be estimated as a continuous phenotype from sequencing reads or array genotyping data. The nature of the genes identified by these analyses suggests that genetic determinants of mLOY reflect general mechanisms of aneuploidy, which we speculate most frequently manifests as mLOY due to the higher capacity of haematopoietic cells to tolerate Y-chromosome loss. This hypothesis is supported by the observation that these same SNPs also predicted X chromosome loss in women, the second most frequent large-scale mosaic event[327].

Pathway analyses identified enrichment of mLOY associations across the genome for cancer and apoptosis pathways. This is further supported by the many well-established cell cycle regulation genes which we observed either as the closest gene to the association signal, or which were implicated via altered expression or protein coding changes. Major mechanistic aspects of the cell cycle, and key regulators of cell-cycle progression were represented by these findings (Figure 6.3), including elements of three major cell cycle checkpoints, and several genes with complementary functional roles in mitosis. *TPX2, CENPN, PMF1* and *ATMIN* are involved in aspects of chromosome alignment during metaphase, spindle assembly, orientation and attachment to chromatids ahead of segregation[328,329] In particular, *TPX2* re-

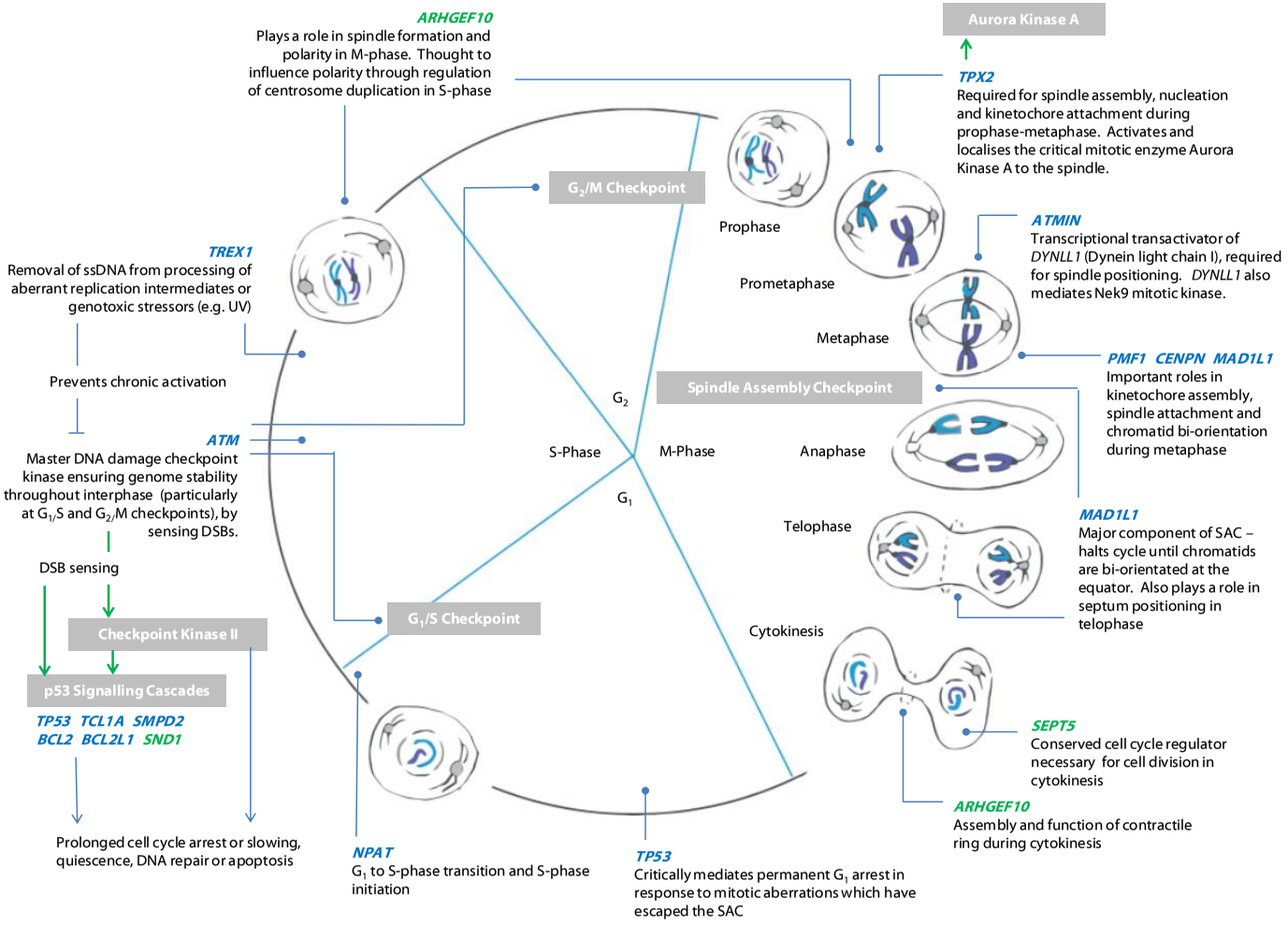

Figure 6.3: Convergence of genes implicated in mLOY on multiple cell cycle processes. Genes falling within GWAS loci are highlighted blue, those implicated by methylation analyses in green. Grey boxes highlight specific checkpoints, signalling cascades, or enzymes of note. Green arrows, activation of a target by phosphorylation; blue arrows, signalling cascade and its ultimate outcome.

cruits the crucial mitotic enzyme, Aurora Kinase A, to the spindle[330], whilst *ATMIN* regulates expression of a dynein motor component (DYNLL1) which critically mediates spindle positioning[331–333] and also modulates Nek9 kinase signalling, required for correct spindle formation and function[334]. Similarly, Rho-GEF 10 (*ARHGEF10*, for which we observe a nearby methylated signal) regulates centrosome duplication and prevents formation of multipolar spindles[335]. We identified a missense variant in *MAD1L1* (MAD1 mitotic arrest deficient like 1), a major component of the spindle assembly checkpoint (SAC). This represents a key cellular safeguard against chromosome mis-segregation (and subsequent ploidy errors), supressing metaphase-anaphase progression until chromatids are bi-orientated on a bipolar spindle at the metaphase plate[287]. During cytokinesis, *SEPT5* (septin 5, implicated in our methylation analysis) encodes a conserved cell cycle regulator required for effective cell division[336], while activation of signalling by Rho-GEF 10 (*ARHGEF10*) facilitates contractile ring ingression to separate the two daughter cells[337].

We also implicated a number of genes with established roles in the replication and stability of nuclear DNA in interphase: replication errors are a key cause of genomic instability and chromosomal fragility[338–340]. G_1 to S-phase transition is dependent on *NPAT*, at least in part through it promoting histone gene transcription[341], while *ATM*, in association with *ATMIN42*, acts as major cell cycle checkpoint kinase dedicated to maintaining genome stability throughout interphase, with particular importance at the G_1/S and G_2/M checkpoints[340]. In response to double-stranded DNA breaks (DSBs) indicative of genomic instability, *ATM* promotes various responses *via* p53 and other factors to promote DNA repair, arrest cell-cycle progression, or otherwise initiate cell cycle exit strategies including apoptosis and senescence[338–340,342]. *TREX1* encodes 3' Repair Exonuclease 1, which digests aberrant replication intermediates and single stranded DNA from genotoxic stress to prevent chronic checkpoint activation[343]. Predicted deleterious missense variants in this gene were recently identified in a mouse GWAS for micronucleus formation, a biomarker of chromosomal breaks, whole chromosome loss and extranuclear DNA[344].

At the later stages of the cell lifespan, several genes implicated by our GWAS findings - including *TP53, TCL1A, SMPD2, BCL2* and *BCL2L1* - functionally impact on apoptotic events[345–349]. Apoptosis is a prime mechanism by which cells with detected DNA damage or ploidy errors may be eliminated[350]: indeed, p53 drives multiple cell-cycle exit responses in response to aberrant mitosis, including G_1 arrest[342,351,352]. The *TP53* variant associated with mLOY in our analyses is the one previously reported for basal cell carcinoma: for this trait, the risk allele changes the AATAAA polyadenylation signal to AATACA, resulting in impaired 3'-end processing of *TP53* mRNA[318]. Our findings also implicated genes involved in spermatogenesis[353,354] (*HENMT1* and *DAZAP1*), and cellular growth and differentiation[355] (*DLK1*).

The genes directly involved in mitotic prophase-metaphase and the SAC have clear roles in averting chromosomal mis-segregation and preventing mis-segregated cells from persisting unchecked; however the mechanisms by which the broader set of genes implicated here may act to promote mLOY remains less clear. We speculate that either many of these genes act in ways that are not currently recognised, or

alternatively that the other highlighted processes outside of cell cycle control and mitosis are important. In particular, as a major mode of cell-cycle exit, the observed enrichment of genes and cascades regulating and effecting apoptosis may play a more passive, permissive, role in enabling mis-segregated cells to survive with ploidy errors, rather than being directly causative of the initial aneuploid event.

Although an initial defect during the cell cycle process is required to generate an aneuploid daughter cell, clonal expansion of the affected progenitor(s) is likely required to drive the lineage to a detectable frequency in the circulating white blood cell population. It is possible that mLOY in haematopoietic precursors confers a proliferative advantage to such cells, leading to a relative enrichment of assayable mLOY progeny. We, therefore, speculate that some loci may operate through this pathway to further facilitate or promote clonal expansion of these cells. Additional functional experimentation in cellular and animal systems is ultimately required to fully elucidate this issue and the role individual associated genes may play in determining mLOY. It is also important to acknowledge that there are likely other, currently unknown, mechanisms by which our associated loci exert their effects.

We observed a substantial shared genetic architecture between mLOY and cancer susceptibility, suggesting that bivariate analyses of these two traits may help to prioritise novel cancer susceptibility loci and elucidate their functions. We were not, however, able to find evidence of a dose-response relationship between these two traits on the basis of MR analyses and reciprocal look-ups. This is perhaps not surprising given that findings from mouse studies in which mitotic checkpoint components are experimentally down-regulated demonstrate an inconsistent relationship between aneuploidy and spontaneous tumorigenesis[287]. It is possible, therefore, that some of our identified genes may promote benign aneuploidy, whereas others may play a role more generally in genome instability. This makes the use of genetic variants associated with mLOY difficult within a Mendelian randomisation framework, as genes with general roles in instability may have different phenotypic consequences to genes that promote aneuploidy in a more stable way.

This of course does not preclude identifying causal risk factors for mLOY. The utility of understanding the underlying genetics of mLOY is exemplified by our positive causal inference for smoking on mLOY, using a genetic instrument for cigarettes per day. More generally, the association between smoking and mLOY suggests that care should be taken to avoid confounding influences such as socioeconomic patterning in epidemiological observations between mLOY and disease. Assuming that the potential for heterogeneity and pleiotropy in the instrument is kept in mind, however, it would seem reasonable to assume that such environmental confounders will be randomised relative to genotype across the 19 mLOY variants. The implication of greater mLOY as a causal exposure for decreased BMI in MR analyses which are (i) robust to heterogeneity and (ii) show no evidence of pleiotropy suggests that our mLOY instrument can be appropriately applied. In this particular case, however, the results should be interpreted cautiously based on its nominal significance ($p \leq 0.05$), which does not survive adjustment for multiple testing. Assuming

that the association is true, it should also be considered that it may to some extent reflect the shared biology of changing body composition, deterioration of muscle mass and the general frailty phenotype which accompanies older age.

In conclusion, our study highlights that estimation of mLOY using genotype array intensity data may serve as a useful quantitative measure of cell cycle efficiency and genome stability, and may thereby add a new approach to the study of cellular ageing and its associations with disease, particularly cancer. In addition to fully evaluating the broader disease relevance of mLOY, future epidemiological studies should look to assess the differential rates at which mLOY changes in individuals over time, its relevance in other tissue types, and further non-genetic modifiable factors which may influence it.

6.5 Contributions

The full list of contributors to the work presented in this chapter is as follows:

Daniel J. Wright, Felix R. Day, Nicola D. Kerrison, Florian Zink, Alexia Cardona, Patrick Sulem, Deborah J. Thompson, Svanhvit Sigurjonsdottir, Daniel F Gudbjartsson, Agnar Helgason, J. Ross Chapman, Steve P. Jackson, Claudia Langenberg, Nicholas J. Wareham, Robert A. Scott, Unnur Thorsteindottir, Ken K. Ong, Kari Stefansson and John R.B. Perry

D.J.W. jointly conceived the project, performed and interpreted main and downstream analyses. Prepared the manuscript in collaboration with colleagues. Oversaw submission and actioned modifications during review process prior to publication.

Jointly conceived the study: J.R.B.P, F.R.D., N.D.K. Statistical analysis: F.R.D., N.D.K., F.Z., A.C., P.S., R.A.S., J.R.B.P. Individual study sample collection, genotyping and phenotyping: S.S., D.F.G., A.H., N.D.K., A.C., F.Z. Individual study principal investigators: C.L., N.J.W., U.T., K.K.O., K.S., J.R.B.P. Project design and interpretation of results: D.J.W., F.R.D., N.D.K., P.S., D.J.T., J.R.C., S.P.J., C.L., N.J.W., U.T., K.K.O., K.S., J.R.B.P.

Chapter 7

Conclusions and Implications

7.1 Summary of Objectives and Findings

Ageing is a composite process of multiple interacting phenotypes spanning from the cellular to whole-organism level, and including changes in muscle tropism, functional indices, aspects of metabolism, genomic stability, and cellular physiology. As well as being informative markers of ageing, many of these phenotypes are also important endpoints in their own right. On the basis that direct study of the composite phenotypes of ageing might allow more direct biological insight into the association between ageing and disease, this PhD set out to conduct the first large-scale population-based genetic discovery of three important but little-studied markers of ageing: hand grip strength as a marker of overall muscle condition and frailty, resting energy expenditure as an indicator of metabolism and energy balance, and mosaic loss of the Y-chromosome, a potential novel marker of genomic instability and replicative capacity with age. Having conducted these discovery efforts, I applied a host of downstream analytical approaches incorporating gene expression, epigenetics, genetic correlations, pathway-based work and partitioned heritability to maximise biological insight, and to understand the shared and separate aetiology of these phenotypes, and their role in cardiometabolic dysfunction.

Through concerted international collaboration and the use of very large population-based cohorts, this thesis has robustly implicated the first variants identified for grip strength (n=16) and mLOY (n=19) in the global literature. In each case, loci identified correspond to genes with a convergent and highly plausible role in the phenotype. Through European and transethnic analyses of REE, three loci of potential interest to this phenotype have additionally been identified. Downstream analyses dramatically enhance our understanding of the basic biology underpinning variation in these traits at population level.

From a translational perspective, the work on grip strength has proved perhaps the most illuminating. Targeted interrogation of the associations with HGS across the genome provided genetic evidence in support of a monoclonal antibody - Bimagrumab (Novartis) - currently being pursued in Phase III trials as a treatment for pathological muscle deterioration[233], and already licensed as an early breakthrough therapy for Sporadic Inclusion Body Myositis (sIBM), an inflammatory condition characterised by progressive wasting of proximal and distal muscles) . Our identification of grip strength as a causal exposure for fracture risk using data from the GEFOS consortium underlines the importance of muscle strength to the maintenance of functional independence and mobility with advanced age. In mLOY, we have demonstrated that major genes implicated in cell cycle control and progression, apoptosis and genomic stability can be identified using this readily-quantifiable and widely-available phenotype, which this thesis highlights as a new parameter to facilitate the study of genome stability and associated conditions at very large population-based scale. The finding that mLOY is inversely correlated with all-cancer risk at population level further underlines this.

The analyses outlined in this work additionally contribute to ongoing high profile discussions in the litera-

ture. For example, this thesis suggests that the genetic influence of *MTCH2* on adiposity is mediated in part through lower REE, but does not support the recently-reported role of *FTO* in thermogenesis[241], or the importance of *MC4R* in REE observed amongst Pima Indians[103]. This PhD does not support a causal role for grip strength in CHD, suggesting that recent work outlining grip strength as a clinical predictor of CHD incidence in low resource settings is not based on an underlying causal relationship, but, rather, on other correlated factors. Whilst the nature of MR analyses precludes a conclusive finding in the case of a null result, one would anticipate that a causal effect would be observed in this instance, if such an effect existed.

This chapter places the work presented throughout this thesis in a wider context; technically, scientifically, and in terms of its application and translational relevance. I firstly assess how the findings of this work might be limited or influenced by major considerations including chance, bias, confounding and error, and specific analytical limitations such as collider bias, whilst outlining the measures that have been applied throughout to mitigate their potential effect. Before drawing final conclusions, I outline in some detail how the findings of this thesis have contributed to the field, discuss their translational and applied relevance, and suggest avenues for further work based on the foundations established by this thesis.

7.2 Possible Limitations and Considerations

7.2.1 Limitations to REE Derivation

Despite the widespread clinical application of indirect calorimetry, consensus protocols for the testing procedure and post-test processing and interpretation of data do not exist[57], and best practice guidelines are geared to the clinical setting. These guidelines typically stipulate rest periods of 30 minutes preceding the test, disregard an initial period at the outset of calorimetry, and define steady state exchange according to strict criteria which often necessitate extended testing durations. Their implementation is restrictive, and a particular challenge in large-scale research environments in which testing procedures must strike a balance between accuracy and throughput whilst minimising participant inconvenience. Working from first principles of calorimetry interpretation, and in collaboration with colleagues, I optimised a framework for cleaning of Fenland calorimetry data to generate a time-series of steady-state breaths physiologically representative of underlying cellular respiration.

During testing, best-practice was applied wherever possible, but one notable deviation was the shortened testing duration required to achieve acceptable throughput in Fenland baseline visits. Whilst the six-minute period is considerably truncated from the recommended duration to achieve steady state[356], a recent systematic appraisal of guidelines has concluded that an overall test duration of five-minute acclimation followed by a five-minute period of steady-state is sufficient to attain representative parameters[57]. Whilst the five-minute steady-state requirement is widely advocated in literature, Reeves and colleagues[357] argue that it is not evidence-based, and suggest that steady-state durations of three minutes generate REE values which differ from five-minute steady-state estimates by less than 3%. It follows, therefore, that observations over the last 120s of our six minute protocol tend towards steady-state, and that residual error is random rather than systematic. In addition, the fasting requirement of REE assessment was technically contravened by the administraion of an oral glucose tolerance test (OGTT) prior to calorimetry. The standardised (75g) glucose dose across all participants mitigates any potential systematic error in REE introduced by pre-test glucose consumption.

Overall, derived REE used in these analyses has high face validity against known correlates including age, sex and fat-free mass, as discussed in Chapter 4. Whilst our reported mean VO_2 over the last 120s of rest is lower than the standard metabolic equivalent of task (MET, 3.5mL/kg/min), this reference value is often considered unrepresentative[248], and a lower observation is in line with the findings of previous studies in healthy populations of similar age[248,358]. Outliers of absolute REE fall within the expected demographics in terms of sex and body mass. Efforts taken throughout data collection and processing give us confidence that estimates are free of systematic error and provide a good indication of absolute REE. Even in the presence of random error, derived phenotypes will correctly capture true inter-individual

variance in RMR, and appropriately rank participants within the population-level distribution. In future, however, the validity of our testing and derivation procedure could be examined by comparison to direct calorimetry as a criterion measure in a representative subset of the Fenland cohort.

7.2.2 Internal and External Validity

Sound epidemiological inference is dependent on a study combining both internal and external validity: that is, the study design and analytical processes are statistically robust, and the findings are generated in a sample which is representative of the population of interest and are generalisable to the real-world setting. Chance, confounding, error and bias can detract from validity, and best efforts have been taken throughout this work to minimise their effect.

Chance Standard p-value thresholds and methods to account for family-wise error rate (FWER) have been applied throughout to fix the risk of type I error (α, the likelihood of declaring a false positive association) at $\leq$5%, in line with standard practice. As is convention, $p \leq 5 \times 10^{-8}$was applied universally as the threshold for association at statistical significance in genome-wide discovery efforts for MAF $\geq$1%, and Bonferroni correction used to conservatively account for multiple testing, assuming that all tests were statistically independent even in situations (such as multiple tissue expression associations) where this may not strictly be true. Replication of genetic associations from discovery-stage analyses in independent, ancestry-matched cohorts, minimises the likelihood that reported associations are due to chance, and mitigates the risk of statistical phenomena such as 'Winner's Curse'. This term is used to refer to the fact that effect sizes (and statistical significance) are often over-estimated at the discovery stage due to the definition of statistical significance based on a binary p-value threshold[359]. Given that effect sizes tend to regress to the mean during stage two follow-up, our exclusive use of effect sizes from combined discovery plus replication analyses moderates the adverse influence of Winner's Curse in downstream MRs in which they are applied as instruments.

Confounding The need to systematically account for confounding issues which limit the capacity for epidemiological inference in standard observational approaches was central to the objectives of this PhD. By applying genetic instruments to model theoretically unconfounded exposures, we were able to estimate causal effects according to Mendelian randomisation. A fuller discussion of the strengths and limitations of these analyses can be found below. To account for population stratification in discovery efforts (confounding by underlying sub-structure in allele frequencies due to ancestry or relatedness), we primarily restricted to individuals of European ancestry as defined by self-report, and applied a linear mixed model (BOLT-LMM) as standard. By empirically accounting for genetic covariance between all samples (based

on a genomic relatedness matrix), LMM have the distinct advantage of mitigating sub-continental ancestral structure, as well as overt and cryptic relatedness, without the necessary need for prior knowledge of this structure. This offers power advantages over the conventional approach of including genomic principal components as covariates to condition for variance attributable to ethnicity. Principal components-based adjustment has, however, been the *de facto* standard since the inception of GWAS and is widely recognised as effective. The majority of replication samples across the analyses provided association statistics according to their standard procedure and thus accounted for population structure using a components-based approach PCs. Systematic assessment of test statistic inflation by λ_{GC} and LD score regression intercept provided confidence that our main discovery models were not residually confounded.

Error and Bias Whereas error, in an epidemiological sense, is used to refer to the random, uncorrelated error occurring in, for example, phenotype measurement within and across studies, bias denotes systematic error which is intrinsic in the study design. The use of standardised protocols for phenotype assessment within studies contributing to this work - as exemplified by UKB[138] provide confidence that the risk of measurement biases is appropriately mitigated. As error is random, it is largely an inverse function of sample size, and is minimised with the increased statistical power offered by the large population-based samples leveraged here. Error may become meaningful if it is structured between stage one and two cohorts. Standard fixed-effect inverse variance-weighted methods was applied in this work to ensure that cohorts contributed appropriately to overall meta-analyses, inversely proportional to the uncertainty surrounding the point estimate of the association of each variant. Formal assessment of heterogeneity across studies suggested that estimates were directly comparable and not subject to differential error by cohort. The potential limitation of residual cohort effects should, however be considered.

As with all cohort-based work, these analyses are prone to healthy volunteer effect[360]; a bias introduced by the phenomenon that, on average, individuals who enrol in population-based cohorts which do not enforce selection criteria based on outcome status are more likely to be healthier and have better health outcomes than their contemporaries. The overall recruitment response rate of 5.5% in UK Biobank[141] is indicative of the likely presence of healthy volunteer effect. By reference to the general population, UKB participants are less socio-economically deprived, older, less likely to smoke or be obese, and suffer 50% less mortality at age 70-74 years[141]. Whilst the healthy cohort effect reduces the representativeness of studies and makes them unsuitable for derivation of descriptive prevalence and incidence rates or population norms, valid assessment of exposure-disease relationships are widely generalisable and do not necessarily require a representative sample given that sufficient phenotypic variability is observed[136,141,361]. Continuing debate in this area should, nonetheless, be acknowledged here.

7.2.3 Collider Bias

In the context of genetics, statistical collision occurs when discovery analyses are adjusted for a heritable covariate which is itself causally influenced by the outcome of interest (a collider); the resulting 'collider bias' may cause spurious genetic associations to be observed. Specifically, variants associated with the collider will be erroneously identified as genetic determinants of the outcome of interest, with a direction of effect which is (a) physiologically implausible and (b) the inverse of the effect observed in analyses not adjusting for the collider. This phenomenon has most clearly been demonstrated in a recent proof-of-concept by Day and colleagues[362], in which autosomal determinants of biological sex were artificially induced in GWAS analyses by adjustment for standing height (which is itself influenced by sex). All identified variants at genome-wide significance were known height-increasing loci, and were associated with odds of being female; the opposite of what would be expected biologically. The implausibility of these associations is self-evident, and clearly illustrates the statistical implications which may arise from inappropriate adjustment of GWAS analyses, or interpretation of adjusted GWAS results without due thought to the risk of statistical collision, even in cases for which the adjustment appears physiologically sensible. Further work has expanded on this, highlighting BMI as a problematic covariate in GIANT meta-analyses[363].

The mLOY discovery (and the main discovery analyses for REE) presented in this PhD are adjusted only for age, sex and other non-heritable covariates, and, therefore, have a very low prior for collision. The hand grip strength discovery, however, is adjusted for BMI and standing height to account for the possibility that strength may scale with muscle size. Given that height is fixed post-adolescence, it is conceptually unlikely that height can be causally influenced by strength variation in adulthood. We were mindful, however, of real possibility of collision by BMI, and took steps to assess its presence by systematically considering the association of known BMI loci[249] with HGS in models including or omitting BMI as a covariate. As discussed more fully in Chapter 3, comparison of the direction of effect of known BMI variants in the main HGS model (age, sex, height and BMI) and a sensitivity GWAS not adjusting for BMI did not provide evidence of collider bias attributable to adjustment for BMI, and suggested its inclusion as a covariate was appropriate.

7.2.4 Limitations to Inferring Causality

Mendelian randomisation offers a powerful solution to deal with many of the issues of observational epidemiology, yet causal inference is only robust if prerequisite assumptions hold. These assumptions have been discussed in some detail in Chapter 2: briefly, the association between the instrument and the outcome of interest must act only *via* the modelled exposure, free of pleiotropy or heterogeneity. Current best-practice approaches to identifying and subsequently accounting for directional pleiotropy (MR-Egger

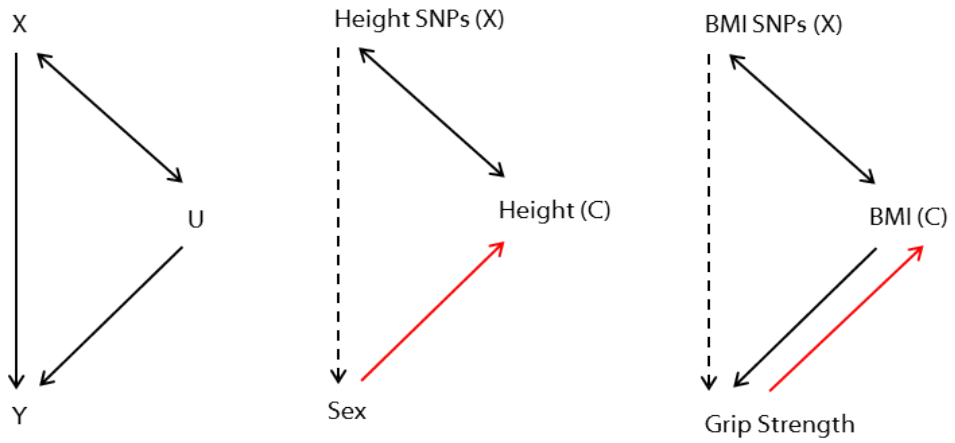

Figure 7.1: Statistical collision illustrated by contrast to confounding. In the association of an exposure X with an outcome Y, a confounder U is a correlate or causal exposure for X, which is also a determinant of Y, but does not lie on the X-Y causal pathway. If the covariate is a causal outcome of Y, it is classed as a collider, C. Adjustment for C will generate a spurious association between X and Y. Unidirectional arrow, causal association; bidirectional arrow, correlation

estimator) or heterogeneity (weighted median estimators) were applied throughout this thesis. Based on a method first described to detect heterogeneity in meta-analyses, MR-Egger allows the intercept term of the MR regression to deviate from zero, providing a quantitative estimate of the presence of directional pleiotropy and a causal β robust to this. Weighted median estimators seek to address issues of heterogeneity and scores comprising a proportion of variants which contravene instrumental varaible assumptions. The contribution of particularly heterogeneous variants to the overall causal estimate is penalised, allowing robust estimates to be generated when as many as half of the variants used to model the exposure are invalid.

A large proportion of the MR estimates presented in this thesis were inconclusive, providing a non-statistically significant association, and highlight a particular limitation of the MR approach. Whereas a statistically significant causal estimate can be interpreted as such, a null estimate cannot be interpreted as absence of a true causal effect. The understanding of power calculations in MR is a developing field, and methods described to date[364,365] are only appropriate in restricted scenarios (for example when considering binary outcomes). Moreover, in two-sample MR, power calculations must inherently be *post-hoc*, and by convention are not undertaken.

Power in MR is primarily a function of the variance explained in the modelled exposure by the instrument, but a fine balance exists between maximising this variance (by expansion of the score), and the accompanying risk of introducing variants which violate instrumental variable assumptions[364]. Use of two-sample approaches conservatively shifts the causal estimate toward the null in the case of this weak-instrument bias, assuming that the effect estimates for the modelled exposure and outcome of interest are drawn from demographically and ethnically similar populations. However, variant choice remains of importance. To minimise weak instruments, MR approaches conventionally restrict to variants robustly associated with the modelled intermediate at genome-wide significance: we followed this convention throughout.

7.3 Implications and the Future

A common criticism of genetic discovery analyses is that conclusions drawn are abstract and cannot be readily translated to clinical or policy settings in a timely manner[366]. This criticism only holds if genetic work is approached with inappropriate expectation of immediate clinical impact, however. In reality, translation may take a number of years, and begins with the major strength of hypothesis-free discovery to empirically elucidate the underlying biology and aetiology of a phenotype. The importance of fully understanding this biology, and the value of genetic evidence in prioritising drug targets, is now recognised as an important measure in improving the efficiency of drug development pipelines and the translation to the clinic[367].

Through the application of genetic discovery in the largest possible population-based samples to date, and the application of downstream work to prioritise functionally-relevant genes, this thesis provides much biological insight into the mechanisms involved in variation in hand grip strength, mosaic loss of Y and resting energy expenditure.

In the case of grip strength, we demonstrate that common genetic variation in proximity to genes implicated in severe monogenic neuromuscular syndromes is associated with normal variation in strength in the population at large. Additionally, we observed important genetic evidence in support of the Novartis compound BYM338, a candidate activin receptor type II (ActRII) antagonist monoclonal antibody being investigated for its hypothesised utility in preserving muscle mass and function in a range of clinical and frailty settings, and licensed (Bimagrumab) as an early breakthrough treatment for the rare degenerative condition, sporadic inclusion body myositis (sIBM)[233]. In recent months, BYM338 has been repositioned as a putative treatment for T2D, on the hypothesis that improvement of body composition amongst the obese could favourably influence insulin sensitivity. Initial results are concordant with this theory[368], and highlight the shared biology between muscle function and metabolic parameters which has been investigated in part in this thesis.

Work presented in Chapter 6 expands on the current literature linking increased mLOY to age, and provides substantial new evidence on the potential of mLOY as marker of basic physiological and ageing processes. The convergence of loci identified by GWAS on diverse aspects of the cell cycle, apoptosis and DNA replication highlight its relevance as a novel quantitative phenotype to assess cell cycle efficiency and genomic instability in large-scale human populations. Whilst we were not able to demonstrate mLOY as a causal exposure for cancer risk, positive genetic correlations indicated a clear shared genetic architecture, and suggest that wider study of this phenotype could offer new insights into processes pertinent to cancer, and possibily drive prioritisation and validation of new targets for intervention. Our demonstration that mLRR-Y can be accurately estimated from commercial genotyping arrays makes this phenotype particularly permissive to further high-impact genetic work with very high power in a comparably short

timeframe. For both mLOY and hand grip strength alike, the imminent release of a further 350,000 genotyped samples from UK Biobank offers an immediate avenue to fundamentally expand discovery analyses, and should be pursued as a priority. In the medium term, initiatives such as the United States' 'All of Us' programme (Precision Medicine Initiative)[369,370] will allow momentum to be maintained in genetic discovery of these traits over coming years. Given that mLOY requires no additional phenotyping - only access to array genotyping - this phenotype is also uniquely placed to leverage the vast repositories or genome-wide genotyping held by commercial direct-to-consumer vendors such as 23andMe and Ancestry.com, and to perform discovery in large non-European populations (e.g., the China-Kadoorie Biobank[371]) with relative ease. Even now, this transition to highly-powered and robust transethnic analyses remains a barrier to the majority of phenotype discovery, which have conventionally been monopolised by European efforts.

Chapter 5 informs the ongoing and often polarising debate surrounding the mechanism of action by which known BMI variants exert their effect on body composition. In contrast to recent work in animal models and human cell lines which implicates *FTO* in pro-thermogenic response and the regulation of adipose browning, and established work implicating *MC4R* in lower REE, our analyses did not support the conclusion that common variants in either gene increases BMI *via* modulation of REE at population scale. We did, however, identify lower REE as a partial mediator of the adiposity-increasing effect of *MTCH2*.

Whilst some promising initial signals were identified, the REE discovery effort presented in Chapter 4 was underpowered. Nonetheless, this analysis represents the largest discovery effort for REE conducted to date, and combines the majority of available data on a global scale. We report that genetic associations for REE are enriched for major respiratory processes, and confirm that known associations between body size and REE are reflected in the shared genetic architecture of these traits. It was disappointing that no genetic instrument for REE was robustly identified, but the international collaboration established during this project sets the foundations for future expanded discovery analyses of REE, which will ultimately implicate sufficient variants to create an instrument. The route to enhanced discovery is not so clear cut for this phenotype as for HGS and mLOY, and will require concerted additional genotyping efforts in new or existing cohorts, but must be pursued in the interests of improving our understanding of this trait and its role in health. Functional work in human cells line and rodent models is likely to offer the greatest potential to inform our knowledge of the role of genes implicated in REE in the short term.

Combined, the discovery analyses described here contribute significantly to our understanding of the genetic aetiology of three functional ageing traits, and will facilitate hand grip strength and mLOY to be modelled as causal exposures by others. MRs must be interpreted with care however. For example, we implicate lower HGS as a 'causal' risk factor for fracture risk, but this association only holds given that HGS is a true proxy of overall muscular strength; i.e. isolated training of grip cannot be used as an intervention to reduce fracture risk. Rather, this finding should be interpreted as a reinforcement of the

need to maintain physical activity and overall strength through general and targeted means in middle and older age.

In conclusion, the work presented here significantly advances our understanding of the role of ageing phenotypes in health and disease. Through considering alternative functional and biological markers of ageing, I have gained insight into the shared genetic aetiology of these traits and their underlying biology, presenting the first large-scale genetic discoveries in each case, and characterising novel genetic variants. The findings of this work have broad relevance to translational and basic science, but efforts must continue to further enhance our knowledge and understanding of these complex topics.

References

1. Ogden, C. L., Carroll, M. D., Kit, B. K. & Flegal, K. M. Prevalence of Childhood and Adult Obesity in the United States, 2011-2012. *JAMA* **311,** 806 (2014).
2. Gallus, S. *et al.* Overweight and obesity in 16 European countries. *Eur. J. Nutr.* **54,** 679–689 (2015).
3. Hossain, P., Kawar, B. & El Nahas, M. Obesity and Diabetes in the Developing World âĂŤ A Growing Challenge. *N. Engl. J. Med.* **356,** 213–215 (2007).
4. Hu, F. B. Globalization of Diabetes: The role of diet, lifestyle, and genes. *Diabetes Care* **34,** 1249–1257 (2011).
5. Prentice, A. M. The emerging epidemic of obesity in developing countries. *Int. J. Epidemiol.* **35,** 93–9 (2006).
6. Withrow, D. & Alter, D. A. The economic burden of obesity worldwide: a systematic review of the direct costs of obesity. *Obes. Rev.* **12,** 131–141 (2011).
7. Seuring, T., Archangelidi, O. & Suhrcke, M. The Economic Costs of Type 2 Diabetes: A Global Systematic Review. *Pharmacoeconomics* **33,** 811–31 (2015).
8. López-Otín, C., Blasco, M. A., Partridge, L., Serrano, M. & Kroemer, G. The hallmarks of aging. *Cell* **153,** 1194–217 (2013).
9. Marcell, T. J. Sarcopenia: Causes, Consequences, and Preventions. *Journals Gerontol. Ser. A Biol. Sci. Med. Sci.* **58,** M911–M916 (2003).
10. Harada, C. N., Natelson Love, M. C. & Triebel, K. L. Normal Cognitive Aging. *Clin. Geriatr. Med.* **29,** 737–752 (2013).
11. Mather, K. A., Jorm, A. F., Parslow, R. A. & Christensen, H. Is telomere length a biomarker of aging? A review. *J. Gerontol. A. Biol. Sci. Med. Sci.* **66,** 202–13 (2011).
12. Pearl, R. *The Biology of Death* (1921).
13. Speakman, J. R. Body size, energy metabolism and lifespan. *J. Exp. Biol.* **208,** 1717–1730 (2005).
14. Harman, D. Aging: A Theory Based on Free Radical and Radiation Chemistry. *J. Gerontol.* **11,** 298–300 (1956).
15. López-Otín, C., Galluzzi, L., Freije, J. M., Madeo, F. & Kroemer, G. *Metabolic Control of Longevity* 2016.
16. Barzilai, N., Huffman, D. M., Muzumdar, R. H. & Bartke, A. *The critical role of metabolic pathways in aging* 2012.
17. Blackburn, E. H. Structure and function of telomeres. *Nature* **350,** 569–73 (1991).
18. Blackburn, E. H. Telomere states and cell fates. *Nature* **408,** 53–56 (2000).
19. Hayflick, L. The limited in vitro lifetime of human diploid cell strains. *Exp. Cell Res.* **37,** 614–636 (1965).
20. Harley, C. B., Futcher, A. B. & Greider, C. W. Telomeres shorten during ageing of human fibroblasts. *Nature* **345,** 458–60 (1990).
21. Saretzki, G. & Zglinicki, T. V.O. N. Replicative Aging, Telomeres, and Oxidative Stress. *Ann. N. Y. Acad. Sci.* **959,** 24–29 (2002).
22. Mundstock, E. *et al. Effect of obesity on telomere length: Systematic review and meta-analysis* 2015.
23. Tzanetakou, I. P., Nzietchueng, R., Perrea, D. N. & Benetos, A. Telomeres and their role in aging and longevity. *Curr. Vasc. Pharmacol.* **12,** 726–34 (2014).
24. Adaikalakoteswari, A., Balasubramanyam, M., Ravikumar, R., Deepa, R. & Mohan, V. Association of telomere shortening with impaired glucose tolerance and diabetic macroangiopathy. *Atherosclerosis* **195,** 83–89 (2007).
25. Shen, Q *et al.* Association of leukocyte telomere length with type 2 diabetes in mainland Chinese populations. *J Clin Endocrinol Metab* **97,** 1371–1374 (2012).
26. Zhao, J., Miao, K., Wang, H., Ding, H. & Wang, D. W. Association between telomere length and type 2 diabetes mellitus: A meta-analysis. *PLoS One* **8** (2013).
27. Haycock, P. C. *et al.* Leucocyte telomere length and risk of cardiovascular disease: systematic review and meta-analysis. *BMJ* **349,** g4227–g4227 (2014).
28. Collaboration, T. T.M. R. Association Between Telomere Length and Risk of Cancer and Non-Neoplastic Diseases: A Mendelian Randomization Study. *JAMA oncology* **3,** 636–651 (2017).
29. Zhan, Y. *et al.* Exploring the Causal Pathway From Telomere Length to Coronary Heart Disease: A Network Mendelian Randomization Study. *Circulation Research* **121,** 214–219 (2017).
30. Codd, V. *et al.* Identification of seven loci affecting mean telomere length and their association with disease. *Nature Genetics* **45,** 422 (2013).
31. Rantanen, T. Muscle strength, disability and mortality. *Scand. J. Med. Sci. Sports* **13,** 3–8 (2003).
32. Morey, M. C., Pieper, C. F. & Cornoni-Huntley, J. Physical fitness and functional limitations in community-dwelling older adults. *Med. Sci. Sports Exerc.* **30,** 715–23 (1998).
33. Syddall, H., Cooper, C., Martin, F., Briggs, R. & Aihie Sayer, A. Is grip strength a useful single marker of frailty? *Age Ageing* **32,** 650–6 (2003).
34. Fried, L. P. *et al.* Frailty in older adults: evidence for a phenotype. *J Gerontol A Biol Sci Med Sci* **56,** M146–56 (2001).
35. Bohannon, R. W. Hand-grip dynamometry predicts future outcomes in aging adults. *J. Geriatr. Phys. Ther.* **31,** 3–10 (2008).
36. Brill, P. a., Macera, C. a., Davis, D. R., Blair, S. N. & Gordon, N. Muscular strength and physical function. *Med. Sci. Sports Exerc.* **32,** 412–416 (2000).
37. Huang, Y *et al.* Physical fitness, physical activity, and functional limitation in adults aged 40 and older. *Med. Sci. Sports Exerc.* **30,** 1430–1435 (1998).

38. Taekema, D. G., Gussekloo, J., Maier, A. B., Westendorp, R. G. J. & de Craen, A. J. M. Handgrip strength as a predictor of functional, psychological and social health. A prospective population-based study among the oldest old. *Age Ageing* **39,** 331–337 (2010).

39. Rantanen, T. *et al.* Muscle strength as a predictor of onset of ADL dependence in people aged 75 years. *Aging Clin. Exp. Res.* **14,** 10–5 (2002).

40. Bohannon, R. W., Magasi, S. R., Bubela, D. J., Wang, Y.-C. & Gershon, R. C. Grip and Knee extension muscle strength reflect a common construct among adults. *Muscle Nerve* **46,** 555–558 (2012).

41. Roberts, H. C. *et al.* A review of the measurement of grip strength in clinical and epidemiological studies: towards a standardised approach. *Age Ageing* **40,** 423–429 (2011).

42. Cruz-Jentoft, A. J. *et al.* Sarcopenia: European consensus on definition and diagnosis: Report of the European Working Group on Sarcopenia in Older People. *Age Ageing* **39,** 412–423 (2010).

43. Frederiksen, H. *et al.* Do children of long-lived parents age more successfully? *Epidemiology* **13,** 334–9 (2002).

44. Chan, J. P. L. *et al.* Genetics of hand grip strength in mid to late life. *Age (Dordr).* **37,** 9745 (2015).

45. Cooper, R., Kuh, D., Hardy, R., Mortality Review Group & FALCon and HALCyon Study Teams. Objectively measured physical capability levels and mortality: systematic review and meta-analysis. *BMJ* **341,** c4467 (2010).

46. Ling, C. H. *et al.* Handgrip strength and mortality in the oldest old population: the Leiden 85-plus study. *Can. Med. Assoc. J.* **182,** 429–435 (2010).

47. Strand, B. H. *et al.* The association of grip strength from midlife onwards with all-cause and cause-specific mortality over 17 years of follow-up in the Tromsø Study. *J. Epidemiol. Community Health* **70,** 1214–1221 (2016).

48. Rantanen, T. *et al.* Midlife muscle strength and human longevity up to age 100 years: a 44-year prospective study among a decedent cohort. *Age (Omaha).* **34,** 563–570 (2012).

49. Leong, D. P. *et al.* Prognostic value of grip strength: findings from the Prospective Urban Rural Epidemiology (PURE) study. *Lancet* **386,** 266–273 (2015).

50. Mainous, A. G., Tanner, R. J., Anton, S. D. & Jo, A. Grip Strength as a Marker of Hypertension and Diabetes in Healthy Weight Adults. *Am. J. Prev. Med.* **49,** 850–858 (2015).

51. Wander, P. *et al.* Greater hand-grip strength predicts a lower risk of developing type 2 diabetes over 10 years in leaner Japanese Americans. *Diabetes Res. Clin. Pract.* **92,** 261–264 (2011).

52. Cetinus, E., Buyukbese, M. A., Uzel, M., Ekerbicer, H. & Karaoguz, A. Hand grip strength in patients with type 2 diabetes mellitus. *Diabetes Res. Clin. Pract.* **70,** 278–286 (2005).

53. Stenholm, S. *et al.* Association between Obesity History and Hand Grip Strength in Older Adults–Exploring the Roles of Inflammation and Insulin Resistance as Mediating Factors. *Journals Gerontol. Ser. A Biol. Sci. Med. Sci.* **66A,** 341–348 (2011).

54. Stenholm, S. *et al.* Sarcopenic obesity: definition, cause and consequences. *Curr. Opin. Clin. Nutr. Metab. Care* **11,** 693–700 (2008).

55. Ortega, F. B., Silventoinen, K., Tynelius, P. & Rasmussen, F. Muscular strength in male adolescents and premature death: cohort study of one million participants. *BMJ* **345,** e7279 (2012).

56. Manini, T. M. Energy expenditure and aging. *Ageing Res. Rev.* **9,** 1–11 (2010).

57. Compher, C., Frankenfield, D., Keim, N. & Roth-Yousey, L. Best practice methods to apply to measurement of resting metabolic rate in adults: a systematic review. *J. Am. Diet. Assoc.* **106,** 881–903 (2006).

58. McNab, B. K. On the utility of uniformity in the definition of basal rate of metabolism. *Physiol. Zool.* **70,** 718–720 (1997).

59. DuBois, E. F. Recent Advances in the Study of Basal Metabolism Part II Basal Metabolism and Surface Area. *J. Nutr.* **3** (1930).

60. Webb, P. The measurement of energy expenditure. *J. Nutr.* **121,** 1897–901 (1991).

61. Ferrannini, E. The theoretical bases of indirect calorimetry: A review. *Metabolism* **37,** 287–301 (1988).

62. WEIR, J. B.D. B. New methods for calculating metabolic rate with special reference to protein metabolism. *J. Physiol.* **109,** 1–9 (1949).

63. Harris, J. A. & Benedict, F. G. A Biometric Study of Human Basal Metabolism. *Proc. Natl. Acad. Sci. U. S. A.* **4,** 370–3 (1918).

64. Cunningham, J. J. Body composition as a determinant of energy expenditure: a synthetic review and a proposed general prediction equation. *Am. J. Clin. Nutr.* **54,** 963–9 (1991).

65. Bosy-Westphal, A *et al.* Effect of organ and tissue masses on resting energy expenditure in underweight, normal weight and obese adults. *Int. J. Obes. Relat. Metab. Disord.* **28,** 72–9 (2004).

66. Buchholz, A. C., Rafii, M. & Pencharz, P. B. Is resting metabolic rate different between men and women? *Br. J. Nutr.* **86,** 641 (2007).

67. Arciero, P. J., Goran, M. I. & Poehlman, E. T. Resting metabolic rate is lower in women than in men. *J. Appl. Physiol.* **75,** 2514–20 (1993).

68. St-Onge, M.-P. & Gallagher, D. Body composition changes with aging: the cause or the result of alterations in metabolic rate and macronutrient oxidation? *Nutrition* **26,** 152–5 (2010).

69. Frisard, M. I. *et al.* Aging, resting metabolic rate, and oxidative damage: results from the Louisiana Healthy Aging Study. *J. Gerontol. A. Biol. Sci. Med. Sci.* **62,** 752–9 (2007).

70. Krems, C, Lührmann, P. M., Strassburg, A, Hartmann, B & Neuhäuser-Berthold, M. Lower resting metabolic rate in the elderly may not be entirely due to changes in body composition. *Eur. J. Clin. Nutr.* **59,** 255–62 (2005).

71. Nelson, K. M., Weinsier, R. L., Long, C. L. & Schutz, Y. Prediction of resting energy expenditure from fat-free mass and fat mass. *Am. J. Clin. Nutr.* **56,** 848–56 (1992).

72. Bogardus, C *et al.* Familial dependence of the resting metabolic rate. *N. Engl. J. Med.* **315,** 96–100 (1986).

73. Johnstone, A. M., Murison, S. D., Duncan, J. S., Rance, K. A. & Speakman, J. R. Factors influencing variation in basal metabolic rate include fat-free mass, fat mass, age, and circulating thyroxine but not sex, circulating leptin, or triiodothyronine. *Am J Clin Nutr* **82,** 941–948 (2005).

74. Luke, A., Dugas, L. & Kramer, H. Ethnicity, energy expenditure and obesity: are the observed black/white differences meaningful? *Curr. Opin. Endocrinol. Diabetes. Obes.* **14,** 370–3 (2007).

75. Désilets, M.-C. *et al.* Ethnic differences in body composition and other markers of cardiovascular disease risk: study in matched Haitian and White subjects from Quebec. *Obesity (Silver Spring).* **14,** 1019–27 (2006).

76. Gannon, B, DiPietro, L & Poehlman, E. T. Do African Americans have lower energy expenditure than Caucasians? en. *Int. J. Obes.* **24,** 4–13 (2000).

77. Hunter, G. R., Weinsier, R. L., Darnell, B. E., Zuckerman, P. A. & Goran, M. I. Racial differences in energy expenditure and aerobic fitness in premenopausal women. *Am. J. Clin. Nutr.* **71,** 500–6 (2000).

78. Albu, J *et al.* Resting metabolic rate in obese, premenopausal black women. *Am. J. Clin. Nutr.* **66,** 531–8 (1997).

79. Foster, G. D., Wadden, T. A. & Vogt, R. A. Resting energy expenditure in obese African American and Caucasian women. *Obes. Res.* **5,** 1–8 (1997).

80. Jakicic, J. M. & Wing, R. R. Differences in resting energy expenditure in African-American vs Caucasian overweight females. *Int. J. Obes. Relat. Metab. Disord.* **22,** 236–42 (1998).

81. Shook, R. P., Hand, G. A. & Blair, S. N. Top 10 Research Questions Related to Energy Balance. en. *Res. Q. Exerc. Sport* (2014).

82. Forman, J. N., Miller, W. C., Szymanski, L. M. & Fernhall, B. Differences in resting metabolic rates of inactive obese African-American and Caucasian women. *Int. J. Obes. Relat. Metab. Disord.* **22,** 215–21 (1998).

83. Kimm, S. Y. S. Effects of Race, Cigarette Smoking, and Use of Contraceptive Medications on Resting Energy Expenditure in Young Women. *Am. J. Epidemiol.* **154,** 718–724 (2001).

84. Williamson, D. F., Kahn, H. S. & Byers, T. The 10-y incidence of obesity and major weight gain in black and white US women aged 30-55 y. *Am. J. Clin. Nutr.* **53,** 1515S–1518S (1991).

85. Weyer, C., Snitker, S., Bogardus, C. & Ravussin, E. Energy metabolism in African Americans: potential risk factors for obesity. *Am J Clin Nutr* **70,** 13–20 (1999).

86. Gallagher, D. *et al.* Small organs with a high metabolic rate explain lower resting energy expenditure in African American than in white adults. *Am J Clin Nutr* **83,** 1062–1067 (2006).

87. Fernández, J. R. *et al.* Association of African genetic admixture with resting metabolic rate and obesity among women. *Obes. Res.* **11,** 904–11 (2003).

88. Manini, T. M. *et al.* European ancestry and resting metabolic rate in older African Americans. *Eur. J. Clin. Nutr.* **65,** 663–7 (2011).

89. Collins, L. C., Cornelius, M. F., Vogel, R. L., Walker, J. F. & Stamford, B. A. Effect of caffeine and/or cigarette smoking on resting energy expenditure. *Int. J. Obes. Relat. Metab. Disord.* **18,** 551–6 (1994).

90. Perkins, K. A. Metabolic effects of cigarette smoking. *J Appl Physiol* **72,** 401–409 (1992).

91. Perkins, K. A., Sexton, J. E. & DiMarco, A. Acute thermogenic effects of nicotine and alcohol in healthy male and female smokers. *Physiol. Behav.* **60,** 305–309 (1996).

92. Hagedorn, T. *et al.* Indirect calorimetry in obese female subjects: Factors influencing the resting metabolic rate. *World J. Exp. Med.* **2,** 58–64 (2012).

93. Blauw, L. L. *et al.* Smoking is associated with increased resting energy expenditure in the general population: The NEO study. *Metabolism* (2015).

94. Weststrate, J. A., Wunnink, I., Deurenberg, P. & Hautvast, J. G.A. J. Alcohol and its acute effects on resting metabolic rate and diet-induced thermogenesis. English. *Br. J. Nutr.* **64,** 413 (2007).

95. Astrup, A *et al.* Caffeine: a double-blind, placebo-controlled study of its thermogenic, metabolic, and cardiovascular effects in healthy volunteers. *Am J Clin Nutr* **51,** 759–767 (1990).

96. Belza, A, Toubro, S & Astrup, A. The effect of caffeine, green tea and tyrosine on thermogenesis and energy intake. *Eur. J. Clin. Nutr.* **63,** 57–64 (2009).

97. Bouchard, C. *et al.* Genetic effect in resting and exercise metabolic rates. *Metabolism* **38,** 364–370 (1989).

98. Fontaine, E *et al.* Resting metabolic rate in monozygotic and dizygotic twins. *Acta Genet. Med. Gemellol. (Roma).* **34,** 41–7 (1985).

99. Bosy-Westphal, A. *et al.* Familial influences and obesity-associated metabolic risk factors contribute to the variation in resting energy expenditure: the Kiel Obesity Prevention Study. *Am J Clin Nutr* **87,** 1695–1701 (2008).

100. Chagnon, Y. *et al.* Linkage and association studies between the melanocortin receptors 4 and 5 genes and obesity-related phenotypes in the Quebec Family Study. *Mol. Med.* **3,** 663–673 (1997).

101. Arrizabalaga, M. *et al.* Preliminary findings on the influence of FTO rs9939609 and MC4R rs17782313 polymorphisms on resting energy expenditure, leptin and thyrotropin levels in obese non-morbid premenopausal women. *J. Physiol. Biochem.* **70,** 255–62 (2014).

102. Nagai, N, Sakane, N, Tsuzaki, K & Moritani, T. UCP1 genetic polymorphism (-3826 A/G) diminishes resting energy expenditure and thermoregulatory sympathetic nervous system activity in young females. *Int. J. Obes. (Lond).* **35,** 1050–5 (2011).

103. Krakoff, J. *et al.* Lower Metabolic Rate in Individuals Heterozygous for Either a Frameshift or a Functional Missense MC4R Variant. *Diabetes* **57,** 3267–3272 (2008).

104. Walston, J. *et al.* Arg64 beta3-adrenoceptor variant and the components of energy expenditure. *Obes. Res.* **11,** 509–11 (2003).

105. Kimm, S. Y. *et al.* Racial differences in the relation between uncoupling protein genes and resting energy expenditure. *Am J Clin Nutr* **75,** 714–719 (2002).

106. Bouchard, C., Perusse, L., Chagnon, Y. C., Warden, C. & Ricquier, D. Linkage Between Markers in the Vicinity of the Uncoupling Protein 2 Gene and Resting Metabolic Rate in Humans. *Hum. Mol. Genet.* **6,** 1887–1889 (1997).

107. Jacobson, P. *et al.* Resting metabolic rate and respiratory quotient: results from a genome-wide scan in the Quebec Family Study. *Am J Clin Nutr* **84,** 1527–1533 (2006).

108. Wu, X. *et al.* A genome scan among Nigerians linking resting energy expenditure to chromosome 16. *Obes. Res.* **12,** 577–81 (2004).

109. Norman, R. A. *et al.* Autosomal genomic scan for loci linked to obesity and energy metabolism in Pima Indians. *Am. J. Hum. Genet.* **62,** 659–68 (1998).

110. Piaggi, P. *et al.* A Genome-Wide Association Study Using a Custom Genotyping Array Identifies Variants in GPR158 Associated with Reduced Energy Expenditure in American Indians. *Diabetes,* db161565 (2017).

111. Astrup, A. *et al.* Meta-analysis of resting metabolic rate in formerly obese subjects. *Am J Clin Nutr* **69,** 1117–1122 (1999).

112. Siervo, M. *et al.* Imposed rate and extent of weight loss in obese men and adaptive changes in resting and total energy expenditure. *Metabolism.* **64,** 896–904 (2015).

113. Westerterp, K. R. Metabolic adaptations to over–and underfeeding–still a matter of debate? *Eur. J. Clin. Nutr.* **67,** 443–5 (2013).

114. Tremblay, A, Royer, M.-M., Chaput, J.-P. & Doucet, E. Adaptive thermogenesis can make a difference in the ability of obese individuals to lose body weight. *Int. J. Obes. (Lond).* **37,** 759–64 (2013).

115. Müller, M. J. & Bosy-Westphal, A. Adaptive thermogenesis with weight loss in humans. *Obesity (Silver Spring).* **21,** 218–28 (2013).

116. Camps, S. G.J. A., Verhoef, S. P. M. & Westerterp, K. R. Weight loss, weight maintenance, and adaptive thermogenesis. *Am. J. Clin. Nutr.* **97,** 990–4 (2013).

117. De Jonge, L. *et al.* Poor sleep quality and sleep apnea are associated with higher resting energy expenditure in obese individuals with short sleep duration. *J. Clin. Endocrinol. Metab.* **97,** 2881–9 (2012).

118. Reinhardt, M. *et al.* A Human Thrifty Phenotype Associated With Less Weight Loss During Caloric Restriction. *Diabetes,* db141881 (2015).

119. Hoffmans, M *et al.* Resting metabolic rate in obese and normal weight women. *Int. J. Obes.* **3,** 111–8 (1979).

120. Ravussin, E, Burnand, B, Schutz, Y & Jequier, E. Twenty-four-hour energy expenditure and resting metabolic rate in obese, moderately obese, and control subjects. *Am J Clin Nutr* **35,** 566–573 (1982).

121. Ravussin, E *et al.* Reduced rate of energy expenditure as a risk factor for body-weight gain. en. *N. Engl. J. Med.* **318,** 467–72 (1988).

122. Buscemi, S, Verga, S, Caimi, G & Cerasola, G. Low relative resting metabolic rate and body weight gain in adult Caucasian Italians. *Int. J. Obes. (Lond).* **29,** 287–91 (2005).

123. Seidell, J. C., Muller, D. C., Sorkin, J. D. & Andres, R. Fasting respiratory exchange ratio and resting metabolic rate as predictors of weight gain: the Baltimore Longitudinal Study on Aging. en. *Int. J. Obes. Relat. Metab. Disord.* **16,** 667–74 (1992).

124. Forsberg, L. A., Gisselsson, D. & Dumanski, J. P. Mosaicism in health and disease âĂŤ clones picking up speed. *Nat. Rev. Genet.* (2016).

125. JACOBS, P. A., BRUNTON, M., COURT BROWN, W. M., DOLL, R. & GOLDSTEIN, H. Change of Human Chromosome Count Distributions with Age: Evidence for a Sex Difference. *Nature* **197,** 1080–1081 (1963).

126. Pierre, R. V. & Hoagland, H. C. Age-associated aneuploidy: loss of Y chromosome from human bone marrow cells with aging. *Cancer* **30,** 889–894 (1972).

127. Dumanski, J. P. *et al.* Mosaic Loss of Chromosome Y in Blood Is Associated with Alzheimer Disease. *Am. J. Hum. Genet.* **98,** 1208–19 (2016).

128. Forsberg, L. A. *Loss of chromosome Y (LOY) in blood cells is associated with increased risk for disease and mortality in aging men* 2017.

129. Stone, J. F. & Sandberg, A. A. Sex chromosome aneuploidy and aging. *Mutat. Res. DNAging* **338,** 107–113 (1995).

130. Wiktor, A *et al.* Clinical significance of Y chromosome loss in hematologic disease. *Genes. Chromosomes Cancer* **27,** 11–6 (2000).

131. Forsberg, L. A. *et al.* Mosaic loss of chromosome Y in peripheral blood is associated with shorter survival and higher risk of cancer. *Nat. Genet.* **46,** 624–8 (2014).

132. Zhou, W. *et al.* Mosaic loss of chromosome Y is associated with common variation near TCL1A. *Nat. Genet.* **48,** 563–8 (2016).

133. Noveski, P. *et al.* Loss of Y Chromosome in Peripheral Blood of Colorectal and Prostate Cancer Patients. *PLoS One* **11,** e0146264 (2016).

134. Bonnefond, A. *et al.* Association between large detectable clonal mosaicism and type 2 diabetes with vascular complications. *Nat. Genet.* **45,** 1040–1043 (2013).

135. Dumanski, J. P. *et al.* Mutagenesis. Smoking is associated with mosaic loss of chromosome Y. *Science* **347,** 81–3 (2015).

136. Collins, R. What makes UK Biobank special? *Lancet* **379,** 1173–1174 (2012).

137. Ollier, W., Sprosen, T. & Peakman, T. UK Biobank: from concept to reality. *Pharmacogenomics* **6,** 639–646 (2005).

138. Sudlow, C. *et al.* UK Biobank: An Open Access Resource for Identifying the Causes of a Wide Range of Complex Diseases of Middle and Old Age. *PLoS Med.* **12,** e1001779 (2015).

139. Allen, N. E., Sudlow, C., Peakman, T. & Collins, R. UK Biobank Data: Come and Get It. *Sci. Transl. Med.* **6,** 224ed4–224ed4 (2014).

140. Besson, H., Brage, S., Jakes, R. W., Ekelund, U. & Wareham, N. J. Estimating physical activity energy expenditure, sedentary time, and physical activity intensity by self-report in adults. *Am. J. Clin. Nutr.* **91,** 106–114 (2010).

141. Fry, A. *et al.* Comparison of Sociodemographic and Health-Related Characteristics of UK Biobank Participants With Those of the General Population. *Am. J. Epidemiol.* 1–9 (2017).

142. Elliott, P. & Peakman, T. C. The UK Biobank sample handling and storage protocol for the collection, processing and archiving of human blood and urine. *Int. J. Epidemiol.* **37,** 234–44 (2008).

143. O'Connell, J. *et al.* Haplotype estimation for biobank-scale data sets. *Nat. Genet.* **48,** 817–20 (2016).

144. Huang, J. *et al.* Improved imputation of low-frequency and rare variants using the UK10K haplotype reference panel. *Nat. Commun.* **6,** 8111 (2015).

145. Abecasis, G. R. *et al.* A map of human genome variation from population-scale sequencing. *Nature* **467,** 1061–73 (2010).

146. Riboli, E *et al.* European Prospective Investigation into Cancer and Nutrition (EPIC): study populations and data collection. *Public Health Nutr.* **5,** 1113–1124 (2003).

147. Day, N *et al.* EPIC-Norfolk: study design and characteristics of the cohort. European Prospective Investigation of Cancer. *Br. J. Cancer* **80 Suppl 1,** 95–103 (1999).

148. Hayat, S. A. *et al.* Cohort profile: A prospective cohort study of objective physical and cognitive capability and visual health in an ageing population of men and women in Norfolk (EPIC-Norfolk 3). *Int. J. Epidemiol.* **43,** 1063–72 (2014).

149. Loh, P.-R. *et al.* Efficient Bayesian mixed-model analysis increases association power in large cohorts. *Nat. Genet.* **47,** 284–290 (2015).

150. Yang, J. *et al.* Common SNPs explain a large proportion of the heritability for human height. *Nat. Genet.* **42,** 565–569 (2010).

151. Loh, P.-R. *et al.* Contrasting genetic architectures of schizophrenia and other complex diseases using fast variance-components analysis. *Nat. Genet.* **47,** 1385–92 (2015).

152. Bulik-Sullivan, B. *et al.* An Atlas of Genetic Correlations across Human Diseases and Traits. *bioRxiv,* 1–44 (2015).

153. Bulik-Sullivan, B. *et al.* An atlas of genetic correlations across human diseases and traits. *Nat. Genet.* **47,** 1236–41 (2015).

154. Bulik-Sullivan, B. K. *et al.* LD Score regression distinguishes confounding from polygenicity in genome-wide association studies. *Nat. Genet.* **47,** 291–295 (2015).

155. Dadd, T., Weale, M. E. & Lewis, C. M. A critical evaluation of genomic control methods for genetic association studies. *Genet. Epidemiol.* **33,** 290–298 (2009).

156. Devlin, B, Roeder, K. & Wasserman, L. Genomic control, a new approach to genetic-based association studies. *Theor. Popul. Biol.* **60,** 155–66 (2001).

157. Yang, J. *et al.* Genomic inflation factors under polygenic inheritance. *Eur. J. Hum. Genet.* **19,** 807–812 (2011).

158. Willer, C. J., Li, Y. & Abecasis, G. R. METAL: Fast and efficient meta-analysis of genomewide association scans. *Bioinformatics* **26,** 2190–2191 (2010).

159. Morris, A. P. Transethnic meta-analysis of genomewide association studies. *Genet. Epidemiol.* **35,** 809–822 (2011).

160. Pruim, R. J. *et al. LocusZoom: Regional visualization of genome-wide association scan results* in *Bioinformatics* **27** (2011), 2336–2337.

161. Yang, J., Lee, S. H., Goddard, M. E. & Visscher, P. M. GCTA: A tool for genome-wide complex trait analysis. *Am. J. Hum. Genet.* **88,** 76–82 (2011).

162. Yang, J. *et al.* Conditional and joint multiple-SNP analysis of GWAS summary statistics identifies additional variants influencing complex traits. *Nat. Genet.* **44,** 369–75, S1–3 (2012).

163. Finucane, H. K. *et al.* Partitioning heritability by functional annotation using genome-wide association summary statistics. *Nat. Genet.* **47,** 1228–35 (2015).

164. Zheng, J. *et al.* LD Hub: a centralized database and web interface to perform LD score regression that maximizes the potential of summary level GWAS data for SNP heritability and genetic correlation analysis. *Bioinformatics,* btw613 (2016).

165. Lonsdale, J. *et al.* The Genotype-Tissue Expression (GTEx) project. *Nat. Genet.* **45,** 580–585 (2013).

166. Zhu, Z. *et al.* Integration of summary data from GWAS and eQTL studies predicts complex trait gene targets. *Nat. Genet.* **48,** 481–487 (2016).

167. Westra, H.-J. *et al.* Systematic identification of trans eQTLs as putative drivers of known disease associations. *Nat. Genet.* **45,** 1238–43 (2013).

168. Gusev, A. *et al.* Integrative approaches for large-scale transcriptome-wide association studies. *Nat. Genet.* **48,** 245–52 (2016).

169. Gamazon, E. R. *et al.* A gene-based association method for mapping traits using reference transcriptome data. *Nat. Genet.* **47,** 1091–1098 (2015).

170. Barbeira, A. *et al.* Integrating tissue specific mechanisms into GWAS summary results. *bioRxiv,* 045260 (2017).

171. Segrè, A. V., Groop, L., Mootha, V. K., Daly, M. J. & Altshuler, D. Common inherited variation in mitochondrial genes is not enriched for associations with type 2 diabetes or related glycemic traits. *PLoS Genet.* **6,** e1001058 (2010).

172. Feng, S., Liu, D., Zhan, X., Wing, M. K. & Abecasis, G. R. RAREMETAL: Fast and powerful meta-analysis for rare variants. *Bioinformatics* **30,** 2828–2829 (2014).

173. De Leeuw, C. A., Mooij, J. M., Heskes, T. & Posthuma, D. MAGMA: Generalized Gene-Set Analysis of GWAS Data. *PLOS Comput. Biol.* **11** (ed Tang, H.) e1004219 (2015).

174. Clarke, T.-K. *et al.* Genome-wide association study of alcohol consumption and genetic overlap with other health-related traits in UK Biobank (N=112 117). *Mol. Psychiatry* (2017).

175. Davies, G *et al.* Genome-wide association study of cognitive functions and educational attainment in UK Biobank (N=112 151). *Mol. Psychiatry* **21,** 758–767 (2016).

176. Sniekers, S. *et al.* Genome-wide association meta-analysis of 78,308 individuals identifies new loci and genes influencing human intelligence. *Nat. Genet.* **49,** 1107–1112 (2017).

177. Hammerschlag, A. R. *et al.* Genome-wide association analysis of insomnia complaints identifies risk genes and genetic overlap with psychiatric and metabolic traits. *Nat. Genet.* (2017).

178. Liu, J. Z. *et al.* A versatile gene-based test for genome-wide association studies. *Am. J. Hum. Genet.* **87,** 139–145 (2010).

179. Hingorani, A. & Humphries, S. Nature's randomised trials. *Lancet* **366,** 1906–8 (2005).

180. Lawlor, D. A., Harbord, R. M., Sterne, J. A. C., Timpson, N. & Davey Smith, G. Mendelian randomization: using genes as instruments for making causal inferences in epidemiology. *Stat. Med.* **27,** 1133–63 (2008).

181. Smith, G. D. & Ebrahim, S. 'Mendelian randomization': Can genetic epidemiology contribute to understanding environmental determinants of disease? *Int. J. Epidemiol.* **32,** 1–22 (2003).

182. Pierce, B. L. & Burgess, S. Efficient design for Mendelian randomization studies: subsample and 2-sample instrumental variable estimators. *Am. J. Epidemiol.* **178,** 1177–84 (2013).

183. Haycock, P. C. *et al.* Best (but oft-forgotten) practices: The design, analysis, and interpretation of Mendelian randomization studies. *Am. J. Clin. Nutr.* **103,** 965–978 (2016).

184. Burgess, S., Butterworth, A. & Thompson, S. G. Mendelian randomization analysis with multiple genetic variants using summarized data. *Genet. Epidemiol.* **37,** 658–665 (2013).

185. Burgess, S., Scott, R. A., Timpson, N. J., Smith, G. D. & Thompson, S. G. Using published data in Mendelian randomization: A blueprint for efficient identification of causal risk factors. *Eur. J. Epidemiol.* **30,** 543–552 (2015).

186. Hemani, G. *et al.* MR-Base: a platform for systematic causal inference across the phenome using billions of genetic associations. *bioRxiv,* 078972 (2016).

187. Machiela, M. J. & Chanock, S. J. LDlink: a web-based application for exploring population-specific haplotype structure and linking correlated alleles of possible functional variants. *Bioinformatics* **31,** 3555–7 (2015).

188. Bowden, J. *et al.* A framework for the investigation of pleiotropy in two-sample summary data Mendelian randomization. *Stat. Med.* **36,** 1783–1802 (2017).

189. Bowden, J., Smith, G. D. & Burgess, S. Mendelian randomization with invalid instruments: Effect estimation and bias detection through Egger regression. *Int. J. Epidemiol.* **44,** 512–525 (2015).

190. Egger, M., Smith, G. D., Schneider, M. & Minder, C. Bias in meta-analysis detected by a simple, graphical test. *BMJ* **315,** 629–634 (1997).

191. Bowden, J., Davey Smith, G., Haycock, P. C. & Burgess, S. Consistent Estimation in Mendelian Randomization with Some Invalid Instruments Using a Weighted Median Estimator. *Genet. Epidemiol.* **40,** 304–314 (2016).

192. Cheung, C.-L. *et al.* Low handgrip strength is a predictor of osteoporotic fractures: cross-sectional and prospective evidence from the Hong Kong Osteoporosis Study. *Age (Dordr).* **34,** 1239–48 (2012).

193. Kärkkäinen, M *et al.* Association between functional capacity tests and fractures: an eight-year prospective population-based cohort study. *Osteoporos. Int.* **19,** 1203–10 (2008).

194. Savino, E. *et al.* Handgrip strength predicts persistent walking recovery after hip fracture surgery. *Am. J. Med.* **126** (2013).

195. Reed, T., Fabsitz, R. R., Selby, J. V. & Carmelli, D. Genetic influences and grip strength norms in the NHLBI twin study males aged 59-69. *Ann Hum Biol* **18,** 425–432 (1991).

196. Arden, N. K. & Spector, T. D. Genetic influences on muscle strength, lean body mass, and bone mineral density: a twin study. *J. Bone Miner. Res.* **12,** 2076–81 (1997).

197. Matteini, A. M. *et al.* Heritability estimates of endophenotypes of long and health life: the Long Life Family Study. *J. Gerontol. A. Biol. Sci. Med. Sci.* **65,** 1375–9 (2010).

198. Sayer, A. A. *et al.* Polymorphism of the IGF2 gene, birth weight and grip strength in adult men. *Age Ageing* **31,** 468–470 (2002).

199. Dato, S. *et al.* UCP3 polymorphisms, hand grip performance and survival at old age: association analysis in two Danish middle aged and elderly cohorts. *Mech. Ageing Dev.* **133,** 530–7 (2012).

200. Matteini, A. M. *et al.* GWAS analysis of handgrip and lower body strength in older adults in the CHARGE consortium. *Aging Cell,* 1–9 (2016).

201. Wain, L. V. *et al.* Novel insights into the genetics of smoking behaviour, lung function, and chronic obstructive pulmonary disease (UK BiLEVE): a genetic association study in UK Biobank. *Lancet. Respir. Med.* **3,** 769–81 (2015).

202. Boettger, L. M., Handsaker, R. E., Zody, M. C. & McCarroll, S. A. Structural haplotypes and recent evolution of the human 17q21.31 region. *Nat. Genet.* **44,** 881–885 (2012).

203. Steinberg, K. M. *et al.* Structural diversity and African origin of the 17q21.31 inversion polymorphism. *Nat. Genet.* **44,** 872–880 (2012).

204. Nikpay, M. *et al.* A comprehensive 1,000 Genomes-based genome-wide association meta-analysis of coronary artery disease. *Nat. Genet.* **47,** 1121–30 (2015).

205. Zheng, H. *et al.* Whole-genome sequencing identifies EN1 as a determinant of bone density and fracture. *Nature* **526,** 112–117 (2015).

206. Han, H. Q., Zhou, X., Mitch, W. E. & Goldberg, A. L. Myostatin/activin pathway antagonism: molecular basis and therapeutic potential. *Int. J. Biochem. Cell Biol.* **45,** 2333–47 (2013).

207. Kaplan, J.-C. & Hamroun, D. The 2015 version of the gene table of monogenic neuromuscular disorders (nuclear genome). *Neuromuscul. Disord.* **24,** 1123–53 (2014).

208. Cohen, S., Nathan, J. A. & Goldberg, A. L. Muscle wasting in disease: molecular mechanisms and promising therapies. *Nat. Rev. Drug Discov.* **14,** 58–74 (2015).

209. Coviello, A. D. *et al.* A genome-wide association meta-analysis of circulating sex hormone-binding globulin reveals multiple Loci implicated in sex steroid hormone regulation. *PLoS Genet.* **8,** e1002805 (2012).

210. Zhai, G. *et al.* Eight common genetic variants associated with serum DHEAS levels suggest a key role in ageing mechanisms. *PLoS Genet.* **7,** e1002025 (2011).

211. Teumer, A. *et al.* Genomewide meta-analysis identifies loci associated with IGF-I and IGFBP-3 levels with impact on age-related traits. *Aging Cell* **15,** 811–824 (2016).

212. Scott, R. A. *et al.* Large-scale association analyses identify new loci influencing glycemic traits and provide insight into the underlying biological pathways. *Nat. Genet.* **44,** 991–1005 (2012).

213. Prokopenko, I. *et al.* A central role for GRB10 in regulation of islet function in man. *PLoS Genet.* **10,** e1004235 (2014).

214. Joshi, P. K. *et al.* Variants near CHRNA3/5 and APOE have age- and sex-related effects on human lifespan. *Nat. Commun.* **7,** 11174 (2016).

215. Liu, J. Z., Erlich, Y. & Pickrell, J. K. Case-control association mapping by proxy using family history of disease. *Nat. Genet.* **49,** 325–331 (2017).

216. Mostafavi, H., Berisa, T., Przeworski, M. & Pickrell, J. K. Identifying genetic variants that affect viability in large cohorts. *bioRxiv.* arXiv: 085969 (2016).

217. Ervasti, J. M. Costameres: the Achilles' heel of Herculean muscle. *J. Biol. Chem.* **278,** 13591–4 (2003).

218. Rybakova, I. N., Patel, J. R. & Ervasti, J. M. The Dystrophin Complex Forms a Mechanically Strong Link between the Sarcolemma and Costameric Actin. *J. Cell Biol.* **150,** 1209–1214 (2000).

219. Dalkilic, I. & Kunkel, L. M. Muscular dystrophies: genes to pathogenesis. *Curr. Opin. Genet. Dev.* **13,** 231–238 (2003).

220. Sonnemann, K. J. *et al.* Cytoplasmic gamma-actin is not required for skeletal muscle development but its absence leads to a progressive myopathy. *Dev. Cell* **11,** 387–97 (2006).

221. Burr, A. R. *et al.* Na+ dysregulation coupled with Ca2+ entry through NCX1 promotes muscular dystrophy in mice. *Mol. Cell. Biol.* **34,** 1991–2002 (2014).

222. Mackler, J. M., Drummond, J. A., Loewen, C. A., Robinson, I. M. & Reist, N. E. The C(2)B Ca(2+)-binding motif of synaptotagmin is required for synaptic transmission in vivo. *Nature* **418,** 340–4 (2002).

223. Dale, J. M. *et al.* The spinal muscular atrophy mouse model, SMAΔ7, displays altered axonal transport without global neurofilament alterations. *Acta Neuropathol.* **122,** 331–41 (2011).

224. Junier, M.-P. What role(s) for TGFα in the central nervous system? *Prog. Neurobiol.* **62,** 443–473 (2000).

225. Lisovoski, F *et al.* Transforming growth factor alpha expression as a response of murine motor neurons to axonal injury and mutation-induced degeneration. *J. Neuropathol. Exp. Neurol.* **56,** 459–71 (1997).

226. Boillée, S, Cadusseau, J, Coulpier, M, Grannec, G & Junier, M. P. Transforming growth factor alpha: a promoter of motoneuron survival of potential biological relevance. *J. Neurosci.* **21,** 7079–88 (2001).

227. Debray, F.-G. *et al.* LRPPRC mutations cause a phenotypically distinct form of Leigh syndrome with cytochrome c oxidase deficiency. *J. Med. Genet.* **48,** 183–9 (2011).

228. Steinberg, S. J. *et al.* Peroxisome biogenesis disorders. *Biochim. Biophys. Acta* **1763,** 1733–48 (2006).

229. Koolen, D. A. *et al.* Mutations in the chromatin modifier gene KANSL1 cause the 17q21.31 microdeletion syndrome. *Nat. Genet.* **44,** 639–641 (2012).

230. Nalls, M. A. *et al.* Large-scale meta-analysis of genome-wide association data identifies six new risk loci for Parkinson's disease. eng. *Nat. Genet.* **46,** 989–93 (2014).

231. Mootha, V. K. *et al.* Identification of a gene causing human cytochrome c oxidase deficiency by integrative genomics. *Proc. Natl. Acad. Sci. U. S. A.* **100,** 605–10 (2003).

232. Julien, M. *et al.* Phosphate-dependent regulation of MGP in osteoblasts: role of ERK1/2 and Fra-1. *J. Bone Miner. Res.* **24,** 1856–68 (2009).

233. Lach-Trifilieff, E. *et al.* An antibody blocking activin type II receptors induces strong skeletal muscle hypertrophy and protects from atrophy. *Mol. Cell. Biol.* **34,** 606–18 (2014).

234. Amato, A. A. *et al.* Treatment of sporadic inclusion body myositis with bimagrumab. *Neurology* **83,** 2239–46 (2014).

235. Yang, N. *et al.* ACTN3 genotype is associated with human elite athletic performance. *Am. J. Hum. Genet.* **73,** 627–631 (2003).

236. Sheffield-Moore, M. & Urban, R. J. An overview of the endocrinology of skeletal muscle. *Trends Endocrinol. Metab.* **15,** 110–115 (2004).

237. Horstman, A. M., Dillon, E. L., Urban, R. J. & Sheffield-Moore, M. The role of androgens and estrogens on healthy aging and longevity. *Journals Gerontol. - Ser. A Biol. Sci. Med. Sci.* **67,** 1140–1152 (2012).

238. Gullett, N. P., Hebbar, G. & Ziegler, T. R. Update on clinical trials of growth factors and anabolic steroids in cachexia and wasting 1 âĂŞ 4. *Curr. Opin. Clin. Nutr. Metab. Care* **91,** 1143–1147 (2010).

239. Clemson, L. *et al.* Integration of balance and strength training into daily life activity to reduce rate of falls in older people (the LiFE study): randomised parallel trial. *BMJ* **345,** e4547 (2012).

240. Edwards, B. J., Song, J., Dunlop, D. D., Fink, H. A. & Cauley, J. A. *Functional decline after incident wrist fractures–Study of Osteoporotic Fractures: prospective cohort study* 2010.

241. Claussnitzer, M. *et al.* FTO Obesity Variant Circuitry and Adipocyte Browning in Humans. *N. Engl. J. Med.* **373,** 895–907 (2015).

242. Lusk, G. ANIMAL CALORIMETRY. Twenty-Fourth Paper ANALYSIS OF THE OXIDATION OF MIXTURES OF CARBOHYDRATE AND FAT. *J. Biol. Chem.* **59,** 41–42 (1924).

243. Mansell, P. I. & Macdonald, I. A. Reappraisal of the Weir equation for calculation of metabolic rate. *Am. J. Physiol.* **258,** R1347–54 (1990).

244. Elia, M. in *Energy Metab. Tissue Determ. Cell. Corollaries* (eds Kinney, J. & Tucker, H.) 61–80 (Raven Press, New York, NY, 1992).

245. Han, B. & Eskin, E. Random-effects model aimed at discovering associations in meta-analysis of genome-wide association studies. *Am. J. Hum. Genet.* **88,** 586–598 (2011).

246. Han, B. & Eskin, E. Interpreting Meta-Analyses of Genome-Wide Association Studies. *PLoS Genet.* **8** (ed Kerr, K.) e1002555 (2012).

247. Ward, L. D. & Kellis, M. HaploReg: A resource for exploring chromatin states, conservation, and regulatory motif alterations within sets of genetically linked variants. *Nucleic Acids Res.* **40** (2012).

248. Byrne, N. M., Hills, A. P., Hunter, G. R., Weinsier, R. L. & Schutz, Y. Metabolic equivalent: one size does not fit all. *J. Appl. Physiol.* **99,** 1112–9 (2005).

249. Locke, A. E. *et al.* Genetic studies of body mass index yield new insights for obesity biology. *Nature* **518,** 197–206 (2015).

250. Wood, A. R. *et al.* Defining the role of common variation in the genomic and biological architecture of adult human height. *Nat. Genet.* **46,** 1173 (2014).

251. Shungin, D. *et al.* New genetic loci link adipose and insulin biology to body fat distribution. *Nature* **518,** 187–196 (2015).

252. Lu, Y. *et al.* New loci for body fat percentage reveal link between adiposity and cardiometabolic disease risk. *Nat. Commun.* **7,** 10495 (2016).

253. InterAct Consortium *et al.* Design and cohort description of the InterAct Project: an examination of the interaction of genetic and lifestyle factors on the incidence of type 2 diabetes in the EPIC Study. *Diabetologia* **54,** 2272–82 (2011).

254. Podmore, C. *et al.* Association of Multiple Biomarkers of Iron Metabolism and Type 2 Diabetes: The EPIC-InterAct Study. *Diabetes Care* **39,** 572–581 (2016).

255. Dudbridge, F. Power and Predictive Accuracy of Polygenic Risk Scores. *PLoS Genet.* **9** (2013).

256. Lee, J.-S. *et al.* Dual targeting of glutaminase 1 and thymidylate synthase elicits death synergistically in NSCLC. *Cell Death Dis.* **7,** e2511 (2016).

257. Allen, E. *et al.* Differential Aspartate Usage Identifies a Subset of Cancer Cells Particularly Dependent on OGDH. *Cell Rep.* **17,** 876–890 (2016).

258. Yang, H. *et al.* SIRT3-dependent GOT2 acetylation status affects the malate-aspartate NADH shuttle activity and pancreatic tumor growth. *EMBO J.* **34,** 1110–1125 (2015).

259. Menzies, K. J., Zhang, H., Katsyuba, E. & Auwerx, J. Protein acetylation in metabolism - metabolites and cofactors. *Nat. Rev. Endocrinol.* **12,** 43–60 (2015).

260. Sakurai, T. The neural circuit of orexin (hypocretin): maintaining sleep and wakefulness. *Nat. Rev. Neurosci.* **8,** 171–181 (2007).

261. Ebrahim, I. O., Howard, R. S. & et al. Kopelman, M. D. The hypocretin/orexin system. *J. R. Soc. Med.* **95,** 227–230 (2002).

262. Rodgers, R. J., Ishii, Y., Halford, J. C. G. & Blundell, J. E. *Orexins and appetite regulation* 2002.

263. Gregor Sutcliffe, J. & De Lecea, L. *The hypocretins: Excitatory neuromodulatory peptides for multiple homeostatic systems, including sleep and feeding* 2000.

264. Sellayah, D., Bharaj, P. & Sikder, D. Orexin Is Required for Brown Adipose Tissue Development, Differentiation, and Function. *Cell Metab.* **14,** 478–490 (2011).

265. Sellayah, D. & Sikder, D. Orexin Restores Aging-Related Brown Adipose Tissue Dysfunction in Male Mice. *Endocrinology* **155,** 485–501 (2014).

266. Zhang, W. *et al.* Orexin neurons are indispensable for stress-induced thermogenesis in mice. *J. Physiol.* **588,** 4117–4129 (2010).

267. Madden, C. J., Tupone, D. & Morrison, S. F. Orexin modulates brown adipose tissue thermogenesis. *Biomol. Concepts* **3** (2012).

268. De Jonge, L. *et al.* Effect of diet composition and weight loss on resting energy expenditure in the POUNDS LOST study. *Obesity (Silver Spring).* **20,** 2384–9 (2012).

269. Llewellyn, C. & Wardle, J. *Behavioral susceptibility to obesity: Gene-environment interplay in the development of weight* 2015.

270. Cornelis, M. C. *et al.* Obesity susceptibility loci and uncontrolled eating, emotional eating and cognitive restraint behaviors in men and women. *Obesity* **22,** E135–E141 (2014).

271. Wardle, J. *et al.* Obesity Associated Genetic Variation in FTO Is Associated with Diminished Satiety. *J. Clin. Endocrinol. Metab.* **93,** 3640–3643 (2008).

272. Micali, N., Field, A. E., Treasure, J. L. & Evans, D. M. Are obesity risk genes associated with binge eating in adolescence? *Obesity* **23,** 1729–1736 (2015).

273. Church, C. *et al.* Overexpression of Fto leads to increased food intake and results in obesity. *Nat. Genet.* **42,** 1086–1092 (2010).

274. Vega, J. A. *et al.* Melanocortin-4 Receptor Gene Variation Is Associated with Eating Behavior in Chilean Adults. *Ann. Nutr. Metab.* **68,** 35–41 (2015).

275. Horstmann, A. *et al.* Common Genetic Variation near MC4R Has a Sex-Specific Impact on Human Brain Structure and Eating Behavior. *PLoS One* **8** (ed Esteban, F. J.) e74362 (2013).

276. Speakman, J. R. The 'Fat Mass and Obesity Related' (FTO) gene: Mechanisms of Impact on Obesity and Energy Balance. *Curr. Obes. Rep.* **4,** 73–91 (2015).

277. Amatruda, J. M., Statt, M. C. & Welle, S. L. Total and resting energy expenditure in obese women reduced to ideal body weight. *J. Clin. Invest.* **92,** 1236–42 (1993).

278. Wyatt, H. R. *et al.* Resting energy expenditure in reduced-obese subjects in the National Weight Control Registry. *Am. J. Clin. Nutr.* **69,** 1189–93 (1999).

279. Baron, R. M. & Kenny, D. a. The moderator-mediator variable distinction in social psychological research: conceptual, strategic, and statistical considerations. *J. Pers. Soc. Psychol.* **51,** 1173–1182 (1986).

280. Lek, M. *et al.* Analysis of protein-coding genetic variation in 60,706 humans. *Nature* **536,** 285–291 (2016).

281. Robinson, A. J., Kunji, E. R. S. & Gross, A. Mitochondrial carrier homolog 2 (MTCH2): the recruitment and evolution of a mitochondrial carrier protein to a critical player in apoptosis. *Exp. Cell Res.* **318,** 1316–23 (2012).

282. Maryanovich, M. *et al.* An MTCH2 pathway repressing mitochondria metabolism regulates haematopoietic stem cell fate. *Nat. Commun.* **6,** 7901 (2015).

283. Buzaglo-Azriel, L. *et al.* Loss of Muscle MTCH2 Increases Whole-Body Energy Utilization and Protects from Diet-Induced Obesity. *Cell Rep.* **14,** 1602–1610 (2016).

284. Bar-Lev, Y. *et al.* Mimp/Mtch2, an obesity susceptibility gene, induces alteration of fatty acid metabolism in transgenic mice. *PLoS One* **11** (2016).

285. Vaisse, C. *et al.* Melanocortin-4 receptor mutations are a frequent and heterogeneous cause of morbid obesity. *J. Clin. Invest.* **106,** 253–262 (2000).

286. Clifton, E. A. D. *et al.* Associations between body mass index-related genetic variants and adult body composition: The Fenland cohort study. *Int. J. Obes.* **41,** 613–619 (2017).

287. Holland, A. J. & Cleveland, D. W. Boveri revisited: chromosomal instability, aneuploidy and tumorigenesis. *Nat. Rev. Mol. Cell Biol.* **10,** 478–487 (2009).

288. Weaver, B. A. A. & Cleveland, D. W. Does aneuploidy cause cancer? *Curr. Opin. Cell Biol.* **18,** 658–67 (2006).

289. Sheltzer, J. M. *et al.* Aneuploidy Drives Genomic Instability in Yeast. *Science (80-.).* **333,** 1026–1030 (2011).

290. Giam, M. & Rancati, G. Aneuploidy and chromosomal instability in cancer: a jackpot to chaos. *Cell Div.* **10,** 3 (2015).

291. Gordon, D. J., Resio, B. & Pellman, D. Causes and consequences of aneuploidy in cancer. *Nat. Rev. Genet.* **13,** 189–203 (2012).

292. Thompson, S. L., Bakhoum, S. F. & Compton, D. A. Mechanisms of chromosomal instability. *Curr. Biol.* **20,** R285–95 (2010).

293. Jacobs, K. B. *et al.* Detectable clonal mosaicism and its relationship to aging and cancer. *Nat. Genet.* **44,** 651–658 (2012).

294. Lippert, C. *et al.* Identification of individuals by trait prediction using whole-genome sequencing data. *Proc. Natl. Acad. Sci.* 201711125 (2017).

295. Skaletsky, H. *et al.* The male-specific region of the human Y chromosome is a mosaic of discrete sequence classes. *Nature* **423,** 825–37 (2003).

296. Wang, K. *et al.* PennCNV: an integrated hidden Markov model designed for high-resolution copy number variation detection in whole-genome SNP genotyping data. *Genome Res.* **17,** 1665–74 (2007).

297. Gudbjartsson, D. F. *et al.* Large-scale whole-genome sequencing of the Icelandic population. *Nat. Genet.* **47,** 435–44 (2015).

298. Li, H. *et al.* The Sequence Alignment/Map format and SAMtools. *Bioinformatics* **25,** 2078–9 (2009).

299. Venables, W. N. & Ripley, B. D. *Modern Applied Statistics with S* (Springer New York, New York, NY, 2002).

300. Sulem, P. *et al.* Identification of low-frequency variants associated with gout and serum uric acid levels. *Nature Genetics* **43,** 1127 (2011).

301. Sulem, P. *et al.* Genome-wide association study identifies sequence variants on 6q21 associated with age at menarche. *Nature Genetics* **41,** 734 (2009).

302. Holm, H. *et al.* Several common variants modulate heart rate, PR interval and QRS duration. *Nat. Genet.* **42,** 117–22 (2010).

303. Bibikova, M. *et al.* High density DNA methylation array with single CpG site resolution. *Genomics* **98,** 288–295 (2011).

304. Lehne, B. *et al.* A coherent approach for analysis of the Illumina HumanMethylation450 BeadChip improves data quality and performance in epigenome-wide association studies. *Genome Biol.* **16,** 37 (2015).

305. Xu, Z., Niu, L., Li, L. & Taylor, J. A. ENmix: a novel background correction method for Illumina HumanMethylation450 BeadChip. *Nucleic Acids Res.* **44,** e20–e20 (2016).

306. Naeem, H. *et al.* Reducing the risk of false discovery enabling identification of biologically significant genome-wide methylation status using the HumanMethylation450 array. *BMC Genomics* **15,** 51 (2014).

307. Houseman, E. A. *et al.* DNA methylation arrays as surrogate measures of cell mixture distribution. *BMC Bioinformatics* **13,** 86 (2012).

308. Aryee, M. J. *et al.* Minfi: a flexible and comprehensive Bioconductor package for the analysis of Infinium DNA methylation microarrays. *Bioinformatics* **30,** 1363–9 (2014).

309. Manning, A. K. *et al.* A genome-wide approach accounting for body mass index identifies genetic variants influencing fasting glycemic traits and insulin resistance. *Nat. Genet.* **44,** 659–69 (2012).

310. Soranzo, N. *et al.* Common variants at 10 genomic loci influence hemoglobin A_1(C) levels via glycemic and nonglycemic pathways. *Diabetes* **59,** 3229–39 (2010).

311. Morris, A. P. *et al.* Large-scale association analysis provides insights into the genetic architecture and pathophysiology of type 2 diabetes. *Nat. Genet.* **44,** 981–90 (2012).

312. Al Olama, A. A. *et al.* A meta-analysis of 87,040 individuals identifies 23 new susceptibility loci for prostate cancer. *Nat. Genet.* **46,** 1103–9 (2014).

313. Eeles, R. *et al.* The genetic epidemiology of prostate cancer and its clinical implications. *Nat. Rev. Urol.* **11,** 18–31 (2014).

314. Thorgeirsson, T. E. *et al.* Sequence variants at CHRNB3-CHRNA6 and CYP2A6 affect smoking behavior. *Nat. Genet.* **42,** 448–53 (2010).

315. Zhu, Z. *et al.* Integration of summary data from GWAS and eQTL studies predicts complex trait gene targets. *Nat. Genet.* **48,** 481–487 (2016).

316. Bonder, M. J. *et al.* Disease variants alter transcription factor levels and methylation of their binding sites. *Nat. Genet.* (2016).

317. Henderson, M. C. *et al.* High-throughput RNAi screening identifies a role for TNK1 in growth and survival of pancreatic cancer cells. *Mol. Cancer Res.* **9,** 724–32 (2011).

318. Stacey, S. N. *et al.* A germline variant in the TP53 polyadenylation signal confers cancer susceptibility. *Nat. Genet.* **43,** 1098–1103 (2011).

319. Walsh, K. M. *et al.* Analysis of 60 reported glioma risk SNPs replicates published GWAS findings but fails to replicate associations from published candidate-gene studies. *Genet. Epidemiol.* **37,** 222–8 (2013).

320. Diskin, S. J. *et al.* Rare variants in TP53 and susceptibility to neuroblastoma. *J. Natl. Cancer Inst.* **106,** dju047 (2014).

321. Ruark, E. *et al.* Identification of nine new susceptibility loci for testicular cancer, including variants near DAZL and PRDM14. *Nat. Genet.* **45,** 686–9 (2013).

322. Chung, C. C. *et al.* Meta-analysis identifies four new loci associated with testicular germ cell tumor. *Nat. Genet.* **45,** 680–5 (2013).

323. Kar, S. P. *et al.* Genome-Wide Meta-Analyses of Breast, Ovarian, and Prostate Cancer Association Studies Identify Multiple New Susceptibility Loci Shared by at Least Two Cancer Types. *Cancer Discov.* 1–17 (2016).

324. Pilling, L. C. *et al.* Human longevity is influenced by many genetic variants: evidence from 75,000 UK Biobank participants. *Aging (Albany. NY).* **8,** 547–60 (2016).

325. Dupuis, J. *et al.* New genetic loci implicated in fasting glucose homeostasis and their impact on type 2 diabetes risk. *Nat. Genet.* **42,** 105–16 (2010).

326. Willems, S. M. *et al.* Large-scale GWAS identifies multiple loci for hand grip strength providing biological insights into muscular fitness. *Nat. Commun.* **8,** 16015 (2017).

327. Machiela, M. J. *et al.* Female chromosome X mosaicism is age-related and preferentially affects the inactivated X chromosome. *Nat. Commun.* **7,** 11843 (2016).

328. Cheeseman, I. M. & Desai, A. Molecular architecture of the kinetochore-microtubule interface. *Nat. Rev Mol. Cell Biol.* **9,** 33–46 (2008).

329. Kline, S. L., Cheeseman, I. M., Hori, T., Fukagawa, T. & Desai, A. The human Mis12 complex is required for kinetochore assembly and proper chromosome segregation. *J. Cell Biol.* **173,** 9–17 (2006).

330. Kufer, T. A. *et al.* Human TPX2 is required for targeting Aurora-A kinase to the spindle. *J. Cell Biol.* **158,** 617–623 (2002).

331. Jurado, S. *et al.* ATM Substrate Chk2-interacting Zn2+ Finger (ASCIZ) Is a Bi-functional Transcriptional Activator and Feedback Sensor in the Regulation of Dynein Light Chain (DYNLL1) Expression. *J. Biol. Chem.* **287,** 3156–3164 (2012).

332. Dunsch, A. K. *et al.* Dynein light chain 1 and a spindle-associated adaptor promote dynein asymmetry and spindle orientation. *J. Cell Biol.* **198,** 1039–1054 (2012).

333. Zaytseva, O. *et al.* The Novel Zinc Finger Protein dASCIZ Regulates Mitosis in Drosophila via an Essential Role in Dynein Light-Chain Expression. *Genetics* **196,** 443–453 (2014).

334. Regue, L. *et al.* DYNLL/LC8 Protein Controls Signal Transduction through the Nek9/Nek6 Signaling Module by Regulating Nek6 Binding to Nek9. *J. Biol. Chem.* **286,** 18118–18129 (2011).

335. Aoki, T., Ueda, S., Kataoka, T. & Satoh, T. Regulation of mitotic spindle formation by the RhoA guanine nucleotide exchange factor ARHGEF10. *BMC Cell Biol.* **10,** 56 (2009).

336. Beites, C. L., Xie, H, Bowser, R & Trimble, W. S. The septin CDCrel-1 binds syntaxin and inhibits exocytosis. *Nat. Neurosci.* **2,** 434–9 (1999).

337. Zuo, Y., Oh, W. & Frost, J. A. Controlling the switches: Rho GTPase regulation during animal cell mitosis. *Cell. Signal.* **26,** 2998–3006 (2014).

338. Mazouzi, A., Velimezi, G. & Loizou, J. I. DNA replication stress: Causes, resolution and disease. *Exp. Cell Res.* **329,** 85–93 (2014).

339. Zeman, M. K. & Cimprich, K. A. Causes and consequences of replication stress. *Nat. Cell Biol.* **16,** 2–9 (2014).

340. Osborn, A. J., Elledge, S. J. & Zou, L. Checking on the fork: the DNA-replication stress-response pathway. *Trends Cell Biol.* **12,** 509–16 (2002).

341. Gao, G. *et al.* NPAT expression is regulated by E2F and is essential for cell cycle progression. *Mol. Cell. Biol.* **23,** 2821–33 (2003).

342. Santaguida, S. & Amon, A. Short- and long-term effects of chromosome mis-segregation and aneuploidy. *Nat. Rev. Mol. Cell Biol.* **16,** 473–485 (2015).

343. Christmann, M. & Kaina, B. Transcriptional regulation of human DNA repair genes following genotoxic stress: Trigger mechanisms, inducible responses and genotoxic adaptation. *Nucleic Acids Res.* **41,** 8403–8420 (2013).

344. McIntyre, R. E. *et al.* A Genome-Wide Association Study for Regulators of Micronucleus Formation in Mice. *G3 (Bethesda).* **6,** 2343–54 (2016).

345. Bieging, K. T., Mello, S. S. & Attardi, L. D. Unravelling mechanisms of p53-mediated tumour suppression. *Nat. Rev. Cancer* **14,** 359–70 (2014).

346. Yabu, T *et al.* Stress-induced ceramide generation and apoptosis via the phosphorylation and activation of nSMase1 by JNK signaling. *Cell Death Differ.* **22,** 258–73 (2015).

347. Laine, J, Künstle, G, Obata, T, Sha, M & Noguchi, M. The protooncogene TCL1 is an Akt kinase coactivator. *Mol. Cell* **6,** 395–407 (2000).

348. Czabotar, P. E., Lessene, G., Strasser, A. & Adams, J. M. Control of apoptosis by the BCL-2 protein family: implications for physiology and therapy. *Nat. Rev. Mol. Cell Biol.* **15,** 49–63 (2014).

349. Haimovitz-Friedman, A, Kolesnick, R. N. & Fuks, Z. Ceramide signaling in apoptosis. *Br. Med. Bull.* **53,** 539–53 (1997).

350. Zhivotovsky, B. & Kroemer, G. Apoptosis and genomic instability. *Nat. Rev. Mol. Cell Biol.* **5,** 752–762 (2004).

351. Uetake, Y. & Sluder, G. Prolonged prometaphase blocks daughter cell proliferation despite normal completion of mitosis. *Curr. Biol.* **20,** 1666–1671 (2010).

352. Ganem, N. J. *et al.* Cytokinesis failure triggers hippo tumor suppressor pathway activation. *Cell* **158,** 833–848 (2014).

353. Lim, S. L. *et al.* HENMT1 and piRNA Stability Are Required for Adult Male Germ Cell Transposon Repression and to Define the Spermatogenic Program in the Mouse. *PLOS Genet.* **11** (ed Frye, M.) e1005620 (2015).

354. Hsu, L. C.-L. *et al.* DAZAP1, an hnRNP protein, is required for normal growth and spermatogenesis in mice. *RNA* **14,** 1814–22 (2008).

355. Falix, F. A., Aronson, D. C., Lamers, W. H. & Gaemers, I. C. Possible roles of DLK1 in the Notch pathway during development and disease. *Biochim. Biophys. Acta - Mol. Basis Dis.* **1822,** 988–995 (2012).

356. Cunha, F. A. *et al.* How long does it take to achieve steady state for an accurate assessment of resting VO2 in healthy men? *Eur. J. Appl. Physiol.* **113,** 1441–7 (2013).

357. Reeves, M. M., Davies, P. S. W., Bauer, J. & Battistutta, D. Reducing the time period of steady state does not affect the accuracy of energy expenditure measurements by indirect calorimetry. *J. Appl. Physiol.* **97,** 130–4 (2004).

358. Sergi, G. *et al.* Resting VO2, maximal VO2 and metabolic equivalents in free-living healthy elderly women. *Clin. Nutr.* **29,** 84–8 (2010).

359. Palmer, C. & Pe'er, I. Statistical correction of the Winner's Curse explains replication variability in quantitative trait genome-wide association studies. *PLoS Genet.* **13** (2017).

360. Froom, P, Melamed, S, Kristal-Boneh, E, Benbassat, J & Ribak, J. Healthy volunteer effect in industrial workers. *J. Clin. Epidemiol.* **52,** 731–5 (1999).

361. Manolio, T. A. & Collins, R. Enhancing the Feasibility of Large Cohort Studies. *JAMA* **304,** 2290 (2010).

362. Day, F. R., Loh, P.-R., Scott, R. A., Ong, K. K. & Perry, J. R. B. A Robust Example of Collider Bias in a Genetic Association Study. *Am. J. Hum. Genet.* **98,** 392–3 (2016).

363. Aschard, H., Vilhjálmsson, B. J., Joshi, A. D., Price, A. L. & Kraft, P. Adjusting for Heritable Covariates Can Bias Effect Estimates in Genome-Wide Association Studies. *Am. J. Hum. Genet.* **96,** 329–339 (2015).

364. Burgess, S. & Thompson, S. G. Avoiding bias from weak instruments in Mendelian randomization studies. *Int. J. Epidemiol.* **40,** 755–64 (2011).

365. Brion, M.-J. A., Shakhbazov, K. & Visscher, P. M. Calculating statistical power in Mendelian randomization studies. *Int J Epidemiol* **42,** 1497–1501 (2013).

366. Evans, J. P., Meslin, E. M., Marteau, T. M. & Caulfield, T. Deflating the Genomic Bubble. *Science (80-.).* **331,** 861–862 (2011).

367. Nelson, M. R. *et al.* The support of human genetic evidence for approved drug indications. *Nat. Genet.* **47,** 856–60 (2015).

368. Garito, T. *et al.* Bimagrumab improves body composition and insulin sensitivity in insulin-resistant individuals. *Diabetes. Obes. Metab.* (2017).

369. Fradkin, J. E., Hanlon, M. C. & Rodgers, G. P. *NIH precision medicine initiative: Implications for diabetes research* in *Diabetes Care* **39** (2016), 1080–1084.

370. Collins, F. S. & Varmus, H. A New Initiative on Precision Medicine. *N. Engl. J. Med.* **372,** 793–795 (2015).

371. Chen, Z. *et al.* China Kadoorie Biobank of 0.5 million people: Survey methods, baseline characteristics and long-term follow-up. *Int. J. Epidemiol.* **40,** 1652–1666 (2011).

Supplementary Materials

Supplementary Figures

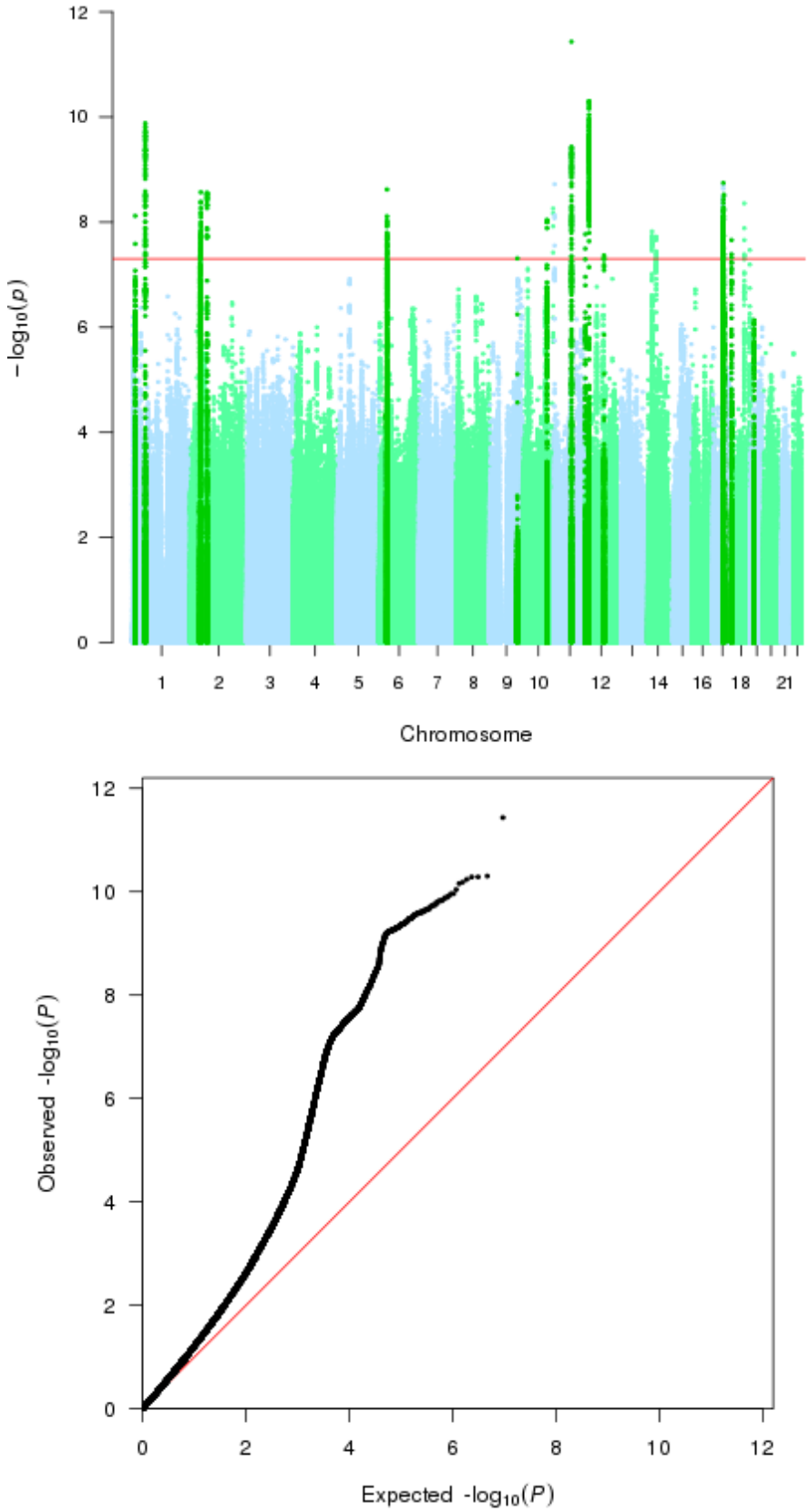

Supplementary Figure 1: Manhattan and QQ-plot of stage one grip strength associations in UK Biobank. Independent loci reaching genomewide significance in combined stage one + two analyses are highlighted bright green. λ_{GC}=1.31, LD score regression intercept = 1.02 (95% CI 0.998-1.042), suggesting that apparent inflation evident in the QQ-plot can be attributed to polygenicity of grip strength. On Manhattan, genomewide significance threshold is indicated; on QQ-plot, red line indicates null effect.

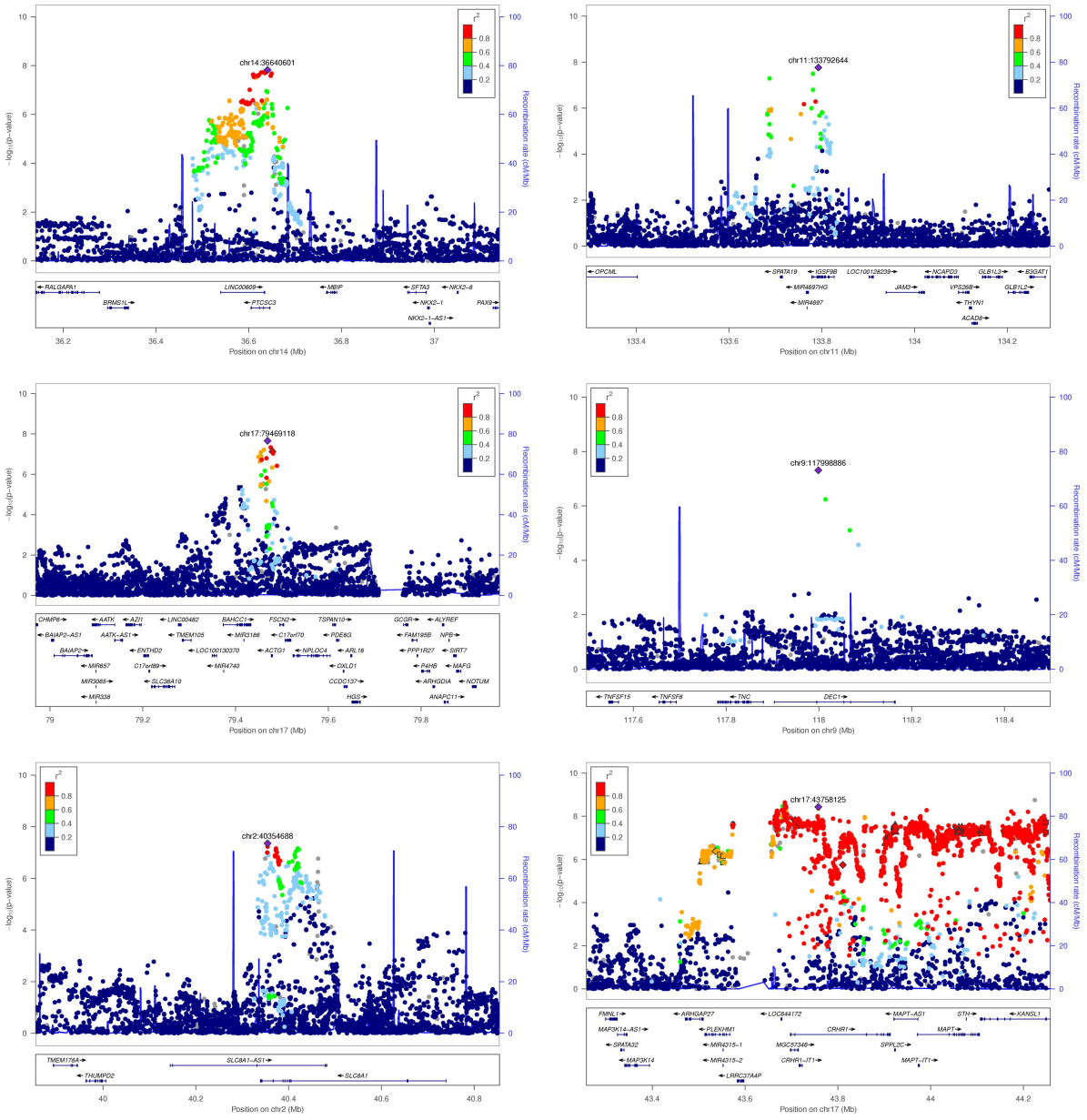

Supplementary Figure 2: Regional association plots of sixteen loci reaching genomewide significance in combined stage one plus two analyses for grip strength. Outlined plot characters denote a variant at suggestive significance ($p=5\times10^{-6}$) with coding consequences. Square, non-deleterious; inverted triangle, stop-gain; triangle, missense; diamond, splice region

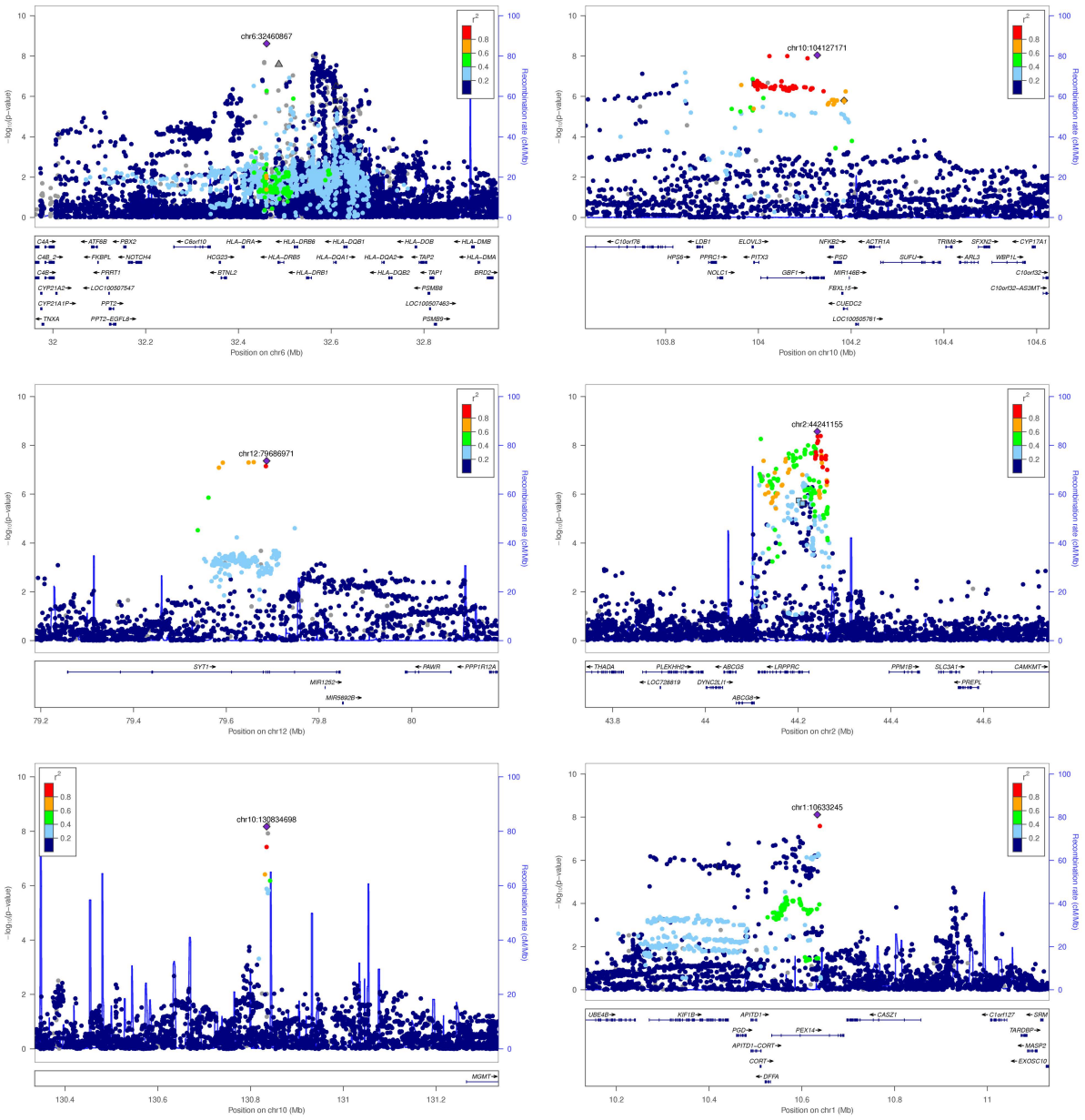

Supplementary Figure 2: Continued

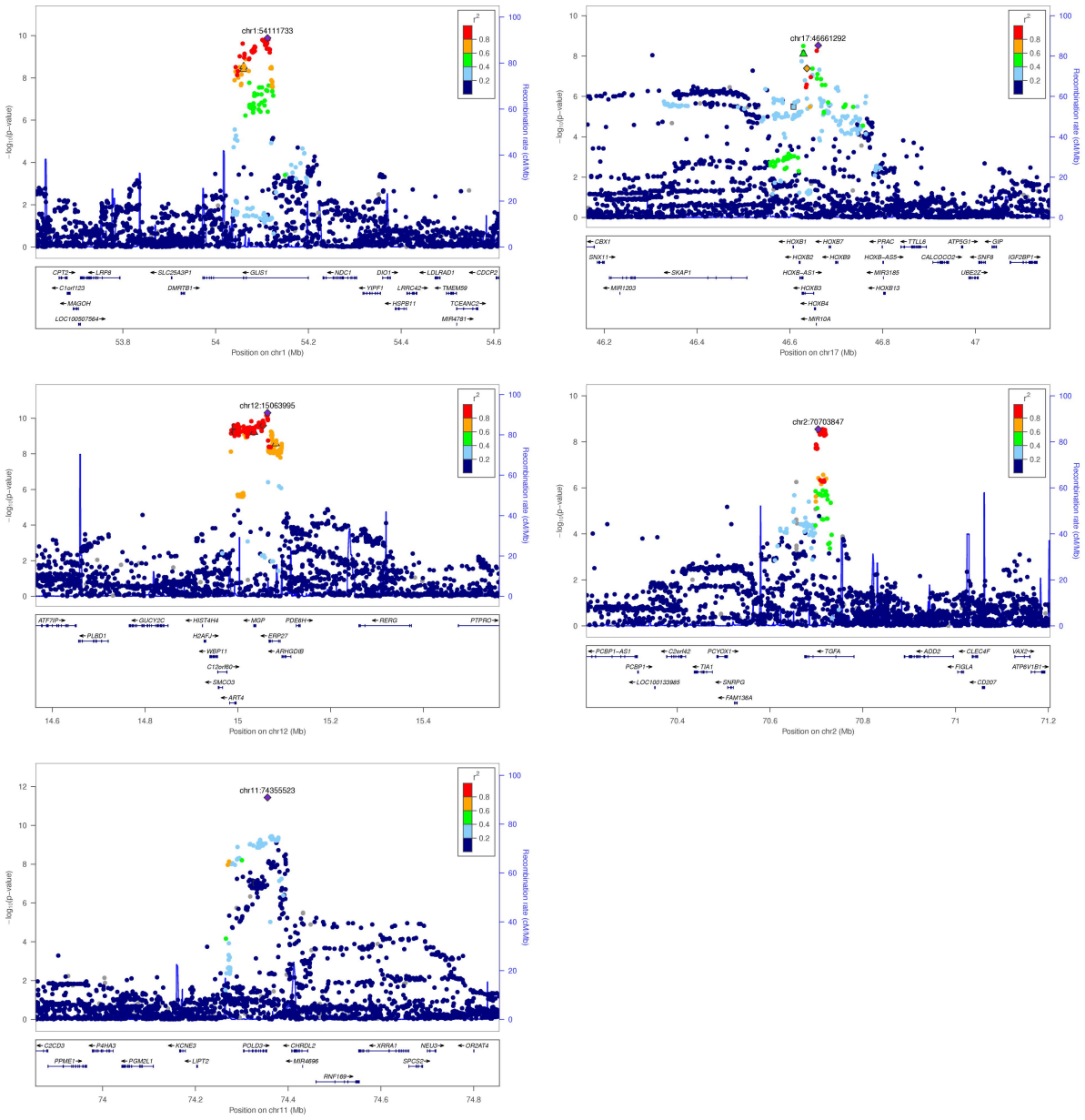

Supplementary Figure 2: Continued

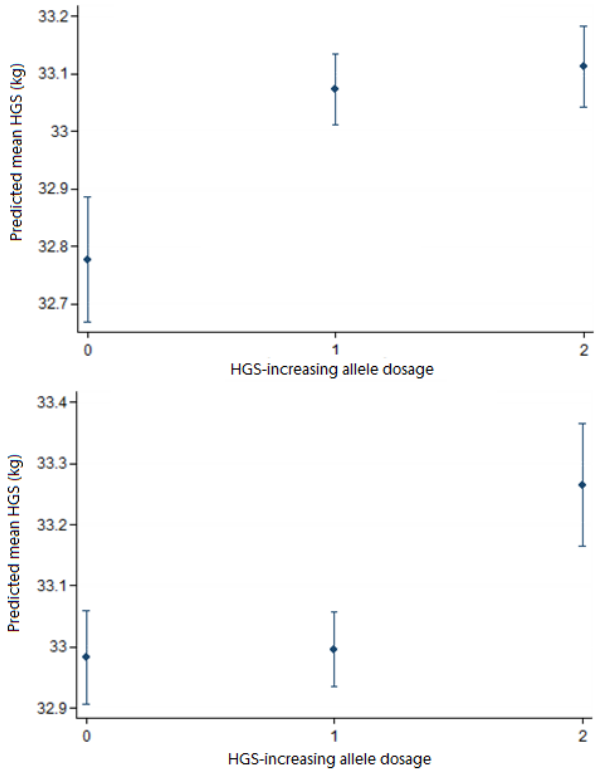

Supplementary Figure 3: Evidence of non-additive genetic association with HGS at two loci. Data shown are predicted mean hand grip strength by best-guess genotype expressed as HGS-increasing allele dosage. *Upper:* rs2273555 in *GBF1*; *Lower:* rs10861798 in *SYT1*. Bars denote 95% confidence interval.

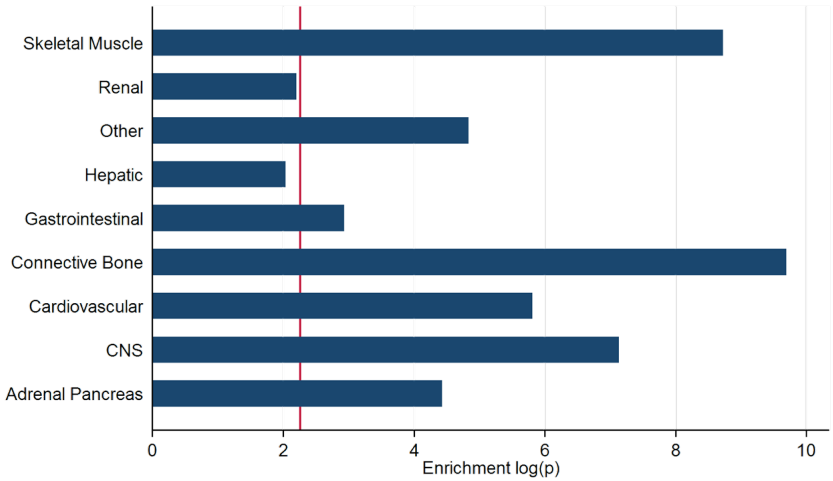

Supplementary Figure 4: Hand grip strength heritability partitioned by major tissue classes. Data shown are log p-values for enrichment in each curated tissue class from LD Score Regression, based on genomewide grip strength association results (adjusted for age, sex, BMI, standing height). Red line indicates Bonferroni-corrected threshold for statistical significance.

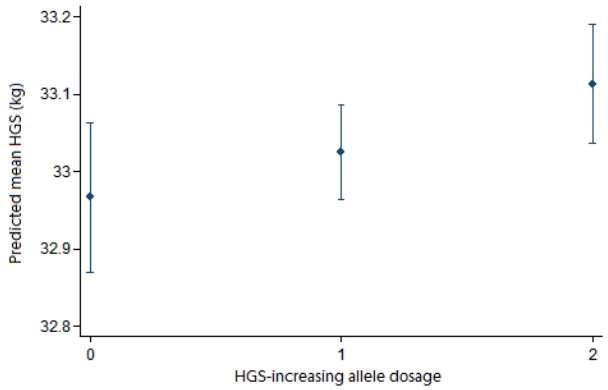

Supplementary Figure 5: Effect of nonsense mutation in *ACTN3* (R577X) on hand grip strength. Data are predicted mean hand grip strength by dosage of the previously-described stop-gain allele at rs1815739 (R577X mutation) in *ACTN3*. Bars denote 95% confidence interval.

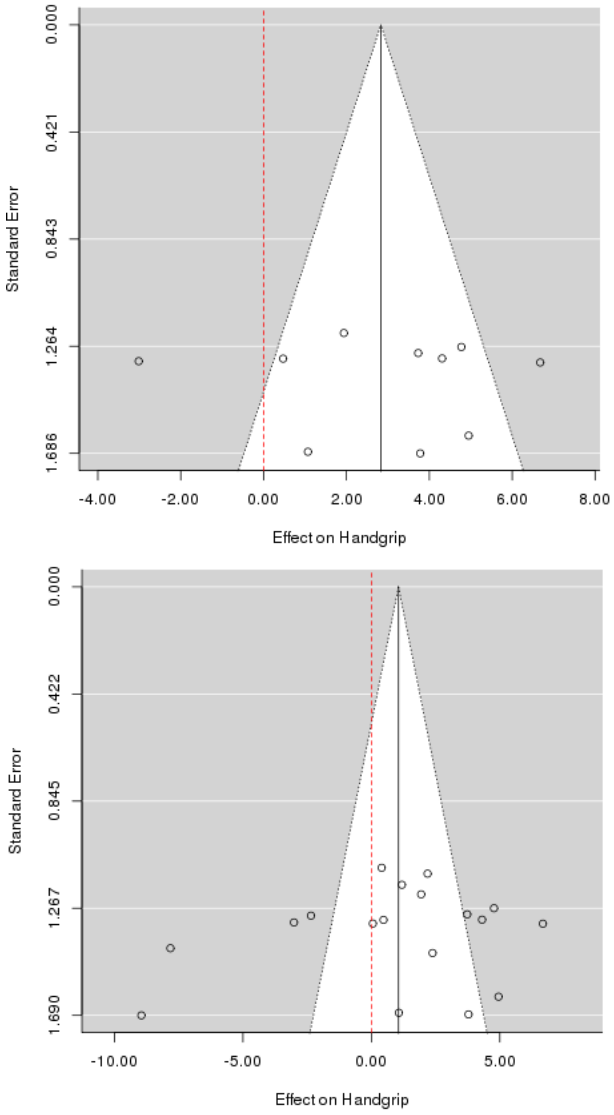

Supplementary Figure 6: Heterogeneity in effect of variants for insulin phenotypes on HGS in MR analyses. Funnel plots indicate the effect of variants included in the scores for two insulin traits on hand grip strength (kg), versus the standard error of this effect. *Upper:* Insulin resistance; *Lower:* Fasting Insulin. The highlighted funnel indicates the expected 95% confidence interval of effect, assuming that the variants in combination have an effect on the trait under an MR framework (black line). The null is indicated by the red dashed line.

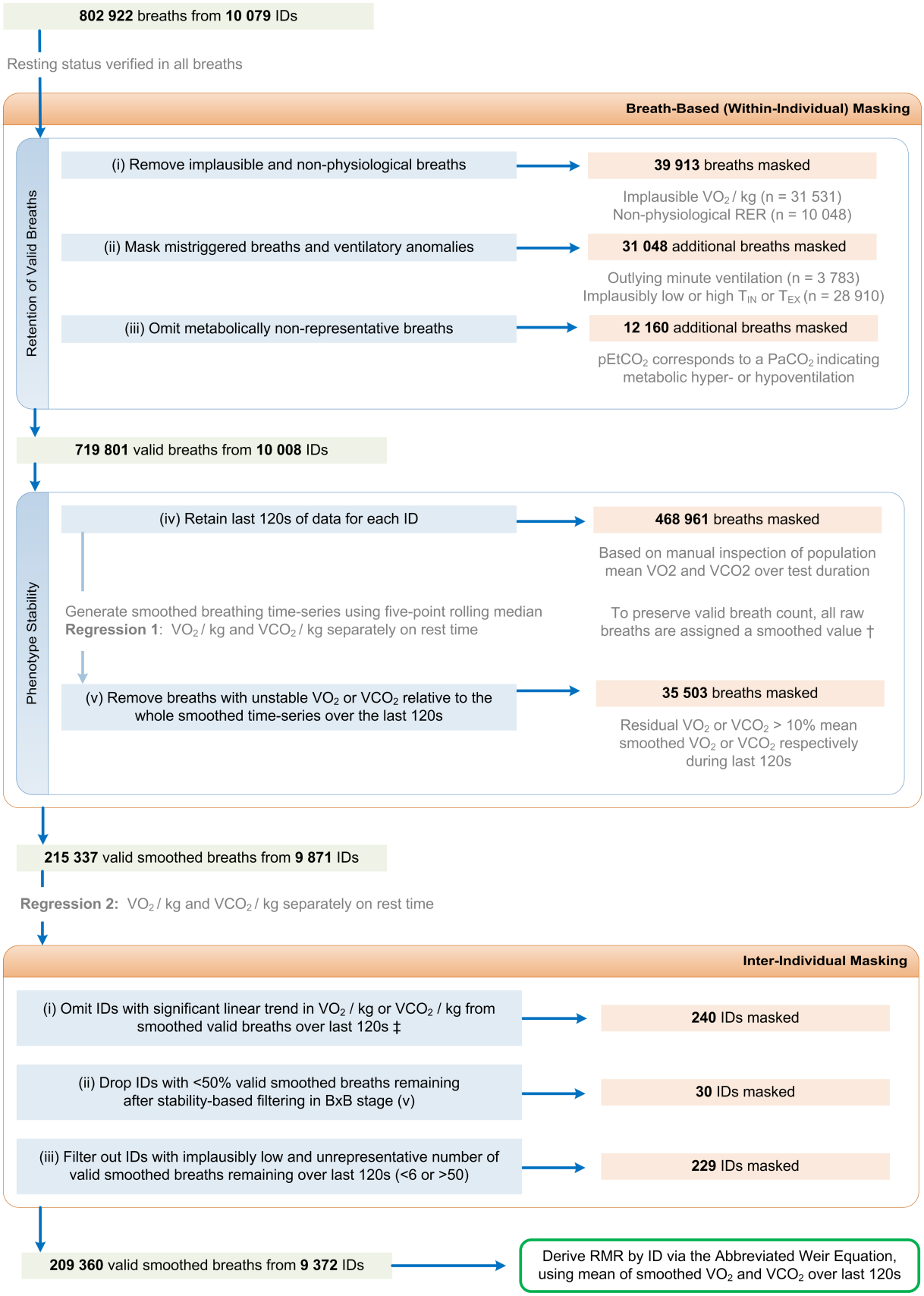

Supplementary Figure 7: Derivation of REE from observed respiratory exchange data
Respiratory exchange parameters measured in participants were processed to ensure they were stable and representative of underlying cellular respiration. VO_2, Oxygen consumption; RER, respiratory exchange rate; T_{IN}, inspiratory duration per breath; T_{EX}, expiratory duration per breath; $pEtCO_2$, end-tidal partial pressure of CO_2; $PaCO_2$, arterial partial pressure of CO_2

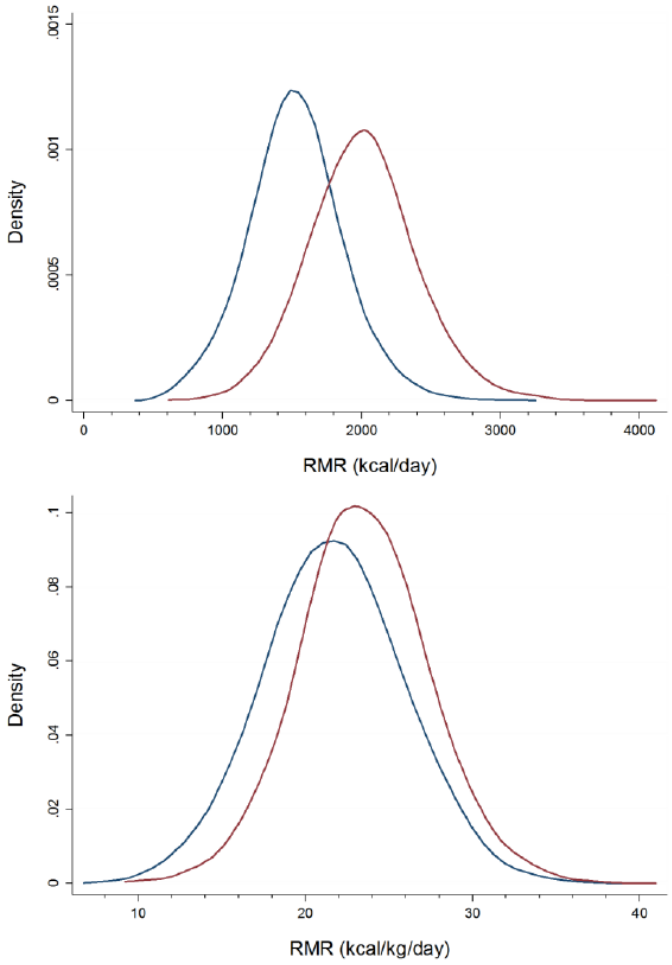

Supplementary Figure 8: Frequency density distribution of REE in Fenland. Data are shown for all 9,372 participants passing quality control for valid breaths and phenotype stability. *Upper:* crude REE. *Lower:* REE normalised to body mass. Kernel density curve generated using Epanechnikov kernel function. Red, male; Blue, female.

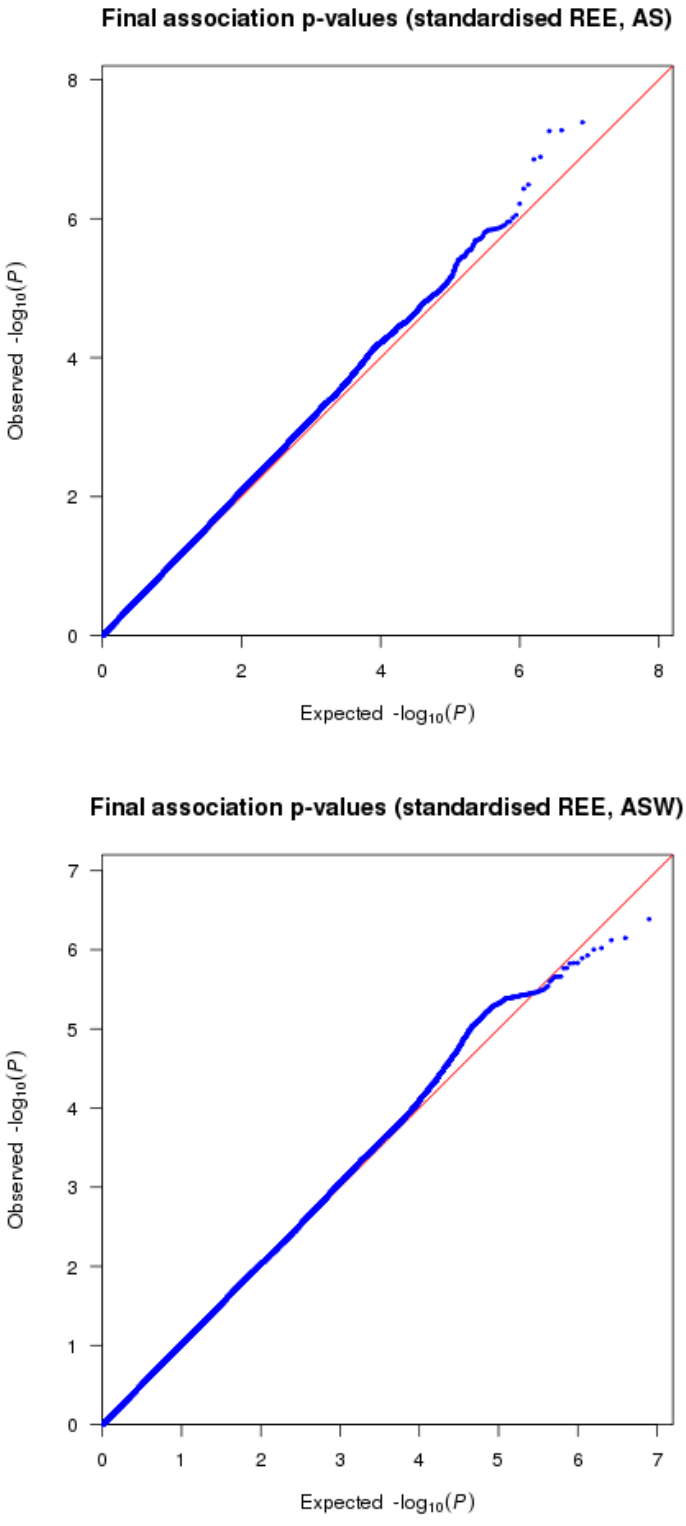

Supplementary Figure 9: QQ-plots of REE associations in combined European meta-analyses. *Upper:* Age and sex-adjusted, λ_{GC} = 1.04, LD score regression intercept = 1.01 (95% CI 0, 1.02). *Lower:* Age, sex and body mass-adjusted, λ_{GC} = 1.01, LD score regression intercept = 1.01.

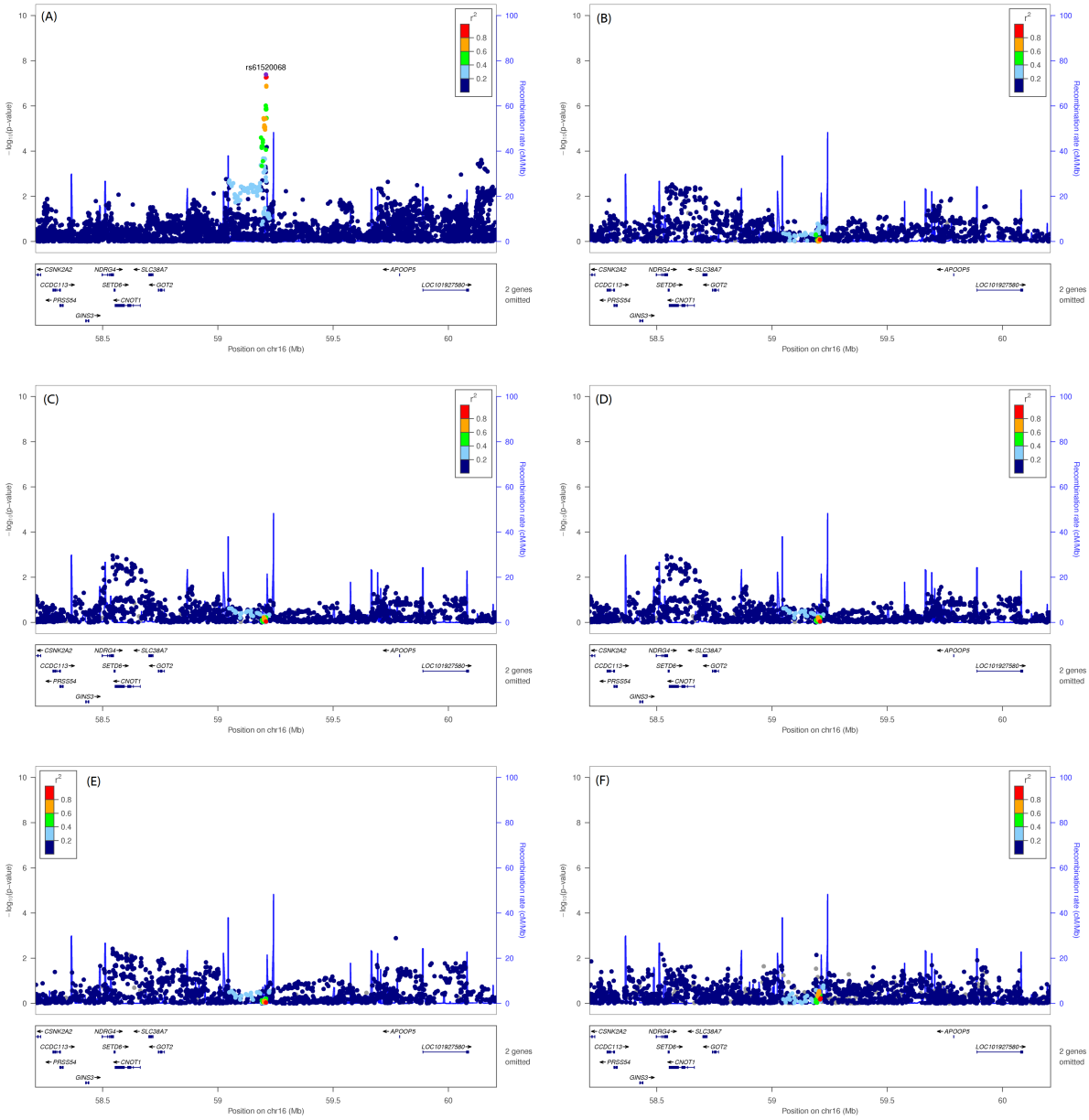

Supplementary Figure 10: *GOT2* locus regional plots for major anthropometric traits. Associations are taken from current GIANT European meta-analyses and elsewhere; details are provided in the main text. Plot character colour indicates linkage disequilibrium with the locus index. (A) Regional association in REE-Gen European discovery, age + sex adjusted (B) BMI (C) Standing height (D) Hip circumference (E) Waist circumference (F) Body fat percentage.

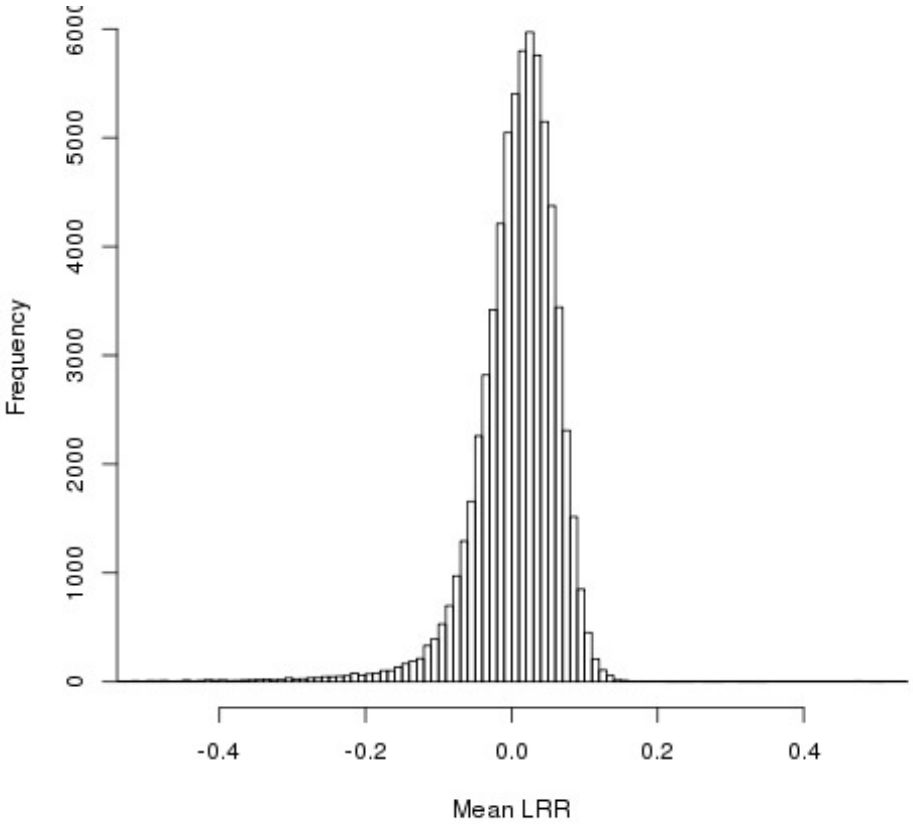

Supplementary Figure 11: Distribution of mLRR-Y amongst 67,034 male participants of UKB

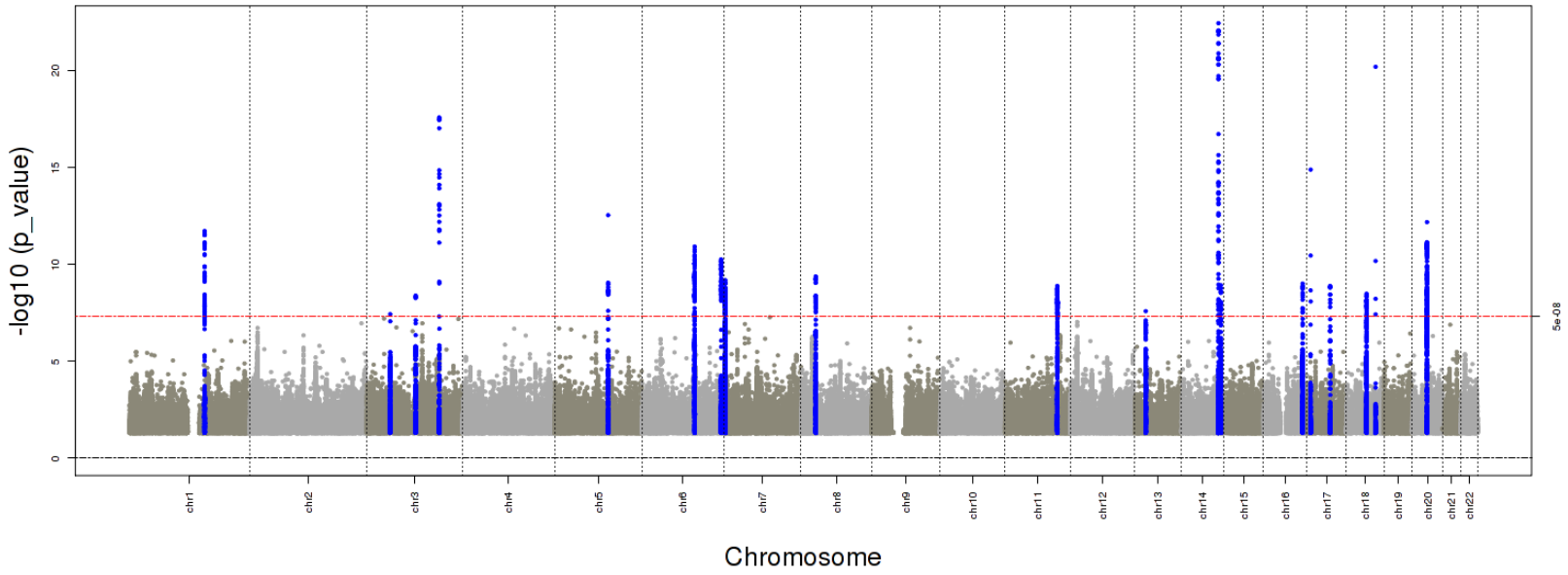

Supplementary Figure 12: Manhattan plot of genome-wide test statistics for mLRR-Y association. Variants shown are restricted to MAF$\geq$1% and imputation info$\geq$0.4. Regions demonstrating potential artefactual associations were additionally removed, as detailed in the Methods. Signals retaining genome-wide significance ($p \leq 5 \times 10^{-8}$) in combined discovery plus replication analyses are highlighted.

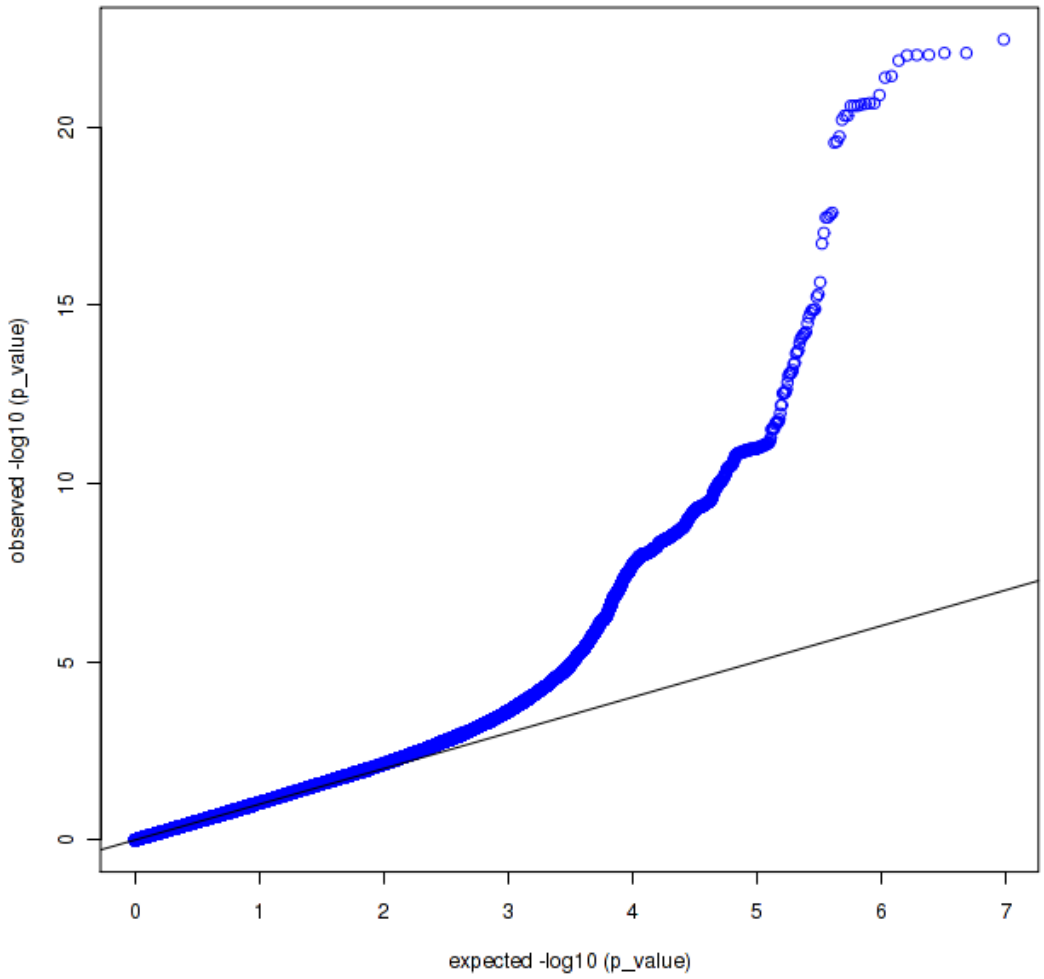

Supplementary Figure 13: Quantile-quantile plot of genome-wide test statistics for mLRR-Y. Line of null effect is shown in black.

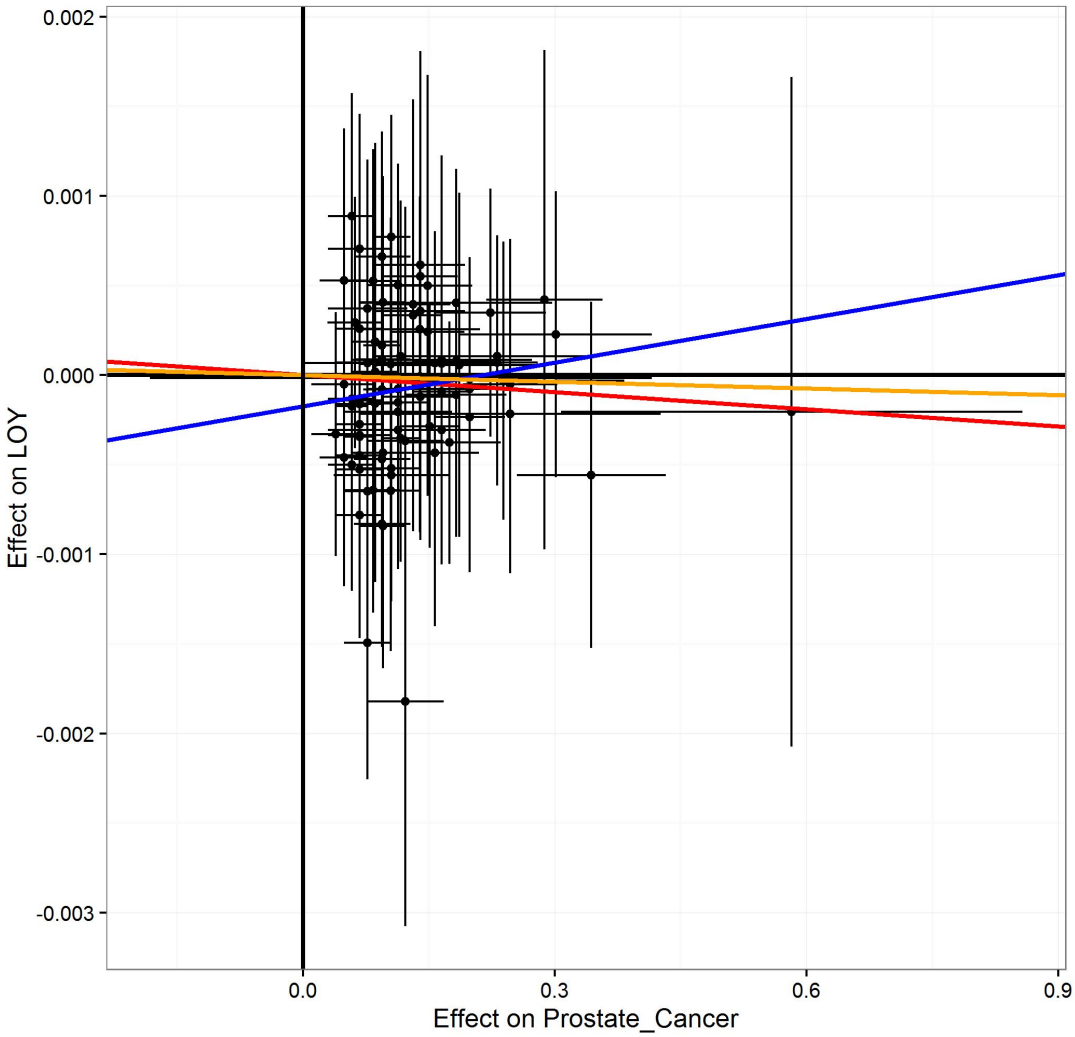

Supplementary Figure 14: Prostate Cancer-mLOY Mendelian randomisation: dosage plot. Each variant previously published for prostate cancer risk is plotted with regard to its additive effect on mLRR-Y. Black lines around each data point, 95% CI of each effect. Coloured lines represent estimates from main and sensitivity MR analyses. Red, IVW (p=0.349); Blue, MR-Egger (p=0.263); Yellow, weighted median (p=0.782); Green (aligned with yellow), penalised weighted median (p=0.772).

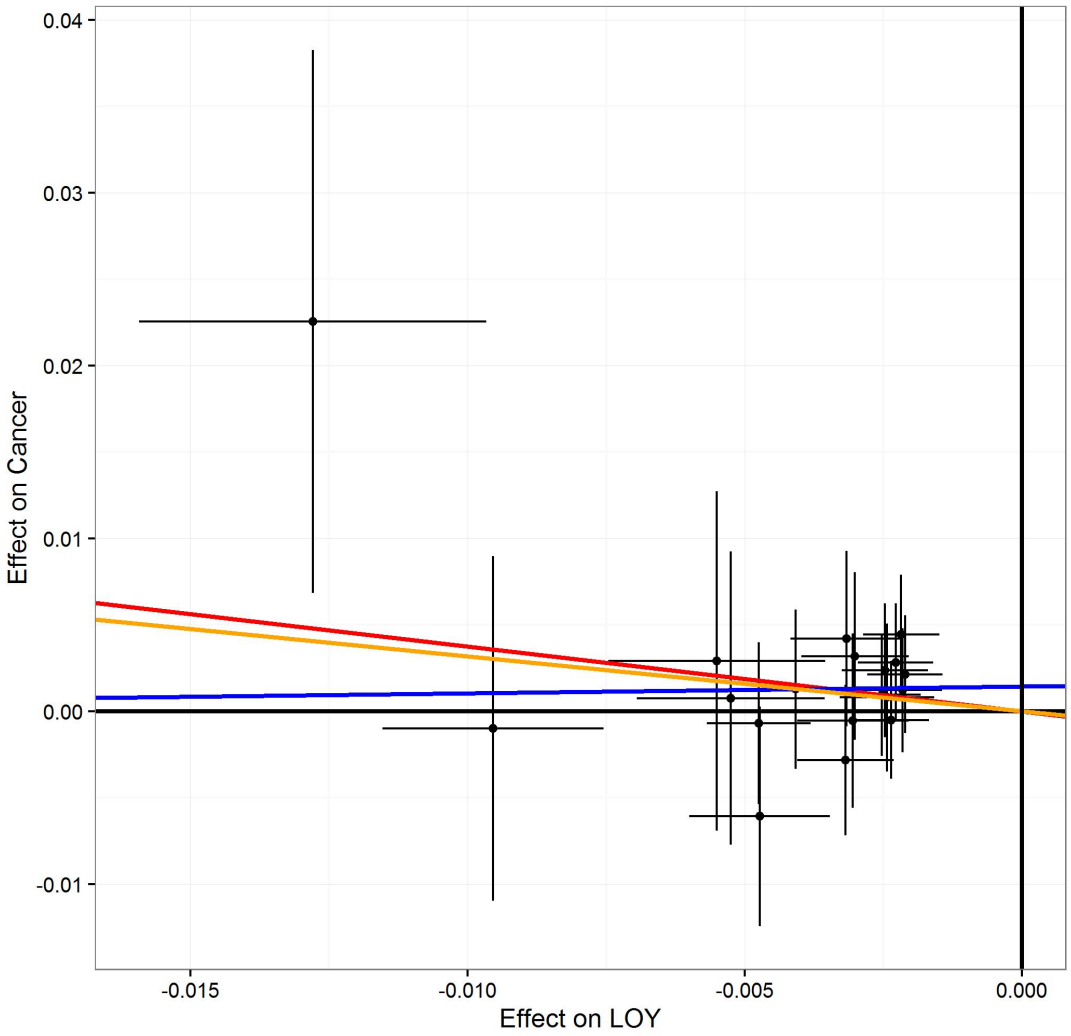

Supplementary Figure 15: mLRR-Y-cancer Mendelian randomisation: dosage plot. Each variant identified for mLRR-Y is plotted with regard to its effect on any-cancer risk (log-OR) in UKB . Black lines around each data point, 95% CI of each effect. Coloured lines represent estimates from main and sensitivity MR analyses. Red, IVW (p=0.0576); Blue, MR-Egger (p=0.938); Yellow, weighted median (p=0.196); Green (aligned with yellow), penalised weighted median (p=0.205).

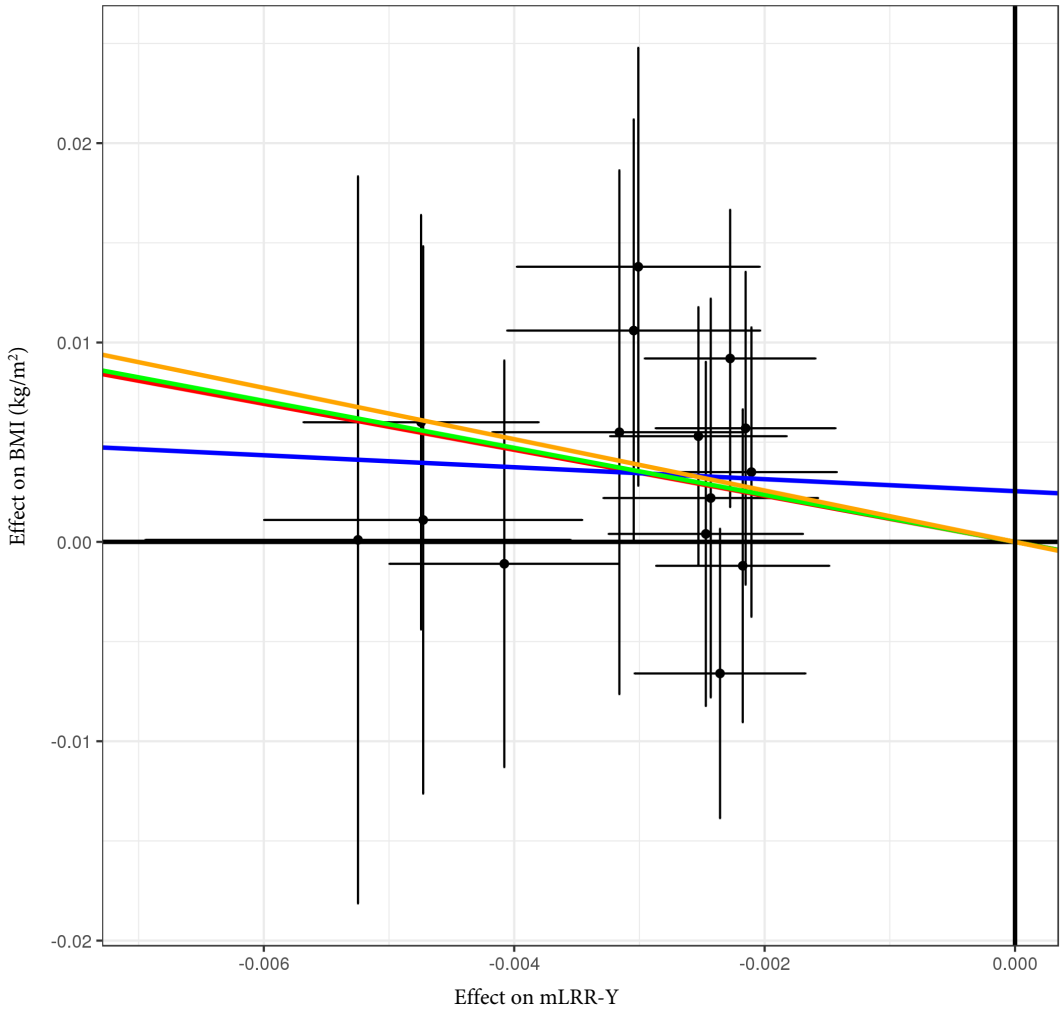

Supplementary Figure 16: mLRR-Y-BMI Mendelian randomisation: dosage plot. Each variant identified for mLRR-Y is plotted with regard to its effect on BMI in GIANT Consortium European Meta-analysis (Locke *et al.*, 2012). Black lines around each data point, 95% CI of each effect. Coloured lines represent estimates from main and sensitivity MR analyses. Red, IVW (p=0.016); Blue, MR-Egger (p=0.862); Yellow, weighted median (p=0.051); Green,penalised weighted median (p=0.034).

Supplementary Tables

	UK Biobank	EPIC-Norfolk	ERF	Health2006	Health2006	Health2008	HCS	Sydney MAS	TwinsUK
Grip Strength Measurement Protocol									
Position during Measurement	Sitting	Standing	Sitting	Sitting	Sitting	Sitting	Sitting or Standing	Sitting or Standing	Sitting
Hands Measured	Both	Both	Non-dominant	Dominant	Dominant	Dominant	Dominant	Dominant	Dominant
Measurements per Hand	1	2	3	3	3	3	3	2 or 3	2
Dynamometer Model	Jamar	Smedley	Jamar	Jamar	Jamar	Jamar	Jamar	Saehan	Bulb Dynamometer
Dynamometer Type	Hydraulic	Spring	Hydraulic	Hydraulic	Hydraulic	Hydraulic	Hydraulic	Hydraulic	Pneumatic
Descriptive Statistics									
N	142,035	7,121	2,058	2,919	2,792	744	2,088	541	3,009
N males	66,743	3,279	903	1,312	1,260	322	1,036	247	308
Mean Age (years) (SD)	56.8 (8.0)	68.8 (8.2)	48.7 (13.8)	49.3 (13.1)	49.5 (12.9)	46.9 (8.2)	66.31 (7.47)	78.18 (4.63)	52.5 (10.9)
Mean BMI (kg/m2) (SD)	27.5 (4.8)	26.8 (4.3)	26.9 (4.6)	25.9 (4.7)	25.9 (4.7)	25.7 (4.3)	28.76 (4.97)	27.29 (4.59)	26.6 (5.2)
Mean Standing Height (cm) (SD)	168.7 (9.2)	166.5 (9.0)	167.5 (9.3)	171.8 (9.2)	171.7 (9.2)	173.1 (9.2)	166.15 (9.55)	163.92 (9.47)	163.6 (7.4)
Mean Maximal HGS (kg) (SD)	33.0 (11.3)	31.1 (10.1)	35.5(11.7)	39.2 (11.4)	39.2 (11.4)	40.2 (11.2)	30.06 (9.86)	26.96 (9.80)	31.7 (8.7)
Genotyping & Imputation									
Genotyping platform	UKB; UKBilEVE	UKB	318K; 370K; 250K	HumanExome	MetaboChip	HumanExome	KP/UCSF	SNP6.0	Hap300; 610Q
Imputation Reference	1000G; UK10K	1000G 3	1000G 3	N/A	N/A	N/A	HapMap 2	HapMap 2	1000G 1
Imputation Software	IMPUTE 3	IMPUTE	MaCH	N/A	N/A	N/A	MaCH	MaCH	IMPUTE 2
Association Analyses									
Association Software	BOLT-LMM	SNPTEST	ProbABEL	PLINK	PLINK	PLINK	GenABEL	mach2qtl	GEMMA
Covariates	ASBH	ASBH	ASBH	ASBH	ASBH	ASBH	AS	AS	ASBH
Population Structure	LMM	PCs	PCs	PCs	PCs	PCs	Exclusion	LMM	

Supplementary Table 1: Study and analytic characteristics of stage one and two grip strength cohorts. Axiom Arrays are an Affymetrix product. Association covariates are A, age; S, sex; B, BMI and H, height. ERF, Erasmus Rucphen Family Study; HCS, Hunter Community Study; MAS, Memory and Ageing Study; LMM, linear mixed model; GRM, genomic relationship matrix; PCs, principal components; KP/UCSF, Kaiser Permanente/University of California at San Francisco.

	Fenland	EPIC-Norfolk
n	9,753	3,098
n males	4,561	1,392
n females	5,192	1,706
Age (years) (SD)	48.46 (7.46)	71.77 (7.47)
Lean Mass Index (kg/m^2)	16.71 (2.22)	16.18 (2.04)
Fat Mass Index (kg/m^2) (SD)	9.22 (3.49)	9.62 (3.28)

Supplementary Table 2: LMI and FMI GWAS cohort characteristics. Data shown are mean (SD) unless otherwise specified

					HGS (Height)			HGS (Height + BMI)			BMI		
rsID	Chr	Pos	EA	AA	Beta	SE	p-value	Beta	SE	p-value	Beta	SE	p-value
rs13107325	4	103188709	C	T	0.191	0.050	1.20E-04	0.200	0.050	5.30E-05	-0.048	0.007	1.83E-12
rs2207139	6	50845490	G	A	-0.120	0.035	5.00E-04	-0.129	0.035	1.90E-04	0.045	0.004	4.13E-29
rs17724992	19	18454825	A	G	-0.090	0.030	2.30E-03	-0.095	0.030	1.40E-03	0.019	0.004	3.41E-08
rs9374842	6	120185665	T	C	-0.086	0.031	5.30E-03	-0.089	0.031	4.10E-03	0.019	0.004	9.67E-08
rs7599312	2	213413231	G	A	0.084	0.030	4.50E-03	0.080	0.030	6.80E-03	0.022	0.003	1.17E-10
rs3817334	11	47650993	C	T	0.061	0.026	0.020	0.067	0.026	0.011	-0.026	0.003	5.14E-17
rs12446632	16	19935389	A	G	-0.099	0.037	7.50E-03	-0.092	0.037	0.013	-0.040	0.005	1.48E-18
rs1928295	9	120378483	C	T	0.058	0.026	0.026	0.061	0.026	0.019	-0.019	0.003	7.91E-10
rs3888190	16	28889486	A	C	-0.055	0.027	0.038	-0.061	0.027	0.021	0.031	0.003	3.14E-23
rs17405819	8	76806584	C	T	-0.067	0.028	0.018	-0.064	0.028	0.024	-0.022	0.003	2.07E-11
rs16851483	3	141275436	G	T	-0.124	0.052	0.018	-0.118	0.052	0.025	-0.048	0.008	3.55E-10
rs17203016	2	208255518	G	A	0.064	0.033	0.047	0.061	0.032	0.059	0.021	0.004	8.14E-08
rs6465468	7	95169514	G	T	-0.053	0.028	0.060	-0.053	0.028	0.060	-0.017	0.004	2.32E-06
rs7141420	14	79899454	T	C	0.054	0.026	0.041	0.049	0.026	0.062	0.023	0.003	1.23E-14
rs7164727	15	73093991	T	C	-0.046	0.028	0.093	-0.051	0.028	0.068	0.018	0.003	6.83E-08
rs9400239	6	108977663	C	T	-0.048	0.029	0.094	-0.052	0.029	0.069	0.019	0.003	1.61E-08
rs977747	1	47684677	T	G	0.051	0.026	0.052	0.047	0.026	0.073	0.017	0.003	8.65E-08
rs2245368	7	76608143	T	C	0.056	0.035	0.110	0.061	0.035	0.078	-0.032	0.006	3.19E-08
rs7903146	10	114758349	T	C	-0.054	0.029	0.060	-0.049	0.029	0.087	-0.023	0.003	1.11E-11
rs10182181	2	25150296	A	G	0.037	0.026	0.150	0.044	0.026	0.091	-0.031	0.003	8.78E-24
rs7899106	10	87410904	A	G	-0.106	0.060	0.078	-0.100	0.060	0.094	-0.040	0.007	2.96E-08
rs29941	19	34309532	A	G	-0.049	0.028	0.077	-0.045	0.028	0.100	-0.018	0.003	2.41E-08
rs16951275	15	68077168	C	T	-0.058	0.031	0.062	-0.051	0.031	0.100	-0.031	0.004	1.91E-17
rs1460676	2	164567689	T	C	-0.059	0.036	0.099	-0.056	0.036	0.120	-0.020	0.004	8.98E-07
rs6477694	9	111932342	C	T	-0.040	0.027	0.140	-0.042	0.027	0.120	0.017	0.003	2.67E-08
rs2365389	3	61236462	C	T	0.046	0.027	0.086	0.039	0.027	0.140	0.020	0.003	1.63E-10
rs4740619	9	15634326	T	C	0.042	0.026	0.110	0.038	0.026	0.140	0.018	0.003	4.56E-09
rs7239883	18	40147671	G	A	-0.035	0.027	0.200	-0.038	0.027	0.160	0.016	0.003	1.63E-07
rs3810291	19	47569003	A	G	-0.033	0.028	0.230	-0.039	0.028	0.160	0.028	0.004	4.81E-15
rs2033732	8	85079709	C	T	0.039	0.030	0.190	0.038	0.030	0.200	0.019	0.004	4.89E-08
rs205262	6	34563164	A	G	0.029	0.029	0.320	0.036	0.029	0.220	-0.022	0.004	1.75E-10
rs11191560	10	104869038	T	C	-0.065	0.049	0.180	-0.060	0.049	0.220	-0.031	0.005	8.45E-09
rs11057405	12	122781897	A	G	0.043	0.042	0.300	0.051	0.042	0.230	-0.031	0.006	2.02E-08
rs9925964	16	31129895	G	A	-0.031	0.024	0.180	-0.028	0.024	0.230	-0.019	0.003	8.11E-10
rs4787491	16	30015337	A	G	-0.035	0.026	0.190	-0.031	0.026	0.240	-0.016	0.003	2.24E-06
rs17024393	1	110154688	C	T	0.109	0.081	0.180	0.094	0.081	0.250	0.066	0.009	7.03E-14
rs2287019	19	46202172	C	T	0.048	0.034	0.160	0.039	0.034	0.250	0.036	0.004	4.59E-18
rs12885454	14	29736838	C	A	-0.025	0.027	0.350	-0.029	0.027	0.290	0.021	0.003	1.94E-10
rs13078960	3	85807590	T	G	-0.039	0.032	0.230	-0.033	0.032	0.300	-0.030	0.004	1.74E-14
rs11165643	1	96924097	C	T	-0.031	0.026	0.240	-0.027	0.026	0.310	-0.022	0.003	2.07E-12
rs3736485	15	51748610	A	G	-0.023	0.026	0.380	-0.026	0.026	0.320	0.018	0.003	7.41E-09
rs1558902	16	53803574	A	T	0.043	0.027	0.100	0.026	0.027	0.330	0.082	0.003	0
rs11847697	14	30515112	T	C	0.066	0.064	0.300	0.061	0.064	0.330	0.049	0.008	3.99E-09
rs6567160	18	57829135	C	T	0.041	0.031	0.180	0.029	0.031	0.340	0.056	0.004	0
rs2080454	16	49062590	A	C	0.022	0.027	0.400	0.026	0.027	0.340	-0.017	0.003	6.55E-08
rs13191362	6	163033350	A	G	0.042	0.039	0.280	0.038	0.039	0.340	0.028	0.005	7.34E-09
rs10733682	9	129460914	A	G	-0.020	0.027	0.440	-0.024	0.027	0.360	0.017	0.003	1.83E-08
rs758747	16	3627358	C	T	-0.028	0.029	0.350	-0.026	0.029	0.380	-0.023	0.004	7.47E-10
rs543874	1	177889480	G	A	-0.016	0.032	0.630	-0.027	0.032	0.400	0.048	0.004	2.62E-35
rs2650492	16	28333411	A	G	-0.017	0.029	0.550	-0.021	0.029	0.450	0.021	0.004	1.91E-09
rs9540493	13	66205704	G	A	0.017	0.026	0.530	0.020	0.026	0.450	-0.017	0.003	1.42E-07
rs3849570	3	81792112	A	C	-0.017	0.027	0.530	-0.020	0.027	0.460	0.019	0.003	2.60E-08
rs11688816	2	63053048	A	G	0.016	0.026	0.540	0.019	0.026	0.470	-0.017	0.003	1.89E-08
rs2121279	2	143043285	T	C	0.029	0.039	0.460	0.028	0.039	0.480	0.024	0.004	2.31E-08
rs2075650	19	45395619	A	G	0.028	0.035	0.430	0.025	0.035	0.480	0.026	0.004	1.25E-08
rs2820292	1	201784287	A	C	-0.023	0.026	0.380	-0.019	0.026	0.480	-0.020	0.003	1.83E-10
rs17094222	10	102395440	C	T	-0.019	0.032	0.550	-0.023	0.032	0.480	0.025	0.004	5.94E-11
rs6804842	3	25106437	A	G	0.015	0.026	0.560	0.018	0.026	0.490	-0.019	0.003	2.48E-09
rs1167827	7	75163169	A	G	-0.022	0.026	0.400	-0.017	0.026	0.510	-0.020	0.003	6.33E-10
rs11126666	2	26928811	G	A	0.019	0.030	0.510	0.019	0.030	0.510	-0.021	0.003	1.33E-09

Supplementary Table 3: Assessment of potential for collider bias by BMI variants in grip strength discovery. Part 1 of 2, continued overleaf. The HGS effect size (kg) of each known BMI locus is shown in models with and without BMI as a covariate. BMI association statistics (effect size in kg/m^2) are taken from GIANT analyses restricted to Europeans - as a result some of the displayed BMI p-values fall short of genomewide significance. All models are adjusted for age and sex.

					HGS (Height)			HGS (Height + BMI)			BMI		
rsID	Chr	Pos	EA	AA	Beta	SE	p-value	Beta	SE	p-value	Beta	SE	p-value
rs492400	2	219349752	T	C	-0.018	0.026	0.490	-0.017	0.026	0.520	-0.016	0.003	4.17E-07
rs1441264	13	79580919	A	G	-0.014	0.027	0.610	-0.017	0.027	0.520	0.018	0.003	6.04E-08
rs9641123	7	93197732	G	C	0.015	0.026	0.580	0.017	0.026	0.530	-0.019	0.004	5.00E-07
rs2112347	5	75015242	G	T	-0.022	0.027	0.410	-0.016	0.027	0.540	-0.026	0.003	6.19E-17
rs10938397	4	45182527	A	G	-0.023	0.026	0.390	-0.016	0.026	0.550	-0.040	0.003	3.21E-38
rs4256980	11	8673939	G	C	-0.012	0.027	0.660	-0.016	0.027	0.550	0.021	0.003	2.90E-11
rs11030104	11	27684517	A	G	0.026	0.032	0.430	0.017	0.032	0.600	0.041	0.004	5.56E-28
rs12566985	1	75002193	G	A	0.017	0.026	0.530	0.014	0.026	0.600	0.024	0.003	3.28E-15
rs16907751	8	81375457	C	T	0.026	0.045	0.560	0.022	0.045	0.620	0.035	0.007	1.25E-07
rs13201877	6	137675541	A	G	0.017	0.039	0.650	0.019	0.038	0.620	-0.023	0.004	2.35E-07
rs1516725	3	185824004	T	C	-0.024	0.038	0.520	-0.018	0.038	0.630	-0.045	0.005	1.89E-22
rs7243357	18	56883319	G	T	-0.021	0.034	0.540	-0.016	0.034	0.630	-0.022	0.004	3.86E-08
rs1016287	2	59305625	T	C	0.018	0.028	0.530	0.013	0.028	0.640	0.023	0.003	2.25E-11
rs7715256	5	153537893	G	T	-0.008	0.026	0.750	-0.012	0.026	0.650	0.016	0.003	1.70E-07
rs11583200	1	50559820	C	T	-0.007	0.027	0.800	-0.011	0.027	0.670	0.018	0.003	1.48E-08
rs11727676	4	145659064	C	T	-0.017	0.044	0.690	-0.018	0.044	0.680	-0.036	0.006	2.55E-08
rs2176598	11	43864278	T	C	-0.007	0.030	0.830	-0.012	0.030	0.700	0.020	0.004	2.97E-08
rs9914578	17	2005136	G	C	0.011	0.032	0.730	0.010	0.032	0.750	0.020	0.004	8.99E-08
rs2176040	2	227092802	G	A	0.007	0.027	0.800	0.008	0.027	0.770	-0.014	0.003	6.06E-06
rs10968576	9	28414339	G	A	-0.001	0.028	0.980	-0.006	0.028	0.830	0.025	0.003	6.61E-14
rs12429545	13	54102206	G	A	0.001	0.039	0.980	0.008	0.039	0.840	-0.033	0.005	1.09E-12
rs17001654	4	77129568	C	G	-0.008	0.035	0.820	-0.006	0.035	0.860	-0.031	0.005	7.76E-09
rs12401738	1	78446761	A	G	0.008	0.027	0.780	0.004	0.027	0.870	0.021	0.003	1.15E-10
rs1808579	18	21104888	T	C	-0.002	0.026	0.940	0.003	0.026	0.900	-0.017	0.003	4.17E-08
rs13021737	2	632348	A	G	-0.009	0.035	0.800	0.004	0.035	0.910	-0.060	0.004	0
rs10132280	14	25928179	A	C	-0.007	0.029	0.810	-0.003	0.029	0.910	-0.023	0.003	1.14E-11
rs1000940	17	5283252	G	A	0.000	0.028	0.990	-0.003	0.028	0.910	0.019	0.003	1.28E-08
rs1528435	2	181550962	T	C	0.006	0.027	0.820	0.002	0.027	0.940	0.018	0.003	1.20E-08
rs12286929	11	115022404	G	A	0.000	0.026	0.990	-0.002	0.026	0.940	0.022	0.003	1.31E-12
rs6091540	20	51087862	C	T	0.003	0.029	0.930	-0.002	0.029	0.940	0.019	0.004	8.02E-08
rs7138803	12	50247468	G	A	-0.007	0.027	0.790	-0.001	0.027	0.970	-0.032	0.003	8.15E-24
rs3101336	1	72751185	T	C	-0.007	0.026	0.800	-0.001	0.026	0.980	-0.033	0.003	2.66E-26
rs12940622	17	78615571	A	G	-0.004	0.026	0.870	-0.001	0.026	0.980	-0.018	0.003	2.49E-09
rs2836754	21	40291740	C	T	0.004	0.027	0.880	0.000	0.027	0.990	0.016	0.003	4.16E-07

Supplementary Table 3: Assessment of potential for collider bias by BMI variants in grip strength discovery. Continued, Part 2 of 2

Index SNP (hg19/GRCh37)	Follow-Up Variants by Cohort							
	EPIC-Norfolk	ERF	HCS	Health2006	Health2008	SMAS	TwinsUK	CHARGE
chr10:104127171	chr10:104127171	chr10:104127171	chr10:104127171			chr10:104127171	chr10:104127171	chr10:104127171
chr10:130837274	chr10:130837274		chr10:130834698			chr10:130834698	chr10:130834698	chr10:130834698
chr11:133792644	chr11:133792644	chr11:133792644				chr11:133781191	chr11:133792644	chr11:133781191
chr11:1479052	chr11:1479052					chr11:1449373	chr11:1479052	chr11:1449373
chr11:74355523	chr11:74355523		chr11:74362531	chr11:74290952		chr11:74362531	chr11:74355523	chr11:74362531
chr12:15063995	chr12:15063995	chr12:15063995	chr12:15063995	chr12:15085950	chr12:14993439	chr12:15063995	chr12:15063995	chr12:15063995
chr12:79686971	chr12:79686971		chr12:79659040				chr12:79686971	chr12:79659040
chr14:36640601	chr14:36640601	chr14:36640601	chr14:36640601	chr14:36649246	chr14:36649246	chr14:36640601	chr14:36640601	chr14:36640601
chr14:55260785	chr14:55260785	chr14:55260785	chr14:55260785	chr14:55265828	chr14:55265828	chr14:55260785	chr14:55260785	chr14:55260785
chr17:43685291:ID	chr17:43685291:ID		chr17:43666906	chr17:43719143	chr17:43719143	chr17:43666906	chr17:43685826	chr17:43666906
chr17:44224940	chr17:44224940		chr17:43991272	chr17:43991272	chr17:43923683	chr17:43991272	chr17:43758125	chr17:43991272
chr17:46661292	chr17:46661292	chr17:46661292	chr17:46661292	chr17:46661292	chr17:46629593	chr17:46661292	chr17:46661292	chr17:46661292
chr17:79469118	chr17:79469118						chr17:79469118	chr17:79378551
chr18:53244414	chr18:53244414	chr18:53244414	chr18:53248151	chr18:53210302	chr18:53210302	chr18:53248151	chr18:53244414	chr18:53248151
chr18:76958587:ID	chr18:76958587:ID	chr18:76951258	chr18:76900411			chr18:76900411	chr18:76958587:ID	chr18:76900411
chr1:10633245	chr1:10633245	chr1:10633245	chr1:10633245	chr1:10592231	chr1:10638604	chr1:10633245	chr1:10633245	chr1:10633245
chr1:54111733	chr1:54111733		chr1:54111733	chr1:54060248	chr1:54060248	chr1:54111733	chr1:54111733	chr1:54111733
chr2:40354688	chr2:40354688		chr2:40354688	chr2:40354688		chr2:40354688	chr2:40354688	chr2:40354688
chr2:44241155	chr2:44241155		chr2:44241781	chr2:44118428		chr2:44241781	chr2:44241155	chr2:44241781
chr2:70703847	chr2:70703847	chr2:70703847	chr2:70703847			chr2:70703847	chr2:70703847	chr2:70703847
chr6:32460867	chr6:32460867		chr6:32577380	chr6:32577380	chr6:32577380	chr6:32577380	chr6:32566635	chr6:32577380
chr9:117998886	chr9:117998886						chr9:117998886	

Supplementary Table 4: Assignment of proxies for the 21 HGS loci in independent follow-up cohorts. In each case, the full list of variants available in each study - whether proxy or not - is provided. Blank cells indicate that no suitable proxy was available for the index variant in the specified cohort. Proxies were defined as the variant with the next-lowest p-value for association with grip strength, with 500kb upstream or downstream of the index. All imputed variants included in the meta-analysis were well imputed (imputation quality $\geq$0.8).

				Stage One (UKB)			Stage Two			Combined					excl. EPIC-Norfolk
rsID	Gene	All.⋆	EAF	Effect	SE	p-value	Effect	SE	p-value	Effect	SE	p-value	N	p_{HET}	Effect
rs958685	*TGFA*	A/C	0.515	0.154	0.026	2.80×10^{-9}	0.1637	0.0397	3.78×10^{-5}	0.1571	0.0217	4.82×10^{-13}	191754	0.966	0.159
rs72979233	*POLD3*	A/G	0.757	0.210	0.030	3.70×10^{-12}	0.1123	0.0407	5.76×10^{-3}	0.1752	0.0242	5.03×10^{-13}	192490	0.206	0.182
rs11614333	*ERP27*	C/T	0.623	0.181	0.027	5×10^{-11}	0.1167	0.04	3.51×10^{-3}	0.1601	0.0226	1.57×10^{-12}	195154	0.641	0.161
rs2288278	*HOXB3*	A/G	0.658	0.162	0.027	3×10^{-9}	0.1466	0.0404	2.84×10^{-4}	0.1574	0.0227	3.76×10^{-12}	195133	0.039	0.154
rs4926611	*GLIS1*	C/T	0.637	0.173	0.027	1.30×10^{-10}	0.1146	0.0409	5.08×10^{-3}	0.1556	0.0225	4.75×10^{-12}	192964	0.308	0.160
rs6687430	*PEX14*	G/A	0.459	0.150	0.026	7.60E-09	0.1241	0.0395	1.66×10^{-3}	0.1423	0.0217	5.58E-11	195176	0.043	0.154
rs10186876	*LRPPRC*	A/G	0.361	0.162	0.027	2.70E-09	0.1127	0.0412	0.006179	0.1469	0.0227	9.75E-11	192490	0.616	0.154
rs374532236	*MGMT*	T/C	0.378	0.157	0.027	5.50×10^{-9}	0.1214	0.0424	4.18×10^{-3}	0.1468	0.0227	1.05×10^{-10}	189701	0.200	0.153
rs10861798	*SYT1*	A/G	0.433	0.145	0.026	4.30×10^{-8}	0.1591	0.0471	7.36×10^{-4}	0.1482	0.0231	1.29×10^{-10}	189160	0.947	0.147
rs78325334	*HLA region*	T/C	0.843	0.228	0.038	2.40×10^{-9}	0.113	0.0501	0.02398	0.1858	0.0304	9.60×10^{-10}	193127	0.201	0.182
rs2273555	*GBF1*	A/G	0.608	0.153	0.027	9.10×10^{-9}	0.0963	0.0411	0.01908	0.1361	0.0223	1.07×10^{-9}	191754	0.204	0.138
rs80103986	*KANSL1*	A/T	0.805	0.201	0.033	1.80×10^{-9}	0.0983	0.0521	0.05936	0.171	0.0281	1.17×10^{-9}	193090	0.382	0.179
rs2110927	*SLC8A1*	C/T	0.269	0.161	0.029	4.40×10^{-8}	0.0979	0.0449	0.02925	0.1422	0.0246	7.70×10^{-9}	192490	0.596	0.144
rs6565586	*ACTG1*	A/T	0.247	0.169	0.030	2.20×10^{-8}	0.0956	0.064	0.1354	0.1556	0.0273	1.23×10^{-8}	187072	0.388	0.167
rs72762373	*DEC1*	A/G	0.030	0.424	0.078	4.90×10^{-8}	0.359	0.2546	0.1586	0.4181	0.0743	1.80×10^{-8}	152162	0.002	0.457
rs34845616	*IGSF9B*	A/G	0.252	0.168	0.030	1.70×10^{-8}	0.0699	0.0487	0.1511	0.1411	0.0254	2.73×10^{-8}	189666	0.174	0.147
rs1169151	*PTCSC3*	G/A	0.419	0.150	0.027	1.50×10^{-8}	0.0536	0.0391	0.17	0.1197	0.022	5.03×10^{-8}	195024		
rs2924322	*TCF4*	A/T	0.119	0.257	0.044	4.40×10^{-9}	0.0726	0.0552	0.1886	0.1859	0.0343	6.08×10^{-8}	195030		
rs7150628	*SAMD4A*	C/T	0.431	0.148	0.026	1.90×10^{-8}	-0.0026	0.0388	0.9466	0.1005	0.0218	3.84×10^{-6}	195180		
rs11606628	*BRSK2*	C/T	0.712	0.173	0.029	1.90×10^{-9}	-0.1093	0.0536	0.04147	0.1096	0.0253	1.48×10^{-5}	187613		
rs34192714	*ATP9B*	T/A	0.279	0.160	0.029	3.40×10^{-8}	-0.0415	0.0472	0.3792	0.1048	0.0247	2.25×10^{-5}	191754		

Supplementary Table 5: Twenty-one loci reaching genomewide significance for hand grip strength in stage I analyses, and their association in stage II and combined analyses. Results are sorted by combined p-value in stages I plus II. Loci in black were independently replicated in stage II cohorts; blue indicates loci were not replicated in stage II but retained a combined p-value at $p\leq5\times10^{-8}$; red loci were neither replicated in stage II nor attained genomewide significance in the combined analyses. p_{HET} indicates the heterogeneity p-value for the 16 loci reaching significance in combined analyses. For each of these loci, the combined effect estimate excluding EPIC Norfolk samples (as used in specified MR analyses in Chapter 3) is also provided

⋆ Alleles are effect/other. Effect estimates are in kg per additional effect allele. EAF; effect allele frequency.

Haplotype Class	Variable	Effect (kg)	Robust SE	p-value
Inversion	H2 (vs. H1)	-0.165	0.036	3.85×10^{-6}
$\alpha/\beta/\gamma$ Copy Number	α	-0.066	0.030	0.027
	β	0.015	0.039	0.712
	γ	-0.039	0.023	0.092
Structural Haplotype	H1.β1.γ1	*Ref.*		
	H1.β1.γ2	-0.035	0.053	0.508
	H1.β1.γ3	-0.058	0.047	0.216
	H1.β1.γ4	-0.576	0.293	0.049
	H1.β2.γ1	0.029	0.041	0.480
	H1.β3.γ1	-0.273	0.428	0.523
	H2.α1.γ2	0.287	0.222	0.196
	H2.α2.γ1	-1.579	1.793	0.379
	H2.α2.γ2	-0.182	0.042	1.24×10^{-5}

Supplementary Table 6: Association of common structural haplotypes at 17q21.31 with grip strength. Effect is additive, in kg per additional CNV/allele/as otherwise specified, and is adjusted for age, sex, BMI, height and genotyping array. H2 denotes inverted haplotype; H1 uninverted.

Behavioural	*Anorexia nervosa* *Bulimia nervosa* Other eating disorders
Neoplasms	All malignant neoplasms *excl. benign skin cancers*
Respiratory	Chronic Obstructive Pulmonary Disease Emphysema Chronic Bronchitis Interstitial Lung Disease Asbestosis Pulmonary Fibrosis Alveolitis (fibrosing/not otherwise specified) Respiratory Failure
Endocrine	Type 1 Diabetes
Neurological	Spinal Cord Disorder Peripheral Neuropathy Motor Neurone Disease Myasthenia Gravis Multiple Sclerosis Other Demyelinating Conditions Cerebral Palsy Parkinson's Disease Dementia (Vascular or otherwise) Alzheimer's Disease Cognitive Impairment Poliomyelitis Spina Bifida Benign Tremor Meningioma Neuroma Spinal Cord or Peripheral Nerve Injury
Musculoskeletal	Arthritis Osteoarthritis Rheumatoid Arthritis Myositis/Myopathy Carpal Tunnel Syndrome Fibromyalgia Dupuytren's Contracture Lateral Epicondylitis (Tennis Elbow)
Cerebrovascular	Stroke (inc Ischaemic and Haemorrhagic)
Systemic Connective Tissue Disorders	Systemic Lupus Erythematosus Sjogren's Syndrome Dermatopolymyositis Scleroderma Raynaud's Phenomenon Vasculitis (inc Polymyalgia Rheumatica) Polyarteritis Nodosa

Supplementary Table 7: Exclusion criteria for grip strength sensitivity analyses in UKB. T1D was defined using an centrally-curated, adjudicated algorithm[1] based on the convergence of multiple indicators to robustly discriminate diabetes cases using the self-reported phenotype data of UKB. Cancers were defined on the basis of a prevalent cancer registration in the UK at the time of enrolment. Other conditions were classified on the basis of self-report at recruitment.

				Discovery n = 142,036			excl. Prevalent Conditions n = 133,360				excl. T1D n = 141,538			
Variant	Gene	All.	EAF	Effect	SE	p-value	Effect	SE	p-value	p_{HET}	Effect	SE	p-value	p_{HET}
rs72979233	POLD3	AG	0.757	0.21	0.030	3.70E-12	0.21	0.033	3.20E-10	0.964	0.21	0.030	1.60E-12	0.925
rs11614333	ERP27	CT	0.623	0.18	0.027	5.00E-11	0.16	0.030	4.50E-08	0.692	0.18	0.028	4.80E-11	1.000
rs4926611	GLIS1	CT	0.637	0.17	0.027	1.30E-10	0.18	0.030	1.30E-09	0.822	0.17	0.027	1.40E-10	1.000
rs80103986	KANSL1	AT	0.805	0.20	0.033	1.80E-09	0.20	0.037	4.30E-08	0.984	0.20	0.033	1.30E-09	0.966
rs78325334	HLA region	TC	0.843	0.23	0.038	2.40E-09	0.13	0.042	2.00E-03	0.084	0.21	0.038	2.90E-08	0.780
rs10186876	LRPPRC	AG	0.361	0.16	0.027	2.70E-09	0.17	0.030	8.20E-09	0.804	0.16	0.027	2.50E-09	0.979
rs958685	TGFA	AC	0.515	0.15	0.026	2.80E-09	0.13	0.028	8.00E-06	0.480	0.15	0.026	2.90E-09	1.000
rs2288278	HOXB3	AG	0.658	0.16	0.027	3.00E-09	0.15	0.030	2.70E-07	0.843	0.16	0.027	6.70E-09	0.937
rs374532236	MGMT	TC	0.378	0.16	0.027	5.50E-09	0.15	0.029	2.50E-07	0.900	0.15	0.027	1.10E-08	0.937
rs6687430	PEX14	GA	0.459	0.15	0.026	7.60E-09	0.17	0.028	4.10E-09	0.656	0.15	0.026	7.60E-09	1.000
rs2273555	GBF1	AG	0.608	0.15	0.027	9.10E-09	0.15	0.029	4.60E-07	0.880	0.15	0.027	8.40E-09	1.000
rs34845616	IGSF9B	AG	0.252	0.17	0.030	1.70E-08	0.16	0.033	7.40E-07	0.875	0.17	0.030	1.90E-08	0.981
rs6565586	ACTG1	AT	0.247	0.17	0.030	2.20E-08	0.17	0.033	1.20E-07	0.893	0.17	0.030	3.20E-08	0.962
rs10861798	SYT1	AG	0.433	0.14	0.026	4.30E-08	0.12	0.029	5.00E-05	0.472	0.14	0.026	6.60E-08	0.957
rs2110927	SLC8A1	CT	0.269	0.16	0.029	4.40E-08	0.16	0.032	9.00E-07	0.945	0.16	0.029	4.20E-08	0.981
rs72762373	DEC1	AG	0.030	0.42	0.078	4.90E-08	0.41	0.085	1.30E-06	0.917	0.43	0.078	2.30E-08	0.921

Supplementary Table 8: Sensitivity analyses for replicated grip strength signals, excluding prevalent disease. Conditions excluded are defined in Supplementary Table 7. All., alleles (effect, other). Effect estimates are in kg per effect allele. Gene shown is the gene within which the signal falls, otherwise the closest gene. n represents the maximum sample size of each model. Signals which do not attain genome-wide significance after exclusions are highlighted in blue. p_{HET} refers to heterogeneity of effect between discovery and restricted analyses; no association is attenuated at statistical significance in restricted vs. discovery models.

Gene	Tissue	Z-Score	$p_{MetaXcan}$	Expression Variance	$n_{Variants}$	Gripstrength Locus	
						Index rsID	Gene
ACTG1	Skeletal Muscle	-5.38	7.50E-08	0.042272	10	rs6565586	*ACTG1*
ARHGAP27	Basal Ganglia - Caudate	-5.73	1.02E-08	0.0253439	7	rs80103986	*KANSL1*
ARHGDIB	Cerebral Cortex	5.08	3.78E-07	0.083278	31	rs11614333	*ERP27*
ARL17A	Basal Ganglia - Caudate	-5.39	7.10E-08	0.1644262	16		
	Cerebral Cortex	-5.19	2.16E-07	0.2059632	42		
	Basal Ganglia - NAcc.	-5.06	4.29E-07	0.2553275	27		
	Hypothalamus	-5.02	5.26E-07	0.1405813	22		
	Cerebellar Hemisphere	-4.95	7.53E-07	0.296909	47		
ASB8	Testis	-5.51	3.49E-08	0.0594337	24		
CHRDL2	Basal Ganglia - Caudate	-4.95	7.56E-07	0.0231122	13	rs72979233	*POLD3*
CRHR1	Basal Ganglia - Putamen	5.37	7.74E-08	0.0155817	14	rs80103986	*KANSL1*
ERP27	Tibial Nerve	6.00	1.98E-09	0.0573961	28	rs11614333	*ERP27*
	Whole Blood	5.91	3.45E-09	0.0250218	11		
FMNL1	Cerebellum	5.04	4.74E-07	0.110669	24	rs80103986	*KANSL1*
GFAP	Tibial Nerve	5.53	3.25E-08	0.0130075	12	rs80103986	*KANSL1*
H2AFJ	Basal Ganglia - NAcc.	6.52	7.26E-11	0.0148962	10	rs11614333	*ERP27*
KIF1B	Whole Blood	-5.79	7.10E-09	0.0730446	50	rs6687430	*PEX14*
LRPPRC	Hippocampus	5.96	2.54E-09	0.0973548	16	rs10186876	*LRPPRC*
	Cerebral Cortex	5.62	1.90E-08	0.1034959	17		
	Testis	5.60	2.16E-08	0.1418592	9		
	Basal Ganglia - Putamen	5.55	2.85E-08	0.0752171	14		
	Basal Ganglia - NAcc.	5.44	5.43E-08	0.0865671	10		
	Cerebellum	5.42	6.12E-08	0.0328546	9		
	Tibial Nerve	5.27	1.34E-07	0.1818902	49		
	Whole Blood	5.25	1.48E-07	0.0399471	21		
LRRC37A	Cerebellum	-5.52	3.35E-08	0.3104757	37		
	Hypothalamus	-5.43	5.64E-08	0.4599563	47		
	Skeletal Muscle	-5.30	1.19E-07	0.1516158	39		
	Basal Ganglia - Caudate	-5.12	3.02E-07	0.2969325	49		
	Cerebellar Hemisphere	-5.12	3.04E-07	0.286255	24		
	Hippocampus	-5.12	3.10E-07	0.0723494	10		
	Whole Blood	-5.11	3.21E-07	0.192233	77		
	Tibial Nerve	-5.06	4.19E-07	0.3424756	53		
LRRC37A2	Hippocampus	-5.55	2.80E-08	0.1788016	20		
	Skeletal Muscle	-5.49	3.92E-08	0.3461513	36		
	Cerebellar Hemisphere	-5.47	4.49E-08	0.2523477	43		
	Basal Ganglia - Caudate	-5.35	8.69E-08	0.2170825	30		
	Tibial Nerve	-5.32	1.02E-07	0.3305588	58		
	Basal Ganglia - NAcc.	-5.28	1.27E-07	0.3082167	42		
	Cerebellum	-5.23	1.71E-07	0.4771353	33		
	Hypothalamus	-5.22	1.79E-07	0.4074591	50		
MAPT	Cerebral Cortex	5.88	4.22E-09	0.0264987	5	rs80103986	*KANSL1*
	Cerebellum	5.53	3.24E-08	0.1219373	14		
	Cerebellar Hemisphere	5.41	6.44E-08	0.1216889	22		
MGP	Tibial Nerve	6.31	2.75E-10	0.0481746	24	rs11614333	*ERP27*
PLEKHM1	Skeletal Muscle	-5.45	5.02E-08	0.0301035	13	rs80103986	*KANSL1*
	Testis	5.23	1.73E-07	0.0280989	16		
	Cerebellar Hemisphere	5.15	2.57E-07	0.2780433	29		
	Cerebellum	5.07	4.04E-07	0.3692071	42		
RAET1G	Testis	-5.12	3.14E-07	0.024732	17		
RP11-182J1.16	Skeletal Muscle	4.98	6.51E-07	0.0340662	11		
SLC35E2B	Tibial Nerve	5.37	8.09E-08	0.2740872	30		
	Skeletal Muscle	5.07	4.06E-07	0.3103245	18		
	Basal Ganglia - Caudate	5.01	5.34E-07	0.1644098	7		
	Testis	4.99	6.04E-07	0.3714615	50		
	Basal Ganglia - Nucleus accumbens	4.93	8.03E-07	0.2226097	25		
SLIT1	Skeletal Muscle	5.35	8.72E-08	0.0591131	25		
SPPL2C	Cerebellar Hemisphere	-5.13	2.96E-07	0.0302724	14		
WDR73	Cerebellum	4.94	7.82E-07	0.0649431	29		
ZNF641	Tibial Nerve	-4.92	8.53E-07	0.051986	10		

Supplementary Table 9: Imputed transcriptome association results for grip strength (MetaXcan) in biologically-relevant tissues. Analyses were restricted to imputed expression levels in all brain tissues, transformed fibroblasts, skeletal muscle, tibial nerve, testis and whole blood. Only protein-coding transcripts associated with gripstrength at statistical significance after Bonferroni correction, and with a high transcriptome imputation quality (minimum MetaXcan Est_Pred_R2 metric 0.01) are shown.

Database	Gene Set ID / Description	External Identifier	FDR	$p_{Magenta}$	Fold Enrichment	Gene Set Size		Reference (PMID)
						Specified	Effective	
Hypothesis-Free Gene Sets								
GO Terms	Positive Regulation of Protein Catabolic Process	GO:1903364	0.026	0.0001	5	11	10	N/A
Reactome	Dual Excision Reaction in GG-NER	Reactome:R-HSA-5696400	0.047	0.0003	6	20	19	N/A
Custom-Defined (Candidate) Gene Sets								
Custom	Myostatin-Activin Signalling through ActRIIA	N/A	0.52	0.53	N/A	16	15	23721881
Custom	Myostatin-Activin Signalling through ActRIIB	N/A	0.48	0.54	N/A	16	15	23721881
Custom	Genes implicated in monogenic muscular dystrophies	N/A	0.43	0.47	N/A	57	52	25625149
Custom	Genes implicated in monogenic myopathies	N/A	0.076	0.017	2.33	60	54	25625149
Custom	Combined set of monogenic myopathies and dystrophies	N/A	0.39	0.19	N/A	104	94	25625149

Supplementary Table 10: Gene set enrichment analyses of hand grip strength associations across the genome. Analyses implemented in MAGENTA using variants with MAF$\geq$0.01 and imputation quality $\geq$0.4. FDR denotes MAGENTA's 95th percentile false discovery rate.

Custom Set	Genes (Entrez ID)
Myostatin-Activin Signalling through ActRIIA	10468; 3624; 2660; 92; 91; 7046; 4087; 4088; 4089; 207; 2308; 2309; 4303; 114907; 84676; 10891
Myostatin-Activin Signalling through ActRIIB	10468; 3624; 2660; 93; 91; 7046; 4087; 4088; 4089; 207; 2308; 2309; 4303; 114907; 84676; 10891
Monogenic muscular dystrophies	58; 825; 859; 1120; 1291; 1292; 1293; 1605; 1674; 1756; 1785; 2010; 2218; 2273; 3679; 3908; 4000; 5339; 6442; 6443; 6444; 6445; 7273; 7415; 8291; 8557; 8813; 8818; 9215; 9499; 9987; 10049; 10329; 10585; 11041; 22954; 23224; 23345; 23347; 23534; 26092; 29925; 29954; 54344; 55624; 57190; 60684; 79147; 79188; 79868; 84197; 84892; 148789; 203859; 284119; 729920; 100288687
Monogenic myopathies	58; 90; 178; 274; 859; 1073; 1272; 1410; 1674; 1785; 2027; 2273; 2318; 2548; 2632; 2660; 2992; 2997; 3920; 3939; 4534; 4607; 4620; 4625; 4703; 5213; 5224; 5230; 5236; 5255; 5339; 5837; 6261; 7072; 7138; 7169; 7170; 7273; 7415; 8106; 8291; 9200; 9499; 9531; 9782; 10020; 10290; 10324; 10616; 11155; 22954; 23479; 51422; 55958; 57190; 131377; 203547; 203859; 246329; 390594
Monogenic myopathies and dystrophies	Myopathies + dystrophies combined and de-duplicated

Supplementary Table 11: Curated custom gene sets for genes implicated in myopathies and muscular dystrophies

Gene	Gene Product	Chr	Gene Start	Gene End	n_{SNPs}	p_{Gene}	Best SNP	p_{SNP}	Rationale for Selection
MSTN	Myostatin	2	190920426	190927455	86	0.102	rs6749852	0.01	A known myokine, key ligand of Activin Receptors
FST	Follistatin	5	52776183	52782964	73	0.117	rs4865546	0.002	Bioneutralising inhibitor of myostatin and activin in the cytosol
INHBA	Inhibin Beta A Subunit	7	41728601	41742706	93	0.05	rs11772877	0.006	Dimerises to form Activin A, the major cellular form of activin
ACVR2A	Activin A Receptor, Type IIA	2	148602086	148688396	103	0.79	rs10171130	0.21	Cell surface receptor of myostatin/activin signalling
ACVR2B	Activin B receptor, Type IIB	3	38495790	38534633	115	0.0002	rs2070489	9.99E-05	Major cell surface receptor of myostatin/activin signalling
FBXO32	Atrogin 1	8	124510127	124553493	142	0.003	rs12548263	0.001	Major atrogene (E3 ubiquitin protein ligase implicated in myofibril breakdown under pro-atrophic signalling)
TRIM63	MuRF-1	1	26377792	26394142	74	0.042	rs3008425	0.012	Major atrogene (E3 ubiquitin protein ligase implicated in myofibril breakdown under pro-atrophic signalling)

Supplementary Table 12: Candidate gene associations with hand grip strength from gene-based analyses. Calculations are based on variants with MAF$\geq$0.01 and imputation quality$\geq$0.8. The number of SNPs included within each gene-based association is denoted by n_{SNPs}; of these, the SNP with the most statistically-significant association with HGS by age is also noted. Chromosomal positions are specified on hg19. Genes were selected primarily based on Han *et al.*[2].

		EAF										
rsID	EA/AA	CEU	JPT	ACB	ASW	OR	LCI	UCI	log(OR)	$SE_{log(OR)}$	P-value	P_{HET}
rs6565586	A/T	0.29	0.76	0.22	0.31	0.98	0.79	1.21	-0.023	0.111	0.8355	0.240
rs6687430	G/A	0.44	0.22	0.79	0.66	0.79	0.48	1.30	-0.235	0.252	0.3516	1.000
rs2288278	A/G	0.60	0.80	0.46	0.54	1.29	0.95	1.76	0.259	0.157	0.1001	0.490
rs2110927	C/T	0.31	0.16	0.68	0.53	0.98	0.82	1.18	-0.016	0.094	0.8627	0.325
rs4926611	C/T	0.67	0.51	0.14	0.22	1.11	0.81	1.53	0.105	0.162	0.5156	0.911
rs2273555	A/G	0.58	0.77	0.55	0.61	0.99	0.84	1.18	-0.008	0.087	0.9293	0.820
rs958685	A/C	0.55	0.64	0.54	0.53	0.98	0.81	1.19	-0.019	0.097	0.8448	0.460
rs11614333	C/T	0.65	0.88	0.68	0.61	0.80	0.67	0.95	-0.225	0.089	0.01167	0.097
rs10186876	A/G	0.33	0.95	0.78	0.81	0.98	0.79	1.21	-0.020	0.109	0.853	1.000
rs72762373	A/G	0.04	NA	NA	0.01	0.60	0.27	1.34	-0.511	0.410	0.2128	1.000
rs34845616	A/G	0.29	0.21	0.04	0.08	1.01	0.64	1.58	0.006	0.229	0.9785	1.000
rs72979233	A/G	0.77	0.64	0.95	0.90	0.84	0.63	1.13	-0.174	0.150	0.2451	1.000

Supplementary Table 13: Effect of strength-associated variants from stage I plus II analyses with odds of elite athletic status in combined analyses of four ethnic groups. Results are aligned to the grip strength-increasing effect allele (EA). OR, odds ratio of athletic status; AA, alternate allele; UCI and LCI, upper and lower limit of 95% confidence interval of OR. Effect allele frequencies (EAF) are provided for each ancestral sub-group in these analyses (European, Japanese, Jamaican and African American) based on the most closely-matched 1000G ancestral population. CEU, Utah residents with Northern and Western European ancestry; JPT, Japanese in Tokyo; ACB, African Caribbean in Barbados; ASW, African ancestry in South-western United States. For the low-frequency variant rs72762373, NA denotes that the variant is monomorphic for the alternate allele in a sub-population, and was omitted from analyses. Full details of contributing cohorts are provided in the Supplementary Note.

Model	Effect Allele	Effect	SE	p-value
Additive - lookup in stage 1 grip strength GWAS results	T	-0.062	0.026	0.018
Dominant - linear regression in unrelated UKB participants	T	-0.062	0.045	0.168
Recessive - linear regression in unrelated UKB participants	T	-0.033	0.053	0.528

Supplementary Table 14: Association of *ACTN3* stop-gain variant rs1815739 (R577X) with grip strength. Effects shown are in kg.

							Grip Strength (Combined)			Capillary Density			Type I Fibres			Type IIA Fibres			Type IIB Fibres		
rsID	Chr	Position	Gene	EA	AA	EAF	Effect	SE	P-value	Effect	SE	P	Effect	SE	P	Effect	SE	P	Effect	SE	P
rs6687430	1	10633245	*PEX14*	G	A	0.459	0.142	0.022	5.58E-11	0.099	0.057	0.0815	-0.056	0.055	0.3107	0.063	0.055	0.2495	0.050	0.055	0.3678
rs4926611	1	54111733	*GLIS1*	C	T	0.637	0.156	0.023	4.75E-12	0.094	0.058	0.1051	-0.006	0.056	0.9142	0.028	0.056	0.6182	0.021	0.056	0.7130
rs2110927	2	40354688	*SLC8A1*	C	T	0.269	0.142	0.025	7.70E-09	0.028	0.065	0.6696	0.177	0.063	0.0048	-0.116	0.063	0.0634	-0.098	0.063	0.1172
rs10186876	2	44241155	*LRPPRC*	A	G	0.361	0.147	0.023	9.75E-11	0.039	0.061	0.5209	-0.020	0.059	0.7342	0.007	0.059	0.8990	0.028	0.059	0.6370
rs958685	2	70703847	*TGFA*	A	C	0.515	0.157	0.022	4.82E-13	-0.003	0.058	0.9627	-0.164	0.056	0.0033	0.043	0.056	0.4441	0.156	0.056	0.0055
rs78325334	6	32460867	HLA	T	C	0.843	0.186	0.030	9.60E-10	-0.007	0.058	0.9087	0.032	0.057	0.5772	-0.005	0.057	0.9328	-0.017	0.057	0.7646
rs72762373	9	117998886	*DEC1*	A	G	0.030	0.418	0.074	1.80E-08	-0.017	0.154	0.9114	0.221	0.150	0.1398	-0.117	0.150	0.4363	-0.193	0.149	0.1940
rs2273555	10	104127171	*GBF1*	A	G	0.608	0.136	0.022	1.07E-09	-0.028	0.056	0.6160	0.007	0.054	0.8915	-0.071	0.055	0.1975	0.062	0.055	0.2574
rs374532236	10	130837274	*MGMT*	T	C	0.378	0.147	0.023	1.05E-10												
rs72979233	11	74355523	*POLD3*	A	G	0.757	0.175	0.024	5.03E-13				-0.197	0.122	0.1078	0.167	0.124	0.1785	0.045	0.125	0.7209
rs34845616	11	133792644	*IGSF9B*	A	G	0.252	0.141	0.025	2.73E-08												
rs11614333	12	15063995	*ERP27*	C	T	0.623	0.160	0.023	1.57E-12	-0.029	0.062	0.6395	-0.023	0.059	0.6891	-0.017	0.059	0.7763	0.029	0.059	0.6197
rs10861798	12	79686971	*SYT1*	A	G	0.433	0.148	0.023	1.29E-10	-0.009	0.060	0.8768	-0.023	0.058	0.6878	0.033	0.058	0.5663	-0.028	0.058	0.6355
rs80103986	17	44224940	*KANSL1*	A	T	0.805	0.171	0.028	1.17E-09												
rs2288278	17	46661292	*HOXB3*	A	G	0.658	0.157	0.023	3.76E-12	-0.078	0.058	0.1783	-0.101	0.056	0.0716	0.030	0.056	0.5979	0.097	0.056	0.0844
rs6565586	17	79469118	*ACTG1*	A	T	0.247	0.156	0.027	1.23E-08	0.059	0.069	0.3867	0.127	0.066	0.0553	-0.013	0.067	0.8452	-0.109	0.067	0.1018

Supplementary Table 15: Association of the sixteen HGS variants with muscle histology parameters. Effects shown are from regression of inverse-normalised percentages, aligned to the grip strength-increasing allele from combined stage I + II results. Blank cells indicate that data is not available. Associations reaching nominal significance ($p \leq 0.05$) are highlighted blue; significant associations allowing for 13 tests are highlighted green.

		Inverse-Variance Weighted					MR-Egger						Weighted Median			Penalised Weighted Median		
Exposure	Exposure Unit	β	SE	p	Coch *Q*	$p_{Coch\ Q}$	β	SE	p	Intercept	$SE_{Intercept}$	$p_{Intercept}$	β	SE	p	β	SE	p
Insulin secretion	SD (30m insulin)	0.237	0.127	6.18E-02	11.005	8.56E-01	0.229	0.338	4.99E-01	0.001	0.021	9.79E-01	0.198	0.174	2.54E-01	0.208	0.184	2.60E-01
Insulin resistance	ln-pmol/L (FI)	2.798	0.909	2.09E-03	38.892	1.21E-05	0.743	5.022	8.82E-01	0.032	0.076	6.77E-01	3.737	0.940	6.99E-05	3.756	0.930	5.40E-05
Fasting insulin	ln-pmol/L (FI)	1.193	0.816	1.44E-01	139.115	3.24E-21	2.515	3.398	4.59E-01	-0.023	0.056	6.88E-01	1.558	0.627	1.29E-02	1.704	0.648	8.55E-03
DHEAS	ln-µmol/L	0.078	0.309	8.00E-01	4.939	2.94E-01	-0.117	0.348	7.37E-01	-0.029	0.026	2.66E-01	-0.077	0.272	7.77E-01	-0.113	0.264	6.68E-01
SHBG	ln-nmol/L	0.185	0.219	3.98E-01	23.635	1.32E-03	0.295	0.283	2.96E-01	-0.017	0.026	5.08E-01	0.191	0.115	9.60E-02	0.189	0.116	1.03E-01
IGF-I	SD	0.196	0.269	4.65E-01	7.393	2.86E-01	-0.279	1.326	8.33E-01	0.030	0.081	7.13E-01	-0.025	0.240	9.18E-01	-0.102	0.244	6.74E-01

Supplementary Table 16: Mendelian randomisation of genetically-predicted sex- and growth-hormone phenotypes to grip strength. Betas are kg change in strength per genetically-predicted unit increase in the exposure, as specified. Coch *Q* denotes Cochran's *Q*-statistic for heterogeneity.

	Exposure		Grip Strength	
Variant	Beta	SE	Beta	SE
SHBG - ln(nmol)/L				
rs10454142	0.023	0.0044	-0.085	0.028
rs17496332	0.028	0.0041	0.004	0.027
rs2411984	0.033	0.0044	-0.050	0.028
rs293428	0.019	0.0042	0.003	0.029
rs3779195	0.28	0.0051	0.053	0.033
rs440837	0.028	0.0047	-0.051	0.032
rs7910927	0.048	0.0039	0.089	0.026
rs8023580	0.03	0.0044	0.017	0.029
DHEA-S - ln(μmol)/L				
rs11761528	-0.16	0.01	0.073	0.046
rs2637125	-0.09	0.01	-0.032	0.036
rs7181230	0.05	0.01	-0.003	0.027
rs2497306	-0.04	0.01	-0.063	0.026
rs2185570	-0.06	0.01	-0.040	0.038
Fasting insulin - ln(pmol)/L				
rs10195252	0.018	0.003	0.035	0.026
rs1167800	0.015	0.003	0.001	0.026
rs1530559	0.013	0.003	-0.102	0.027
rs17036328	0.014	0.005	0.015	0.040
rs2126259	0.031	0.005	0.037	0.043
rs2745353	0.015	0.003	0.065	0.026
rs2943645	0.016	0.003	0.007	0.027
rs3822072	0.010	0.003	0.049	0.026
rs459193	0.019	0.003	0.089	0.030
rs4846565	0.015	0.003	0.103	0.027
rs4865796	0.016	0.003	-0.048	0.028
rs6822892	0.010	0.003	0.037	0.028
rs6912327	0.015	0.005	0.036	0.032
rs731839	0.017	0.003	0.062	0.028
rs780094	0.022	0.003	0.009	0.027
rs7903146	0.022	0.004	0.049	0.029
rs860598	0.012	0.004	-0.112	0.036
rs974801	0.016	0.003	-0.038	0.027
Insulin resistance - ln(pmol)/L				
rs731839	0.017	0.003	0.062	0.028
rs17036328	0.014	0.005	0.015	0.040
rs4865796	0.016	0.003	-0.048	0.028
rs10195252	0.018	0.003	0.035	0.026
rs459193	0.019	0.003	0.089	0.030
rs3822072	0.010	0.003	0.049	0.026
rs2943645	0.016	0.003	0.007	0.027
rs4846565	0.015	0.003	0.103	0.027
rs2745353	0.015	0.003	0.065	0.026
rs6822892	0.010	0.003	0.037	0.028

Supplementary Table 17: Variants applied in MR analyses to model hormonal phenotypes as causal exposures for grip strength. Part 1 of 2, continued overleaf. Reference details for each score are provided in the main text. Betas are expressed in the units specified for each exposure. Grip strength data are from stage I analyses in UKB.

	Exposure		Grip Strength	
Variant	Beta	SE	Beta	SE
Insulin secretion - SD 30-min insulin				
rs10811661	0.083	0.029	0.076	0.034
rs10830963	0.076	0.025	-0.020	0.029
rs10946398	0.061	0.023	0.003	0.028
rs11603334	0.051	0.028	0.015	0.036
rs11605924	0.069	0.021	0.047	0.026
rs11672660	0.130	0.034	0.030	0.033
rs12686676	0.015	0.021	0.008	0.026
rs12779790	0.068	0.028	-0.035	0.034
rs13266634	0.041	0.024	0.053	0.028
rs174550	0.031	0.022	-0.009	0.027
rs4502156	0.050	0.022	0.006	0.026
rs4607517	0.032	0.033	0.004	0.034
rs5015480	0.061	0.021	0.058	0.026
rs5215	0.038	0.022	0.014	0.027
rs560887	0.047	0.023	-0.025	0.028
rs7903146	0.060	0.025	0.049	0.029
rs7957197	0.062	0.027	-0.058	0.033
rs933360	0.079	0.024	0.005	0.029
IGF-I - SD IGF-I				
rs1065656	0.053	0.009	0.056	0.028
rs2153960	0.051	0.009	-0.043	0.029
rs509035	0.049	0.009	-0.005	0.028
rs700753	0.089	0.009	-0.009	0.027
rs780093	0.064	0.009	0.007	0.027
rs934073	0.051	0.009	0.005	0.028
rs978458	0.059	0.009	0.091	0.030

Supplementary Table 17: Variants applied in MR analyses to model hormonal phenotypes as causal exposures for grip strength (continued). Part 2 of 2.

			Inverse Variance-Weighted					MR-Egger						Weighted Median			Penalised Weighted Median		
Trait	Dataset	Scale of β	β	SE	p	Coch *Q*	$p_{Coch\ Q}$	β	SE	p	Intercept	$SE_{Intercept}$	$p_{Intercept}$	β	SE	p	β	SE	p
Fracture Risk	GEFOS	log(OR)	-0.052	0.025	0.038	1.473	1.000	-0.670	0.267	0.012	0.099	0.041	0.016	-0.069	0.032	0.031	-0.075	0.032	0.019
Coronary Heart	CARDIoGRAMplusC4D	log(OR)	-0.011	0.023	0.631	1.873	1.000	0.146	0.127	0.249	-0.027	0.022	0.207	-0.017	0.024	0.985	0.000	0.023	0.470
Myocardial Infarction	CARDIoGRAMplusC4D	log(OR)	-0.021	0.027	0.433	2.307	1.000	0.197	0.144	0.170	-0.038	0.025	0.123	-0.012	0.027	0.463	0.020	0.027	0.648
Lean Mass Index	Fenland + EPIC-Norfolk	kg/m^2	0.072	0.040	0.074	2.699	1.000	-0.314	0.195	0.106	0.064	0.032	0.043	0.095	0.054	0.066	0.095	0.052	0.075
Fat Mass Index	Fenland + EPIC-Norfolk	kg/m^2	0.013	0.084	0.878	6.171	0.977	-0.836	0.401	0.037	0.141	0.065	0.031	0.045	0.101	0.647	0.046	0.101	0.657
Lumbar Spine BMD	GEFOS	SD	0.040	0.023	0.086	2.331	1.000	0.150	0.134	0.262	-0.019	0.023	0.404	0.051	0.021	0.025	0.052	0.023	0.014
Femoral Neck BMD	GEFOS	SD	0.019	0.016	0.229	1.279	1.000	0.052	0.095	0.582	-0.006	0.016	0.725	0.015	0.017	0.395	0.016	0.018	0.377
Forearm BMD	GEFOS	SD	-0.002	0.026	0.953	1.495	1.000	0.115	0.146	0.429	-0.020	0.025	0.415	-0.035	0.037	0.347	-0.035	0.037	0.346

Supplementary Table 18: Mendelian randomisation of genetically-predicted grip strength to selected morbidities. Betas are per additional strength-increasing allele, in the units specified. Coch *Q* denotes Cochran's *Q*-statistic for heterogeneity

Phenotype	Source	r2	z-score	p-value
Coronary Heart Disease	CARDIoGRAMplusC4D	-0.045	-0.006	0.362
Fat Mass Index	Fenland + EPIC-Norfolk	-0.128	-1.943	0.052
Lean Mass Index	Fenland + EPIC-Norfolk	0.258	4.189	2.80E-05
Bone Mineral Density (Forearm)	GEFOS	0.164	1.558	0.119
Bone Mineral Density (Femoral Neck)	GEFOS	0.123	2.595	0.0095
Bone Mineral Density (Lumbar Spine)	GEFOS	0.156	3.441	0.0006

Supplementary Table 19: Genetic correlations of grip strength with selected phenotypes. Correlations shown are with UKB discovery (stage I) analyses

	Fenland	NEO	QFS	BLSA	ICSHIB	Pima
Study Information						
Population	British	Dutch	French Canadian	US Citizens	Nigerian	Pima Indians
Ancestry	European	European	European	European/African	African	Native American
Age Range at Recruitment (years)	30-65	40-65	18-65	29-97	13-85	18-46
Location	Cambridgeshire, UK	Leiden, Netherlands	Quebec City, Canada	Baltimore, MD	Igbo-Ora, Nigeria	Phoenix, AZ
Recruitment Period	2005-2015	2008-2012	1989-2002	Ongoing	1998-2000	1982-2004
Contributing Sample Size	8,491	1,242	762	669	188	509
Indirect Calorimetry Protocol						
Fasting Duration (hr)	Overnight	Overnight	Overnight	Overnight	Overnight	Overnight
Stimulants Prohibited	Caffeine, Nicotine	N/A	N/A	Caffeine, Nicotine	Caffeine, Nicotine	Caffeine, Nicotine
OGTT Administered	Yes	No	Yes	No	No	No
Testing Time of Day	0700-1200		0700-1100	0600-0800	0700-1100	0700-1000
Participant Position	Supine	Supine	Semi-reclined	Supine	Supine	Supine
Calorimeter Model or Protocol	Jaeger Oxycon Pro	Jaeger Oxycon Pro	Zirconia Cell O_2 Analyser	Cosmed K4b2	Delta Trac II	Parvo Medics TrueOne 2400
Calorimeter Supplier	CareFusion, San Diego, CA	CareFusion, San Diego, CA	Thermox Instruments, Pittsburgh, PA	Not Known	Sensor Medics, Anaheim, CA	Not Known
Sampling Frequency	Breath-by-Breath	Breath-by-Breath	Breath-by-Breath	Breath-by-Breath	Continuous Flow	Breath-by-Breath
Participant Interface	Facemask	Facemask	Ventilated Hood	Facemask	Ventilated Hood	Ventilated Hood
Testing Duration (min)	6	30	30	15	30-45	
Derivation Equation	Abbreviated Weir	Elia & Livesey	Abbreviated Weir	Abbreviated Weir	Abbreviated Weir	Lusk

Supplementary Table 20: Cohorts contributing to the REEGen Consortium. NEO, Netherlands Epidemiology of Obesity Cohort; QFS, Quebec Family Study; BLSA, Baltimore Lomngitudinal Study of Ageing; ICSHIB, International Collaborative Study of Hypertension in Blacks; Pima, NIH/NIDDK Pima Indian Study. Note: the total n contributed by Fenland is less than the number of individuals for whom REE was initially calculated due to lower availability of samples with intersecting genotyping data in this subcohort

	Male	Female	All
n	4325	5047	9372
Age (years)	48.9 (7.6)	48.9 (7.4)	48.9 (10.0)
Body Mass (kg)	86.2 (13.9)	71.2 (14.6)	78.1 (16.1)
Body Mass Index (kg/m^2)	27.3 (4.0)	26.4 (5.2)	26.8 (4.7)
Fat Mass (kg)	25.4 (8.2)	27.4 (10.2)	26.5 (9.3)
Lean Mass (kg)	57.4 (6.8)	41.5 (5.3)	48.8 (10.0)
Relative Body Fat Mass (%)	29.0 (5.8)	37.5 (7.0)	33.5 (7.7)
Relative Lean Mass (%)	67.3 (5.7)	59.3 (6.7)	63.0 (7.4)
Breaths passing QC	20.8 (7.1)	23.7 (7.3)	22.3 (7.4)
Breaths failing QC	5.5 (4.3)	4.9 (4.3)	5.2 (4.3)
Resting VO_2 (mL/kg/min)	3.33 (0.55)	3.06 (0.59)	3.18 (0.59)
Resting VCO_2 (mL/kg/min)	3.03 (0.60)	2.84 (0.56)	2.92 (0.59)
RER	0.91 (0.07)	0.93 (0.07)	0.92 (0.07)
REE (kcal/24hr)	2008.5 (384.15)	1525.1 (336.40)	1748.17 (432.55)
REE (kcal/kg/24hr)	23.5 (3.91)	21.7 (4.23)	

Supplementary Table 21: Univariate characteristics of derived REE and associated traits in Fenland. Unless specified, data are mean (SD). DXA data are available for 9296 participants of the final 9372 passing all quality control stages for REE derivation. Data shown for lean and fat masses reflect this figure.

	Beta	SE	p-value
Model 1 (n = 7,689)			
Age (per 10-year increase)	-320.18	19.83	1.01E-57
Sex (Males vs Females)	1859.63	29.44	<5.00E-300
BMI (kg/m2)	777.74	14.78	<5.00E-300
Model 2 (n = 7,689)			
Age (per 10-year increase)	-279.85	20.64	2.15E-41
Sex (Males vs Females)	1412.84	51.34	4.63E-159
Total LM (kg)	747.15	43.99	1.55E-63
Total FM (kg)	461.70	18.73	3.11E-129
Total BM (kg)	-307.74	35.94	1.33E-17

Supplementary Table 22: Association of REE with basic anthropometric covariates. For each model, associations are calculated in participants with complete data available for REE, genotyping, and all covariates. Betas and SEs are change in REE (kJ/day) per SD increase in exposure, unless otherwise stated. Models include all variables shown as covariates, and are additionally adjusted for REE device, ambient test temperature during calorimetry, and OGTT test status (Y/N).

								European				Transethnic								
					EAF			IVW				Fixed			Random			Han-Eskin	Binary		
Source	rsID	Chr	Gene	All.	Eur.	ICSHIB	Pima	Beta	SE	p-value	n	Beta	SE	p-value	Beta	SE	p-value	p-vale	p-value	n	MAC
European	rs61520068	16	*GOT2*	A/G	0.5	0.94	0.65	0.08	0.014	4.11E-08	11164	0.07	0.014	2.81E-07	0.01	0.066	0.869	3.86E-07	1.15E-07	11861	11449
Transethnic	rs12527963	6	*HCRTR2*	C/T	0.99	0.03	0.51					0.33	0.061	4.12E-08	0.33	0.061	4.12E-08	5.83E-08	8.50E-08	1665	2781
Transethnic	rs12034996	1	*VCTN1*	C/T	0.01	0.92	0.86					0.24	0.071	7.66E-04	0.36	0.304	0.241	1.85E-08	3.91E-09	1939	213

Supplementary Table 23: Variants associated with REE in European and transethnic discovery, independent of age and sex. Data are shown for all variants reaching genome-wide significance in at least one European or Transethnic model. Betas are additive SD change in REE per effect allele. European associations for the two transethnic variants are not shown due to low frequency in the European sample.

		Gene Set Size		GSEA		
Source	Gene Set	Original	Effective	p-value	FDR	Enrich.
KEGG	Citrate Cycle/TCA Cycle	32	27	2.18E-02	2.50E-01	1.71
GO	TCA Cycle Enzyme Complex	11	11	3.40E-02	1.93E-01	2.00
Biocarta	ETC Pathway	12	9	4.99E-02	1.62E-01	2.50
Reactome	Glycolysis	29	24	1.20E-01	4.31E-01	1.50
GO	Negative Regulation of Release of Cytochrome C from Mitochondria	17	16	1.87E-01	5.33E-01	1.50
Reactome	Pyruvate Metabolism	19	16	1.90E-01	4.63E-01	1.50
GO	Oxaloacetate Metabolic Process	11	11	2.84E-01	5.70E-01	1.33
GO	Proton Transporting ATP Synthase Complex	22	22	2.97E-01	6.01E-01	1.17
Reactome	TCA Cycle and Respiratory ET	141	109	3.81E-01	7.67E-01	1.07
GO	Respiratory Chain Complex IV Assembly	18	17	4.25E-01	8.32E-01	1.25
KEGG	Glycolysis Gluconeogenesis	62	54	4.90E-01	8.21E-01	1.00
GO	Regulation of Release of Cytochrome C from Mitochondria	44	43	5.17E-01	7.86E-01	1.00
Reactome	Respiratory ET: ATP Synthesis by Chemiosmotic Coupling and Heat Production by UCP	98	77	5.63E-01	7.65E-01	1.00
GO	Hydrogen Peroxide Metabolic Process	30	24	5.76E-01	7.96E-01	1.00
KEGG	Pyruvate Metabolism	40	38	6.40E-01	7.74E-01	0.90
Reactome	Respiratory Electron Transport	79	61	6.97E-01	7.76E-01	0.93
Biocarta	Glycolysis Pathway	10	9	7.06E-01	8.16E-01	1.00
GO	Positive Regulation of Release of Cytochrome C from Mitochondria	28	28	7.32E-01	7.48E-01	0.86
GO	Respiratory Chain	80	74	7.79E-01	8.14E-01	0.84
GO	Mitochondrial ET: Ubiquinol to Cytochrome C	14	13	8.75E-01	8.25E-01	0.67
GO	Electron Transport Chain	94	87	9.08E-01	8.80E-01	0.77

Supplementary Table 24: Enrichment of REE associations for selected respiratory pathways. Gene set size is expressed in number of genes - effective size denotes the gene set used in analysis after filtering of the input set based on gene size and proximity. Results are sorted by enrichment p-value. Enrich indicates the fold-enrichment of REE associations in this pathways, based on permutation. FDR, permutation-based false discovery rate; ET, electron transport; TCA, tricarboxylic acid

		REE_{AS}		
Trait	PMID	r_G	SE	p-value
Height	20881960	0.5747	0.1038	3.10E-08
BMI	20935630	0.7076	0.1336	1.18E-07
Waist Circumference	25673412	0.9296	0.1994	3.14E-06
Waist-to-hip Ratio	25673412	0.6594	0.1461	6.41E-06
Hip Circumference	25673412	0.834	0.1864	7.68E-06
Body Fat Percentage	26833246	0.3834	0.12	0.0014
HOMA-IR	20081858	0.5554	0.1895	0.0034
Fasting Insulin	22581228	0.3931	0.1569	0.0122
Type 2 Diabetes	22885922	0.274	0.1218	0.0244
Parental age at death	27015805	-0.3959	0.2068	0.0556
Maternal age at death	27015805	-0.3366	0.1876	0.0727
Fasting Pro-insulin	20081858	0.3617	0.2062	0.0794
HOMA-B	20081858	0.2847	0.1788	0.1114
Fasting Glucose	22581228	0.2115	0.1335	0.113
Amyotrophic Lateral Sclerosis	27455348	0.2004	0.2056	0.3299
Paternal age at death	27015805	-0.1464	0.1738	0.3995
Femoral Neck BMD	26367794	0.0864	0.1157	0.455
Coronary Artery Disease	26343387	0.0583	0.0815	0.4743
Lumbar Spine BMD	26367794	0.0794	0.1157	0.4927
Adiponectin	22479202	-0.0641	0.1873	0.7323
HbA1C	20858683	-0.0418	0.1492	0.7791
Parkinson's disease	19915575	0.0314	0.1121	0.7792
Sitting height ratio	25865494	0.0366	0.1521	0.8099
Alzheimer's disease	24162737	-0.0283	0.1608	0.8603
Forearm BMD	26367794	0.0278	0.2698	0.918

Supplementary Table 25: Genetic correlations of REE with selected anthropometric, ageing and cardiometabolic phenotypes. PMID indicates original source of GWAS summary statistics for trait. BMD, bone mineral density; HOMA-IR, ; HOMA-B

	REE_{AS} (kJ/24hr)			REE_{RES} (kJ/24hr)			BMI_{AS} (kg/m^2)			BFP_{AS} (%)			
rsID	Beta	SE	p-value	Beta	SE	p-value	Beta	SE	p-value	Beta	SE	p-value	n
rs3817334	-43.44	24.59	0.077	-73.72	21.05	4.65E-04	0.19	0.08	0.013	0.24	0.11	0.023	7689
rs9641123	-43.25	24.64	0.079	-51.88	21.1	0.014	0.07	0.08	0.402	0.12	0.11	0.238	7689
rs7138803	102.6	24.94	3.93E-05	49.93	21.39	0.02	0.31	0.08	8.08E-05	0.32	0.11	2.96E-03	7671
rs7599312	-50.99	27.85	0.067	-47.38	23.87	0.047	-0.02	0.09	0.817	-0.01	0.12	0.951	7686
rs12566985	48.84	24.47	0.046	41.41	20.96	0.048	0.05	0.08	0.495	-0.07	0.11	0.482	7689
rs9400239	52.07	26.83	0.052	44.84	22.99	0.051	0.04	0.08	0.637	-0.08	0.12	0.508	7689
rs17094222	-55.01	30.41	0.071	-50.47	26.05	0.053	-0.01	0.1	0.88	0.02	0.13	0.863	7689
rs1808579	-17.28	24.39	0.479	-39.45	20.89	0.059	0.14	0.08	0.079	0.32	0.1	2.62E-03	7689
rs1528435	58.52	24.88	0.019	37.95	21.31	0.075	0.13	0.08	0.092	0.16	0.11	0.146	7689
rs12286929	-9.67	24.12	0.688	-36.72	20.66	0.076	0.17	0.08	0.023	0.27	0.1	0.01	7689
rs6804842	51.82	24.67	0.036	32.44	21.13	0.125	0.12	0.08	0.127	0.15	0.11	0.144	7689
rs543874	74.07	30.05	0.014	36.49	25.75	0.157	0.24	0.09	0.013	0.18	0.13	0.165	7689
rs6477694	41.21	25.35	0.104	29.53	21.71	0.174	0.07	0.08	0.351	0.13	0.11	0.228	7689
rs7243357	53.24	31.86	0.095	36.77	27.29	0.178	0.09	0.1	0.381	0.15	0.14	0.27	7689
rs12401738	59.03	25.18	0.019	28.32	21.58	0.189	0.19	0.08	0.018	0.16	0.11	0.137	7689
rs1928295	-13.83	24.29	0.569	-25.55	20.8	0.219	0.07	0.08	0.356	0.04	0.1	0.702	7665
rs11165643	37.02	24.52	0.131	25.08	21.01	0.233	0.08	0.08	0.309	0.13	0.11	0.222	7689
rs11126666	9.62	27.68	0.728	-28.13	23.7	0.235	0.22	0.09	0.012	0.14	0.12	0.244	7647
rs7164727	-1.17	25.69	0.964	-25.84	22	0.24	0.16	0.08	0.054	0.13	0.11	0.23	7689
rs3888190	36.45	24.94	0.144	24.5	21.37	0.252	0.07	0.08	0.346	0.18	0.11	0.088	7689
rs2365389	-15.16	24.51	0.536	-22.81	21	0.277	0.05	0.08	0.559	0.21	0.11	0.048	7689
rs492400	-42.03	24.51	0.086	-22.49	21	0.284	-0.12	0.08	0.123	-0.17	0.11	0.097	7689
rs9540493	-4.45	24.46	0.855	-21.91	20.95	0.296	0.11	0.08	0.153	0.18	0.1	0.094	7655
rs758747	-1.2	28.03	0.966	-24.4	24.01	0.31	0.14	0.09	0.111	0.16	0.12	0.178	7689
rs10968576	41.38	25.93	0.111	21.96	22.22	0.323	0.11	0.08	0.194	0.09	0.11	0.43	7689
rs2121279	-45.6	36.77	0.215	-30.37	31.5	0.335	-0.09	0.12	0.423	-0.02	0.16	0.882	7689
GRS_{95}	13.85	2.79	7.21E-07	-2.29	2.4	0.339	0.1	0.01	2.08E-29	0.11	0.01	2.21E-19	7689
rs11847697	-18.53	58.4	0.751	-46.82	50.02	0.349	0.15	0.18	0.404	-0.03	0.25	0.903	7689
rs13021737	72.4	31.82	0.023	25.43	27.26	0.351	0.28	0.1	5.26E-03	0.22	0.14	0.114	7689
rs1167827	59.3	24.84	0.017	19.58	21.28	0.358	0.25	0.08	1.44E-03	0.17	0.11	0.12	7689
rs6091540	11.85	26.58	0.656	-20.39	22.77	0.371	0.19	0.08	0.021	0.21	0.11	0.063	7689
rs17203016	-24.74	30.94	0.424	-22.35	26.5	0.399	-0.03	0.1	0.783	-0.05	0.13	0.734	7689
rs12429545	50.4	37.25	0.176	26.14	31.91	0.413	0.14	0.12	0.228	0.01	0.16	0.969	7689
rs977747	27.84	24.66	0.259	16.51	21.12	0.434	0.08	0.08	0.319	0.25	0.11	0.019	7689
rs3736485	9.29	24.42	0.704	16.25	20.91	0.437	-0.03	0.08	0.715	0.07	0.1	0.486	7689
rs2033732	-19.2	27.53	0.486	-18.28	23.59	0.438	-0.01	0.09	0.923	-0.1	0.12	0.419	7689
rs1000940	7.18	26.1	0.783	-17.23	22.36	0.441	0.15	0.08	0.075	0.2	0.11	0.068	7689
rs10733682	21.31	25.55	0.404	16.4	21.89	0.454	0.03	0.08	0.71	0.01	0.11	0.917	7689
rs4256980	-10.33	25.28	0.683	-15.94	21.65	0.462	0.04	0.08	0.628	0.2	0.11	0.069	7689
rs3101336	29.24	24.94	0.241	-14.63	21.37	0.494	0.27	0.08	5.33E-04	0.18	0.11	0.098	7689
rs12446632	-6.14	35.22	0.862	-20.55	30.17	0.496	0.09	0.11	0.415	-0.14	0.15	0.342	7689
rs1516725	25.97	35.31	0.462	-20.32	30.24	0.502	0.28	0.11	0.011	0.22	0.15	0.15	7689
rs1441264	-17.89	25.01	0.474	-14.37	21.42	0.502	-0.02	0.08	0.817	-0.13	0.11	0.214	7689
rs7903146	-14.22	26.69	0.594	-14.88	22.86	0.515	0	0.08	0.995	0.02	0.11	0.865	7689
rs4787491	23.99	24.42	0.326	13.6	20.92	0.516	0.07	0.08	0.389	0.03	0.1	0.761	7689
rs11030104	41.81	29.65	0.159	16.31	25.4	0.521	0.16	0.09	0.084	0.17	0.13	0.174	7671
rs10182181	27.73	24.51	0.258	-13.01	20.99	0.535	0.25	0.08	1.35E-03	0.31	0.11	3.35E-03	7689
rs2245368	1.85	32.45	0.954	-15.22	27.79	0.584	0.08	0.1	0.407	-0.08	0.14	0.546	7689
rs16951275	12.02	28.65	0.675	13.42	24.54	0.585	-0.01	0.09	0.915	-0.03	0.12	0.83	7689
rs16851483	41.61	47.24	0.378	-21.76	40.46	0.591	0.4	0.15	8.03E-03	0.55	0.2	6.50E-03	7689

Supplementary Table 26: Association of 95 known BMI variants with REE in the Fenland cohort. Part 1 of 2, continued overleaf. Effect shown is additive per BMI-increasing allele based on GIANT consortium data - effect size for BMI shown here may be negative due to lack of power. Variants are sorted by p-value of association with REE_{RES}. GRS_{95} denotes the additive effect of all 95 variants combined into a single dosage score. BMI and BFP are residualised for age and sex. REE is residualised for age, sex, OGTT and technical parameters (see main text); REE_{RES} additionally residualised for BMI.

	REE_{AS} (kJ/24hr)			REE_{RES} (kJ/24hr)			BMI_{AS} (kg/m^2)			BFP_{AS} (%)			
rsID	Beta	SE	p-value	Beta	SE	p-value	Beta	SE	p-value	Beta	SE	p-value	n
rs13078960	14.54	30.27	0.631	-13.78	25.93	0.595	0.18	0.1	0.062	0.2	0.13	0.132	7689
rs2080454	40.56	25.08	0.106	10.91	21.49	0.612	0.19	0.08	0.017	0.29	0.11	7.07E-03	7689
rs11583200	8.82	24.55	0.719	-10.64	21.03	0.613	0.12	0.08	0.125	0.23	0.11	0.029	7689
rs29941	2.95	26.24	0.911	-11.3	22.48	0.615	0.09	0.08	0.291	0.12	0.11	0.285	7689
rs7141420	2.61	24.34	0.915	-10.46	20.85	0.616	0.08	0.08	0.307	0.17	0.1	0.094	7687
rs2650492	3.51	27.55	0.898	-11.43	23.6	0.628	0.1	0.09	0.266	0.22	0.12	0.063	7689
rs1460676	-18.17	32.72	0.579	-12.6	28.03	0.653	-0.05	0.1	0.658	-0.04	0.14	0.802	7689
rs12940622	29.43	24.24	0.225	8.54	20.77	0.681	0.14	0.08	0.074	0.09	0.1	0.396	7689
rs7899106	-0.73	53.61	0.989	-18.27	45.92	0.691	0.11	0.17	0.512	-0.11	0.23	0.634	7687
rs2176040	3.08	25.06	0.902	-8.2	21.47	0.703	0.06	0.08	0.412	0.21	0.11	0.051	7689
rs6567160	50.36	28.37	0.076	-9.08	24.31	0.709	0.36	0.09	5.37E-05	0.36	0.12	2.96E-03	7689
rs2207139	33.13	32.53	0.309	-9.5	27.87	0.733	0.27	0.1	8.82E-03	0.22	0.14	0.119	7689
rs17024393	56.59	78.53	0.471	-22.72	67.27	0.736	0.49	0.25	0.05	0.74	0.34	0.027	7689
rs12885454	9.8	25.12	0.696	-7.19	21.52	0.738	0.1	0.08	0.2	0.22	0.11	0.043	7689
rs13191362	-3.03	36.63	0.934	10.22	31.38	0.745	-0.07	0.12	0.518	-0.16	0.16	0.302	7689
rs205262	40.19	27.17	0.139	6.58	23.28	0.777	0.2	0.09	0.017	0.15	0.12	0.21	7689
rs2836754	52.4	25.23	0.038	6.05	21.62	0.779	0.29	0.08	3.12E-04	0.28	0.11	0.011	7689
rs2176598	-1.22	28.43	0.966	6.46	24.35	0.791	-0.04	0.09	0.685	-0.05	0.12	0.684	7689
rs3849570	-29.99	25.33	0.236	-5.74	21.7	0.791	-0.14	0.08	0.072	-0.14	0.11	0.205	7689
rs16907751	54.85	40.83	0.179	8.8	34.98	0.801	0.28	0.13	0.032	0.19	0.18	0.277	7689
rs13201877	-17.21	35.82	0.631	-7.51	30.69	0.807	-0.05	0.11	0.654	-0.18	0.15	0.247	7689
rs9914578	4.21	29.88	0.888	6.2	25.59	0.809	-0.01	0.09	0.941	0.12	0.13	0.369	7689
rs11727676	18.35	41.71	0.66	-8.62	35.73	0.809	0.17	0.13	0.203	0.14	0.18	0.422	7689
rs11057405	41.06	40.38	0.309	7.9	34.59	0.819	0.21	0.13	0.104	0.26	0.17	0.128	7689
rs6465468	-8.44	26.84	0.753	5.14	23	0.823	-0.08	0.08	0.325	-0.06	0.12	0.629	7689
rs2112347	20.27	25.15	0.42	4.38	21.55	0.839	0.09	0.08	0.275	-0.03	0.11	0.747	7689
rs17001654	18.82	34.16	0.582	5.71	29.27	0.845	0.08	0.11	0.48	0.13	0.15	0.393	7689
rs13107325	50.57	46.19	0.274	7.71	39.57	0.846	0.26	0.15	0.073	0.09	0.2	0.647	7689
rs17724992	0.63	28.2	0.982	4.53	24.15	0.851	-0.03	0.09	0.748	-0.03	0.12	0.794	7689
rs10938397	27.4	24.65	0.266	-3.93	21.11	0.852	0.2	0.08	0.011	0.25	0.11	0.017	7689
rs17405819	9.79	26.67	0.714	-4.15	22.84	0.856	0.1	0.08	0.224	0.14	0.11	0.229	7689
rs2820292	-6.7	24.31	0.783	-3.66	20.83	0.861	-0.03	0.08	0.723	0.04	0.1	0.681	7689
rs9581854	-14.48	30.83	0.639	-4.51	26.41	0.864	-0.07	0.1	0.498	-0.12	0.13	0.371	7689
rs2033529	-54.31	65.47	0.407	-9.15	54.71	0.867	-0.27	0.23	0.249	-0.18	0.31	0.563	979
rs9925964	19.89	24.67	0.42	-2.49	21.13	0.906	0.14	0.08	0.074	0.27	0.11	0.011	7689
rs2287019	32.32	32.38	0.318	3.19	27.74	0.908	0.17	0.1	0.102	0.06	0.14	0.688	7689
rs2075650	24.08	36.07	0.504	3.36	30.9	0.913	0.12	0.11	0.288	0.1	0.15	0.532	7689
rs1558902	48.74	24.38	0.046	-2.14	20.89	0.918	0.3	0.08	7.95e-05	0.4	0.1	1.28E-04	7689
rs7715256	19.13	24.16	0.429	1.87	20.7	0.928	0.09	0.08	0.229	0.09	0.1	0.399	7689
rs4740619	-0.7	24.36	0.977	1.79	20.87	0.932	-0.01	0.08	0.877	0	0.1	0.991	7689
rs11688816	22.88	24.23	0.345	-1.63	20.75	0.937	0.14	0.08	0.061	0.12	0.1	0.249	7689
rs3810291	-3.8	25.85	0.883	-0.97	22.15	0.965	-0.01	0.08	0.855	-0.09	0.11	0.42	7689
rs7239883	23.6	24.88	0.343	0.71	21.32	0.974	0.13	0.08	0.089	0.13	0.11	0.233	7689
rs11191560	36.74	43.41	0.397	1	37.19	0.978	0.22	0.14	0.114	-0.06	0.19	0.736	7680
rs10132280	-0.04	26.53	0.999	0.38	22.73	0.987	0	0.08	0.993	-0.12	0.11	0.299	7689
rs9374842	25.11	28.5	0.378	-0.27	24.41	0.991	0.14	0.09	0.113	0.1	0.12	0.418	7689
rs1016287	19.61	26.48	0.459	0.19	22.68	0.993	0.12	0.08	0.166	0.09	0.11	0.44	7689

Supplementary Table 26: Association of 95 known BMI variants with REE in the Fenland cohort. Part 2 of 2.

					Bottom 5% mLRR-Y			Top 5% mLRR-Y		
rsID	Chr.	Pos.	EA	AA	log(OR)	SE	p-value	log(OR)	SE	p-value
rs1122138	14	96180242	C	A	0.0417	0.0050	9.60E-17	-0.0083	0.0050	9.40E-02
rs17758695	18	60920854	C	T	0.0576	0.0109	1.40E-07	-0.0385	0.0105	2.60E-04
rs59633341	3	150018880	D	I	0.0334	0.0048	2.70E-12	0.0025	0.0049	6.10E-01
rs78378222	17	7571752	T	G	-0.0856	0.0161	1.10E-07	0.0205	0.0177	2.50E-01
rs2736609	1	156202640	C	T	-0.0196	0.0037	9.70E-08	0.0014	0.0038	7.10E-01
rs13191948	6	109634599	C	T	0.0189	0.0036	1.60E-07	-0.0069	0.0037	5.90E-02
rs35091702	8	30279470	I	D	-0.0188	0.0041	4.20E-06	0.0085	0.0041	4.00E-02
rs4721217	7	1973579	C	T	-0.0185	0.0036	3.20E-07	0.0047	0.0037	2.00E-01
rs137952017	14	101176090	D	I	0.0193	0.0052	1.90E-04	-0.0135	0.0052	9.30E-03
rs56084922	5	111061883	A	G	-0.0322	0.0067	1.50E-06	0.0099	0.0070	1.60E-01
rs60084722	20	30355738	I	D	0.0221	0.0045	1.20E-06	-0.0118	0.0046	1.00E-02
rs381500	6	164478388	C	A	0.0188	0.0036	1.80E-07	-0.0036	0.0037	3.20E-01
rs12448368	16	81044947	T	C	-0.0215	0.0053	5.00E-05	0.0036	0.0054	5.10E-01
rs4754301	11	108048541	G	A	-0.0163	0.0036	5.20E-06	0.0060	0.0036	9.80E-02
rs77522818	17	47817373	A	T	0.0419	0.0091	3.60E-06	-0.0174	0.0089	5.10E-02
rs11082396	18	42080720	T	C	-0.0280	0.0052	7.60E-08	0.0140	0.0054	9.50E-03
rs13088318	3	101242751	A	G	-0.0193	0.0038	2.60E-07	0.0058	0.0039	1.30E-01
rs10687116	13	41678081	D	I	-0.0152	0.0045	8.10E-04	0.0080	0.0046	7.90E-02
rs115854006	3	48388170	C	T	0.0394	0.0106	1.90E-04	-0.0213	0.0104	4.20E-02

Supplementary Table 27: Effect of the 16 mLOY variants on dichotomised mLRR-Y. Effects are shown for the topmost and lowermost 5% of participants ranked by mLRR-Y, by comparison to the median 25% in each case. Insertion-deletion variants are coded I/D. Only two variants reach statistical significance at $p \leq 5 \times 10^{-8}$ in these dichotomised analyses (highlighted red), illustrating the increased statistical power of considering mLRR-Y as a continuous trait in discovery analyses

CpG	Chr.	Pos.	Effect	SE	*T*-value	p-value	Nearest Gene	GWAS Locus
cg24405270	7	141401010	-0.0421	0.0041	-10.17	2.73E-24	*KIAA1147*	
cg06010724	5	79911547	0.0350	0.0042	8.24	2.22E-16	*DHFR*	
cg24718722	10	129536818	0.0350	0.0044	8.01	1.11E-15	*FOXI2*	
cg19509778	10	129537308	0.0346	0.0043	8.02	1.11E-15	*FOXI2*	
cg07823670	1	35222618	0.0328	0.0046	7.20	6.04E-13	*GJB5*	
cg07546011	2	233274509	0.0308	0.0043	7.13	1.03E-12	*ALPPL2*	
cg02317313	12	122235206	0.0306	0.0045	6.82	8.79E-12	*LOC338799*	
cg00691598	8	1810526	0.0344	0.0050	6.82	9.00E-12	*ARHGEF10*	
cg01788994	4	96469264	-0.0288	0.0043	-6.63	3.30E-11	*UNC5C*	
cg07159847	12	58122341	0.0285	0.0045	6.37	1.90E-10	*AGAP2*	
cg11294269	12	132685428	0.0275	0.0044	6.24	4.24E-10	*GALNT9*	
cg22585988	1	161059327	0.0273	0.0044	6.15	7.59E-10	*PVRL4*	
cg24299740	11	134252804	0.0266	0.0044	6.10	1.06E-09	*B3GAT1*	
cg05304393	16	1545405	0.0287	0.0047	6.08	1.24E-09	*TELO2*	
cg08634229	6	169326603	0.0266	0.0044	6.05	1.48E-09	*SMOC2*	
cg02307597	19	17402942	0.0291	0.0048	6.03	1.65E-09	*ABHD8*	
cg25095973	10	48413850	0.0262	0.0044	5.96	2.51E-09	*GDF2*	
cg13935577	12	107974897	0.0265	0.0045	5.96	2.57E-09	*BTBD11*	
cg05796223	16	21532721	0.0273	0.0046	5.94	2.89E-09	*SLC7A5P2*	
cg24843003	19	1409547	0.0280	0.0047	5.92	3.28E-09	*DAZAP1*	
cg01303141	17	77952109	0.0262	0.0045	5.88	4.19E-09	*TBC1D16*	
cg21468274	17	7339835	0.0255	0.0044	5.80	6.73E-09	*TMEM102*	*TP53*
cg20442078	2	27531360	0.0253	0.0044	5.75	8.75E-09	*UCN*	
cg26315984	1	173176501	-0.0247	0.0044	-5.62	1.89E-08	*TNFSF4*	
cg09911083	17	7754956	0.0314	0.0056	5.61	2.02E-08	*KDM6B*	*TP53*
cg00328227	1	109204325	0.0274	0.0049	5.60	2.18E-08	*HENMT1*	
cg13249146	12	132887349	0.0245	0.0044	5.58	2.39E-08	*GALNT9*	
cg00317577	15	83239908	0.0297	0.0053	5.58	2.39E-08	*CPEB1*	
cg03339609	19	34662636	0.0279	0.0050	5.54	2.98E-08	*LSM14A*	
cg14644418	10	129536661	0.0242	0.0044	5.51	3.67E-08	*FOXI2*	
cg20116579	17	7288001	0.0244	0.0044	5.50	3.81E-08	*TNK1*	*TP53*
cg06783429	7	127673038	0.0243	0.0044	5.48	4.24E-08	*SND1*	
cg05726109	22	19709755	0.0243	0.0044	5.47	4.55E-08	*SEPT5*	
cg16572910	1	43880657	0.0274	0.0051	5.40	6.48E-08	*SZT2*	
cg14782678	17	7339721	0.0237	0.0044	5.39	7.23E-08	*TMEM102*	*TP53*
cg27529647	1	151300868	0.0240	0.0045	5.37	7.69E-08	*PI4KB*	

Supplementary Table 28: Differentially-methylated CpG positions associated with mLRR-Y. Effect shown is change in mLRR-Y per SD increase in methylation at the specified CpG. All CpGs are physically independent of GWAS signals for mLRR-Y, with the exception of the four indicated sites falling within a 1mB window of *TP53*

DMP			*cis*-meQTLs					Association with mLRR-Y (UKB)			
CpG	Chr.	Pos.	rsID	Pos	All.	*Z*-score	p-value	EAF	Effect	SE	p-value
cg00317577	15	83239908	rs185018922	83183986	A/C	4.39	1.12E-05	0.935	0.002	0.0007	5.40E-03
			rs12438312	83363323	G/A	31.1	2.41E-212	0.412	0.000	0.0004	2.60E-01
			rs28664062	83414429	C/T	-8.54	1.37E-17	0.839	0.000	0.0005	5.10E-01
			rs66500181	83459370	C/T	-4.74	2.13E-06	0.530	0.000	0.0004	7.20E-01
			rs140228545	83030117	G/A	-5.91	3.33E-09				
cg00328227	1	109204325	rs17025036	109150720	T/C	15.34	3.95E-53	0.935	-0.001	0.0007	4.20E-02
			rs144231308	109200742	C/T	-5.88	4.15E-09	0.918	0.000	0.0006	5.60E-01
cg01303141	17	77952109	rs73423941	77943468	T/C	4.41	1.05E-05	0.892	-0.001	0.0006	1.70E-01
			rs3169601	77909438	C/T	-9.95	2.44E-23	0.697	0.000	0.0004	5.80E-01
			rs1542102	78003406	C/G	5.28	1.27E-07	0.792	0.000	0.0004	7.80E-01
			rs1561812	78061027	C/T	-4.16	3.20E-05	0.412	0.000	0.0004	9.80E-01
cg02307597	19	17402942	rs2288544	17337025	T/C	-4.72	2.39E-06	0.778	0.000	0.0004	9.10E-01
cg02317313	12	122235206	rs2515729	122279333	T/A	-4.6	4.14E-06	0.212	0.001	0.0004	1.80E-01
			rs1168668	122227451	C/G	9.64	5.25E-22	0.189	0.000	0.0004	4.90E-01
cg03339609	19	34662636	rs872236	34685617	G/C	-17.69	5.41E-70	0.805	0.001	0.0004	3.80E-02
			rs74401830	34711072	A/G	8.82	1.12E-18	0.670	0.000	0.0004	2.50E-01
cg05726109	22	19709755	rs9680714	19571194	T/C	-4.17	3.00E-05	0.860	0.000	0.0005	6.00E-01
cg06783429	7	127673038	rs7809182	127521056	G/C	9.36	7.77E-21	0.703	0.000	0.0004	7.90E-01
cg07159847	12	58122341	rs4760169	58118847	C/T	-10.74	6.82E-27	0.870	0.000	0.0005	3.90E-01
			rs7965287	58188696	C/G	5.92	3.26E-09	0.667	0.000	0.0004	7.10E-01
cg13935577	12	107974897	rs61648172	107813364	T/C	5.57	2.60E-08	0.924	0.002	0.0007	1.50E-02
			rs7138971	107724891	T/G	-20.6	2.98E-94	0.724	-0.001	0.0004	2.70E-02
			rs6539329	107786705	G/A	-5.13	2.92E-07	0.452	0.000	0.0003	2.40E-01
			rs856887	107725814	G/A	8.62	6.71E-18	0.226	0.000	0.0004	4.50E-01
cg14644418	10	129536661	rs1926181	129586689	A/C	-4.17	3.06E-05	0.203	0.001	0.0004	2.40E-01
			rs77244569	129535455	A/G	-19.75	8.82E-87	0.868	0.000	0.0005	9.90E-01
cg14782678	17	7339721	rs35894069	7395176	A/G	6.12	9.36E-10	0.640	0.000	0.0004	2.80E-01
			rs117208279	7337862	A/G	-28.31	2.32E-176	0.927	0.000	0.0007	5.90E-01
			rs111269607	7367810	A/G	5.31	1.12E-07	0.925	0.000	0.0007	6.90E-01
cg20116579	17	7288001	rs7208523	7288228	T/C	-11.57	5.57E-31	0.886	-0.002	0.0006	8.80E-04
			rs60684900	7264760	T/C	-5	5.71E-07	0.901	-0.001	0.0007	1.60E-01
			rs114576150	7307950	G/T	-4.38	1.18E-05	0.908	0.001	0.0006	2.80E-01
cg20442078	2	27531360	rs72817542	27526681	G/C	-3.94	8.21E-05	0.792	0.000	0.0004	3.80E-01
			rs61737373	27423913	A/G	5.12	2.98E-07	0.943	0.001	0.0007	4.90E-01
cg21468274	17	7339835	rs35894069	7395176	A/G	6.9	5.28E-12	0.640	0.000	0.0004	2.80E-01
			rs4796305	7336055	G/T	5.45	5.02E-08	0.915	0.000	0.0006	4.80E-01
			rs34662267	7333058	A/C	-27.66	1.99E-168	0.927	0.000	0.0007	5.80E-01
cg22585988	1	161059327	rs11577230	161053644	T/C	-5.6	2.17E-08	0.886	0.001	0.0005	2.00E-01
cg24299740	11	134252804	rs10894808	134256805	T/C	-4.43	9.55E-06	0.874	0.001	0.0005	1.70E-01
cg24718722	10	129536818	rs12777108	129632527	G/A	6.19	5.88E-10	0.832	0.000	0.0005	5.20E-01
			rs72843197	129590057	C/G	4.88	1.06E-06	0.814	0.000	0.0005	7.60E-01
			rs72843150	129535239	T/C	-24.75	3.49E-135	0.868	0.000	0.0005	9.70E-01
cg24843003	19	1409547	rs11881021	1441600	C/T	-6.54	6.18E-11	0.697	-0.001	0.0004	1.70E-01
cg27529647	1	151300868	rs11204798	151273726	C/G	-7.7	1.38E-14	0.233	0.001	0.0004	3.80E-02
			rs34834099	151502427	T/C	9.9	4.05E-23	0.933	-0.001	0.0007	7.30E-02
			rs6695344	151178491	G/A	9.64	5.57E-22	0.369	0.001	0.0004	1.40E-01
			rs3811402	151119745	C/G	-6.05	1.49E-09	0.920	0.001	0.0006	1.60E-01
			rs3828054	151512895	G/A	3.96	7.57E-05	0.881	0.000	0.0005	8.60E-01
			rs76061334	151182876	T/C	-19.6	1.67E-85	0.891	0.000	0.0006	9.30E-01

Supplementary Table 29: *cis*-meQTLs for mLRR-Y differentially-methylated positions, with corresponding mLRR-Y association statistics. *Z*-score reflects the direction and magnitude at which the meQTL effect allele is associated with methylation of the CpG. For mLRR-Y, Effect is change in mLRR-Y per meQTL effect allele.

Published PCa Risk Loci[A]								Lookup in mLOY (UKB)			
rsID	Chr.	Pos.	EA	AA	OR	95% CI	Gene[B]	EAF	Effect[C]	SE	p-value
rs16901979	8	128124916	A	C	1.79	(1.36âĂŞ2.34)		0.034	-0.0002	0.0010	0.830
rs1447295	8	128485038	A	C	1.62			0.103	0.0001	0.0006	0.800
rs817826	9	110156300	C	T	1.41	(1.29, 1.54)	*RAD23B-KLF4*	0.146	-0.0006	0.0005	0.260
rs10486567	7	27976563	A	G	0.74	(0.66, 0.83)	*JAZF1*	0.234	0.0002	0.0004	0.580
rs12621278	2	173311553	A	G	0.75	(0.70, 0.80)	*ITGA6*	0.937	0.0004	0.0007	0.550
rs103294	19	54797848	C	T	1.28	(1.21, 1.36)	*LILRA3*	0.774	-0.0001	0.0004	0.900
rs11649743	17	36074979	G	A	1.28	(1.07, 1.52)	*HNF1B*	0.813	-0.0002	0.0005	0.630
rs1571801	9	124427373	A	C	1.27	(1.10, 1.48)	*DAB21P*	0.269	0.0000	0.0004	0.940
rs6983267	8	128413305	G	T	1.26	(1.13, 1.41)		0.520	0.0001	0.0003	0.760
rs12653946	5	1895829	T	C	1.26	(1.20, 1.33)	*IRX4*	0.418	0.0001	0.0004	0.840
rs10993994	10	51549496	T	C	1.25	(1.17, 1.34)	*MSMB*	0.392	0.0003	0.0004	0.330
rs7127900	11	2233574	A	G	1.22	(1.17, 1.27)		0.187	-0.0002	0.0004	0.600
rs4430796	17	36098040	A	G	1.22	(1.15, 1.30)	*HNF1B*	0.519	0.0000	0.0003	0.950
rs339331	6	117210052	T	C	1.22	(1.15, 1.28)	*RFX6*	0.693	-0.0001	0.0004	0.840
rs2735839	19	51364623	G	A	0.83	(0.75, 0.91)	*KLK2/KLK3*	0.854	0.0001	0.0005	0.910
rs2055109	3	87467332	C	T	1.2	(1.13, 1.29)		0.243	-0.0001	0.0004	0.780
rs1859962	17	69108753	G	T	1.2	(1.14, 1.27)		0.465	0.0001	0.0003	0.820
rs4962416	10	126696872	C	T	1.2	(1.07, 1.34)	*CTBP2*	0.289	0.0004	0.0004	0.290
rs7931342	11	68994497	G	T	0.84	(0.79, 0.90)		0.511	-0.0004	0.0003	0.270
rs2660753	3	87110674	T	C	1.18	(1.06, 1.31)		0.096	0.0001	0.0006	0.880
rs636291	1	10556097	A	G	1.18	(1.12-1.24)	*PEX14*	0.672	-0.0003	0.0004	0.410
rs1512268	8	23526463	A	G	1.18	(1.14, 1.22)	*NKX3.1*	0.584	-0.0001	0.0004	0.790
rs9600079	13	73728139	T	G	1.18	(1.12, 1.24)		0.448	0.0001	0.0003	0.850
rs9364554	6	160833664	T	C	1.17	(1.08, 1.26)	*SLC22A3*	0.307	0.0001	0.0004	0.860
rs902774	12	53273904	A	G	1.17	(1.11, 1.24)	*KRT8*	0.144	-0.0004	0.0005	0.380
rs5759167	22	43500212	G	T	0.86	(0.83, 0.88)	*BIL/TTLL1*	0.504	-0.0003	0.0003	0.410
rs1938781	11	58915110	C	T	1.16	(1.11, 1.21)	*FAM111A*	0.210	0.0002	0.0004	0.570
rs2252004	10	122844709	G	T	1.16	(1.10, 1.22)		0.091	0.0005	0.0006	0.400
rs1983891	6	41536427	T	C	1.15	(1.09, 1.21)	*FOXP4*	0.280	0.0004	0.0004	0.350
rs13385191	2	20888265	G	A	1.15	(1.10, 1.21)	*C2orf43*	0.232	-0.0001	0.0004	0.770
rs721048	2	63131731	A	G	1.15	(1.10, 1.21)	*EHBP1*	0.198	0.0005	0.0004	0.200
rs11650494	17	47345186	A	G	1.15	(1.09, 1.22)	*SPOP,HOXB13*	0.087	0.0006	0.0006	0.310
rs10086908	8	128011937	T	C	0.87	(0.81, 0.94)		0.704	0.0003	0.0004	0.500
rs2242652	5	1280028	G	A	0.87	(0.84, 0.90)	*TERT*	0.805	0.0000	0.0004	0.990
rs2292884	2	238443226	G	A	1.14	(1.09, 1.19)	*MLPH*	0.254	0.0004	0.0004	0.320
rs76934034	10	46082985	T	C	1.14	(1.10, 1.18)	*MARCH8*	0.906	0.0003	0.0006	0.590
rs80130819	12	48419618	A	C	1.13	(1.08, 1.17)	*RP1-228P16.4*	0.920	-0.0018	0.0006	0.004
rs12480328	20	49527922	T	C	1.13	(1.08, 1.17)	*ADNP*	0.927	-0.0004	0.0007	0.580
rs8008270	14	53372330	G	A	0.89	(0.86, 0.93)	*FERMT2*	0.816	0.0001	0.0004	0.820
rs6062509	20	62362563	A	C	0.89	(0.66, 0.92)	*ZGPAT*	0.673	0.0000	0.0004	0.960
rs1933488	6	153441079	A	G	0.89	(0.87, 0.92)	*RSG17*	0.597	-0.0004	0.0004	0.320
rs11672691	19	41985587	A	G	1.12	(1.03, 1.21)		0.251	-0.0003	0.0004	0.440
rs6465657	7	97816327	C	T	1.12	(1.05, 1.20)	*LMTK2*	0.465	-0.0002	0.0003	0.550
rs8102476	19	38735613	C	T	1.12	(1.08, 1.15)		0.535	0.0005	0.0003	0.150
rs10934853	3	128038373	A	C	1.12	(1.08, 1.16)	*EEFSEC*	0.269	-0.0002	0.0004	0.690
rs3771570	2	242382864	A	G	1.12	(1.08, 1.17)	*FARP2*	0.163	-0.0001	0.0005	0.870
rs10936632	3	170130102	A	C	0.9	(0.88, 0.93)	*CLDN11/SKIL*	0.521	0.0008	0.0003	0.027
rs620861	8	128335673	C	T	0.9	(0.84, 0.96)		0.365	-0.0006	0.0004	0.120
rs17021918	4	95562877	C	T	0.9	(0.87, 0.93)	*PDLIM5*	0.652	-0.0005	0.0004	0.150
rs12155172	7	20994491	A	G	1.11	(1.07, 1.15)	*SP8*	0.220	0.0001	0.0004	0.880
rs11135910	8	25892142	A	G	1.11	(1.07, 1.16)	*EBF2*	0.170	-0.0006	0.0005	0.160
rs684232	17	618965	G	A	1.1	(1.07, 1.14)	*VPS53,FAM57A*	0.356	0.0004	0.0004	0.260
rs17599629	1	150658287	G	A	1.1	(1.07, 1.13)	*GOLPH3L*	0.235	-0.0008	0.0004	0.038
rs17694493	9	22041998	G	C	1.1	(1.06, 1.13)	*CDKN2B-AS1*	0.136	-0.0004	0.0005	0.390
rs4245739	1	204518842	A	C	0.91	(0.88, 0.95)	*MDM4,PIK3C2B*	0.723	-0.0005	0.0004	0.230
rs1894292	4	74349158	G	A	0.91	(0.89, 0.94)	*AFM,RASSF6*	0.512	0.0002	0.0003	0.630
rs11568818	11	102401661	A	G	0.91	(0.88, 0.94)	*MMP7*	0.454	0.0001	0.0003	0.800
rs7611694	3	113275624	A	C	0.91	(0.88, 0.93)	*SIDT1*	0.597	-0.0008	0.0004	0.018
rs7679673	4	106061534	C	A	0.91	(0.88, 0.94)	*TET2*	0.629	0.0007	0.0004	0.063
rs3850699	10	104414221	A	G	0.91	(0.89, 0.94)	*TRIM8*	0.711	-0.0001	0.0004	0.830
rs7153648	14	61122526	C	G	1.09	(1.04, 1.13)	*SIX1*	0.087	0.0001	0.0006	0.910
rs7141529	14	69126744	G	A	1.09	(1.06, 1.12)	*RAD51L1*	0.503	0.0002	0.0003	0.590

Supplementary Table 30: Effect of published autosomal risk loci for prostate cancer on mLOY. Part 1 of 2, continued overleaf. [A] Source detailed in main chapter. [B] Nearest gene. [C] Change in mLRR-Y per additional prostate cancer EA (risk-increasing). PCa, prostate cancer excluding benign prostate hyperplasia. Six PCa risk loci falling on the X-chromosome, and three autosomal variants with unacceptable imputation quality, are omitted from this look-up.

Published PCa Risk Loci								Lookup in mLOY (UKB)			
rsID	Chr.	Pos.	EA	AA	OR	95% CI	Gene[B]	EAF	Effect[C]	SE	p-value
rs10009409	4	73855253	T	C	1.09	(1.06, 1.12)	*COX18*	0.289	-0.0002	0.0004	0.680
rs2238776	22	19757892	G	A	1.09	(1.06, 1.12)	*TBX1*	0.801	0.0000	0.0004	0.970
rs10187424	2	85794297	A	G	0.92	(0.89, 0.94)	*GGCX/VAMP8*	0.428	-0.0006	0.0003	0.066
rs7241993	18	76773973	G	A	0.92	(0.89, 0.95)	*SALL3*	0.306	0.0005	0.0004	0.160
rs1465618	2	43553949	A	G	1.08	(1.03, 1.12)	*THADA*	0.792	0.0004	0.0004	0.380
rs12543663	8	127924659	C	A	1.08	(1.00, 1.16)		0.314	0.0001	0.0004	0.860
rs12500426	4	95514609	A	C	1.08	(1.05, 1.12)	*PDLIM5*	0.445	-0.0006	0.0003	0.061
rs11214775	11	113807181	G	A	1.08	(1.05, 1.11)	*HTR3B*	0.720	-0.0015	0.0004	0.000
rs3096702	6	32192331	A	G	1.07	(1.04, 1.10)	*NOTCH4*	0.401	-0.0008	0.0004	0.026
rs9287719	2	10710730	C	T	1.07	(1.04, 1.09)	*NOL10*	0.478	-0.0001	0.0003	0.680
rs1270884	12	114685571	A	G	1.07	(1.04, 1.10)	*TBX5*	0.483	-0.0003	0.0003	0.430
rs4713266	6	11219030	C	T	1.07	(1.04, 1.09)	*NEDD9*	0.514	-0.0004	0.0003	0.200
rs56232506	7	47437244	A	G	1.07	(1.05, 1.09)	*TNS3*	0.465	-0.0003	0.0003	0.320
rs8014671	14	71092256	G	A	1.07	(1.05, 1.10)	*TTC9*	0.596	-0.0002	0.0004	0.650
rs11902236	2	10117868	A	G	1.07	(1.03, 1.10)	*TAF1B:GRHL1*	0.278	0.0007	0.0004	0.068
rs10875943	12	49676010	C	T	1.07	(1.04, 1.10)	*TUBA1C/PRPH*	0.275	-0.0005	0.0004	0.170
rs6869841	5	172939426	A	G	1.07	(1.04, 1.11)	*FAM44B*	0.211	-0.0002	0.0004	0.700
rs2273669	6	109285189	G	A	1.07	(1.03, 1.11)	*ARMC2,SESN1*	0.145	-0.0003	0.0005	0.500
rs9443189	6	76495882	G	A	1.07	(1.04, 1.11)	*MYO6*	0.145	0.0003	0.0005	0.600
rs2427345	20	61015611	G	A	0.94	(0.91, 0.97)	*GATAS,CABLES2*	0.373	0.0003	0.0004	0.410
rs1775148	1	205757824	C	T	1.06	(1.03, 1.08)	*SLC41A1*	0.363	-0.0001	0.0004	0.710
rs1218582	1	154834183	G	A	1.06	(1.03, 1.09)	*KCNN3*	0.441	0.0009	0.0004	0.012
rs1041449	21	42901421	G	A	1.06	(1.04, 1.09)	*TMPRSS2*	0.446	-0.0002	0.0004	0.620
rs12051443	16	71691329	A	G	1.06	(1.03, 1.08)	*PHLPP2*	0.362	-0.0005	0.0004	0.160
rs2121875	5	44365545	G	T	1.05	(1.02, 1.08)	*FGF10*	0.673	-0.0005	0.0004	0.210
rs2928679	8	23438975	T	C	1.05	(1.01, 1.09)	*SLC25A37*	0.528	-0.0001	0.0003	0.880
rs130067	6	31118511	G	T	1.05	(1.02, 1.09)	*CCHCR1*	0.197	0.0005	0.0004	0.220
rs6763931	3	141102833	T	C	1.04	(1.01, 1.07)	*ZBTB38*	0.443	-0.0003	0.0003	0.340

Supplementary Table 30: Effect of published autosomal risk loci for prostate cancer on mLOY, Continued. Part 2 of 2

mLOY SNPs						All-Cancer			excl. Skin		
rsID	EA	AA	EAF	Effect	p-value	log(OR)	SE	p-value	log(OR)	SE	p-value
rs1122138	C	A	0.84	-0.005	3.6E-23	0.0026	0.0018	1.40E-01	0.0021	0.0016	1.90E-01
rs17758695	C	T	0.97	-0.01	6.4E-21	-0.0023	0.0037	5.40E-01	-0.0030	0.0034	3.80E-01
rs59633341	D	I	0.16	-0.004	2.6E-18	0.0026	0.0017	1.30E-01	0.0025	0.0016	1.20E-01
rs78378222	T	G	0.99	-0.013	1.3E-15	-0.0267	0.0060	7.50E-06	-0.0166	0.0055	2.60E-03
rs2736609	C	T	0.64	-0.003	1.9E-12	-0.0020	0.0013	1.30E-01	-0.0029	0.0012	1.80E-02
rs13191948	C	T	0.54	-0.002	1.2E-11	0.0013	0.0013	3.20E-01	0.0009	0.0012	4.50E-01
rs35091702	I	D	0.26	-0.002	4.2E-10	0.0004	0.0015	7.70E-01	0.0009	0.0013	4.90E-01
rs4721217	C	T	0.60	-0.002	6.5E-10	-0.0040	0.0013	2.10E-03	-0.0030	0.0012	1.20E-02
rs137952017	D	I	0.85	-0.003	1.2E-09	0.0004	0.0018	8.30E-01	-0.0004	0.0017	8.20E-01
rs56084922	A	G	0.92	-0.005	2.9E-13	0.0020	0.0024	3.90E-01	0.0028	0.0022	2.00E-01
rs60084722	I	D	0.79	-0.003	6.6E-13	-0.0013	0.0016	4.40E-01	-0.0018	0.0015	2.40E-01
rs381500	C	A	0.55	-0.002	5.7E-11	0.0016	0.0013	2.00E-01	0.0008	0.0012	4.80E-01
rs12448368	T	C	0.87	-0.003	9.8E-10	-0.0043	0.0019	2.40E-02	-0.0040	0.0017	2.20E-02
rs4754301	G	A	0.45	-0.002	1.3E-09	-0.0003	0.0013	8.30E-01	-0.0002	0.0012	8.60E-01
rs77522818	A	T	0.96	-0.005	1.3E-09	-0.0008	0.0032	8.00E-01	-0.0015	0.0029	6.10E-01
rs11082396	T	C	0.87	-0.003	3.3E-09	-0.0011	0.0019	5.60E-01	-0.0008	0.0017	6.40E-01
rs13088318	A	G	0.66	-0.002	4.1E-09	-0.0011	0.0013	4.00E-01	-0.0009	0.0012	4.60E-01
rs10687116	D	I	0.20	-0.002	2.6E-08	-0.0001	0.0016	9.60E-01	0.0006	0.0015	6.80E-01
rs115854006	C	T	0.96	-0.006	3.7E-08	0.0009	0.0037	8.00E-01	0.0005	0.0034	8.80E-01

Supplementary Table 31: Association of the 19 mLOY variants with cancer registrations in UKB. Effect is change in mLRR-Y per effect allele. log(OR), odds of having received a registration for cancer vs. control status. For brevity, alleles at insertion-deletion variants have been coded as I/D; the original alleles are detailed in the main chapter

			IVW Estimator			MR-Egger					Weighted Median			Penalised Weighted Median		
Exposure	n_{VAR}	Outcome	Effect	SE	p	$p_{Intercept}$	Effect	SE	p	p_{Het}	Effect	SE	p	Effect	SE	p
T2D	29	mLOY	0.000	0.001	0.921	0.300	0.001	0.001	0.380	1	0.000	0.001	0.768	0.000	0.001	0.774
mLOY	15	T2D	-0.366	1.386	0.792	0.164	-4.964	3.572	0.165	5.39E-18	-0.525	1.723	0.761	-0.526	1.794	0.769
FI	17	mLOY	0.010	0.006	0.105	0.440	-0.010	0.026	0.713	1	0.008	0.008	0.363	0.007	0.008	0.377
mLOY	15	FI	-0.083	0.364	0.821	0.057	-2.121	1.274	0.096	3.20E-01	0.075	0.524	0.885	0.484	0.532	0.363
HbA1c	11	mLOY	-0.001	0.004	0.755	0.138	-0.013	0.009	0.139	1	-0.002	0.005	0.645	-0.002	0.005	0.625
mLOY	15	HbA1c	-0.822	0.576	0.153	0.890	-0.540	2.131	0.800	4.18E-05	-0.901	0.576	0.118	-0.816	0.548	0.137
FG	29	mLOY	-0.002	0.003	0.453	0.490	0.001	0.005	0.872	1	-0.001	0.004	0.837	-0.001	0.004	0.893
mLOY	15	FG	-0.061	0.359	0.865	0.838	-0.303	1.259	0.810	3.37E-03	-0.463	0.488	0.342	-0.492	0.489	0.314
BMI	96	mLOY	0.000	0.002	0.923	0.594	-0.002	0.004	0.655	1	-0.002	0.002	0.526	-0.002	0.002	0.515
mLOY	15	BMI	-1.154	0.483	0.017	0.606	-0.300	1.728	0.862	4.62E-03	-1.179	0.604	0.051	-1.288	0.608	0.034

Supplementary Table 32: Bidirectional Mendelian randomisation between mLRR-Y and selected cardiometabolic phenotypes. mLRR-Y instrument (15 biallelic variants, weights from combined discovery plus replication) is aligned to mLRR-Y decreasing alleles (i.e., greater mLOY). Otherwise, effects are expressed as change in outcome per unit increase in exposure; Body mass index (BMI) is quantified in kg/m^2, fasting insulin (FI) in lm(pmol/L), fasting glucose (FG) in mmol/L, and glycated haemoglobin (HbA1c) in % haemoglobin. n_{VAR} denotes number of variants used in the instrument; p_{Het}, p-value of *Q*-statistic for heterogeneity applied to IVW estimator; $p_{Intercept}$, p-value of intercept from MR-Egger

Supplementary Notes

Hand Grip Strength: Stage II & Additional Cohorts

CHARGE Consortium

Fourteen cohorts contributed to the CHARGE grip strength GWAS:

AGES-Reykjavik The AGES-Reykjavik Study is a population-based study of older individuals from the 40-year long Reykjavik Study. Participants were aged between 66 and 96 years and were randomly recruited between 2002 and 2006 from surviving Reykjavik Study members[3]. Informed consent was obtained from all participants. Details of the investigations and local institutional review board approvals are described in the study's baseline article[3].

Cardiovascular Health Study The CHS is a population-based cohort study of risk factors for CHD and stroke in adults $\geq$65 years conducted across four field centers[4]. The original predominantly Caucasian cohort of 5,201 persons was recruited in 1989-1990 from random samples of the Medicare eligibility lists; subsequently, an additional predominantly African-American cohort of 687 persons was enrolled for a total sample of 5,888. DNA was extracted from blood samples drawn on all participants at their baseline examination in 1989-90. In 2007-2008, genotyping was performed at the General Clinical Research Center's Phenotyping/Genotyping Laboratory at Cedars-Sinai using the Illumina 370CNV BeadChip system on 3980 CHS participants who were free of CVD at baseline, consented to genetic testing, and had DNA available for genotyping.

Framingham Heart Study The Framingham Heart Study (FHS) was initiated in 1948 to study determinants of cardiovascular disease and other major illnesses. The original cohort included 5,209 men and women, aged 28-62 years at enrollment who have undergone routine biennial examinations[5]. In 1971, Offspring of the original cohort participants and Offspring spouses including 5,124 men and women, aged 5 to 70 years, were enrolled into the Framingham Offspring Study. Offspring participants have been examined approximately every 4 years. In the 1990s, DNA was obtained for genetic studies from surviving original cohort and Offspring participants. All participants provided informed consent for all assessments through the Boston University Medical Center IRB.

Health ABC Between March 1997 and July 1998, 3,075 black and white men and women aged 70 to 80 were recruited to participate in the Health, Ageing and Body Composition (Health ABC) Study; characteristics of the cohort have been described elsewhere[6]. Medicare beneficiary listings were used to recruit in metropolitan areas surrounding Pittsburgh, Pennsylvania, and Memphis, Tennessee. Eligibility criteria included having no difficulty walking one-quarter of a mile, climbing 10 steps, or performing activities of daily living (transferring, bathing, dressing, and eating); no history of active treatment for cancer in the prior 3 years; and no plans to move from the area within 3 years.

Health & Retirement Study The Health and Retirement Study (HRS) is a longitudinal survey of a representative sample of Americans over the age of 50. The current sample is over 26,000 persons in 17,000 households. The study interviews respondents every two years about income and wealth, health and use of health services, work and retirement, and family connections[7]. DNA was extracted from saliva collected during a face-to-face interview in the respondents' homes. These data represent respondents who provided DNA samples and signed consent forms in 2006 and 2008.

InCHIANTI The study participants consisted of men and women, aged 65 and older, who participated in the *Invecchiare in Chianti (Aging in the Chianti Area, InCHIANTI)* study, conducted in two small towns in Tuscany, Italy. The rationale, design, and data collection have been described elsewhere, and the main

outcome of this longitudinal study is mobility disability[8]. Briefly, in August 1998, 1270 people aged 65 years and older were randomly selected from the population registry of Greve in Chianti (pop. 11,709) and Bagno a Ripoli (pop. 4,704), and of 1,256 eligible subjects, 1,155 (90.1%) agreed to participate. Participants received an extensive description of the study and participated after written, informed consent. The study protocol complied with the Declaration of Helsinki and was approved by the Italian National Institute of Research and Care on Aging Ethical Committee and by the Institutional Review Board of the Johns Hopkins University School of Medicine.

Lothian Birth Cohorts The Lothian Birth Cohort 1921 (LBC1921) cohort consists of 550 relatively healthy individuals, 316 females and 234 males, assessed on cognitive and medical traits at 79 years of age. They were born in 1921, most took part in the Scottish Mental Survey of 1932, and almost all lived independently in the Lothian region (Edinburgh City and surrounding area) in Scotland. When tested, the sample had a mean age of 79.1 years (SD = 0.6). A full description of participant recruitment and testing can be found elsewhere[9]. Ethics permission for the study was obtained from the Lothian Research Ethics Committee (LREC/1998/4/183). The research was carried out in compliance with the Helsinki Declaration. All subjects gave written, informed consent.

The Lothian Birth Cohort 1936 (LBC1936) consists of 1,091 relatively healthy individuals assessed on cognitive and medical traits at 70 years of age. They were born in 1936, most took part in the Scottish Mental Survey of 1947, and almost all lived independently in the Lothian region of Scotland. The sample of 548 men and 543 women had a mean age 69.6 years (SD = 0.8). A full description of participant recruitment and testing can be found elsewhere[10]. Ethics permission for the study was obtained from the Multi-Centre Research Ethics Committee for Scotland (MREC/01/0/56) and from Lothian Research Ethics Committee (LBC1936: LREC/2003/2/29). The research was carried out in compliance with the Helsinki Declaration. All subjects gave written, informed consent.

Sydney Memory and Aging Project The Memory and Aging Project (MAP) is a longitudinal clinical-pathologic cohort study of aging. The study enrolls older adults without known dementia who agree to an annual assessment of risk factors, blood donation and a structured clinical evaluation[11]. All participants sign an Anatomical Gift Act and agree to the donation of brain, the entire spinal cord and selected nerve and muscles at the time of death. Study participants are primarily recruited from retirement communities throughout northeastern Illinois. Since October 1997, about 1,650 participants have completed their baseline evaluation. The follow-up rate of survivors exceeds 90%, and the autopsy rate exceeds 80%.

Religious Orders Study The Religious Order Study (ROS) is a longitudinal clinical-pathologic cohort study of aging. The study enrolls older adults without known dementia who agree to an annual assessment of risk factors, blood donation and a detailed evaluation[12]. All participants sign an Anatomical Gift Act and agree to donation of brain at the time of death. Study participants are primarily Catholic priests, nuns and brothers from about 40 groups in 12 states. Since January 1994, over 1,100 participants completed their baseline evaluation. Both the follow-up rate among survivors and the autopsy rate exceed 90

Osteoporotic Fractures in Men Study The Osteoporotic Fractures in Men Study (MrOS) is a multicenter prospective, longitudinal, observational study of risk factors for vertebral and all non-vertebral fractures in older men, and of the sequelae of fractures in men[13,14]. The original specific aims of the study include: (1) to define the skeletal determinants of fracture risk in older men, (2) to define lifestyle and medical factors related to fracture risk, (3) to establish the contribution of fall frequency to fracture risk in older men, (4) to determine to what extent androgen and oestrogen concentrations influence fracture risk, (5) to examine the effects of fractures on quality of life, (6) to identify sex differences in the predictors and outcomes of fracture, (7) to collect and store serum, urine and DNA for future analyses as directed by emerging evidence in the fields of aging and skeletal health, and (8) define the extent to which bone

mass/fracture risk and prostate diseases are linked. From March 2000 to April 2002, 5994 community dwelling ambulatory men aged 65 years or older were recruited from six communities in the United States (Birmingham, AL; Minneapolis, MN; Palo Alto, CA; Monongahela Valley near Pittsburgh, PA; Portland, OR; and San Diego, CA). Inclusion criteria were designed to provide a study cohort that is representative of the broad population of older men. The MrOS inclusion criteria were: (1) ability to walk without the assistance of another, (2) absence of bilateral hip replacements, (3) ability to provide self-reported data, (4) residence near a clinical site for the duration of the study, (5) absence of a medical condition that (in the judgment of the investigator) would result in imminent death, (6) ability to understand and sign an informed consent, and (7) 65 years or older. To qualify as an enrollee, the participant had to provide written informed consent, complete the self-administered questionnaire (SAQ), attend the clinic visit, and complete at least the anthropometric, DEXA, and vertebral X-ray procedures. The institutional review board at each center approved the study protocol, and written informed consent was obtained from all the participants.

Study of Health in Pomerania The Study of Health in Pomerania (SHIP) is a population based in West Pomerania, the north-east area of Germany[15,16]. A sample from the population aged 20 to 79 years was drawn from population registries. First, the three cities of the region (with 17,076 to 65,977 inhabitants) and the 12 towns (with 1,516 to 3,044 inhabitants) were selected, and then 17 out of 97 smaller towns (with less than 1,500 inhabitants), were drawn at random. Second, from each of the selected communities, subjects were drawn at random, proportional to the population size of each community and stratified by age and gender. Only individuals with German citizenship and main residency in the study area were included. Finally, 7,008 subjects were sampled, with 292 persons of each gender in each of the twelve five-year age strata. In order to minimize drop-outs by migration or death, subjects were selected in two waves. The net sample (without migrated or deceased persons) comprised 6,267 eligible subjects. Selected persons received a maximum of three written invitations. In case of non-response, letters were followed by a phone call or by home visits if contact by phone was not possible. The SHIP population finally comprised 4,308 participants (corresponding to a final response of 68.7%). This study includes data of 320 individuals with complete GWAS data who participated in the 10-year follow-up examinations (SHIP-2).

Study of Osteoporotic Fractures The Study of Osteoporotic Fractures (SOF) is a prospective multicenter study of risk factors for vertebral and non-vertebral fractures[17]. From 1986 to 1987, 9704 community dwelling women aged 65 years or older were recruited from population-based listings in four U.S. areas: Baltimore, Maryland; Minneapolis, Minnesota; Portland, Oregon; and the Monongahela Valley, Pennsylvania. The SOF participants were followed up every four months by postcard or telephone to ascertain the occurrence of falls, fractures and changes in address. The SOF inclusion criteria were: 1) 65 years or older, (2) ability to walk without the assistance of another, (3) absence of bilateral hip replacements, (4) ability to provide self-reported data, (5) residence near a clinical site for the duration of the study, (6) absence of a medical condition that (in the judgment of the investigator) would result in imminent death, and (7) ability to understand and sign an informed consent. To qualify as an enrollee, the participant had to provide written informed consent, complete the self-administered questionnaire (SAQ), attend the clinic visit, and complete at least the anthropometric measures. The institutional review board at each center approved the study protocol, and written informed consent was obtained from all the participants.

Tasmanian Study of Cognition & Gait TASCOG is a study of cerebrovascular mechanisms underlying gait, balance and cognition in a population-based sample of Tasmanian people aged at least 60 years[18]. Individuals aged 60âĂŞ86 years (n = 395) living in Southern Tasmania, Australia, were randomly selected from the electoral roll between 2006 and 2008 to participate in the study. Individuals were excluded if they lived in a nursing home, had a contraindication for magnetic resonance scanning (MRI) or were unable to walk without a gait aid. Participants underwent brain MRI scans and genotyping. DNA was extracted from peripheral blood samples by proteinase K digestion following cell lysis, then phenol-chloroform purifica-

tion. DNA was genotyped using Illumina Hap370CNV chips at the University of Queensland Diamantina Institute, Princess Alexandra Hospital, Brisbane, Australia, for 370 participants, and call rates were greater than 97% for all samples. Genotypes for 22 individuals were excluded, either because they were closely related to other individuals, they were outliers in a population ancestry analysis or their sex predicted from genotypes did not match sex as recorded in the database. Among the 348 remaining participants with available genome-wide data, after exclusion of 2 participants with dementia, 3 with posterior circulation infarcts on MRI and 3 with insufficient MRI image quality, 340 individuals were available for the present analysis on hippocampal volume.

TwinsUK The TwinsUK registry now consists of about 12,000 monozygotic (MZ) and dizygotic (DZ) twins aged 18 to 103 years. About 83% of the registry is female (mean age of 55 years). The registry now contains 51% MZ and 49% DZ twins. Between 1992 and 2004, twins were invited for a full comprehensive visit and several project-led studies. More than 7,000 twins responded to some of the annual questionnaires and 5,725 attended a comprehensive visit. Apart from a lifelong lower weight in MZ twins of around 1 kg, all other age-matched characteristics of these volunteer twins were found not to differ from a singleton population-based cohort of British women[19]. Between April 2004 and May 2007, all the 6,740 active twins on the registry were invited for a 1-day clinical visit, of whom 3,725 twins attended and 1,299 twins posted their blood DNA samples via their general practitioners. The age of participants ranged between 18 and 82 years (mean 52.5 Âś 13 years) and 3,299 of the clinic attendants (89%) were female.

Further Stage II Samples

Erasmus Rucphen Family Study The Erasmus Rucphen Family genetic isolate study (ERF) is a prospective family based study located in the southwestern Netherlands[20]. This young genetic isolate was founded in the midâĂŘeighteenth century and minimal immigration and marriages occurred between surrounding settlements due to social and religious reasons. The ERF population includes 3,465 individuals that are living descendants of 22 couples with at least six children baptized. The study protocol was approved by the medical ethics board of the Erasmus MC Rotterdam, the Netherlands. The baseline demographic data and measurements of the ERF participants were collected around 2002 to 2006. All the participants filled out questionnaires on socio-demographics, disease and medical history and lifestyle factors, and were invited to the research center for an interview and blood collection for biochemistry and physical examinations. In the main follow-up of the study by May, 2016 (follow up from 9 to 14 years), 1,940 baseline participants' records were scanned in the general practitionerâĂŹs database.

Health 2006 and 2008 Cohorts The Health2006 study is a general population-based study (started in 2006) designed to investigate lifestyle-related chronic diseases such as coronary heart disease, diabetes, musculoskeletal disorders, asthma, allergy, chronic lung diseases and mental disorders in men and women aged 18 to 69 years. The Health2008 study (started in 2008) is an extension of the Health2006 study using essentially similar collection methods, investigating men and women aged 30 to 60 years, living in the same municipalities as participants from Health2006. A random sample of potential volunteers was obtained from the Danish Civil Registration system. All participants were Danish adults living in 11 municipalities in the south-western part of the greater Copenhagen area, Denmark. Pregnant women were excluded. All participants had measurements done at the Research Centre for Prevention and Health at the Copenhagen University Hospital in Glostrup. Participants were asked to be fasting at the day of examination for a detailed clinical examination when blood samples were collected. Written informed consent was obtained from all participants and the study was approved by the Ethical Committee of Copenhagen County and the Danish Data Protection Agency. The study is registered at www.clinical.trials.com.

Hunter Community Study The HCS[21] is a population-based study comprised of middle-aged to older adults aged 55-85 years from Newcastle, Australia. Voting registration in Australia is compulsory and participants were recruited randomly from the electoral roll. Potential participants were excluded if they could not speak English and/or if they lived in an aged-care facility. The final sample included 3207 participants. Ethics approval was obtained from the Hunter New England Local Health District and University of Newcastle Human Research Ethics Committees and written informed consent was obtained from all participants. Comprehensive data was collected including samples for genetic analyses.

Sydney Memory & Ageing Study The Sydney MAS[22] is a longitudinal population-based study, which recruited community-dwelling adults aged 70-90 years at baseline from Sydney. In Australia voting registration is compulsory and participants were recruited randomly from the electoral roll. Exclusion criteria included a diagnosis of dementia, schizophrenia or bipolar disorder and medical or psychological conditions that would prevent them from completing assessments. The final sample was comprised of 1,037 participants at baseline. Ethics approval for Sydney MAS was granted by the Human Research Ethics Committees of the University of New South Wales and the South Eastern Sydney and Illawarra Area Health Service. Written informed consent was provided by all participants. A wide range of data was collected including samples donated for genetic analyses.

TwinsUK Additional Samples In addition to the TUK sample contained within CHARGE, Twins UK contributed 3009 additional genotyped grip strength samples that were not included in the pre-existing CHARGE GWAS discussed above. The TwinsUK cohort (www.twinsuk.ac.uk) is an adult twin British registry shown to be representative of singleton populations and the United Kingdom population[19]. The mean age of the 3009 individuals was 52.5 (Âś10.9) years. Ethical approval was obtained from the GuyâĂŹs and St. ThomasâĂŹ Hospital Ethics Committee. Written informed consent was obtained from every participant to the study.

Athlete case-control studies

European Athletes The European Athlete study consists of white European sprint and power athletes (n=395) and approximately geographically-matched white European controls (n=726). Participant DNA was whole genome amplified and normalised before SNP-based genotyping at each of the sixteen grip strength SNPs identified in combined analyses (Sequenom). Genotyping was conducted at the Australian Genome Research Facility (AGRF). 12 SNPs passed quality control (HWE pâL'ě0.05) and genotype associations between cases and controls were assessed using conditional logistic regression with country as a covariate (conducted in R). All participants supplied written informed consent, which was approved by each respective cohortâĂŹs institution. This includes approval by the institutional review boards of the the ChildrenâĂŹs Hospital at Westmead (2003/086), The Royal ChildrenâĂŹs Hospital Human Research Ethics Committee (35172), the Pomeranian Medical University Ethics Committee, Universidad Pablo Olavide, The Lithuanian National Committee of Biomedical Ethics, Aristotle University of Thessaloniki Research Committee, The Ethics Committee of the University of Cagliari, Ghent University Hospital, Belgium and the Nottingham Trent University Ethical Review Committee.

Japanese Athletes The Japanese cohort is comprised of 54 international sprint/power track and field athletes and 406 geographically matched controls. Total DNA was isolated from venous blood and saliva by QIAamp DNA Blood Maxi Kit (QIAGEN, Hilden, Germany) and OrageneÂůDNA (DNA genotek, Ontario, Canada), respectively. DNA Samples from all subjects were genotyped on the HumanOmniExpress BeadChip (Illumina). Ten of the sixteen replicated SNVs associated with grip strength in the present study were available in this Japanese population either directly or by proxy (r2âL'ě0.8). Genotyping quality of each polymorphism was checked by visually in GenomeStudio (Illumina). This study is part of the Japanese Human Athlome Project, focusing on the study of genes associated with physical performance

and its related phenotypes[23]. Written consent was obtained from each subject, and the study was approved by the Ethics Committees of Juntendo University, the Japanese National Institute of Health and Nutrition and the Japan Institute of Sports Sciences.

Jamaican and US Athletes This cohort is comprised of high-level black athletes (n=167) and geographically matched controls (n=478). Samples were genotyped using the HumanOmniExpress or Omni1-Quad BeadChips (Illumina). Standard GWAS quality control was applied to the genotype data. Genetic associations were evaluated by logistic regression with adjustment for population structure. Genotype imputation with IMPUTE2 using the 1000G phase 3 reference panels was then conducted to increase power of GWA scans. This investigation aims to understand the influence of common genetic variants on performance through the use of athletic populations enriched with high-level competitors. All participants supplied written informed consent, which was approved by the UHWI/UWI/FMS Ethics Committee, University of West Indies, Jamaica and participating institutions in the United States.

Genetic Factors for Osteoporosis (GEFOS) Consortium

The GEFOS consortium is an international collaboration of investigators dedicated to identify the genetic determinants of osteoporosis (http://www.gefos.org/). The original any-type of fracture GWAS meta-analysis comprised 24 GWA studies (20,439 cases, 78,843 controls) from populations across North America, Europe, East Asia and Australia, with a variety of epidemiological designs and patient characteristics. Cases were individuals (>18 years) with fractures confirmed by medical, radiological or questionnaire reports. When possible, fractures of the fingers, toes and skull were excluded from analyses. GWAS genotyping was done by each study following standard manufacturer protocols followed by imputation to 2.5 million SNPs from HapMap Phase II.

Muscle Histology

The muscle histology study was performed on 656 men from three independent cohorts of Swedish ancestry. These cohorts included Uppsala Longitudinal Study of Adult Men (ULSAM, n=482)[24], Malmö Men (MM, n=128)[25] and Malmö Exercise Intervention (MEI, n=46)[26]. The ULSAM cohort included non-diabetic males of age 71.0 Âś 0.64 years and body-mass index (BMI) 26.3 Âś 3.4 kg/m2. The MM cohort consists of non-obese males aged 65.9 Âś 2.0 years and with BMI 26.4 Âś 3.4 kg/m2, including 50 individuals with diagnosed Type II diabetes (T2D). The MEI cohort consists of male subjects aged 37.7 Âś 4.3 years, VO2MAX 32.0 Âś 5.0 ml/kg/min and BMI 28.0 Âś 3.1kg/m2 with (n=22) and without (n=24) a first degree family member with T2D. The primary phenotypes included in the GWA-analysis were percentage of (i) type I, (ii) type IIa, and (iii) Type IIx fibres, as well as capillary density, calculated as number of capillaries divided by total number of fibres. Phenotypes were inverse-normalised for analysis. Genotype data in each cohort were imputed up to 35 million variants from the 1000 Genomes âĂIJall ancestriesâĂİ reference panel (March 2012). Prephasing of haplotypes and imputation were performed using ShapeIT and IMPUTE2, respectively. The association within each cohort was performed using SNPTEST frequentist score additive model test.

Appendix 1

REEGen Consortium Analysis Plan

Resting Energy Expenditure GWAS Analysis Plan (1000G Imputed)

Version 2.1, distributed 9th March 2016.

Prepared by the Resting Energy Expenditure Genetics Consortium (REE-Gen).
Please contact Dan Wright (dan.wright@mrc-epid.cam.ac.uk) with any questions.

---

1 Genotyping & Imputation

We request that all studies are imputed to 1000G, Phase III. If your study is imputed to a different reference panel, please let us know. We can meta-analyse results using different imputation strategies, including HapMap.

We presume that pre-imputation sample QC was performed to account for call rate, heterozygosity, relatedness (unless participants are related by study design) and outlying ethnic ancestry. If you have questions, would like to discuss imputation quality control thresholds, or an imputation protocol is required, please get in touch.

2 Association Analyses

GWAS of REE will be conducted using z-score standardised residual REE (after adjustment for covariates) as the outcome. Follow the steps detailed in **2.1** to **2.3** to generate the residuals and conduct the analyses. Please bear in mind the following points:

Derivation of REE The trait of interest is total daily REE (kJ / 24hr). For consistency, this should have been generated *via* the abbreviated Weir Equation using VO_2 and VCO_2 from steady-state resting calorimetry in thermoneutral, fasted participants. If an alternative derivation equation has been used, please recalculate the REE using the Weir approach if possible:

REE (kJ / 24hr) = 4.184 (1.44 (3.9 VO_2 + 1.1 VCO_2))

Note that VO_2 and VCO_2 in this equation are **mL/min,** not **mL/min/kg**

The original abbreviated Weir equation (shaded green) calculates the REE in kcal / 24hr. An adjustment factor has been included in the above formula to convert this kcal result to kJ, based on 1 kcal = 4.184 kJ. Please double-check that your REE phenotype is expressed as kJ / 24hr, not kcal. Contact us with any questions.

Population Stratification In the Fenland Study, we have conducted initial genome-wide analyses using BOLT-LMM, which implements GWAS using linear mixed models. LMM have the particular benefit of not being liable to sub-ethnic population stratification when applied to a population of known continental ancestry (e.g. white Europeans), precluding the need to include genomic PCs as indicators of underlying structure. The method also confers power benefits in large population-based studies. If convenient, please consider using this tool (available from http://www.hsph.harvard.edu/po-ru-loh/software/). Dan will be happy to discuss and share scripts. If using linear regression-based software for the association analyses (e.g. SNPTest), please adjust for underlying population structure using your standard approach (e.g. genomic PCs, the number of which can be defined by each study).

Known Relatedness Some of the contributing cohorts use family-based recruitment. In these cases, please take any usual steps to account for relatedness within the sample (whilst maximising sample size for REE). This will usually involve conditioning the analyses on a kinship matrix. Note that BOLT-LMM can also help here .

Indels, CNVs and Multiallelic SNPs If available in your genotyping data, please retain all such variants for analysis alongside biallelic SNPs. Depending on naming, we may be able to standardise these centrally and retain for meta-analysis.

In All Models: Assume additive genetic effect. Please do not impute missing phenotypes or omit true outliers (i.e. those which correspond to a real observation). Do not apply genomic correction to results, nor filter results based on imputation quality; we can do so centrally.

Standard Covariates: All models should be adjusted for age at calorimetry (years) and biological sex. Age squared can also be included as a covariate if this is usual for your study, explains additional variance, or a non-linear age-REE association is expected. Depending on your study design, adjust for study-specific covariates as required; e.g. for study site if a multi-centre study, or device ID if calorimetry was measured using different devices for different participants. As discussed on the TC, ambient air temperature during calorimetry (°C) should be included as a covariate where available.

2.1 Generate Residuals of REE

- Trait is total daily REE (kJ / 24hr)
- Derived (where possible*) via* the Abbreviated Weir Equation using steady-state VO_2 and VCO_2 from resting calorimetry in fasted, thermoneutral participants (see above).

Using linear regression, generate a set of crude REE residuals for each of the three models:

Model 1 (Baseline): REE (kJ/24hr) ~ Standard Covariates
Model 2 (Weight-Adjusted): REE (kJ/24hr) ~ Standard Covariates + Weight (kg)
Model 3 (Weight and Height-Adjusted): REE (kJ/24hr) ~ Standard Covariates + Weight (kg) + Height (m)

2.2 Standardise REE Residuals

Standardise each set of residuals from 2.1 by applying a z-score transformation – i.e. to produce a distribution with mean = 0 and standard deviation = 1.

This step can be easily run in STATA using the `zscore` command or in R using the `scale` function

2.3 Genome-Wide Association

Conduct genome-wide association for all three sets of standardised residuals:

A) Standardised REE residuals from Baseline Model ~ Population Structure
B) Standardised REE residuals from Weight-adjusted Model ~ Population Structure
C) Standardised REE residuals from Weight and Height-adjusted Model ~ Population Structure

We encourage you to consider using BOLT-LMM for these analyses, but please feel free to apply your current pipeline if more convenient. Apply your normal approach (e.g. inclusion of genomic PCs) to account for population structure if using a linear regression (rather than LMM) software. Take usual steps to account for relatedness in your study.

3 Returning Data

3.1 File Format

Results for each model should be returned as a separate tab-delimited text file including both typed and imputed variants, one variant per line (multiple lines may be required if the variant is multiallelic, see below). For each variant, please provide the variables shown in the table. The first line of the file should contain these variable names as a header. Denote missing data with a full-stop/period (".").

Variable Name	Details	Format
snp	Unique SNP identifier, e.g. rsID	rsID
chr	Chromosome	Integer
pos	Base pair coordinate, build 37 (hg19)	Integer
effect_allele	Allele to which effect estimate corresponds	String **(see below)**
other_allele	Alternative allele at this position	String **(see below)**
n	Number of individuals analysed	Integer
eaf	Observed frequency of effect_allele in study cohort	Numeric
hwe_p	Hardy-Weinberg p-value for variant (NA if imputed)	Numeric
beta	Effect size corresponding to effect_allele	Numeric
se	Standard error of effect size (uncorrected for GC)	Numeric
pval	p-value of association (uncorrected for GC)	Numeric
info	Imputation quality (0-1)	Numeric
typed	= 1 if variant was typed rather than imputed	1 or missing (".")

Flagging Typed Variables The *typed* indicator is not included in BOLT-LMM output; please flag typed variants manually. As BOLT provides separate output files for typed and imputed loci, typed loci can be quickly flagged by reading in the typed results and generating *typed ==1* for all observations, before appending the imputed results file.

Hardy-Weinberg Equilibrium For variant QC during meta-analysis, we ask that HWE p-values are returned. In SNPTEST, HWE p-values can be outputted by specifying the `–hwe` option. BOLT cannot currently output HWE p-values, which will need to be merged in from another source. Should you need to calculate these from scratch, exact Hardy-Weinberg tests can be run in PLINK using the `--hardy` option. Please calculate p-values using the exact (as opposed to asymptotic) Hardy-Weinberg test for all participants. Contact Dan if you have any queries.

Allele Coding For biallelic SNPs, the effect allele and other allele should be specified as A/C/T/G. For other variant types, please report alleles using your normal practice. All biallelic variants should be reported one variant per line in the returned file. For multiallelic variants, more than one line may be reported for the same genomic coordinate (i.e. chromosomal position) to represent the different combinations of alleles at the site. We will harmonise variant coding ahead of meta-analysis.

Provide all values for all analysed variants exactly as displayed in association output.

Do not correct for genomic control

Please do not apply any filtering to results (for example, based on MAF or imputation quality)

Please include HWE p-value to facilitate variant QC during meta-analysis

3.2 Association File Names

Files should be named using the convention:

`[Ancestry]_GWAS_residREE_zstand_[Model]_[Study]_[Software]_[Date]_[Initials].txt`

Ancestry	*EUR* for White European, *AFR* for Black African descent, *PIM* for Pima Indian.
Model	*as* for baseline, *asw* for weight-adjusted, *aswh* for weight and height-adjusted
Study	Study Abbreviation: QFS, NEO, ICSHIB, BLSA, PIMA etc.
Software	Software used to run GWA analyses (e.g. BOLT, SNPtest etc.)
Date	Analysis date (DDMMYY)
Initials	Initials of person uploading file

`e.g. EUR_GWAS_residREE_zstand_as_Fenland_BOLT_150316_DW.txt`

3.3 Cohort Details

Please provide **descriptive statistics** of your cohort using the spreadsheet distributed with this analysis plan (REEGen_Additional_Information_Sheet_V2_March2016_Final.xlsx).

Descriptives should be restricted to the individuals included in the GWAS.

Please additionally provide **histograms** for each set of standardised residuals generated, plus the non-residualised crude REE phenotype (kJ / 24hr) – i.e. four histograms in total. Please provide each histogram as a separate image file (e.g. .png) named:

`Distribution_residREE_zstand_[Model]_[Study].png`

For example, for standardised REE residuals from the weight-adjusted model:

`Distribution_residREE_zstand_asw_Fenland.png`

Name the non-residualised REE phenotype distribution as

`Distribution_REE_crude_[Study].png`

3.4 Data Upload

An SFTP site hosted by the MRC Epidemiology Unit is provided for return of results.

Host	`sftp.mrc-epid.cam.ac.uk`
Username	`sftp-REE-Gen`
Password	E-mail Dan when you are ready to upload; he will provide password by phone.

Unix and MacOS X: Use `sftp` or `scp` at the terminal

Windows: We suggest using FileZilla (http://sourceforge.net/projects/filezilla). Connect your client to the host.

To minimise upload size, please compress all files being returned into a zip archive or similar (named with the study name, date of upload, and initials of the person uploading), then upload the archive.

Supplementary References

1. Eastwood, S. V. *et al.* Algorithms for the Capture and Adjudication of Prevalent and Incident Diabetes in UK Biobank. *PLoS One* **11** (ed Herder, C.) e0162388 (2016).
2. Han, H. Q., Zhou, X., Mitch, W. E. & Goldberg, A. L. Myostatin/activin pathway antagonism: molecular basis and therapeutic potential. *Int. J. Biochem. Cell Biol.* **45,** 2333–47 (2013).
3. Harris, T. B. *et al.* Age, Gene/Environment Susceptibility-Reykjavik Study: multidisciplinary applied phenomics. *Am. J. Epidemiol.* **165,** 1076–87 (2007).
4. Fried, L. P. *et al.* The Cardiovascular Health Study: design and rationale. *Ann. Epidemiol.* **1,** 263–76 (1991).
5. DAWBER, T. R., MEADORS, G. F. & MOORE, F. E. Epidemiological approaches to heart disease: the Framingham Study. *Am. J. Public Health Nations. Health* **41,** 279–81 (1951).
6. Harris, T. B. *et al.* Waist circumference and sagittal diameter reflect total body fat better than visceral fat in older men and women. The Health, Aging and Body Composition Study. *Ann. N. Y. Acad. Sci.* **904,** 462–73 (2000).
7. Sonnega, A. *et al.* Cohort Profile: the Health and Retirement Study (HRS). *Int. J. Epidemiol.* **43,** 576–85 (2014).
8. Ferrucci, L *et al.* Subsystems contributing to the decline in ability to walk: bridging the gap between epidemiology and geriatric practice in the InCHIANTI study. *J. Am. Geriatr. Soc.* **48,** 1618–25 (2000).
9. Deary, I. J., Whiteman, M. C., Starr, J. M., Whalley, L. J. & Fox, H. C. The Impact of Childhood Intelligence on Later Life: Following Up the Scottish Mental Surveys of 1932 and 1947. *J. Pers. Soc. Psychol.* **86,** 130–147 (2004).
10. Deary, I. J. *et al.* The Lothian Birth Cohort 1936: a study to examine influences on cognitive ageing from age 11 to age 70 and beyond. *BMC Geriatr.* **7,** 28 (2007).
11. Bennett, D. A. *et al.* The Rush Memory and Aging Project: study design and baseline characteristics of the study cohort. *Neuroepidemiology* **25,** 163–75 (2005).
12. Bennett, D. A., Schneider, J. A., Arvanitakis, Z. & Wilson, R. S. Overview and findings from the religious orders study. *Curr. Alzheimer Res.* **9,** 628–45 (2012).
13. Blank, J. B. *et al.* Overview of recruitment for the osteoporotic fractures in men study (MrOS). *Contemp. Clin. Trials* **26,** 557–68 (2005).
14. Orwoll, E. *et al.* Design and baseline characteristics of the osteoporotic fractures in men (MrOS) study–a large observational study of the determinants of fracture in older men. *Contemp. Clin. Trials* **26,** 569–85 (2005).
15. John, U *et al.* Study of Health In Pomerania (SHIP): a health examination survey in an east German region: objectives and design. *Soz. Praventivmed.* **46,** 186–94 (2001).
16. Völzke, H. *et al.* Cohort profile: the study of health in Pomerania. *Int. J. Epidemiol.* **40,** 294–307 (2011).
17. Cummings, S. R. *et al.* Appendicular bone density and age predict hip fracture in women. The Study of Osteoporotic Fractures Research Group. *JAMA* **263,** 665–8 (1990).
18. Callisaya, M., Blizzard, L., McGinley, J. & Srikanth, V. Risk of falls in older people during fast-walking âĂŞ The TASCOG study. *Gait Posture* **36,** 510–515 (2012).
19. Moayyeri, A., Hammond, C. J., Hart, D. J. & Spector, T. D. The UK Adult Twin Registry (TwinsUK Resource). *Twin Res. Hum. Genet.* **16,** 144–9 (2013).
20. Henneman, P *et al.* Prevalence and heritability of the metabolic syndrome and its individual components in a Dutch isolate: the Erasmus Rucphen Family study. *J. Med. Genet.* **45,** 572–7 (2008).
21. McEvoy, M. *et al.* Cohort profile: The Hunter Community Study. *Int. J. Epidemiol.* **39,** 1452–63 (2010).
22. Sachdev, P. S. *et al.* The Sydney Memory and Ageing Study (MAS): methodology and baseline medical and neuropsychiatric characteristics of an elderly epidemiological non-demented cohort of Australians aged 70-90 years. *Int. Psychogeriatr.* **22,** 1248–64 (2010).
23. Pitsiladis, Y. P. *et al.* Athlome Project Consortium: a concerted effort to discover genomic and other "omic" markers of athletic performance. *Physiol. Genomics* **48,** 183–90 (2016).
24. Hedstrand, H. A study of middle-aged men with particular reference to risk factors for cardiovascular disease. *Ups. J. Med. Sci. Suppl.* **19,** 1–61 (1975).
25. Mootha, V. K. *et al.* Identification of a gene causing human cytochrome c oxidase deficiency by integrative genomics. *Proc. Natl. Acad. Sci. U. S. A.* **100,** 605–10 (2003).
26. Elgzyri, T *et al.* First-degree relatives of type 2 diabetic patients have reduced expression of genes involved in fatty acid metabolism in skeletal muscle. *J. Clin. Endocrinol. Metab.* **97,** E1332–7 (2012).